STORE-OPERATED CALCIUM CHANNELS REGULATED BY HYPEROSMOLARITY AS A MECHANISM UNDERLYING ENDOTHELIAL DYSFUNCTION IN THE HYPERSOMOLAR CONDITION

Thomas Gordon Hallett

Submitted in accordance with the requirements for the degree of

Doctor of Philosophy

The University of Hull and The University of York

Hull York Medical School

August 2020

Contents

Acknowledgements

I thank Dr S.Z Xu for his guidance and supervision throughout this process.

I also thank Dr N. Daskidilou and Dr B. Zheng for their work on these channels before me, thanks to their work I had a foundation on which to build.

Dr B Zheng was responsible for the creation of the Orai mCherry/STIM-GFP HEK 293-TRex cells and Dr Daskidilou published data (referenced in this thesis) on the effect of hyperglycaemia on the activity of Orai channels.

I thank my parents for their support and encouragement and love throughout my studies.

Finally, I dedicate this thesis to my darling wife Teodora, her patience and strength spurred me on to be better and to do better.

The Hours (Orai) have as their charge, the vast sky and Mount Olympos, to open and close the dense darkness which guards the home of the Immortals

The Illiad 05.750

Soli deo gloria

List of Figures

List of Tables

Author's Declaration

I confirm that this work is original and that if any passage(s) or diagram(s) have been copied from academic papers, books, the internet or any other sources, these are clearly identified by the use of quotation marks and the reference(s) is fully cited. I certify that, other than where indicated, this is my own work and does not breach the regulations of HYMS, the University of Hull or the University of York regarding plagiarism or academic conduct in examinations. I have read the HYMS Code of Practice on Academic Misconduct, and state that this piece of work is my own and does not contain any unacknowledged work from any other sources.

Abstract

Introduction

Hyperosmolarity is a concomitant factor to the hyperglycaemia observed in diabetes mellitus, a disease known to affect the function of endothelial cells and cause vascular damage. Previous studies have found that hyperglycaemia is capable of reducing the viability of endothelial cells and altering the activity of store-operated Ca^{2+} entry (SOCE). This study aims to determine the role of hyperosmolarity on the endothelial function and the activity of SOCE and Orai channels.

Methods

In this study, hyperosmolarity was simulated (*in vitro*) via the addition of mannitol at clinically relevant concentrations (19.5, 30 & 60 mM). Physical & biochemical assays were employed to determine the effect this stimulus had on endothelial function. Ca^{2+} imaging was employed to measure the effect of hyperosmolarity on Orai channel activity and the role of Reactive Oxygen Species was investigated with the use of biochemical dyes (H_2DCFDA. Mitosox & Amplex red).

Results

Hyperosmolarity reduced endothelial cell migration (41% fewer migrated cells compared to control P=<0.0001) and increased the number of dead cells per field (160% increase from control P=<0.0001). SOCE was reduced under hyperosmolar conditions in human aortic endothelial cells and endothelial cell line (EA.hy926). SOCE in primary endothelial cells was found to be mediated by Orai channels, which was demonstrated by transfection of Orai siRNAs.

All three types of Orai channels (Orai1-3) were sensitive to hyperosmolarity in the HEK293 cells overexpressing STIM1/Orai with all three subtypes showing a >50% reduction in peak influx compared with untreated cells (*P*=<0.05 for all groups). Cytosolic reactive oxygen species (ROS) and mitochondrial ROS were increased by hyperosmolarity. Hydrogen peroxide was capable of reducing SOCE in a concentration-dependent manner.

Conclusion

These results suggest that the reduced SOCE by hyperosmolarity may be mediated by an increase in intracellular ROS concentration. The findings in this study suggest that store-operated Orai channels regulated by hyperosmolarity may act as a new underlying mechanism for causing diabetic vascular injury, which allows further therapeutic exploration for diabetic complications.

Abbreviations

2-APB	2-Aminoethoxydiphenyl borate
CRAC	Calcium release-activated current
DM	Diabetes Mellitus
DMEM	Dulbeco's modified eagle media
DMSO	Dimethylsulphoxide
ECF	Extracellular fluid
EGTA	Ethylene glycol tetra-acetic acid
eNOS	Endothelial Nitric Oxide synthase
ETC	Electron transport chain
FBS	Foetal bovine serum
FCCP	Carbonyl cyanide-p-trifluoromethoxyphenylhydrazone
GFP	Green fluorescent protein
GPCR	G-protein coupled receptor
H_2DCFDA	2',7'-dichlorodihydrofluorescein diacetate
HEK 293	Human embryonic kidney 293 cells
HEPES	4-(2-hydroxyethyl)-1-piperazineethanesulfonic acid
HG	Hyperglycaemia
HHS	Hyperosmolar hyperglycaemic state
IP_3	Inositol triphosphate
NADPH	Nicotinamide adenine dinucleotide phosphate
NOX	NAPDH oxidase
Pen/Strep	Penicillin-Streptomycin

PBS	Phosphate buffered saline
ROI	Region of interest
ROS	Reactive oxygen species
SAM	Sterile Alpha Motif
SOAR	STIM/ORAI activating region
SOCE	Store-operated calcium entry
SOD	Superoxide dismutase
STIM	Stromal interaction molecule
TG	Thapsigargin
TRP	Transient receptor potential channel
TRPC	Transient receptor potential canonical channel
TRPV	Transient receptor potential vanilloid channel

Chapter 1

Introduction

1.1 Introduction

Diabetes mellitus (DM) is a growing global health problem with an estimated prevalence of 424 million patients worldwide in 2017 which is 8.8% of the global population (Standl et al., 2019). Diabetes affects around 4% of the UK population, with this proportion predicted to rise in line with increasing levels of obesity (Holman et al., 2015). DM places a large burden on the healthcare system in the UK with a total cost to the economy being £23.7 billion, constituting both direct costs and indirect costs in 2010/2011 (Hex et al., 2012). These costs will continue to rise and research into the prevention and treatment of DM is of great economic benefit to both developed and developing countries.

It is not just the cost of DM that is of concern but the consequences and impact it has on a patient's health and life expectancy. For example, diabetic men and women over 50 had an average reduction in life expectancy of 7.5 and 8.2 years, respectively (Franco et al., 2007). This reduction in life expectancy is associated with the vascular complications of DM, which are caused by the chronic hyperglycaemic state (Leibson and Narayan, 2005). The state of chronic hyperglycaemia (HG) is found in both types of diabetes, although in type 2 diabetes the symptoms are far less severe in the early stages, which can lead to substantial vascular injury even before diagnosis (Caballero et al., 1999, Caballero, 2003). Type II diabetes is becoming a focus for several Western economies as a growing health crisis, although it is accepted that to battle this disease both societal policy change and advanced medical research must work together in order to turn the tide against this endocrine disease (Whiting et al., 2011).

1.1.1 Blood glucose and diabetes

Glucose is the primary metabolic fuel utilised by the human body for the generation of Adenosine triphosphate (ATP). This molecule (ATP) goes on to provide the chemical energy required for the majority of cellular processes that must occur for tissues, organs and, indeed, the whole body to function (Gajewski et al., 1986). Glucose is primarily sourced from the dietary intake of sugars which are digested down into more basic sugars to allow for their absorption into the bloodstream. These simple sugars are characterised by whether their carbonyl group is exposed, in the case of reducing sugars, (e.g. glucose) or un-exposed in the case of non-reducing sugars (e.g. sucrose) (Hewitt and Pryde, 1920). The process of how glucose is regulated once it has entered into the blood is crucial to understanding one of the key bioenergetic principles of the human body.

Insulin is a peptide hormone that is produced in the pancreas by the β-cells found within the islets of Langerhans. Insulin is released from β-cells when glucose enters the cell, primarily via the GLUT2 transporter. The GLUT2 transporter has relatively low affinity for glucose, in comparison to other glucose transporters, and as such glucose will only enter via this channel when there is an elevated concentration of plasma glucose (Schnedl et al., 1994). After the glucose enters the β-cells it undergoes phosphorylation leading to an increase in the intracellular Adenosine triphosphate: Adenosine diphosphate (ATP:ADP) ratio (Konrad et al., 1996). This prevents potassium ions from leaving the cell (via facilitated diffusion) causing membrane depolarization and subsequent activation of voltage-gated Ca^{2+} channels (Braun et al., 2008).

The increase in cytosolic Ca^{2+} leads to the release of insulin into the blood plasma; this insulin then goes on to increase the level of glucose uptake within the cells of target tissues (e.g., adipose tissue and skeletal muscle) by causing the GLUT4 transporter to be incorporated into the plasma membrane of the target cells (Klip et al., 1990). This lowers the level of blood glucose to the normal homeostatic level which in a healthy human will be no greater than 5.5 mmol/l when fasting or no greater than 7.8 mmol/l 2 hours after a meal and no greater than 11.1 mmol/l when tested at a random interval (Hill et al., 2011) (Diabetes UK, 2019).

Insulin is only one part of the homeostatic mechanism responsible for maintaining optimum glucose levels. A second major component is the hormone glucagon, which has an end tissue action that opposes the action of insulin, that being the release of glucose from tissues into the plasma (Wewer Albrechtsen et al., 2017). The major tissue types that glucagon acts upon to cause the release of glucose into the bloodstream are the liver and skeletal muscle (Kraft et al., 2017). Glucagon is another peptide hormone that is produced in the pancreas, although produced in the α-cells in the islets of Langerhans, and it is released when blood glucose levels are too low (hypoglycaemia) (Mitrakou et al., 1991).

Diabetes mellitus (DM) is a metabolic disorder characterised by chronic hyperglycaemia caused by disturbances in carbohydrate and lipid metabolism (Alberti and Zimmet, 1998). The changes in carbohydrate and lipid metabolism are caused either by the impaired secretion of the hormone insulin from the pancreas (β-cells) or by the impaired action of insulin on target tissues (American Diabetes Association, 2010).

There are two types of DM, i.e., type 1 and type 2. A common clinical manifestation for both types of DM is the elevation of blood glucose to pathological levels (Olokoba et al., 2012). The World Health Organisation gives the diagnostic criteria for DM as a plasma glucose level of ≥7.0 mmol/L when fasting or over ≥11.1 mmol/L 2 hours after glucose intake (World Health Organization, 2006). The HbA1c test (or glycated haemoglobin) is a way of measuring the average plasma glucose over a prolonged period, and WHO recommended its use in DM diagnosis in 2011 (World Health Organization, 2013). The cut-off value for the definite diagnosis of DM is 48 mmol/mol (6.5 %) of HbA1c (Cohen et al., 2010). HbA1c is also a good predictor of peripheral arterial disease as it can be used to measure a patient's long-term glucose control and help to calculate their risk of vascular complications (Selvin et al., 2006).

Two important terms to define within the topic of blood glucose regulation are hyperglycaemia and hypoglycaemia. Hyperglycaemia is an elevated blood glucose level (> 7 mmol/l fasting) and has acute effects on the body, for example, an increase in urine output and increased thirst (Spira et al., 1997, Buoite Stella et al., 2018). Hypoglycaemia is a condition of low blood glucose that can occur in both healthy and diabetic populations; a person will be considered hypoglycaemic if their blood sugar is < 3.9 mmol/l although some have suggested this criterion should be shifted to < 3.0 mmol/l (Heller et al., 2019). In more recent studies there is increasing consensus around the definition of a pre-diabetic state, with a common diagnostic criteria being a fasting blood glucose level of between 5.6-7 mmol/l (Bansal, 2015). This condition is increasing in prevalence throughout the world and can be a valuable diagnosis as “pre-diabetes” can be more easily managed or reversed through modification of diet compared to Type II diabetes (Lim et al., 2011).

It is important to note that it is very rare for a healthy, non-diabetic, person to become hypoglycaemic and this may usually only result from some extreme circumstances such as fasting or excessive alcohol intake over a short period of time (Fischer et al., 1986). Even fasting should not produce a hypoglycaemic state, as the body is capable of maintaining a functional concentration of blood glucose through the process of gluconeogenesis (Hatting et al., 2018). Hypoglycaemia also has acute effects on the body such as a loss of consciousness as well as causing confusion and lethargy (Malouf and Brust, 1985).

Type 1 DM is known as insulin-dependent diabetes, which is caused by the autoimmune destruction of pancreatic β-cells, leading to impaired secretion of insulin (Daneman, 2006). The pathophysiology of type 1 DM depends on autoimmune damage resulting from both genetic predisposition and viral infection (Åkerblom et al., 2002). The invasion of immune cells and the over-production of chemokines and inflammatory markers leads to apoptosis of the β-cells (Cnop et al., 2005), thereby preventing insulin production. Patients of type 1 diabetes require insulin therapy (Atkinson and Eisenbarth, 2001). Type 1 diabetes can be controlled through the use of insulin and glucose monitoring and if a patient shows good therapy concordance then they can avoid some of the more severe consequences of the disease (Chatterjee, 2006). Patient concordance is a major area of research within diabetes treatment research, particularly with type 1 patients. There is an increasing prevalence of psychological disorders associated with type 1 diabetes, for example, the unique condition diabulimia whereby a patient may forgo essential insulin infusions in order to reduce their weight (Hastings et al., 2016).

If type 1 diabetes is not controlled well (with proper glucose monitoring and insulin dosage) then a patient may experience ketoacidosis due to the inability to utilise the elevated levels of blood glucose (Luethi et al., 2016). Ketones are produced by breaking down fat in a process known as ketogenesis to provide an alternative energy source because the body cannot utilize the available glucose, due to lack of insulin, in ketoacidosis, these ketones reach such a level that it produces an acidotic (low blood pH) state (Dashti et al., 2004). Ketogenesis is a normal physiological process intended to utilize stored fat, unlike the pathological state of ketoacidosis (Stadie, 1958). The keto-acidotic condition is generally only observed in type one diabetes although it has been documented in patients suffering from type 2 diabetes where the level of insulin produced has reduced significantly (Gosmanov et al., 2014, Welch and Zib, 2004).

Type 2 DM, formally known as non-insulin-dependent diabetes, is characterised by a resistance to insulin as well as impaired pancreatic secretion of insulin (Kahn, 1998). The cause of type 2 diabetes is a significant field of scientific enquiry that consists of the investigation into potential causative factors (Dardano et al., 2014). A leading hypothesis is that type 2 DM is strongly correlated with obesity, and as such there may be a causative factor within the pathophysiology of obesity (Astrup & Finer, 2000) (Al-Goblan et al., 2014). Both genetic and environmental factors lead to insulin resistance and thus impaired homeostatic control of glucose (Florez, 2008).

Another clinical condition with the name diabetes but with very different pathogenesis and very different implications for the body is diabetes insipidus. The most common form of this disease (central) involves a lack of the hormone vasopressin which leads to greatly elevated urine output and increased thirst (Kalra et al., 2016). This disease can cause kidney damage and although rare is still a significant cause of morbidity for those who suffer from the disease (Bockenhauer and Bichet, 2015).

1.1.2 Diabetic vascular damage

Chronic hyperglycaemia impairs the activity and reduces the viability of vascular endothelial and smooth muscle cells (Lund et al., 2000). One impact upon large blood vessels (the macrovascular system) is the narrowing of the vascular lumen via atherosclerosis which is potentiated by both diabetes and dyslipidaemia (Beckman et al., 2002).

Atherosclerosis is the loss of elasticity within a blood vessel leading to the formation of an atheromatous plaque which eventually can lead to vascular occlusion (due to the narrowing of the vessel) as well as plaque rupture leading to clot formation and potential major ischemic episodes such as cardiovascular ischaemia (Ference et al., 2017) (de Vries et al., 2012). Diabetes is only one risk factor that has been shown to be linked with atherosclerosis formation-for example: age and being of the male gender are significant risk factors (Collins et al., 2009, Fairweather, 2015). Atherosclerosis is an insidious condition as it often shows no clinical symptoms until the level of vascular occlusion/damage caused is at a very significant level (Näslund et al., 2019). One paper by Duncan *et al* describes how the low-level systemic inflammation associated with diabetes may be a contributing factor to the increased risk of atherosclerosis in diabetic patients (Duncan et al., 2003). One significant effect that hyperglycaemia has on the microvasculature is the alteration of vasoconstrictive/dilative properties within these small vessels which in turn can lead to impairment of blood flow to the surrounding tissues (Schramm et al., 2006).

Vasoconstriction (narrowing of the lumen through the constriction of the vascular wall/muscle) is a normal reaction to some stimuli (for example peripheral vasoconstriction to prevent heat loss in cold condition) (Castellani and Young, 2016). Vasoconstriction is, in healthy people, often a short-lived vascular response, although diabetic patients have been shown to have reduced levels of bioavailable Nitric oxide (NO) which is a potent vasodilator (Modin et al., 2001). With reduced NO compared to healthy patients there is a greater chance of end tissue damage due to vasoconstrictive ischaemia and this is theorised to contribute to the vascular complications of DM (Vinik et al., 2001).

Impaired vascular reactivity contributes to hypertension and further increases the risk of a significant cardiovascular event, thereby contributing to the mortality of DM (Caballero et al., 1999). A leading cause of cardiovascular disease (a macrovascular complication) is atheroma formation, which is strongly associated with DM (Beckman et al., 2002b). HG causes an elevation in circulating lipid and initial endothelial damage leading to a greater chance of atheroma formation (Al-Sharea et al., 2019). This, in turn, contributes to coronary heart disease, leading to an increased risk of myocardial infarction (Stranders et al., 2004). The macrovascular damage caused by prolonged HG also leads to an increased risk of acute cerebral ischaemia and stroke (Gilmore and Stead, 2006).

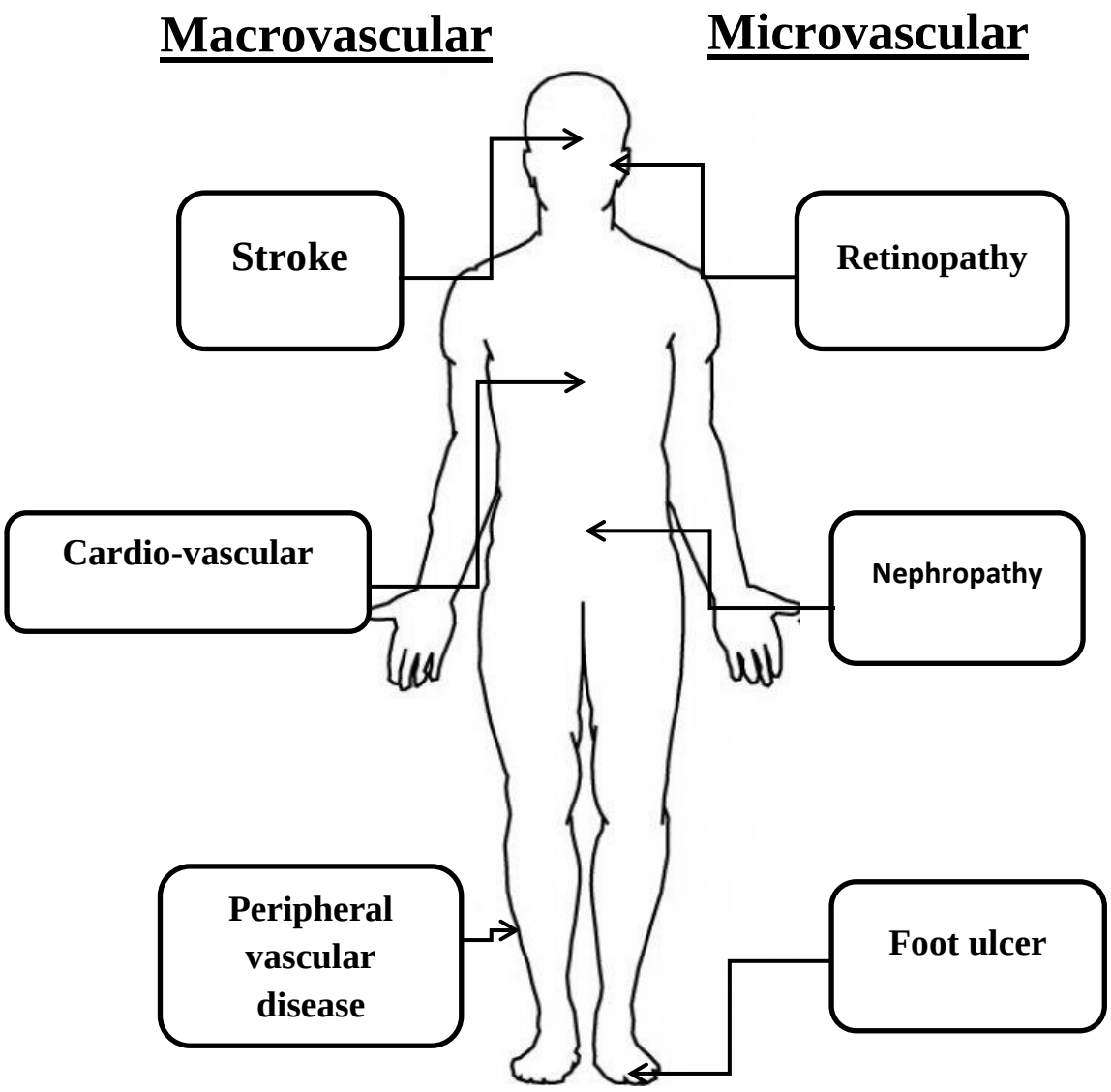

Fig. 2.1 Common complications of diabetes. Both peripheral and visceral complications are shown in this diagram, showing the major morbidities of DM.

The vascular complications that are caused by DM range in their severity of mortality and morbidity. For example, vascular injury can lead to diabetic foot ulcers as well as stroke and cardiovascular disease (Donnelly et al., 2000). The physical and biochemical stress that the blood vessels are placed under in chronic HG has a profound effect on a patient's overall health as time progresses. This is because in both the large and the small blood vessels HG causes vascular injury (Maile et al., 2007). A common form of diabetic microvascular injury is diabetic retinopathy as it occurs in ¾ of all patients who have been diagnosed with DM for greater than 15 years (Klein et al., 1984). The development of diabetic retinopathy is complicated but it is agreed that elevated blood sugar causes the pathological changes in the eye such as thickening of the vascular basement membrane and degeneration of the retinal capillaries (Engerman, 1989). Diabetic retinopathy is a disease that severely impacts patient quality of life and leads to blindness (Sivakumar et al., 2005); although some vascular complications of DM such as increased cardiovascular risk carry with them increased mortality (Sheetz and King, 2002).

One of the most severe conditions caused by microvascular diabetic blood vessel injury is diabetic nephropathy, as it is capable of causing end-stage renal disease and kidney failure (Thomas et al., 2015). The kidney is a multifunctional organ that plays a key role in several homeostatic mechanisms that are needed to maintain bodily function and health (Higgins et al., 2004). One such function is in the filtration of smaller molecules (for example salts and urea) out of the blood in order to be excreted in the urine which prevents the toxic build-up of metabolic end-products(Caulfield and Farquhar, 1975).

This filtration takes place at the renal corpuscle (found within the cortex of the kidney- see Fig 2.2) which is found at the beginning of the nephron and compounds with lower molecular weights pass through and form the ultra-filtrate which may go on to be excreted as urine (Tojo et al., 2008). Molecules of lower molecular weight are not all excreted as urine because another major function of the kidney is resorption. Resorption of small molecules takes place in different parts of the nephron - for example, Na^+ ions are reabsorbed in the collecting tubules partially by the action of Na^+/K^+ ATPase pumps (Frömter et al., 1973). Ca^{2+} is one of the molecules that is reabsorbed from the ultra-filtrate to a high degree (99%) (Hoenderop et al., 2001).

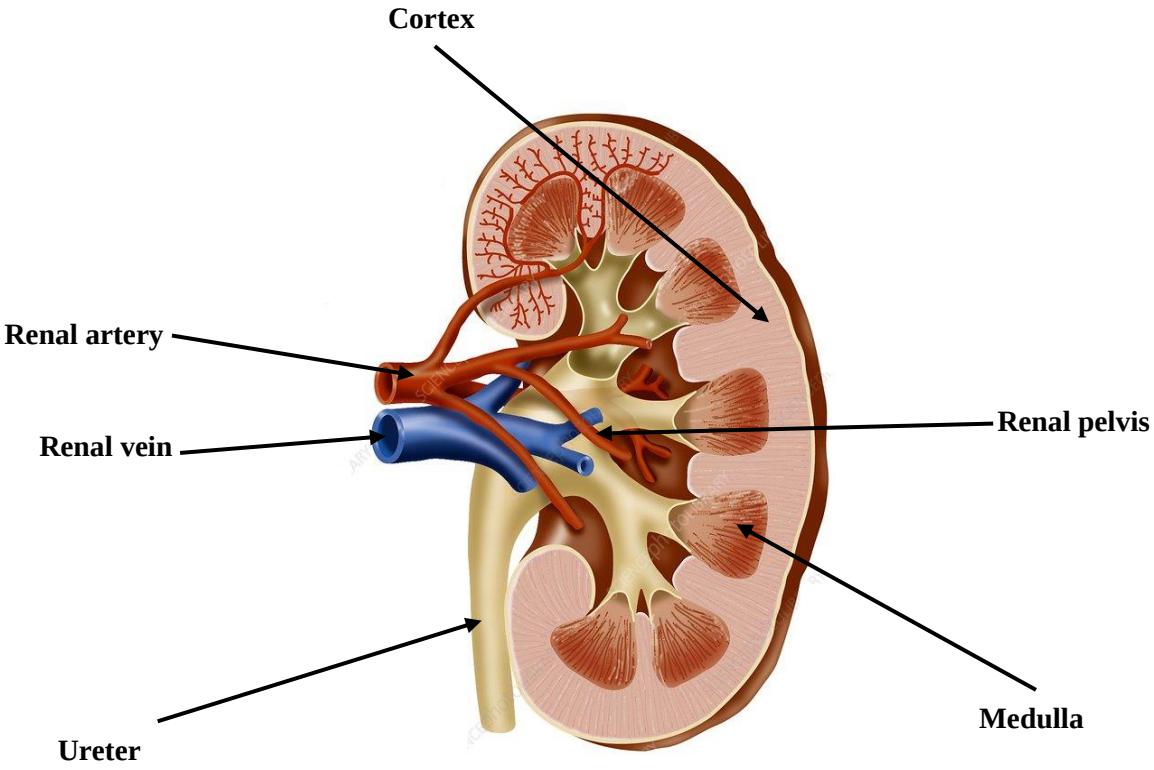

Fig.2.2-Figure adapted from (Velho and Velho, 2013) showing the anatomy of the human kidney.

One fundamental hypothesis as to how DM leads to nephropathy is by the alteration of inflammatory pathways as well as the haemodynamic and metabolic changes that lead to nephrotic damage (Navarro-González et al., 2011). This diabetic kidney damage contributes to the morbidity of diabetes (Young et al., 2003). It is also reported that diabetic nephropathy occurs in 40% of patients diagnosed with diabetes within their lifetime (Gross et al., 2005). Diabetic foot ulcers are a source of disability for DM patients that are caused by peripheral ischemia, infection and neuropathy; although not a life-threatening condition it can have a considerable impact on a DM patient's quality of life (Jeffcoate and Harding, 2003).

1.2 Mechanisms of diabetic vascular injury

Diabetic vascular damage is caused by a complex combination of the direct physical (haemodynamic) damage to the vasculature as well as cellular and physiological changes to the cells that make up the vascular system (Cooper et al., 2001). One of the haemodynamic factors that contribute to diabetic vascular injury is hypertension, which is present in 60% of people diagnosed with type 2 diabetes by the age of 75 in the US (Garber, 1995). Hypertension, otherwise known as high blood pressure, is a serious chronic medical condition. The clinical guidance published by the National Institute of Health and Care Excellence (NICE) states that the diagnostic criteria for hypertension are a singular blood pressure observation of $\geq$140/90 mmHg as well as an ambulatory blood pressure of $\geq$135/85 mmHg (average taken over the waking hours of three days) (NICE, 2019).

Hypertension is capable of producing morphological changes within blood vessel walls such as endothelial dysfunction and remodelling of the vasculature (Hsueh and Anderson, 1993). Haemodynamic changes are but one of the elements of diabetic vascular injury, as prolonged hyperglycaemia also causes metabolic changes and osmotic stress, both of which can be seen in Fig. 1.2, and contribute to the damage of diabetic vessels (Madonna and De Caterina, 2011). Hypertension does not only affect the vascular endothelial cells but it has been shown to lead to hyper-proliferation of perivascular adipose tissue (Li et al., 2011) as well as negatively impacting the proliferation and functionality of vascular smooth muscle cells found within the tunica media of blood vessels (Wu and Juurlink, 2002). Hypertension may be asymptomatic for many patients at the earliest stages although some symptoms of the condition include severe headaches, impaired vision and chest pains (Yannoutsos et al., 2014).

Two critical studies (DCTT 1995 & (King et al., 1999)) have shown hyperglycaemia to be a contributory cause of diabetic vascular complications. Both of these working groups found that the strict control of hyperglycaemia leads to a reduction in diabetic vascular injury (DCCT 1995; King et al., 1999). Both studies were very highly powered with over 1000 patients per population group; these studies followed nearly the same methodology although one used a North American population (King et al 1999) whereas the other was performed on a UK population. These large sample sizes are advantageous as it is known that the morbidity of type II diabetes can be affected by patient demographics such as race and gender, with African American and Polynesian populations being at greater risk of developing vascular complications (Spanakis and Golden, 2013).

The cell types that are most prone to undergo alterations in their metabolism are those which are not capable of significantly modulating glucose transport in the event of high intracellular glucose (Heilig et al., 1995)&(Nichols et al., 2008). These include neuronal cells as well as smooth muscle cells within the vascular system, although within the vascular system the cell type most prone to hyperglycaemic damage are endothelial cells (Meng et al., 2014). In the overabundance of intracellular glucose, injury-prone cells downregulate glucose entry and alter their energetic profile to survive the HG stress stimulus (Brownlee, 2001).

There are four major pathways detailing how hyperglycaemia can lead to metabolic changes, thereby causing diabetic vascular injury, these pathways/mechanisms are not thought to work in isolation but rather it is hypothesised that they synergistically produce metabolic changes within various cell types under the hyperglycaemic condition (Peiró et al., 2016). Firstly, it has been shown that there is an increase in polyol pathway flux that is associated with elevated glucose levels (Tang et al., 2012) (Wilson et al., 1992). Aldose reductase is the first enzyme in the polyol pathway and it has a low affinity for glucose within the non-diabetic population. The Wilson 2012 paper showed that within DM this enzyme is used to a much greater degree, therefore leading to an increased level of sorbitol production. This, in turn, produces intracellular hyperosmolarity, potentially initiating cell death in severe hyperosmolar episodes (Aquilano et al., 2007).

The second metabolic change that has been shown to result from hyperglycaemia is the increased production of advanced glycation end-products (AGE) within the hyperglycaemic condition (Wells-Knecht et al., 1995). AGE's are produced in the event of intracellular HG through several pathways and it is the accumulation of these AGEs that increases the concentration of intracellular Reactive Oxygen Species (ROS) as well as the activation of NF-Kb potentially leading to cellular death (Giardino et al., 1994).

Thirdly, it has been shown that the activation of protein kinase C (a key regulator of the function of many intracellular proteins) is linked with intracellular HG (Ishii et al., 1998). This is because protein kinase C is activated by diacylglycerol (DAG), during the HG condition the *de novo* synthesis of DAG is increased, leading to an increase in the activity of protein kinase C which will go on to both upregulate and inhibit the activity of many other key metabolic proteins (Kuboki et al., 2000).

The fourth change of cellular metabolism that is associated with HG is the increased flux through the Hexosamine pathway; during the HG condition excess glucose can be shuttled into the Hexosamine pathway (Kolm-Litty et al., 1998). This, in turn, leads to the production of o-linked glycoproteins that are capable of upregulating the expression of several transcription factors, for example Transforming growth factor alpha (TGF-α) and plasminogen activator inhibitor 1 (PAI-1) (Du et al., 2001). These factors can, in turn, lead to changes in cellular proliferation and maturation as well as the overproduction of intracellular ROS (Kim et al., 2010).

It has been found that urea induced ROS generation was exacerbated and driven by a marked increase in the utilization of the hexosamine pathway when measured in human aortic endothelial cells and mouse models (D'Apolito et al., 2015). It has also been suggested that it is an increase in hexosamine pathway usage that could be an early marker for beta cell dysfunction in DM (Evans et al., 2003). These findings are sometimes suggested to be indicative of a dynamic relationship between the "damage pathways" and the hyperglycaemic condition whereby it may be the case that the pathways induced produce a positive feedback loop, potentially leading to a greater sensitivity to the hyperglycaemic condition (Brereton et al., 2016).

The four pathways discussed lead to the alteration of many cellular growth factors and other proteins. One thing that these pathways have in common is that all of them have been discovered to be produced not just by HG but more specifically, they have been linked to an increase in intracellular ROS (Yan, 2018). It is well known that the ROS increase associated with HG is capable of producing oxidative stress, itself a condition capable of leading to alterations of cellular function and even apoptosis (Brownlee, 2005). One major source of intracellular ROS, even in a normal physiological state, is the mitochondrion (Mailloux et al., 2016).

The mitochondrial electron transport chain overproduces ROS such as superoxide (O2-) in the hyperglycaemic state due to more glucose being oxidised in the TCA cycle leading to the back up of electrons at coenzyme Q in the chain, producing the superoxide ROS (Nishikawa et al., 2000). ROS also act as signalling molecules leading to apoptosis or necrosis (Buetler et al., 2004).

An increase in intracellular reactive oxygen species generated under hyperglycaemic conditions is capable of altering many signalling processes that can contribute to diabetic vascular injury and, interestingly, the concomitant factor of hyperosmolarity is capable of producing an increase in intracellular ROS (Deng et al., 2015). Additional detail on the generation of intracellular reactive oxygen species can be found in section 1.5.2 of this chapter.

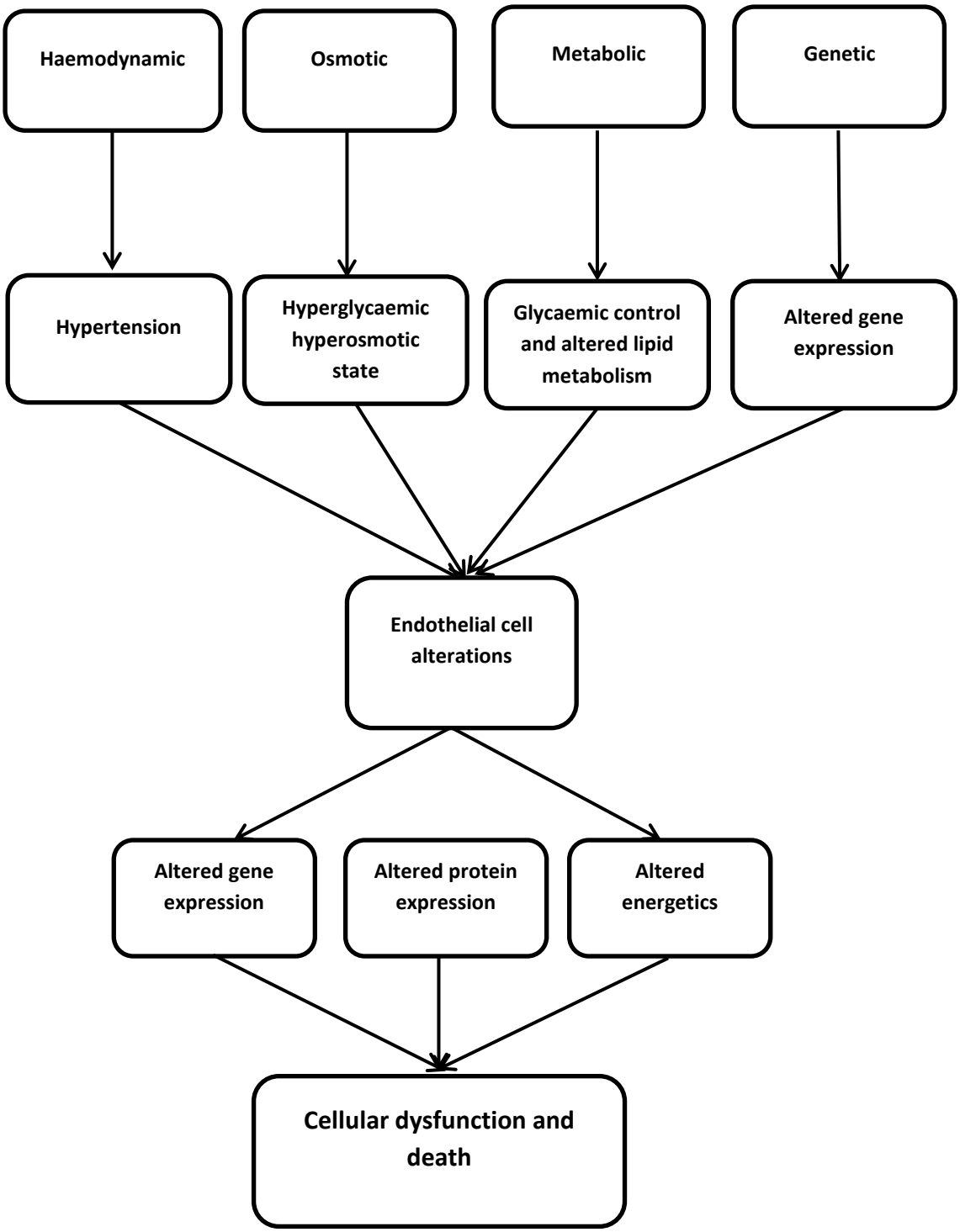

Fig. 1.2 Schematic diagram for the mechanisms of diabetic vascular injury adapted from (Rask-Madsen and King, 2013).

1.3 Osmolarity

Osmolarity is defined as the concentration of osmotically active particles within a solution relative to the concentration of solvent molecules within that solution. For the purpose of physiological studies, this solvent is always water (Vujovic et al., 2018). As a worked example, the osmolarity of a NaCl (salt) solution increases if more particles of NaCl (dissociated into Na^+ & Cl^-) are added or if particles of H_2O are taken away or evaporated. Conversely, if the level of free water is increased e.g. the solution is diluted with water then the total osmolarity of the solution has been decreased. Osmolarity and osmolality are different measurements used to describe the same physical property they differ in one key way: osmolarity is the measure of soluble particles relative to the volume of the solvent material whereas osmolality is the measure of soluble particles relative to the mass of the solvent particles. For this reason osmolarity (volume dependant) is affected by temperature and pressure whereas these factors do not have to be taken into account when calculating osmolality (Caon, 2008).

The normal osmolarity for human plasma is between 285-295 mOsm/L (Hooper et al., 2015). Osmolarity and the osmotic forces placed upon the cells of the body facilitate the diffusion of ions across the plasma membrane, which controls many processes within the cells and maintains an optimum cell volume (Lang et al., 1998). For this reason, it is crucial that plasma osmolarity is maintained within strict parameters for changes in extracellular osmolarity can change the intracellular osmolarity (Natarajan et al., 1997) (Verkman et al., 1996). This change in intracellular osmolarity is capable of producing a change in the expression of proteins and regulation of some genes; for example, a change in osmolarity is capable of changing the expression of Collagen 1 & 2 within intervertebral discs (Wuertz et al., 2007) as well as the osmosensitivity of some cell surface ion channels (Strotmann et al., 2000).

One such example is the Transient receptor potential channel v-4 (TRPV4) which is known to play a role in osmosensation and proven to contribute to nociception (Alessandri-Haber et al., 2004). One of the most notable changes that cells will undergo following a change in ECF osmolarity is a reduction or increase in volume (Verkman et al., 1996). If plasma osmolarity increases then cell volume will decrease and cell volume will increase when plasma osmolarity is reduced, this is due mostly to the movement of water moving down the osmotic gradient primarily via aquaporins (Soergel et al., 1968). This can have an immediate effect upon the function and viability of a cell depending on its ability to rectify and buffer this response, extreme changes in osmolarity lead to cell death and lysis (Hasler et al., 2005).

1.3.1 osmolarity in health and disease

Hyperosmolarity within the clinical setting is often defined as a sustained plasma osmolarity of over 320 mOsm/L and can be caused by several disease states (Hooper et al., 2015). One example is renal failure, whereby the kidneys are no longer able to properly regulate the balance of osmolytes and free water within the plasma (Conte et al., 1990). Another less common example is acute alcohol poisoning which can produce clinical hyperosmolarity as ethanol is capable of increasing serum osmolarity through increasing the loss of free water through urination and itself acting as an osmolytes (Kraut and Kurtz, 2008). The symptoms of mild to moderate hyperosmolarity include; thirst, dizziness and dry mouth (Pasquel and Umpierrez, 2014). Severe hyperosmolarity is capable of causing neurological and nephritic damage and therefore may present with symptoms such as the loss of consciousness or haematuria (Rybka and Mistrík, 2015).

One of the most clinically significant osmolytes that are capable of causing hyperosmolarity is glucose which under normal circumstances is tightly controlled by the action of hormones (insulin and glucagon) controlling the storage and release of free glucose into the plasma (Drucker, 2007). Therefore, one of the most common causes of clinical hyperosmolarity is diabetes, a common metabolic disease that impairs the standard physiological systems of glucose control. Although this is only when diabetes is uncontrolled through both diet and medication, as controlled diabetes would not lead to dangerously elevated blood glucose and therefore would not be a cause of clinical hyperosmolarity. Hypoosmolarity (clinically low plasma/extracellular fluid (ECF) osmolarity) is often associated with either solute or salt depletion (hyponatraemia). This is concomitant with the over-retention of water (Mp et al., 1971).

Hyponatraemia is commonly defined clinically as a serum osmolarity of lower than 280 mOsm/kg (Milionis et al., 2002) and can occur commonly from over-hydration or, paradoxically, from diarrhoea. Although diarrhoea causes an increased loss of water in the stools if this water loss is replaced with a hypotonic solution (e.g. water) the depletion of sodium and other essential ions will not be corrected, leading to hyponatremia and hypoosmolarity (Pizarro et al., 1983). Clinical hypoosmolarity can lead to cerebral oedema the symptoms of which include; nausea, faintness and in severe cases coma and death (Gullans and Verbalis, 1993). Hyponatremia is treated with isotonic supplementation delivered orally in mild cases and intravenously in severe cases (Sterns et al., 2013).

1.3.2 Hyperosmolarity and diabetic vascular injury

The plasma osmolarity of patients suffering from diabetes is elevated by increased blood glucose, which is thought to negatively impact vascular cells, alongside the effects of the diabetic hyperglycemia (Lorenzi et al., 1986). It is not just chronic plasma osmolarity that can damage but also acute hyperglycemic/ hyperosmotic episodes such as the hyperosmolar hyperglycemic state (HHS) (Umpierrez et al., 1996).

The diagnostic criteria for diabetic HHS are as follows: a plasma glucose concentration of >30 mmol/l and effective serum osmolarity >320mosmol/kg (Wolfsdorf et al., 2014). HHS is sometimes referred to as hyperosmolar non-ketotic state and is a condition common in type 2 DM sufferers and is a medical emergency as there can be an immediate threat to life (Delaney et al., 2000). Serum glucose in excess of 30 mmol/L would usually lead to the production of ketones within a patient with type one diabetes (Chiasson et al., 2003). This is because a lack of insulin (the major biochemical hallmark of the condition) in the presence of hyperglycaemia will result in ketogenesis (this can be seen in serum glucose concentrations of >10 mmol/L) (Gosmanov et al., 2014). It is therefore important to differentiate between the diabetic ketogenesis present in patients with uncontrolled type 1 diabetes and HHS which is a condition seen in patients with uncontrolled type 2 diabetes. Because type 2 diabetic patients produce sufficient insulin there would not necessarily be a marked increase in the production of ketones because the level of insulin would not be low enough to lead to ketogenesis (Willix et al., 2019). Because some patients with type 2 diabetes do develop a reduction of insulin production, it is possible for a patient with type 2 diabetes to develop HHS and manifest ketosis although this is not the usual aetiology of the condition (Kim et al., 2016).

It is clear then that acute hyperosmolarity is a well-documented complication of diabetes although it is not just the acute condition that is capable of causing damage, and the prolonged hyperglycaemia is capable of causing vascular injury in DM (Wachtel et al., 1991). It has also been identified that hyperosmolarity can affect the contraction and volume reduction of cardiac myocytes in streptozotocin-induced diabetic rats; this indicates that the hyperosmotic state produced by diabetic HG is capable of producing pathological changes in experimental diabetic conditions (Howarth et al., 2002). It is worth noting that there is some debate as to the usefulness of streptozoticin in rat models as the drug destroys both the α & β cells of the pancreas as well as being hepatotoxic (Goyal et al., 2016).

Therefore, it has been suggested that the data generated within these studies may not be good predictors of what occurs in the human clinical condition, although the technique remains a popular way to induce a "diabetes-like" state for the purposes of drug screening and other preliminary work (Yau et al., 2018). The acute HSS condition can contribute to diabetic vascular injury and reduce endothelial integrity if the hyperosmolarity is remedied the damage would still be done to the vascular cells increasing the risk of atheroma and cardiovascular disease (Pinhas-Hamiel and Zeitler, 2007). Therefore the immediate treatment goal for HHS is the normalization of plasma glucose and osmolarity in order to minimize the damage caused to vulnerable tissues such as the retina and kidney (Pasquel and Umpierrez, 2014).

Diabetic hyperosmolarity has also been shown to delay the vasoconstriction response to noradrenaline via latent endothelial cell signalling responses (Fortes et al., 1984). Changes in extracellular osmolarity have also been shown to increase the activity of Ca^{2+} permeable channels such as the TRPV 1,2&4 (Strotmann et al., 2000). In diabetes, hyperosmolarity is not just caused by the increased concentration of plasma glucose alone but also through hyperglycemia-induced osmotic diuresis, where the elevated glucose leads to the increase of sodium and may lead to excessive cellular dehydration (particularly within the vascular compartment) (Roscoe et al., 1975)

1.4 Hyperglycaemia and Ca^{2+} homeostasis

Calcium functions as a messenger molecule and plays an essential role in metabolism and cell signalling (Fig. 1.3). For example, Ca^{2+} is one essential component of the generation of neurological signals and the synchronisation of neuronal cell impulses (Gutierrez et al., 2009). One such example of the role of Ca^{2+} within neuronal cells is the use of Ca^{2+} as a secondary messenger molecule to propagate a signal across synaptic ribbons, this is done through the Cav1.3 subgroup of voltage-gated Ca^{2+} channels (Brandt et al., 2005). Ca^{2+} is also an important messenger molecule at the neuromuscular junction as it is responsible for the transfer of the signal from neuronal cells to muscular cells (Van der Kloot, 1978). Ca^{2+} is also an essential molecule within the coagulation cascade as it is required as it is essential in combining the FXa and FX1a complexes to allow for the formation of thrombin which will lead to fibrinogen formation and ultimately to haemostasis being achieved (Artim-Esen et al., 2017, Mikaelsson, 1991).

Ca^{2+} is not merely a potent and essential secondary messenger molecule but it is also essential as an intracellular messenger, for example, Ca^{2+} is one of the molecules that is known to modulate apoptosis (Li et al., 2018, Klarić et al., 2012). Ca^{2+} overload is capable of "tipping the balance" of pro-apoptotic (BCL-2- BAX) and anti-apoptotic proteins leading to a signalling cascade that triggers controlled cell death (Basset et al., 2006). It is for this reason that it is hypothesised that calcium overload in neuronal cells may be one of the causative factors in some neurodegenerative medical conditions (Rosenstock et al., 2004, Arundine and Tymianski, 2003). Ca^{2+} is an intracellular messaging molecule that influences both ATP production and whole-cell bioenergetics through the uptake of cytosolic Ca^{2+} into the mitochondria (Jouaville et al., 1999)&(Adinolfi et al., 2005). This can lead to an increase in mitochondrial Reactive Oxygen Species (ROS) production which when combined with a pathological condition such as Ca^{2+} overload can lead to cell death (Wagner et al., 2011) & (Peng and Jou, 2010).

It has been well established that ROS can contribute to the endothelial dysfunction caused by hyperglycaemia in DM (Callaghan et al., 2005). It has also been shown that ROS causes endothelial dysfunction by interfering with Ca^{2+} signalling (Elliott and Koliwad, 1995). Ca^{2+} signalling has been shown to be altered in patients suffering from non-insulin controlled diabetes (Nagasaka et al., 1995). Hyperglycaemia has been shown to alter Ca^{2+} homeostasis in multiple ways including intracellular Ca^{2+} compartmentalisation in cardiomyocytes (Clark et al., 2003).

As well as alterations described at the cellular level it has also been established that there is a net loss of free serum Ca^{2+} within the hyperglycaemic condition (Sundararaghavan et al., 2017). Research has found that diabetic patients do suffer from a reduction of serum Ca^{2+} which contributes to an increased risk of bone formation disorders, including osteoporosis (Jackuliak and Payer, 2014). This loss of Ca^{2+} is not thought to arise from the malabsorption of Ca^{2+} but rather an increase in urinary excretion due to chronic elevation in active parathyroid hormone (Nagasaka et al., 1995). This alteration to Ca^{2+} homeostasis at a whole-body level is also reflected at a cellular level, for example, the intracellular Ca^{2+} concentration of neuronal cells was impaired in hyperglycaemic conditions during reperfusion following ischaemia (Araki et al., 1992).

Because both hyperglycaemia and the concomitant increase in intracellular ROS are capable of altering cellular Ca^{2+} homeostasis it is prudent to explore the role of cytosolic Ca^{2+} signalling in more detail. Work performed in our laboratory by (Daskoulidou et al., 2015) has demonstrated that Store-operated Ca^{2+} entry is altered (increased) in endothelial cells that are exposed to hyperglycaemic conditions. This alteration was thought to be caused by an increased expression of the Orai channels, key in generating the Store-operated Ca^{2+} entry, therefore, suggesting that an increase in intracellular Ca^{2+} concentration may be one of the contributing factors to diabetic endothelial dysfunction. This was also reflected in the direct activation of a SOCE-like current within EA,hy926 cells when exposed to a transient hyperglycaemic condition as measure by “patch-clamp” electrophysiology (Daskoulidou et al, 2015).

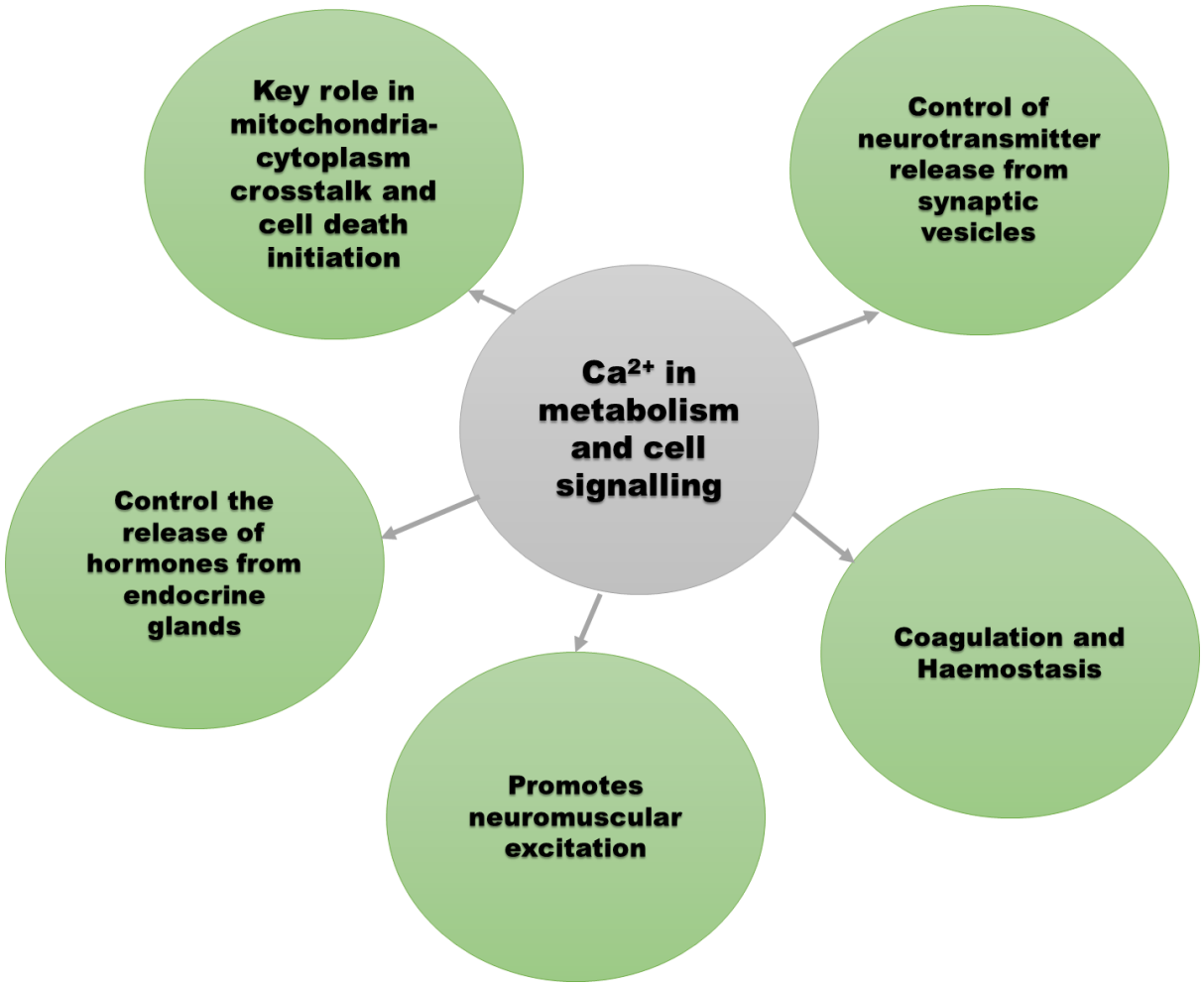

Fig. 1.3 Major functions of Ca^{2+} in a mammalian cell

1.5 Ca^{2+} and cellular function

In the blood plasma, the concentration of free ionized Ca^{2+} is regulated to within a small physiological range between 1.3 and 1.5 mmol/L, this concentration is approximately half of the total plasma calcium concentration usually ranging between 2 and 2.6 mmol/L. (Wang et al., 2018) & (Pan et al., 2014). Ca^{2+} is sometimes known as the life-giving and life-sustaining signalling molecule, due to its role in reproduction (sperm motility and ovum fertilization) as well as its role in key excitable cells (neurons, and skeletal muscle) (McCalley et al., 2014), (Rahman et al., 2014) (Bernhardt et al., 2018). Ca^{2+} is not just a "life-giving" molecule due to its role in early fertilisation but Ca^{2+} transport is also key the development in the development in the foetal skeleton as it must be transported from the maternal placenta to the foetus, this process is mediated by the calcium-sensing receptor (CaSR) (Ellinger, 2016).

Ca^{2+} plays a vital role in the initiation of apoptosis during cellular and extracellular stress (Mattson and Chan, 2003). Apoptosis is the process of controlled cell death which minimises the occurrence of collateral damage at the tissue level (Han et al., 2018). Apoptosis is a morphologically distinct mechanism of cell death that can occur as both to control normal cellular populations within tissues and as a response to infection or damage as triggered by the immune system (Pollack et al., 2002). Apoptosis initiation can differ by cell type with some cells expressing receptors such as tumour necrosis factor (TNF) which must bind with a ligand to initiate apoptosis (Chau et al., 2004). Whereas other cells have an apoptosis pathway that must be blocked by a survival factor (e.g. hormone and growth factors) in order to initiate apoptosis (Kalimuthu and Se-Kwon, 2013). The morphological features of apoptosis are well known, for example, cells undergoing apoptosis will shrink and undergo pyknosis visible under light microscopy (Van Cruchten and Van den Broeck, 2002).

This is in stark contrast to an uncontrolled form of cell death, necrosis, which leads to the release of many pro-inflammatory cytokines and can cause significant collateral damage to healthy cells (Rock and Kono, 2008). Whether a cell undergoes controlled (apoptotic) or uncontrolled (necrotic) cell death is largely dependent upon the stimulus causing cell death (e.g. genomic damage vs thermal cell destruction) (Fink and Cookson, 2005). Initiation of apoptosis can be caused by an influx of calcium into the cell via plasma membrane channels, causing the mitochondria to take up Ca^{2+} thereby causing the release of cytochrome (Stojanovic et al., 2005).

Cytochrome C release triggers the Inositol trisphosphate (IP3) receptor at the Endoplasmic Reticulum (ER). This leads to store depletion of ER Ca^{2+} stores and increasing cytosolic Ca^{2+} concentration, leading to further cytochrome c release from the mitochondria and formation of the apoptosome (Mattson and Chan, 2003). A more recent discovery into the role that Ca^{2+} plays in cell death is the interplay between the "guardian of the genome" p53, a tumour suppressor and the flux of Ca^{2+} between the endoplasmic reticulum (ER) and the mitochondria (Bittremieux and Bultynck, 2015). It was found that p53 localises within the ER under stress conditions and causes an increase in the level of cytoplasmic Ca^{2+} via modulation of the Sarco/ER Ca^{2+}-ATPase (SERCA) pump activity.

This interplay between intracellular calcium and the tumour suppressor p53 has expanded the understanding of the importance of Ca^{2+} in the development of cancer as demonstrated in (Giorgi et al., 2015). Ca^{2+} channel expression and activity has been suggested as another marker and potential target within oncology. For example, Transient receptor cation channel vanilloid 6 (TRPV6) is overexpressed within some breast cancer tissue samples and it has been hypothesised that inhibition of these channels may provide a novel treatment for oestrogen receptor-negative breast cancer patients (Weber et al., 2016).

It is well established that the dysregulation of Ca^{2+} influx is capable of causing a disease state such as Alzheimer's disease (Demuro et al., 2005). It has been reported that intracellular neuronal Ca^{2+} concentration is elevated when the neurons are in close proximity to amyloid deposits (Arbel-Ornath et al., 2017). These alterations in Ca^{2+} homeostasis within Alzheimer's disease are not merely transient as it has been found that essential calcium-binding/regulating proteins calmodulin and calcineurin activity is altered in a way that may lead a loss in neuronal plasticity and ultimately to a loss of memory (Xia and Storm, 2005) (Caillard et al., 2000). This supports earlier work that has found that some changes in Ca^{2+} homeostasis within neuronal cells are age-dependent and this may be a contributing factor in age-related neuronal degeneration and memory loss (Oh et al., 2013).

1.5.1 Ca^{2+} efflux and influx

Ca^{2+} can enter the cell through diverse Ca^{2+} channels including through voltage-gated, store-operated, receptor-operated and stretch-activated channels. In excitable cells, such as skeletal muscle and cardiomyocytes, the voltage-gated Ca^{2+} channels, such as L-type Ca^{2+} channels, provide a key pathway for Ca^{2+} to enter the cells (Helton et al., 2005). It has been shown that the initiation of a store-operated Ca^{2+} current can inhibit the activity of L-type voltage-gated channels. This appears to be achieved by preventing depolarisation via the voltage-gated channels through the non-selective binding of the stromal interaction molecule with the L type channels (Park et al., 2010). The major Ca^{2+} entry pathway in non-excitable cells is the store-operated channels in this pathway; the release (depletion) of intracellular Ca^{2+} stores leads to the activation of channels in the plasma membrane. This Ca^{2+} influx, also called store-operated Ca^{2+} entry, or previously known as capacitive Ca^{2+} entry (Venkatachalam et al., 2002, Petersen and Berridge, 1996).

First experimental evidence for the existence of this pathway was the electrophysiological recordings of the calcium release-activated calcium current in mast cells and T cells (Prakriya and Lewis, 2003). Voltage-gated Ca^{2+} channels are expressed within the plasma membrane of excitable cells (cells that form part of an electrochemical circuit, for example, neuronal cells and muscle cells). At physiological resting potential (without excitation) voltage-gated Ca^{2+} channels are closed, they should only open when the cell becomes de-polarised (for example during a nervous impulse); it is because of this electrical potential activation that these channels are termed "voltage-gated" (Calderon-Rivera et al., 2015).

Upon activation, the voltage-gated channels allow for the influx of Ca^{2+} into the cytoplasm of the cell (Gomez-Ospina et al., 2006); this influx can go on to lead to contraction of the cell (in the example of skeletal muscle) as well as allowing for the activation of other PM ion channels, such as K^+ channels (DAVILA, 1999). Formally the voltage-gated channels were termed according to their characteristic activity (for example L-type calcium channel which was so-called because the current generated by the channel was long-lasting) (Koschak et al., 2001). Although in the year 2000 a new nomenclature was suggested that would better classify the voltage-gated channels according to their molecular structure, this would become the Cav system of naming (Ertel et al., 2000). The voltage-gated Ca^{2+} are responsible for some cellular and physiological processes. For example, the activity of the $Ca_{v1.1}$ channel is linked to gene regulation and cellular secretion, as seen in a study which showed that insulin secretion was impeded by Ca_{v1} suppression (Schulla et al., 2003). This is not the only important role that voltage-gated Ca^{2+} channels play in human physiology: for example, the $Ca_{v2.2}$ subfamily is required for the normal function of mammalian sensory neurons (Chai et al., 2017).

Voltage-gated Ca^{2+} channels are characterised by their "speed of reactivity" as compared with other forms of Ca^{2+} influx (Armstrong and Hille, 1998). Receptor-mediated Ca^{2+} is a term used to describe the entry of Ca^{2+} into cells following the activation of a plasma membrane receptor that in turn increases the level of Ca^{2+} being transported into the cell (Rink, 1990). One of the significant channel types that can be responsible for calcium entry is the transient receptor potential channels (TRP) which are a family of non-selective cation channels that serve many functions (Clapham et al., 2001). TRP channels mediate the flux of cation channels down the electrochemical gradient, leading to an increase of intracellular [Ca^{2+}] and TRP channels play a significant role in both excitable and non-excitable cells (Ramsey et al., 2006). TRP channels have been implicated in endothelial dysfunction with TRPC4 dysfunction being implicated in the compromise of the endothelial barrier function; as well as other subtypes contributing to overall endothelial dysfunction (Kwan et al., 2007).

Transient receptor potential (TRP) channels are a good example of receptor-mediated Ca^{2+} influx resulting from activation of receptors (Clapham, 2007). The TRPC (canonical) family of channels are known to be activated by phospholipase C as well as some variants being sensitive to diacylglycerol produced within the cell (Venkatachalam et al., 2003). Although the TRPC family is not ubiquitous in function and structure, some variants have been known to be activated through alternative pathways. For example, TRPC5 has been shown to be activated by the extracellular redox protein thioredoxin (Xu et al., 2008). It has also been shown that β-catenin activates TRPC6 expressing podocytes, and this may be linked to cellular damage associated with the high glucose condition (Li et al., 2013).

The TRPC1 variant within this class of channel proteins has been shown to not just be activated via the usual receptor-ligand mechanism, it has been shown that this channel can be activated by stretching the plasma membrane (Maroto et al., 2005). Receptor-mediated Ca^{+2} entry as mediated by the TRPC family of channels is commonly observed within neuronal tissue, specifically within the corticolimbic parts of the brain such as the prefrontal cortex (Fowler et al., 2007). One TRP channel subtype that has been found to contribute to the diabetic pathological state is the TRPM7 subtype as reported by Huang et al (2018). Their work demonstrated that this channel plays a role in the ER stress response under hyperglycaemic conditions, which leads to neuronal cell apoptosis. It is not just the action of TRP channels having a direct effect on cellular viability and apoptosis that is of interest but also the interactions that TRP subtypes have with other Ca^{2+} channels. Especially the contribution of the TRPC1 subtype to SOCE through both its ability to be activated by STIM and its subsequent ability to contribute to the Ca^{2+} influx generated by Orai1 in the event of ER Ca^{2+} store depletion (Ambudkar et al., 2017) & (Kim et al., 2009). This interaction is an important discovery into how the SOCE comes about.

Ca^{2+} influx is but one element of calcium transport, calcium efflux makes up the second half of the dynamic. Ca^{2+} efflux is the term used to describe the transportation of Ca^{2+} from within the cell to the extracellular space or the release of Ca^{2+} from the endoplasmic reticulum (ER) into the intracellular fluid (Johny et al., 2017). One receptor responsible for triggering such a release from the ER is the Ryanodine receptors which when activated move calcium from the lumen of the endoplasmic reticulum into the cytosolic space, this is essential in the contraction of skeletal muscle cells (Marx et al., 1998). Ryanodine receptors have also been found to play a significant role in the initiation of store-operated Ca^{2+} entry (Uehara et al., 2002).

As can be seen in the previous sections Ca^{2+} signalling is responsible for the normal function of many cell types and physiological processes, for example in the contraction of skeletal muscle (Robison et al., 2017). But Ca^{2+} is not only responsible for the mediation of signals during normal physiological stress conditions, as it is a key messaging molecule in the initiation of cell death (Selvaraj et al., 2016). Many stimuli are capable of causing cellular stress and even death, for example, hypoxia is capable of initiating apoptosis as well as necrosis within the cells of the peripheral vascular system (Michiels, 2004). Metabolic dysregulation, including in the hypoxic state, does not just lead to an alteration in the calcium dynamics of cells, it also leads to the production of reactive oxygen species (ROS) which in themselves are potent messenger molecules capable of producing a wide range of cellular effects from death to vasodilation (Chidgey et al., 2016, Schenk and Fulda, 2015).

1.5.2 Reactive oxygen species in health and disease

Reactive oxygen species are chemically reactive molecules that have the ability to reduce (donate electrons) to other compounds due to the presence of a free oxygen electron (Wang et al., 2004). Examples of common ROS include:

- Superoxide
- Peroxide
- Hydroxyl radicals
- Nitric oxide

These ROS are produced as a natural by-product of cellular metabolism, due to the use of oxygen as a terminal electron acceptor within the electron transport chain (Scialò et al., 2017). Of course when under metabolic stress, for example, hyperglycaemia or hypoxia, the production of ROS is greatly increased and this, in turn, can alter the physiological condition of the cell (Lambros and Plafker, 2016). ROS are even capable of introducing deleterious mutations to nuclear Deoxyribonucleic acid (DNA) (Trifunovic et al., 2005)

ROS produced via mitochondrial metabolism such as this are known as "mitochondrial ROS" and although they are a major source of intracellular (endogenous) ROS there are several other intracellular sources that are important to mention (Engelmann et al., 2005). The mitochondria produce ROS from the electron transport chain, which is found within the inner membrane of the mitochondria (Kühlbrandt, 2015), the ROS produced ar a result of the oxidative phosphorylation pathway (Takamura et al., 2008).

The primary ROS species generated under this mechanism is superoxide (O^-) which results from the partial chemical reduction of O_2 by "leaked" electrons from complexes I & III of the electron transport chain (Zhao et al., 2019). This Superoxide can the go on to be dismutated by superoxide dismutases 1 & 2 (SOD 2 is specific to the mitochondrial matrix) to form hydrogen peroxide, and it is these two ROS species (O^- and H_2O_2) that are considered the "mitochondrial ROS" (Suthammarak et al., 2013).

When the rate of electron entry into the respiratory chain is mismatched with the rate of electron transport through the electron transport chain there is an increase in ROS generation (Jin and Bethke, 2002). This mismatch can be caused by a number of stimuli, including hypoxia and cellular stress (Guzy et al., 2005). Interestingly the hydrogen peroxide produced by the dismutation of superoxide by SOD is not considered a "radical" but rather a stable reactive oxygen species (Wu et al., 1996). Incidental H_2O_2 generation can be mitigated with the action of catalase breaking down the hydrogen peroxide into O_2 and H_2O although this process cannot buffer all of the H_2O_2 produced under cellular stress (Collin, 2019). This H_2O_2 in the presence of metal ions (Fe^{2+}) can be catalysed into hydroxyl radicals, which are a particularly reactive and potentially damaging form of ROS (Zhao, 2019).

The electron transport chain is not the sole source of free radical generation within the mitochondria, evidence has suggested that the commonly membrane-bound NAPDH oxidase (NOX) proteins may also be able to localise within the mitochondria (Kuroda et al., 2010). NAPDH Oxidase 4 (NOX 4) is a member of the NOX family that is known to be localised within the mitochondria (Graham et al., 2010). This Protein can generate superoxide, independent of the electron transport chain and has been shown to have its activity regulated by an ATP binding motif on the NOX 4 protein (Shanmugasundaram et al., 2017). The superoxide generation by this NOX 4 protein contributes to the overall ROS generation of the mitochondria; and has been found to have increased localisation and activity in some disease states, for example, the activity of NOX 4 in the mitochondria is elevated in aortic fibrosis (Canugovi et al., 2019). NOX 4 localisation within the mitochondria is also increased within the kidney tissues of a diabetic mouse model, indicating that there is a potential for increased oxidative stress placed upon the cell, not just through the alteration in bioenergetics associated with the condition but also by the

activity of the NOX 4 protein(Block et al., 2009). Finally, this increase in mitochondrially localised NOX 4 activity has been shown to be increased by the process of ageing- potentially helping to understand the process of how our cells adapt and change as a result of age (Vendrov et al., 2015). It is clear then that mitochondrial ROS production is not a simple process of a simple "electron leak" but rather is influenced by the action of several complex interactions and processes that lead to the generation of total mitochondrial ROS.

ROS production in health and disease is a major area of research as there are many disease states that have been associated with alterations in ROS production. One example of this is the research of the role of ROS in oncogenesis and cancer progression (Ogrunc et al., 2014) It has been found that ROS can play a role in the development of cancer via DNA damage caused by excessive ROS (Ma et al., 2018). Interestingly ROS generation is not always identified as a causative or proliferative factor in cancer cells but has also been identified a playing an important role in tumour suppression and in preventing the proliferation of some cancer cells (Tong et al., 2015). A contemporary research topic highlighting the importance of ROS in disease is in the recent findings that mitochondrial ROS production is elevated in cells infected by the Severe Acute Respiratory Syndrome Coronavirus-2 (SARS-CoV-2/ COVID-19).

It appears that cells infected with the virus become highly glycolytic, increasing the production of Hypoxia-inducible factor 1 alpha (HIF-1α) which can alter monocyte metabolism and inhibit the T-cell immune response (Cavounidis and Mann, 2020). This demonstrates that ROS production and functionality is a complex area with potential therapeutic benefits that impact some of the most important diseases within the modern era.

The mechanism by which one of the other major sources of intracellular ROS is the peroxisome, a metabolically active organelle which is a known source of several ROS including hydroxyl and superoxide radicals (del Río and López-Huertas, 2016). The peroxisome is a membrane-bound organelle found in the cytoplasm of the majority of eukaryotic cells, its primary function is in the breaking down of long-chain fatty acids through beta-oxidation (Wanders et al., 2016).

This oxidation is dependent upon the peroxisome's ability to produce ROS (H_2O_2) and this beta-oxidation of fatty acids is an essential step in the generation of cellular energy from long-chain fatty acids (Herzog et al., 2018). The H_2O_2 is generated by peroxisomes primarily through the action of peroxidases which transfer hydrogen from cellular metabolites to molecular Oxygen (Lismont et al., 2019). The generation of ROS is not the only major function of peroxisomes, they also play an essential role in the scavenging ROS to prevent oxidative stress (Bonekamp et al., 2009).

This antioxidant functionality is achieved by a number of antioxidant enzymes which includes catalase and superoxide dismutase (SOD) (Al-Qabandi et al., 2012). The antioxidant function is thought to be not just a negative feedback mechanism in opposition to the generation of H_2O_2 by the peroxisome but also as a potential cellular defence from other sources of oxidative stress (Bonekamp et al., 2009). The peroxisome has been identified as a key organelle in some important processes, for example, it has been found that the proliferation of peroxisomes is associated with an increase in apoptotic cell death (Roberts et al., 1998). This may be one of the reasons why abnormalities in peroxisome activity have been associated with some age-related conditions within humans (Terlecky et al., 2006). Of interest to this body of work is the research that has revealed that the catalase activity of peroxisomes is inhibited in diabetic mouse models, perhaps suggesting a role in the increased oxidative stress seen in DM (Walton and Pizzitelli, 2012).

Another source of extramitochondrial ROS is seen in the endoplasmic reticulum itself, this complex network is responsible for the packaging and production of cellular proteins as well as being responsive to cellular stress conditions through communication/crosstalk with the mitochondria (Zeeshan et al., 2016). One way that the ER is known to be a producer of ROS is through oxidative protein folding and formation of disulphide bonds via the action of the enzyme protein disulphide isomerase, which is estimated to be responsible for over 25% of ER generated ROS (Cao and Kaufman, 2014).

The ROS generated within the ER have a great potential to affect numerous cellular mechanisms, due to the role of the ER as a central protein folding apparatus, under conditions of oxidative stress, the ER ROS can lead to alterations in protein oxidation and structure which in turn alter the activity of those proteins (England et al., 2006).

It is clear that the generation of intracellular ROS is not just the purview of the mitochondrion but rather is also contributed to by other major cellular organelles. So far, though, only sources of endogenous ROS have been discussed (ROS generated by the cells own internal mechanisms) but exogenous ROS are also a potential major contributor to oxidative stress (Phaniendra et al., 2015). Exogenous ROS often arise from an external change in environment that causes an increase in ROS production due to the stress placed upon cells (ROS). Some of these sources include environmental pollutants as well as tobacco smoke and heavy metals. These stimuli (apart from in the case of some environmental pollutants) do not involve the direct intake of ROS but involve the reaction of cells to the change in producing ROS (Pizzino et al., 2017). One source of exogenous ROS that can directly produce ROS within the body without being dependent on cellular metabolism is ionizing radiation, whereby radiolysis of water molecules can produce several ROS including hydroxyl and superoxide radicals (Leach et al., 2001).

The production of ROS, whether through endogenous or exogenous means is both essential for normal physiological function but if the level of ROS grows too high without abatement from scavengers then what is essential can become detrimental and harmful at not just the cellular level but also at the whole-body level (Poljsak et al., 2013). It is for this reason that antioxidants are often explored as potential protective/preventative agents to the oxidative damage caused by increased ROS levels (Kefer et al., 2009).

1.5.3 Reactive oxygen species and store-operated calcium entry

DM can produce increased oxidative stress within several cell types, for example, it has been shown that vascular endothelial cells produce more ROS under experimentally induced diabetic conditions (Shaw et al., 2014) (Lee et al., 2003). It has also been shown by (Zhang et al., 2015) that hyperglycaemia, at levels expected with poorly controlled diabetes, was capable of significantly increasing the concentration of intracellular ROS within hippocampal neurons.

It is not unreasonable to postulate that the hyperosmolarity associated with HG could be driving some of the oxidative stress within vascular endothelial cells (Nedeljkovic et al., 2003). Research that has been performed on the relationship between ROS and the activity of SOCE proteins as it may mechanistically link any relationship between disease states such as hyperglycaemia and change in SOCE channel activity (Niemeyer, 2017). It has been established that SOCE can be initiated (independent of ER Ca^{2+} depletion) by H_2O_2 as described in Hawkins et al (Hawkins et al., 2010). In this paper, it was suggested that oxidative stress alters the thiol groups of cysteines within the EF-hand of STIM proteins resulting in S-glutathionylation the EF-hand. This mimics the effect of ER Ca^{2+} depletion leading to STIM oligomerization and the generation of the SOCE influx (Hawkins et al., 2010) (Grupe et al., 2010, Tornquist et al., 1999).

1.6 Store-operated Ca^{2+} entry

For a long time, the molecular basis of store-operated Ca^{2+} entry that was responsible for producing the typical calcium release-activated current (CRAC) was unknown until genetic screening in Drosophila and HeLa cells identified two proteins that were essential to this pathway (Feske et al., 2006). These were the stromal interaction molecules (STIM1-2), responsible for sensing depleted intracellular Ca^{2+} stores at the endoplasmic reticulum (Liou et al., 2005). The next significant discovery was the Orai proteins, which are responsible for the formation of store-operated channels. Orai is named after heaven's gatekeeper in Greek mythology and the Orai1-3 subtypes were known as CRACM1-3 (Vig et al., 2006).

Earlier studies in SOCE were performed on immune cells, such as mast cells and Jurkat T or rat basophilic leukaemia cells (Yeromin et al., 2006). It is now known that SOCE is a necessary component in T-cell activation (Smith-Garvin et al., 2009). The Orai1 channel mutation associated with one hereditary form of severe combined immunodeficiency syndrome (SCIDS) that lead to the discovery of the Orai1 protein and its role as a CRAC pore-forming unit (Thompson et al., 2009). Three homologs of the Orai protein have been identified (Orai 1, Orai 2 & Orai 3) using genetic and proteomic analysis and differences in their actions have also been discovered (Yuan et al., 2009), (Mercer et al., 2006). Although the majority of the early research into these channels was performed in Drosophila the scientific community is now beginning to understand the significant role that these SOCE proteins have to play in various human cells. This includes the important discovery of the ICRAC in immune cell activation and as well as this the channels have been found to play an essential role in the function of this in vascular endothelial cells and smooth muscle cells (Potier et al., 2009).

Although the main molecular components required for SOCE have been discovered for just over a decade the complex interactions that STIM & Orai have with other proteins have only recently been elucidated. For example, there have been recent discoveries of a co-localised protein molecule, called STIMATE, that has a role in STIM activation, allowing for STIM oligomerisation and endoplasmic reticulum structural re-arrangement to facilitate SOCE (Hooper & Soboloff, 2015).

The discovery of the SOCE Apparatus (STIM & Orai) not only filled an essential gap in our knowledge as to the proteins responsible for the control of Ca^{2+} store filling, but it also opened up new areas of research into the interaction between these proteins and other Ca^{2+} channels (Badou et al., 2013). One such example is in the relationship between $Ca_{V1.2}$ (L-type) voltage-gated Ca^{2+} channel protein and STIM, where two separate studies have found that where STIM is overexpressed the activity of the $Ca_{V1.2}$ channel is decreased and where STIM expression has been reduced the intensity of the $Ca_{V1.2}$ current is increased (Park et al., 2010). These findings have led to the hypothesis that STIM is capable of initiating SOCE in non-excitable cells and inhibiting voltage-gated calcium entry in excitable cells. $Ca_{V1.2}$ is not the only voltage calcium channel that STIM has been found to interact with $Ca_{V3.1}$ (T-type) channel activity has also been shown to be inhibited by STIM in cardiomyocyte cells (Stojanovic et al., 2005). It has been suggested that this inhibitory effect that STIM has on $Ca_{V3.1}$ may be present in order to prevent pathological levels of Ca^{2+} influx, as it has been shown that high levels of cytosolic Ca^{2+} within cardiomyocytes contributes to cardiac arrhythmia (Sedej et al., 2010).

1.6.1 STIM structure and function

It was work performed by Roos et al (2005) that characterized the second essential component of the SOCE system, the CRAC channel activating protein, STIM1. This was achieved by performing genetic knockdown studies in HeLa cells and these identified two proteins that were necessary for ER Ca^{2+} release detection in SOCE, they were STIM1 and STIM2 (Stathopulos et al., 2009). STIM1&2 share 61% sequence homogeneity and are functionally very similar (Roos et al., 2005). Both STIM1&2 have an endoplasmic reticulum (ER) luminal N-terminus with Ca^{2+} sensing EF-hand domain, one transmembrane segment and a cytosolic strand that is capable of binding to and activating Orai channels (Soboloff et al., 2006).

When intracellular Ca^{2+} stores are depleted the luminal STIM1 EF-hand loses Ca^{2+}, this causes the homomerization and the translocation of STIM1 to the plasma membrane following this the ER-PM junctions are formed and STIM punctate or clusters can interact and activate the Orai proteins (Frischauf et al., 2001). STIM1 is the Ca^{2+} sensing component of the SOCE pathway and it is an intracellular protein located in the endoplasmic reticulum, although some studies have seen STIM1 transiently present in the plasma membrane (Carrasco & Meyer, 2011).

Using Ca^{2+} imaging, transfected cells overexpressing the STIM1 protein (with a fluorescent tag) this aggregation response can easily be visualized and the formation of STIM1 clusters at the plasma membrane can be seen and even quantified (Daskoulidou et al., 2015).

Within a normal resting cell that has not undergone Ca^{2+} depletion, STIM1 is evenly distributed throughout the endoplasmic reticulum and it can move along microtubules (Brandman et al., 2007). When Ca^{2+} stores are depleted STIM1 oligomerizes this leads to slower transport along the microtubules but ultimately forms the Puncta located at the ER-PM junctions (Barr et al., 2008). It is the initial di/oligomerization on the luminal side of STIM1 that is the initial process of STIM1 mediated SOCE (Luik et al., 2006).

The ER luminal section of STIM1 contains a canonical and hidden EF-hand followed by a sterile α-motif (SAM) (Stathopulos et al., 2009). The EF-Hand is considered to be the true Ca^{2+} sensing part of the protein as it consists of a helix-loop-helix motif where the negatively charged aspartate and glutamate amino-acids can bind Ca^{2+} providing that the concentration is high enough (stores are full) (Prakriya, 2013a). When Ca^{2+} stores are depleted the EF-SAM area of the STIM1 protein becomes unstable and this allows for the oligomerization of STIM in the response to Ca^{2+} depletion (Hogan et al., 2010). This is how STIM1 acts as a Ca^{2+} sensor in this pathway but the essential part of the protein responsible for activating Orai and rectifying Ca^{2+} depletion is the cytosolic portion of STIM1. A full schematic diagram of the STIM1 protein can be seen in Fig. 1.4.

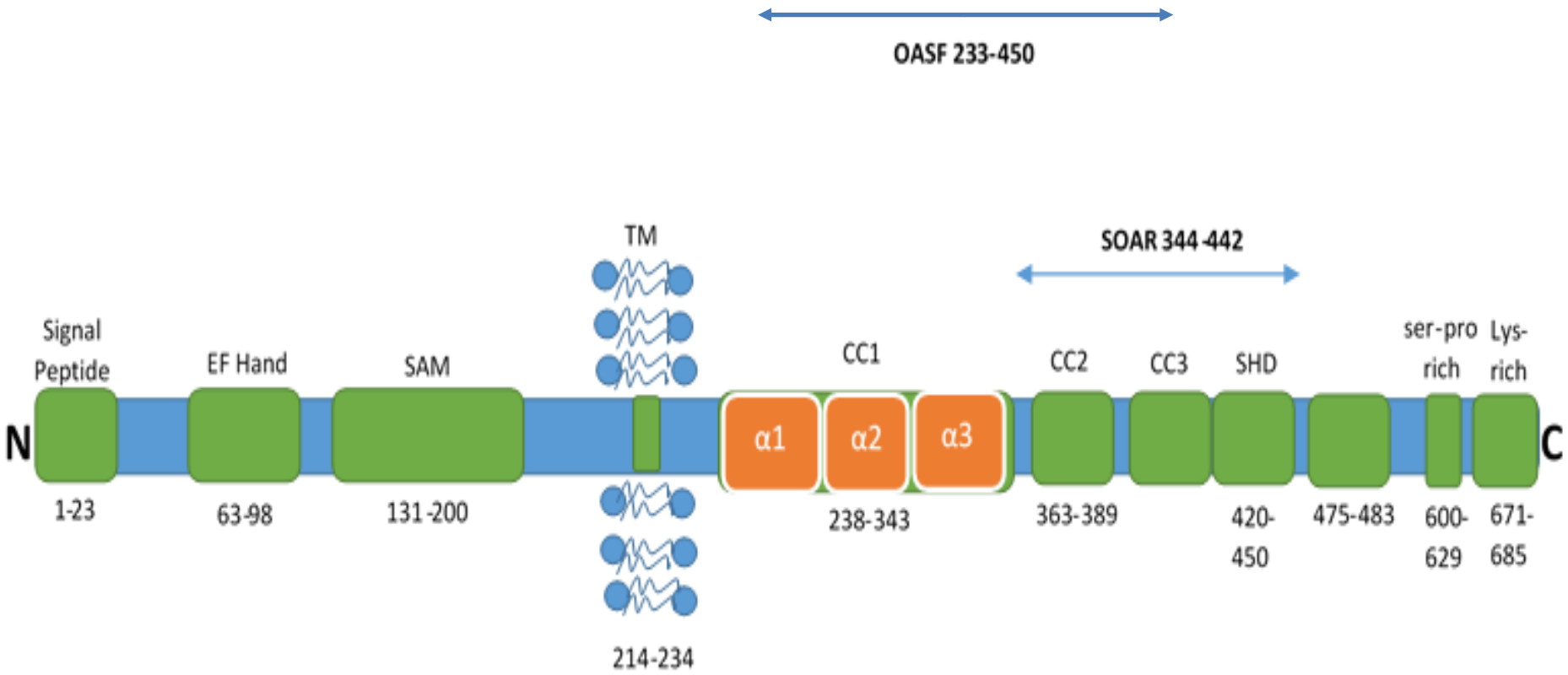

Fig 1.4 Schematic structure of STIM1 protein. The EF and sterile alpha motif (SAM) domains on the ER side of the protein. ER/SAM destabilisation leads to the activation of STIM1 and this allows for the STIM-ORAI cascade to begin SOAR= STIM ORAI activating region. Figure adapted from Rosado et al, 2016

1.6.2 Orai structure and function

There are three subtypes of human Orai protein (Orai 1-3). Each Orai monomer is made up of 4 transmembrane domains, with both the N and C terminals present on the cytosolic side, two extracellular loops, and one intracellular loop connecting the subunits to form the signal Orai hexamer channel (Penna et al., 2008)(Hou et al., 2012). Others have hypothesised that the Orai protein for a hexamer, the same conformation that was identified in Drosophila *sp* via crystallisation studies (Hou et al., 2012). Each CRAC channel is made up of an oligomer of Orai subunits and there can be no CRAC mediated Ca^{2+} entry without the formation of the Orai oligomer, as initiated by the STIM1 protein following Ca^{2+} depletion from ER stores (Prakriya, 2013b). It is assumed that the transmembrane domains of the Orai proteins are the key areas that allow for Orai multimerization. This is because of the cytosolic strands of the protein is still activated and can form the CRAC channel (Cai & Clapham, 2012).

The crystal structure of the Orai channel was published by Hou et al (2012) and this structure revealed that it is the transmembrane 1 helices (TM1) that form the selective Ca^{2+} pore in the centre of the hexamer. Opening of this channel occurs when the 6 TM4 helices conformationally transduce into TM-1 helices to form the outward turned open-pore which is highly selective for Ca^{2+}. This model has been confirmed by the recent publication of the open Orai channel structure (Liu et al., 2019). The published structure of Orai can be seen in Fig. 1.5. Under normal conditions, where Ca^{2+} is not depleted, Orai is distributed throughout the cytosol and it is only upon interaction with STIM-1 puncta with the intact c-terminus of the Orai protein that Orai subunits form the CRAC producing pore at the plasma membrane of the cell (Moccia et al., 2015). Below in Fig.1.5 there is a schematic diagram showing the structure of the Orai 1 protein with important functional areas highlighted (Rosado et al., 2016).

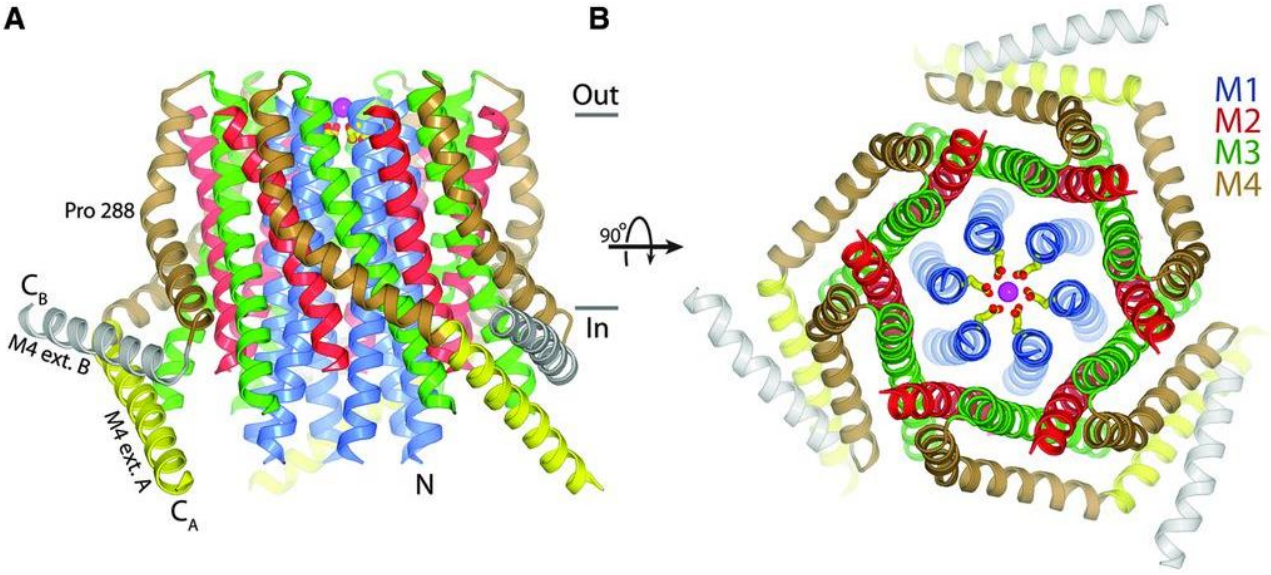

Fig 1.5- Published 3D crystal structure of Orai as presented in Hou et al (2012). A. clearly shows the c terminus of the Orai protein essential in STIM communication B. Shows the 6 TM1 alpha helices that form the selective Ca^{2+} pore as described in Liu et al (2019).

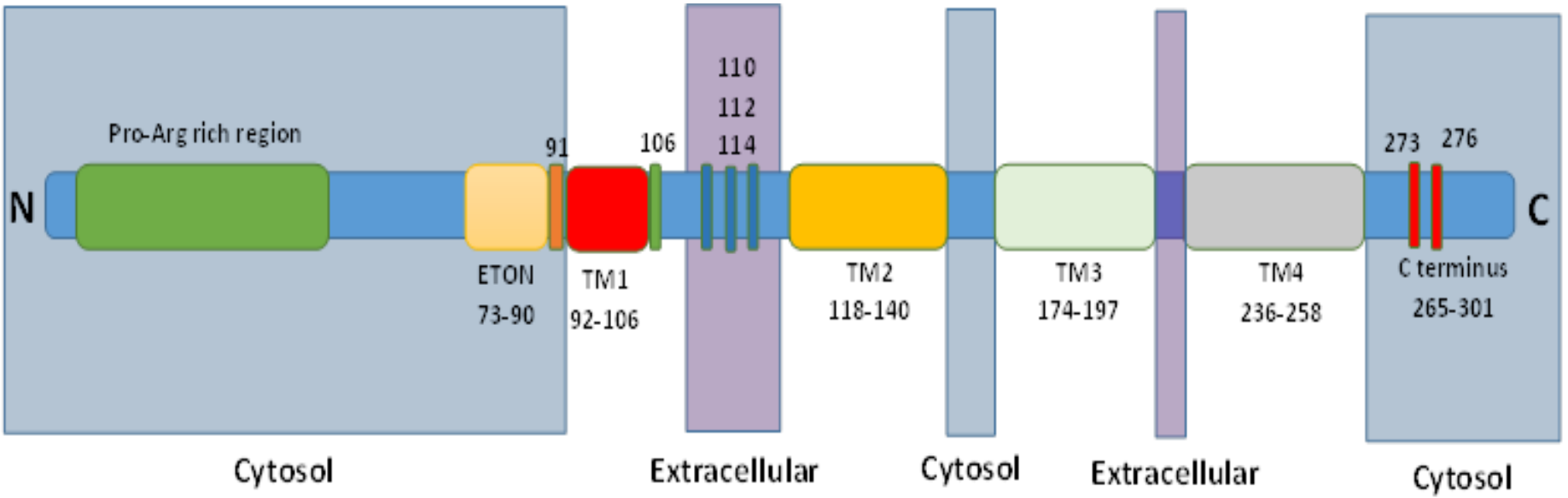

Fig. 1.6 Schematic diagram for Orai 1. The C-terminus strand is important in the interaction between STIM1 and Orai. ETON: Extended membrane Orai N Terminal. Figure adapted from Rosado et al., 2016

1.6.3 Mechanism of Orai channel activation

It is the dissociation of Ca^{2+} from the STIM EF hand-Sterile Alpha Motif (SAM) domain (following ER Ca^{2+} depletion) that leads to the destabilization of STIM1 (Stathopulos et al., 2008). The EF-SAM can be thought of as the Ca^{2+} sensing element of the STIM protein as it is this domain that remains conformationally inert in the presence of full Ca^{2+} ER stores, and once Ca^{2+} dissociates from this element of the STIM protein the EF-SAM hand can become conformationally active (Zheng et al., 2011). That causes the movement and aggregation of STIM proteins along the microfilaments of the endoplasmic reticulum (Barr et al., 2008). Leading to the localisation of STIM towards the plasma membrane, allowing for the formation of STIM puncta; which are the point of STIM aggregation formed between the ER and plasma membrane where Ca^{2+} ions will be entering (Barr et al., 2009). These puncta allow for the interaction STIM with Orai proteins found within the cytosol (Derler et al., 2009). Orai is then reversibly trapped at the plasma membrane by the interaction of the c-terminus of Orai with the STIM1 puncta (Frischauf et al., 2009). This causes the multimerization of the Orai subunits to form the CRAC producing Orai channel and this allows for the store-operated entry of Ca^{2+} into the cell (Várnai et al., 2009) (Fig 1.6). This system is controlled by a negative feedback loop that ensures when Ca^{2+} concentrations are rectified the SOCE can be stopped; this is done by the newly in-fluxed Ca^{2+} causing STIM1 to dissociate from Orai when it reaches normal cytosolic concentrations as Ca^{2+} once again binds to the EF-hand of the STIM1 molecule (Taylor, 2006).

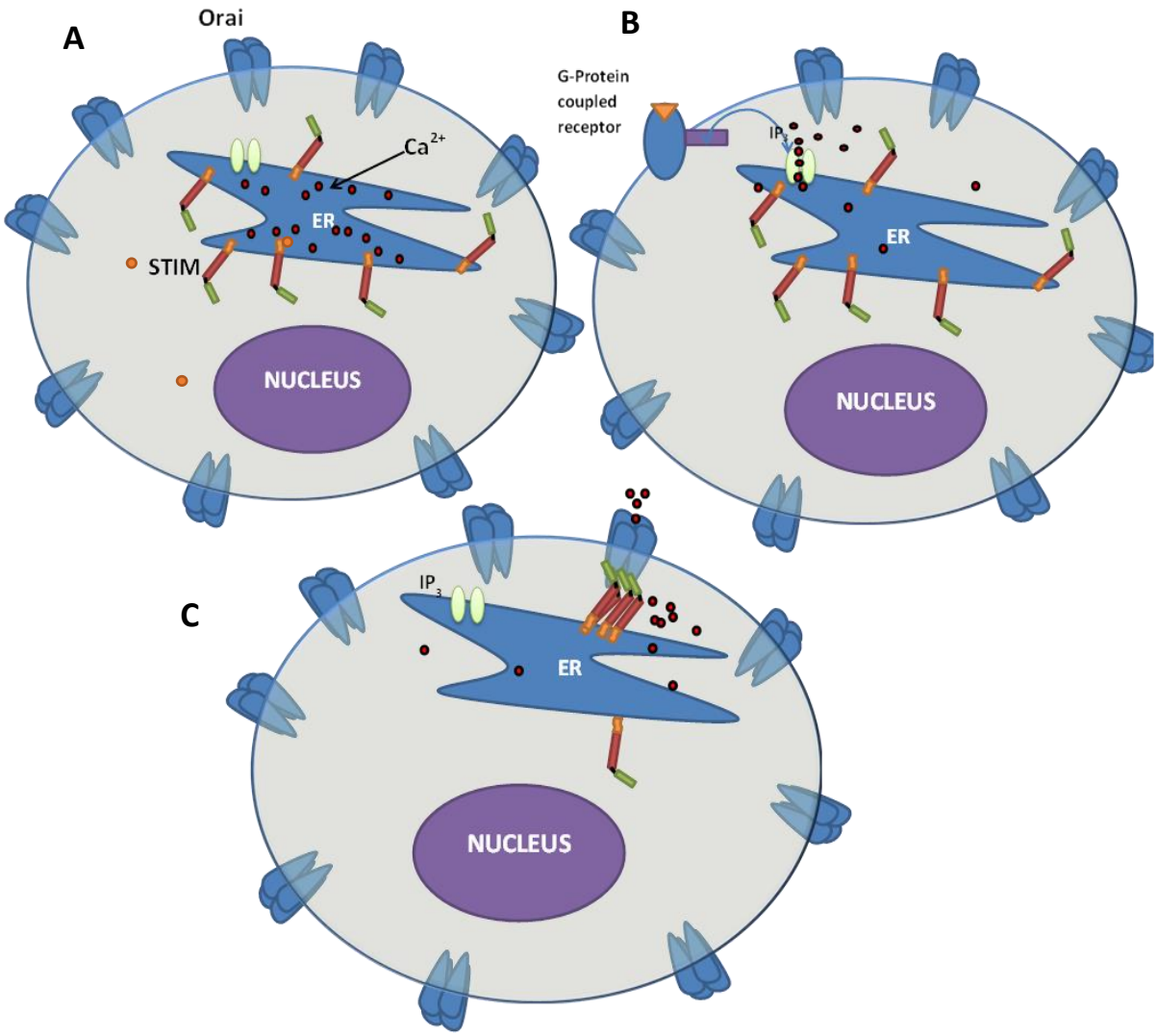

Fig. 1.6 Activation of ORAI channel by STIM1. (A) In a quiescent state, cells contain a level of stored Ca^{2+} (B) Ca^{2+} can be depleted from the ER through cell signalling pathways that utilize G-protein coupled receptors and the ER receptor IP-3. (C) As the ER concentration of Ca^{2+} has fallen Ca^{2+} dissociated from the EF-SAM domain of STIM allowing for the movement of STIM to the plasma membrane and thereby allowing STIM to recruit ORAI subunits so that a CRAC channel can be formed and the Ca^{2+} levels can be restored to normal cytosolic levels. Adapted from Daskoulidou et al (2015).

1.6.4 Pharmacological regulation of Orai/STIM channels

Ca^{2+} is a critical biological ion, responsible for the regulation of many processes within cells, such as the transcription of genes or the regulation of cell death and proliferation. Therefore, the SOCE pathway is of interest to the field of medical science. This is because as we understand how SOCE works there will be new drug targets found that can be used to alter the Ca^{2+} balance of the cell (Bergmeier et al., 2013). A number of pathologies can benefit from better understanding the SOCE pathway for example in some cancers the inositol triphosphate receptor (IP3R) is overexpressed (Lappano and Maggiolini, 2011) and SOCE is elevated and this allows for the abnormal proliferation of the cancer cells. Another pathology that could benefit from better understanding the factors that impact SOCE would be severe combined immunodeficiency syndrome as the SOCE proteins are known to be dysfunctional and are a major contributing factor to this disease state (Feske et al., 2006). By understanding the behaviour and regulation of STIM and Orai new pharmacological targets can be found; leading to the development of drugs that can reduce the hyper-proliferative signals that are found within cancer cells as shown in the TRPC study performed by Jiang et al (2013). There is also an interest of whether SOCE can be targeted as a pathway for immune system modulation because STIM and Orai are responsible for the activation of several immune cell types there is potential for the development of immuno-suppressive or immune-stimulant drugs that target the STIM/Orai system (Panyi et al., 2014).

Any pharmacological intervention targeting the STIM/Orai apparatus would have to consider the impact that the drug would have on different cell types and on the many cellular processes that are controlled by Ca^{2+} (Bogeski et al., 2010a). The presence of STIM/Orai SOCE within vascular endothelial cells and smooth muscle that makes these proteins pharmacologically interesting. Particularly to those seeking to prevent the vascular complications of diabetes (Giachini et al., 2009). It has been shown previously that hyperglycaemic conditions modulate the activity and expression of Orai channels and are capable of upregulating SOCE (Daskoulidou et al., 2015). It is now important that we understand the mechanisms by which hyperglycaemia modulated the activity of STIM and Orai, for example, does the osmotic stress induced by hyperglycaemia activate CRAC and SOCE?

1.7 Aims of the study and hypothesis

Diabetic hyperglycaemia is capable of causing damage to the vasculature so it is important to understand the underlying mechanism of injury. Some TRP channels have been shown to be osmosensitive (Guilak, Leddy & Liedtke, 2010) and hyperglycaemia has been shown to alter SOCE (Daskoulidou et al., 2014). The first hypothesis to be tested is that hyperosmolarity will reduce the intensity of SOCE via the modulation of STIM-Orai activity. With the null hypothesis being that hyperosmolarity will have no effect on the intensity of SOCE.

The secondary hypothesis in this project is that the underlying mechanism of reduced SOCE under the hyperosmotic condition is, at least in part, due to an increase in intracellular ROS. With the null hypothesis being that intracellular ROS generated under the hyperosmolar condition is not capable of reducing the activity of SOCE proteins. Hyperosmolarity has always been seen as a simple consequence of hyperglycaemia (which it is) but this thesis postulates that hyperosmolarity is an overlooked and insidious contributor to endothelial cell dysfunction in DM. By identifying a potential new mechanism for damage and vascular injury, SOCE proteins might be further explored as pharmacological targets in the treatment of DM.

The aims are:

1. To determine the effect of hyperosmolarity on endothelial cell function by measuring migration, proliferation, and cell death.
2. To determine the effect of hyperosmolarity on SOCE in vascular endothelial cells and study the contribution of Orai in hyperosmolarity-induced Ca^{2+} response.
3. To investigate if hyperosmolarity can increase ROS production and if so, the underlying mechanism will be explored.

Chapter 2

Materials & Methods

2.1 Materials

Dulbecco's Modified Eagle Medium (DMEM) F12 cell growth media, foetal bovine serum and 0.25% Trypsin/EDTA were purchased from Thermo Fisher Scientific (Loughborough, UK). Cell culture plasticware (cell culture flasks, serological pipettes and tubes) were purchased from Sarstedt (Leicester, UK). All standard salt compounds and sugars (sucrose and mannitol) were purchased from Merck as well as the FuraPE3-AM Ca^{2+} dye, WST-1 cell proliferation assay reagent solution and propidium iodide were purchased from Roche (Welwyn, UK).

The cell-permeant 2',7'-dichlorodihydrofluorescein diacetate (H2DCFDA) intracellular ROS indicator was purchased from Merck (Watford UK,). Superoxide detection dye and Amplex red intracellular peroxide indicator were purchased from Thermo Fisher (Loughborough UK).

Orai 1-3 siRNAs were purchased from Sigma and the Lipofectamine 2000 reagent used for the siRNA knockdown experiments was purchased from Thermo Fischer UK. Thapsigargin and 2-APB were purchased from Merck UK (Watford, UK,). EA.hy926 (Human umbilical vein cell line CRL2922) cells were purchased from American Type Culture Collection (ATCC) (Middlesex, UK,). HEK 293 T-Rex (Embryonic human kidney CRL 1573) cells were purchased from Thermo Fisher UK (Loughborough, UK, 2013), and were transfected with Orai 1-3 m-cherry and STIM-1 green fluorescent protein (GFP) by Dr Bo Zheng (Zeng, 2012). Human aortic endothelial cells (HAEC C11271) and endothelial cell growth medium were purchased from PromoCell (Heidelberg, Germany). HK-2 (Human kidney proximal tubule CRL2190) cells were purchased from ATCC (Middlesex, UK). Sodium pyruvate and hydrogen peroxide were purchased from Merck (Watford, UK). Flexstation 3 pipette tips were purchased from Molecular devices (Wokingham, UK).

2.2 Ethical considerations

No specific ethical approval was sought, nor required, for any of the experiments performed in this thesis. All cell lines were purchased and no patient data was obtained or stored during the course of study.

All solutions used in this study are listed in Table 2.1.

Table 2.1. list of bath and salt solutions used in experiments

Solution	Compound concentration (mM)
Hanks Balanced Salt Solution	NaCl 137; KCl 5.4; NaH_2PO_4 0.34; K_2HPO_4 0.44; $CaCl_2$ 0.01; HEPES 10; D-glucose 8; pH adjusted to 7.4 using NaOH
standard bath solution (containing 1.5 mM Ca^{2+})	NaCl 130; KCl 5; $MgCl_2$ 1.2; $CaCl_2$ 1.5; HEPES 10; D-glucose 8; pH adjusted to 7.4 using NaOH
Ca^{2+} free bath solution	NaCl 130; KCl 5; $MgCl_2$ 1.2; EGTA 0.4; HEPES 10; D-glucose 8; pH adjusted to 7.4
PBS	NaCl 137; KCl 2.7; $Na_2HPO_4 \bullet 12H_2O$ 10; KH_2PO_4 2; pH adjusted to 7.4 using HCl

2.2 Methods

2.2.1 Cell culture

Cells (EA.hy926, HEK293, and HK2) were grown in Dulbecco's Modified Eagle Medium/Nutrient Mixture F-12 (Invitrogen, UK) supplemented with 10% foetal bovine serum (FBS) and 100 units/ml penicillin and 100µg/ml streptomycin. Cells were passaged upon reaching confluence (~75% flask coverage) using Trypsin/EDTA (0.25%) after washing with phosphate-buffered saline (PBS). Cells were treated with trypsin at 37°C for 5 minutes. Following this, the trypsin was deactivated using serum-containing media and cell clumps were broken up via pipette aspiration. Cells were seeded into cell culture flasks at a density of 1000 cells per ml. For experimentation, higher seeding densities were used (up to 2000 cells/ml).

Primary Human Aortic Endothelial Cells (HAEC's) were cultured in endothelial basal medium 2 (EBM-2) (PromoCell, Heidelberg, Germany). These cells were passaged at ~60% confluence and a lower concentration of dissociation reagent was used 0.05% (Trypsin/EDTA). The standard supplementation mix (C-39216) was included in the media as well as 10% FBS. To avoid phenotype changes, HAECs at passages 2 and 3 were used in this study. These cells were grown to lower confluence because their proliferative ability is known to diminish above 70% (Hayasaka et al., 2007).

Ea.hy 926 cells were purchased and used as an endothelial cell model due to their high level of genetic and morphological stability at high passage numbers (Bauer et al., 1992) as well as being well established *in vitro* models for vascular endothelial cells (Ahn et al., 1995). Although there is an understanding that these cells may have lost some endothelial cell characteristics following immortalisation and stabilisation these remain a very useful tool for early screening and experimentation. The HEK 293 cell line was chosen due to its high rate of success for transfected gene translation and protein production (Ward et al, 2011). As well as being a cell line that finds its origin within the kidney, an organ of the body known for the regulation of osmolarity (Danziger and Zeidel, 2015).

The HK-2 cells were used as an *in vitro* model of the proximal tubule of the kidney; this is a well-established cell line that has been used in this way within several papers (Gildea et al., 2010)& (Jenkinson et al., 2012). The HAEC cells were purchased as they are a primary cell isolate they are known to better model vascular endothelial cells as they have a greater level of expression of endothelial markers and grow to form a distinct endothelial monolayer (Sprague et al., 1997). These primary cells were grown in the recommended medium supplied by the manufacturer, this is because in order to maintain endothelial morphology for several passages these cells require precise supplementation with endothelial growth factors as well as other key messaging molecules (Promocell manual 2019). All other cell lines were grown in DMEM-F12 media containing penicillin/streptomycin as well as 10% Foetal bovine serum (FBS), this cell culture method has been published previously in (Zeng et al., 2017).

2.2.2 Cell migration assay

The method involves creating a scratch in a confluent monolayer of endothelial cells to measure how many cells migrate into the scratched gap in a given timeframe (Liang et al., 2007). EA.hy926 cells were seeded onto 6*35 mm (2 ml volume) round cell culture dishes and grown to 90% confluence; following this, the plates are scratched in a set pattern using a sterile implement of 1mm diameter. The scratched and dead cells are then washed away using room temperature Phosphate buffered saline (PBS) and 2 ml of the cell culture media (DMEM/F12) was placed into the dishes. This washing step was used to ensure that any scratched cells were not able to re-adhere to the base of the dish.

Control groups had media with no supplementation and just the basal level of glucose (5.5 mM) as the osmotically active sugar. The two experimental groups contained supplemented sucrose and mannitol at a 19.5 mM final concentration, these sugars were chosen as they are osmotically active but are not metabolised by the endothelial cells directly (Better et al., 1995). These cells were then incubated at 37 °C (5% CO2) for 48 hrs. Following this growth period, the cells (in 35 mm dishes) were transported to the microscopy suite in a heated container at 37 °C.

After the incubation period, photomicrographs were taken of the wound area in predetermined locations allowing 10 areas to be counted per 2ml dish. The number of cells that migrated into the scratched area was counted by the investigator manually (with any cells on the border of the scratched area being excluded). The manual cell counts were each repeated twice as well as being confirmed by the CellC cell counting software, with the parameters set to only include cells within the middle 90% of the scratched zone. The number of cells that migrated into the scratched area was taken as a measure of endothelial cell migration.

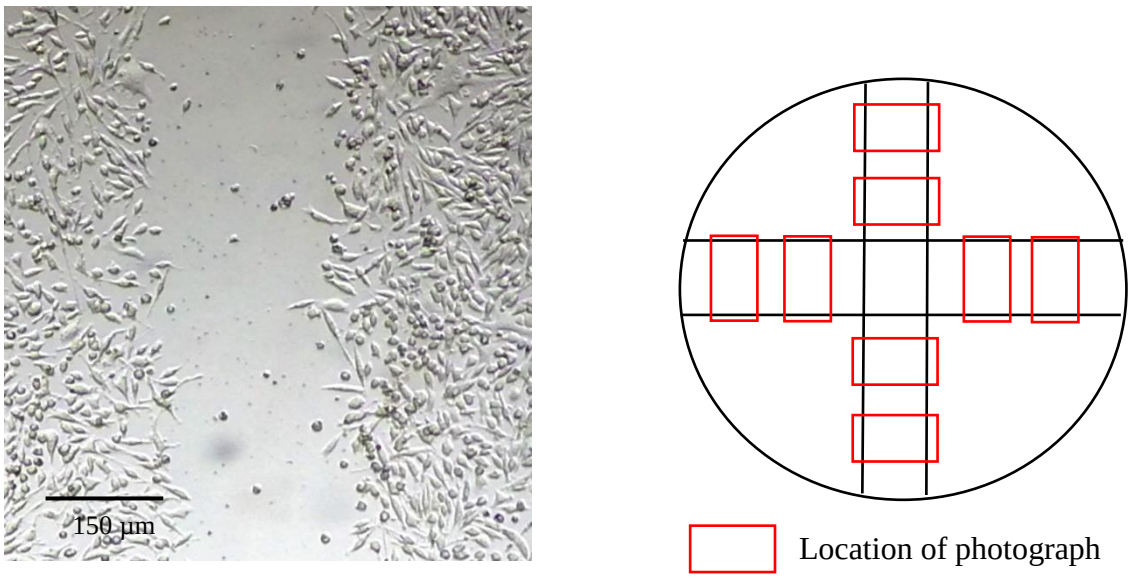

Fig 2.1. A. Example photo of cell EA.hy926 wound healing assay B. Schematic showing the predetermines photograph zones for each 2 ml dish

All photographs were taken using a Nikon LV 150 bright field microscope with exposure and focus settings remaining the same between every replicate (exposure was 0.25s for all images). All experiments were performed in triplicate and eight photographs were taken per plate, thereby generating 24 images per group from three different plates receiving the same condition.

2.2.3 Cell proliferation assay

A WST-1 cell viability/proliferation assay was performed to determine whether the hyperosmolar condition is capable of reducing endothelial cell viability and proliferation. (Roche, Welwyn, UK). The WST-1 assay is used to measure the relative abundance of the NADPH dependent oxidoreductase enzymes, and the level of reaction is correlated to the number of viable cells (Berridge et al., 2005). The compound changes colour upon incubation with these enzymes and this compound can be quantified by colourimetry and absorbance using a plate reader, this can be seen in Fig 2.2 (Ngamwongsatit et al., 2008). The colour change is caused by the conversion of the WST-1 (a tetrazolium salt) into formazan by the mitochondrial succinate-tetrazolium-reductase system, this formation of Formazan produces a colour change from very light pink to dark red (Yin et al., 2013).

The relative absorbance is then taken to correlate with the number of viable cells present within a sample population. Ea.hy926 cells were seeded into a 96 well plate either in the control media (containing no osmotic sugar supplement) or in media containing an additional 19.5 mM of sucrose or mannitol. These sugars were selected because they are osmolytes similar to glucose but they cannot be taken up by the cells (Olmstead, 1953). Each experimental group (negative control, sucrose, glucose and mannitol) was repeated eight times.

The 96 well plate was incubated for 48 hrs, after which the media was aspirated and 40µl of the WST-1 at working concentration was added to each well. This working concentration was taken from the manufacturer's instruction manual for the compound and was a 1:2500 dilution in sterile PBS.

The reason for aspirating the growth media before the addition of WST-1 is because the growth media contains phenol red, a compound that would be detected using an absorbance plate reader. The plate was then incubated at 37 °C for another 2 hrs. Following this, the plate was then read using the Flexstation3 96-well plate reader measuring absorbance at 450 and 605 nm. The plate reader was set to ambient temperature, as the plate would only need to be kept at this temperature for less than 2 minutes and this is not expected to significantly affect the results of the experiment.

All results generated from the assay are normalised against a well containing the WST-1 reagent but no cells, this allows for the removal of any background absorption that is present from the light red/pink WST-1 reagent.

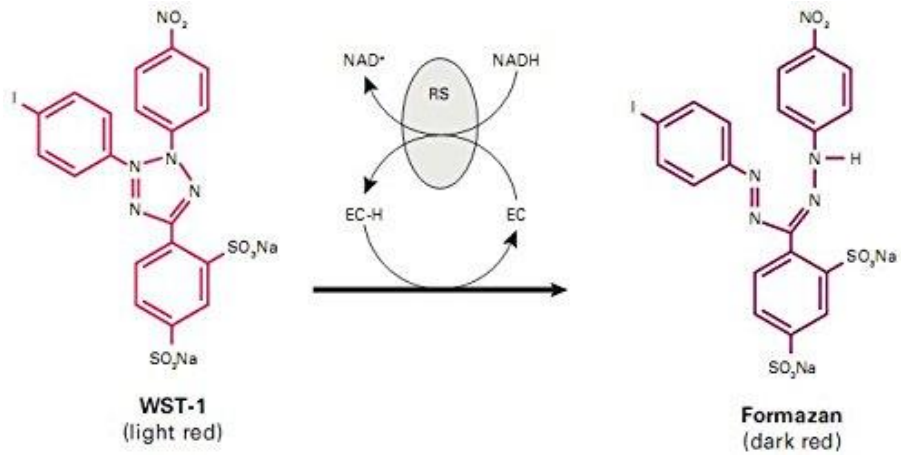

Fig 2.2. Diagram showing the conversion of the WST-1 salt being converted by the succinate-tetrazolium-reductase system (represented by R) into the dark red Formazan compound. Figure is from ROCHE WST-1 Assay kit instructions for use Issue 7 2017

2.2.4 Cell death assay

Propidium iodide binds to DNA and becomes fluorescent when bound with fragmented/damaged DNA. Because a dying or dead cell would have undergone DNA fragmentation, the nucleus of these cells will be easily seen under the right fluorescent excitation and emission wavelengths (Riccardi and Nicoletti, 2006). The protocol used in this experiment is adapted from a protocol published by (Cummings and Schnellmann, 2004) (EA.hy926 cells were seeded into 96 well plates at a seeding density of 5000 cells per ml and were grown in DMEM-F12 media containing penicillin/ streptomycin as well as 10% FBS supplementation.

All wells were marked prior to seeding to determine the zones that would be used for taking photographs; these zones were to be the same for every dish used to prevent observer bias in zone selection. After 24 hours the media was replaced with the media introducing the experimental condition (mannitol, sucrose or hydrogen peroxide as the positive control), and this was incubated at 37°C 5% CO_2 for a further 24 hours. For the experiments where the wells were analysed by taking fluorescence microscope photographs cell counting was performed using the CellC software (CellC, Tampere University, 2008). These cells were fixed (in 2% paraformaldehyde) before taking the photographs to capture the 24hr time point precisely.

The paraformaldehyde needs to be removed prior to the loading of the PI as this compound can affect dye loading (Poole et al., 1996). 40µl of Propidium iodide in PBS (working concentration of 10µg/ml) was added to each well to be stained, the dye was allowed to permeate the cells at room temperature for 2 hours. After removing the excess dye by washing (aspiration and replacement of bath solution three times) with PBS a fluorescence microscope capable of measuring red fluorescence (Ex: 493 nm Em: 636 nm) pictures were taken of the cells within the wells within the predetermined zones. Dead/dying and total cell counts can then be taken with the CellC software or manually, allowing for the determination of total dead cells and the proportion of cells that were dead in comparison to the total population.

For plates that were measured using the Flexstation3 plate reader using an endpoint reading (Ex: 493 nm Em: 636 nm). These cells did not need to be fixed with paraformaldehyde before reading the plates as the direct fluorescence reading is much quicker than the use of a fluorescence microscope to take photographs. The purpose behind using a plate reader to measure the intensity of fluorescence is to confirm the results observed in the photographic analysis as this could be open to miscounting and sample bias even with controls in place. Because PI causes dense nuclear staining in dead or dying cells (Riccardi and Nicoletti, 2006) it is predicted that the greater the total fluorescence intensity per well the greater the number of densely stained nuclei are present within that well and therefore a greater proportion of dead or dying cells. Wells were checked immediately prior to plate reading to ensure that contamination or excess dye could not interfere with the results.

2.2.5 Intracellular Ca^{2+} measurement

To test the effect of hyperosmolarity on the cellular Ca^{2+} efflux and influx a Ca^{2+} dye is used to visualise and measure the relative concentration of intracellular Ca^{2+}. By using appropriate bath solutions and specific activation compounds in a live fluidic system (Flexstation3) this dye can be used to measure the intensity of the multi-step SOCE process (Zeng et al., 2017).

The dye selected for the measurement of Ca^{2+} efflux and influx was FuraPE3-AM, a membrane-permeable derivative of the common Fura-2 intracellular Ca^{2+} dye, this membrane permeability characteristic results from the esterification of the base molecule (acetoxymethyl ester AM) (Garaschuk et al., 2006). The FuraPE3-AM dye crosses the cell membrane and the AM ester is removed by intracellular esterases this then allows the dye to bind to intracellular Ca^{2+} and become active (Gunter et al., 1988). FuraPE3-AM is prepared and stored within a 1 mM stock solution of dimethylsulphoxide (DMSO) and for the purposes of imaging, experiments is often loaded into cells in the presence of 0.01% Pluronic acid which increases both the permeability of the dye and helps to ensure complete de-esterification leading to more even dye loading (Maruyama et al., 1989). 0.01% Pluronic acid (Pluronic F127) was not used in these plate reader assays due to the fact that the Flexstation3 takes eight readings per well from different areas and any local dye loading anomalies should not affect the final reading as well as dye loading and de-esterification being visually confirmed before the start of each plate reading session. The FuraPE3-AM is solubilised in DMSO and because of this; all the negative control groups set for experiments using this dye contained a like-for-like volume of DMSO in order to ensure that the DMSO was not capable of interfering with the results of the experiment.

Adherent cells are seeded onto a 96 well plate and incubated at 37 °C/ 5% CO_2 for 48 hours. For stably transfected HEK293 cells tetracycline is added to the cell culture media at the stage of seeding the 96 well plates (to a concentration of 1µg/ml). This tetracycline concentration is also added to the negative control groups for experiments using these cells. This experiment was also performed using the EA.hy926 cell lines and HAEC cells and these were not treated with tetracycline because they did not contain a transfected tetracycline activated sequence.

When cells have reached 80% confluence the growth media is aspirated and 40µl of FuraPE3-AM dye (working concentration of 2 µg/ml in Ca^{2+} free solution) is added to each of the wells. The plate is incubated at 37°C for 30 minutes to allow for dye loading. After incubation, the cells are washed with standard Ca^{2+} bath solution to remove excess dye and the wells have 100 µl of Ca^{2+} free solution added before Flexstation3 recording. The Flexstation 3 (Molecular Devices, Wokingham, UK) is then set to dispense up to 3 live fluidic additions from a prepared compound plate and for the FuraPE3-AM dye, the excitation wavelengths must be set at 340nm & 380nm with both of the emission wavelengths being set at 510nm. All compound additions are prepared at a concentration that allows for the dilution factors (1:5,1:6,1:7) depending on the number of the addition and presuming a 100 µL starting volume and a 25 µL addition volume. Data for FuraPE3-AM is presented as a ratio between the two excitation wavelengths (340nm/380nm) and is normalised to a basal fluorescence to account for small differences in intracellular dye concentrations between groups as well as other variables such as cell thickness.

To investigate the effect of hyperosmolarity on SOCE the cells underwent a pre-treatment with the hyperosmolar condition following the Ca^{2+}dye loading for 5 minutes this using a Ca^{2+} free bath solution. Following this pre-treatment, the 96 well plate was placed in the Flexstation3 at 37°C and two live fluid additions were programmed. Thapsigargin (TG) was added at 100 s, this SERCA blocker was used to cause calcium efflux from the ER (Daskoulidou et al., 2015), this was then followed at 450 s by the addition of the standard bath solution containing a final diluted concentration of 1.5 mM Ca^{2+}. This addition of standard bath solution was added to initiate SOCE following depletion of the ER Ca^{2+} stores. For the HEK 293 cells overexpressing the Orai 3-mcherry protein, an alternative protocol was used to initiate SOCE. This is because it is known that 2-Aminoethoxydiphenyl borate (2-APB) can pharmacologically initiate SOCE without the need to deplete the ER Ca^{2+} stores, this was used as the first fluidic addition (final concentration of 50 µM), this methodology was demonstrated in the Daskoulidou et al 2015 paper.

The HEK296 Trex cells used in this experiment were transfected using the lipofectamine 3000 technique as described in the paper by(Zeng et al., 2017). Cells were transfected with STIM-1-Green fluorescence protein (GFP) cassette and one of the three Orai subtypes which were tagged with the m-cherry sequence. This allows the cells to overexpress these ion channels and thereby allowed for the investigation into the specific Orai subtypes. The success of the stable transfection was confirmed using western-blot (Zeng et al, 2017) and before every experiment, with these transfected cells the overexpression of the protein was confirmed visually using a fluorescence microscope using both red and green filters to detect the fluorescent tags used.

2.2.6 Cell surface area/volume

In order to assess the effect that the hyperosmolar condition would have on the volume of endothelial cells a cell volume reduction experiment was performed. The expected shrinkage response to hypertonic solutions is a well known and established scientific concept (Kajimura & Curry, 1999). This experimental protocol was adapted from (Kajimura and Curry, 1999).

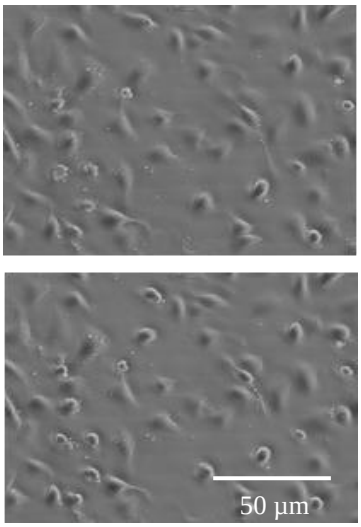

Fig 2.3 Example photographs of the pictures analysed in the cell volume/surface area experiment. (A) Cells prior to addition of 30 mM mannitol (B). Cells after 5 min incubation with 30 mM mannitol.

Both EA.hy926 and HEK293 (transfected and non-transfected) cells were grown to 60-70% confluence in sterile 24-well plates. For each cell type culture media was replaced by standard 1.5 mM Ca^{2+} bath solution in the control condition and with the addition of 30, 60 and 90 mM mannitol in the test conditions n=5 per group. In each experiment, a picture was taken of a suitable field (containing a minimum of 30 distinct cells) before the addition of control or hyperosmotic mannitol bath solution.

A second picture was taken at either 5 minutes for endpoint measurement or at set intervals for a time-course experiment. Cell volume was measured by photographic analysis of the cells by CellC cell counting software (Harvard, open access). Each cell at the beginning of the assay had an applied region of interest (ROI). Meaning that the original outer perimeter of the cell was recorded prior to the addition of the experimental condition and it was a reduction in this perimeter that was measured by the software example photographs of the images analysed for this method can be seen in Fig 2.3.

2.2.7 Intracellular ROS detection using H_2DCFDA

The intracellular dye used was 2',7'-dichlorodihydrofluorescein diacetate (H_2DCFDA) this is a chemically reduced form of fluorescein and upon entering a cell the intracellular esterases and oxidants cleave the acetate groups within the compound producing the highly fluorescent 2',7'-dichlorofluorescein (DCF) (Wu and Yotnda, 2011) this can be seen in Fig 2.4. The dye is prone to oxidation if exposed to air and therefore is dissolved within DMSO, to prevent oxidation of the compound, and stored at -20 °C to prevent premature oxidation of the dye, it was also used no more than 4 weeks post preparation.

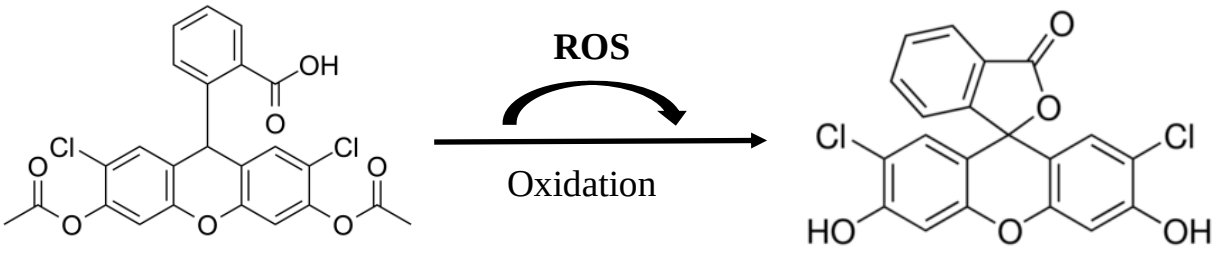

H_2DCFDA- Non-fluorescent

DCF-fluorescent

Fig 2.4 Equation showing the reaction of H_2DCFDA to the presence of ROS producing the fluorescent compound DCF. Fig. adapted from manufacturers manual

Because H_2DCFDA is a fluorescein derivative it is important to ensure that the loading media is free of colourimetric dyes such as phenol red because these indicators can increase background fluorescence and interfere with the results (Zielonka et al., 2014). For this reason, the standard bath solution was chosen to be the dye-loading medium as this has the advantage of maintaining consistency between experiments as well as not containing primary and secondary amines, which could cause extracellular de-esterification of the dye (Carpéné et al., 2016).

The dye was loaded into both EA.hy926 and HK2 cells for these experiments for 30 minutes before the experiment at 37 °C with a dye loading concentration of 2 µM which is within the loading media. This loading media was changed before experimentation to prevent bleaching during fluorescence detection. The 96 well plates were placed into the Flexstation3 for fluorescent measurement (Ex: 493 nm Em: 520 nm). Fluorescence was measured on a time course setting of measurement every 30 seconds over a period of 60 minutes. For this experiment, the Flexstarion3 was kept at a temperature of 37°C for the duration and was kept at 5% CO_2 to prevent these factors causing an increase in intracellular ROS (Krasensky-Wrzaczek and Kangasjarvi, 2018).

Hyperosmotic (19.5, 30 and 60 mM mannitol) or positive control (100 µM H_2O_2) conditions were applied by Flexstation 3 compound transfer at a time point. Compound plate solutions were prepared at a 5* concentration to allow for dilution of 25 µl of fluid into 100 µl within the 96 well test plate.

2.2.8 MitoSOX superoxide detection assay

To detect intracellular superoxide specific fluorescent dye, MitoSOX was used (ThermoFischer, UK, 2016) as this is a fluorogenic dye that enters the mitochondrion and is activated by the superoxide by-product of mitochondrial oxidative phosphorylation. This assay also allows for the investigation as to whether the hyperosmolar condition is capable of increasing the level of superoxide and by inference determine an effect on the oxidative phosphorylation pathway (Kuznetsov et al., 2011). The hyperosmolar condition was achieved via the addition of mannitol at various concentrations to the Ca^{2+} bath solution. This standard bath solution contains 1.5 mM concentration of Ca^{2+} in order to mimic the normal plasma concentration of ionised Ca^{2+} which ranges from 1.3-1.5 mM (Ross et al, 2011). For this experiment adherent cells (EA.hy926 and HAEC) were seeded onto 96 well plates and grown to 70% confluence at 37 °C and 5% CO2 (DMEM/12 media was used for the EA.hy926 cells and EBCM-2 was used for the HAEC cells). The MitoSOX dye was loaded into the cells according to the manufacturer's instructions (loading vehicle was standard bath solution: contents specified within the materials section of this chapter). The working concentration of the MitoSOX dye was 5 µM, and the cells were loaded with the dye for 30 minutes at 37 °C, taking care not to expose the dye to light to avoid bleaching.

Dye activity was confirmed using a visual check under inverted fluorescence microscopy, all living cells produce superoxide via mitochondrial oxidative phosphorylation so therefore all cells would fluoresce red after loading with mitosox (Boguca & Wojtczak, 1966). For this reason, sodium azide was used as a control group to confirm the specificity of the Mitosox activity. Sodium azide is known to scavenge and quench the singlet superoxide anion which could be used as a confirmation of the dye fluorescence checked visually before experimentation was due to mitochondrial superoxide because any cells treated with 2µm sodium azide would not show fluorescence (Boguca & Wojtczak, 1966). Carbonyl cyanide-p-trifluoromethoxyphenylhydrazone (FCCP) was used as a positive control in these experiments because it is a known disrupter of mitochondrial oxidative phosphorylation leading to significant superoxide production (To et al, 2011).

The plate was read in a time-course manner using the Flexstation3 using the settings recommended by the manufacturer for MitoSOX detection (Ex: 510/Em: 580 nm). The Mitosox reagent is supplied in aliquots, each sufficient for one 96 well plate of experiments, the reagent is dissolved in DMSO immediately before experimentation as the reagent is easily oxidised and cannot be prepared in advance. The dye was diluted to its working concentration in standard 1.5 mM Ca^{2+} bath solution and was kept in the dark to prevent photobleaching before the experiment, for this reason, all preparation was performed in a dark room and the cells were covered with tin foil for transportation into the plate reader.

2.2.9 Amplex red extracellular peroxide detection assay

To test the effect of hyperosmolarity on the production of extracellular peroxide reactive oxygen species the Amplex Red dye was used (ThermoFischer, UK, 2016), as this dye is known to be able to specifically detect the presence of peroxide radicles in the presence of horseradish peroxidase (HRP) (Votyakova and Reynolds, 2004). This is because the dye is reduced in the presence of HRP and forms the fluorescent compound resorufin in direct proportion to the amount of hydrogen peroxide in the solution (Mishin et al, 2010), this can be seen in Fig 2.5. The protocol used for this experiment is adapted from Votyakova & Reynolds (2004).

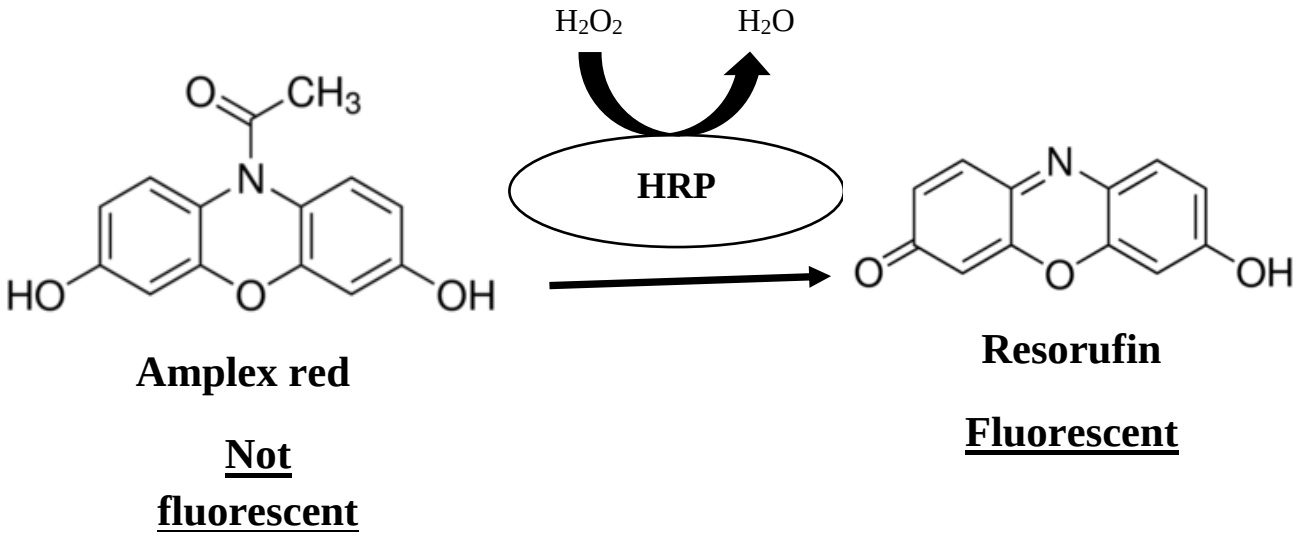

Fig 2.5 Equation showing reduction of Amplex red in the presence of Horseradish peroxidase (HRP) and hydrogen peroxide to form the fluorescent compound resorufin. Adapted from Mishin et al (2010).

Adherent cells (EA.hy926 and HAEC) were seeded into 96 well plates and grown at 37°C & 5% CO_2 until they reached 70-80% confluence. The reason for selecting relatively low confluence was to avoid complete dye bleaching and conversion, which may happen with the Amplex red dye in the presence of a very large number of cells producing peroxide in response to cellular stress. Upon reaching confluence the cell culture media was removed and replaced with Ca^{2+} bath solution containing 1.5 mM Ca^{2+} to mimic plasma Ca^{2+} concentrations (Goldstein et al, 1990). That same solution contained the working concentration of Amplex red (50 µM) as well as the required concentration of horseradish peroxidase (10 u/ml) that allows for the dye to become active in the presence of peroxide anions. It was at this point that the different groups including the hyperosmolar mannitol groups and the positive (H_2O_2) control groups were initiated. The cells were then incubated with the Amplex red for 1 hour for 37 °C and the fluorescence intensity was measured using the Flexstation3 (Ex:530/Em:590 nm).

2.2.10 siRNA transfection

Small interfering RNA (siRNA) was transfected into living cells using the Lipofectamine 2000 transfection reagent in a protocol adapted from the paper published by (Zeng et al, 2017). The specific siRNA's used in these experiments were designed and produced by Thermo Fischer (2010, UK) the Lipofectamine 2000 transfection kit was also purchased from this company. The concentration of siRNA used in each well was 2.5 µg/µL and this was mixed with the Lipofectamine reagent in a 1:1 ratio (25 µl diluted siRNA: 25 µl diluted Lipofectamine 2000 reagent) (Zeng et al, 2017).

Both siRNA and Lipofectamine were diluted and combined using OptiMEM medium (no serum to increase transfection efficiency). 50 µl of the Lipid/siRNA complex was added to the wells of the 96 well plate containing 100 µl OptiMEM media and the cells were incubated with the transfection complex for 24 hr (initial transfection took place when cells were 50% confluent). This allowed for the Lipofectamine 2000 ample time to permeablise the cell membrane and in turn introduce the siRNA sequences into the cell as described in (Cardarelli et al., 2016).

OptiMEM media was used because it is a low serum growth medium, the cationic Lipofectamine can be inhibited in high serum concentration mediums so this OptiMEM media is intended to improve transfection efficiency (Rashid et al, 2019). To ensure the specificity of the cellular response a scrambled form of the target sequence was co-transfected with the DS-red DNA which was used as a transfection confirmation tracer.

Following the initial 24 hr incubation, the media was replaced with either standard DMEM/F12 for EA.hy926 cells or ECBM-2 for Human Aortic Endothelial Cells (HAEC). The cells were incubated for a further 24 hrs and transfection was then confirmed by viewing the cells under fluorescence microscopy (DS-red tracer DNA was transfected as a control/confirmation group). If cells had reached at least 80% confluence (and a minimum of 90% positive transfection) then the subsequent Ca^{2+} dynamics experiments were performed. The siRNA sequence targets and transfection efficiency are all published in the paper listed in the publications section of this thesis.

The siRNA sequences used in the experiments were as follows:

Orai1: CGAGCACUCCAUGCAGGCG

Orai2: CGUGCCUAUCGACCCCUCU

Orai3: AGCUUCCAGCCGCACGUCU

2.3 Statistics

Data are presented as mean ±SEM. Students t-test was performed where only two groups were being compared and a P value of less than 0.05 was used as the cut off for null hypothesis rejection. For mean comparison between groups, a one-way analysis of variance (ANOVA) was performed. If a significant difference was observed after the ANOVA test a Tukey post hoc test or a Bonferroni's post hoc analysis was performed to identify which groups differed significantly. As with the t-test, the cut off for rejecting the null hypothesis was a P-value below 0.05. In all cases where the ANOVA test was used as the data was observed to be normally distributed.

Origin Pro8 was used for data presentation and graph generation as well as for statistical analysis of the data (OriginLab 8.0) IBM SPSS statistical package was also used for some statistical analysis (SPSS v19.0). Automated micrograph cell counting was performed using the open-access software CellC (CellC, Tampere, USA).

All experiments were powered sufficiently to allow for the statistical tests mentioned above to be performed, all Ca^{2+} dynamics experiments were performed with n=8 wells and because the sample populations were taken from homogenous cell populations this allows for the use of an ANOVA with post hoc Tukey/Bonferroni analysis. This same number of replicates were performed for all of the ROS assays and the siRNA transfection. For the endothelial cell migration assay, there were 8 images taken per group performed in triplicate which is n=24 images per group, this allowed for a one-way ANOVAto be performed under the same assumptions of a homogenous sample population.

Chapter 3

Hyperosmolarity causes endothelial cell dysfunction by the impairment of SOCE

3.1 Introduction

Hyperglycaemia is not only responsible for alterations in cell signalling and gene regulation due to oxidative stress but is also associated with the increase of osmolarity which is capable of producing cellular osmotic stress (Brownlee, 2001)& (Hashim and Zarina, 2012). Transient elevations in plasma osmolarity occur commonly in diabetes and a persistently elevated level of plasma osmolarity is life-threatening, for example, the hyperglycaemic and hyperosmolar state (HHS) in diabetes, which can cause significant damage to the endothelial layer of blood vessels (Yasuda et al., 2009). Some early work done by Luh *et al* 1996 found that bovine endothelial cells were capable of resisting modest hyperosmolarity without effecting the proliferative ability of the cells (Luh et al., 1996)

Research performed by Affonso *et al* suggests that hyperosmolarity is capable of reducing the vasoconstrictive reactivity of vascular endothelial cells (Affonso et al., 2003). Looking beyond endothelial cells it has been found that hyperosmolarity is capable of causing the accumulation of Myo-inositol within renal cells, potentially contributing to the increased excretion of Myo-inositol commonly found within the urine of diabetic patients with diabetic nephropathy (Bissonnette et al., 2008). Hypoosmolarity has also been shown to increase the rate of cell death within human proximal kidney tubule cells (Jenq et al, 1999).

These papers describe the effect that hyperosmolarity has on endothelial cells as well as kidney cells; far less work has been done in investigating the mechanism by which the hyperosmolar condition is causing these negative cellular effects. Madonna *et al* have described how glucose-induced hyperosmolarity increases angiogenesis within retinal tissue via the increased expression of aquaporin 1 and cyclooxygenase 2. This paper does suggest that hyperosmolarity is capable of resulting in significant changes within the cells apart from the physical shrinkage and remodelling expected under this condition (Madonna et al, 2016).

Our research group has shown that hyperglycaemia is capable of increasing SOCE intensity through the enhancement of the expression of Orai and STIM in endothelial cells (Daskoulidou et al., 2015). However, it is unclear if the osmolarity, a concomitant factor can change the activity of SOCE proteins in its own right. The aim of this chapter is therefore two-fold, firstly to determine any detrimental effect that hyperosmolarity has on the viability (migration, proliferation, death and surface area) of endothelial cells; and secondly to determine whether the modulation of SOCE is a contributory factor to the cellular dysfunction observed in the hyperosmolar condition.

Hypothesis 1: Hyperosmolarity will reduce the viability of endothelial cells as measured by migration, proliferation, cell death and volume/surface area assays.

Hypothesis 2: A reduction in SOCE intensity will be observed within the endothelial cells in response to the hyperosmolar condition.

3.2 Methods

Endothelial cell viability testing performed in this chapter uses the established endothelial cell line EA.hy926 as an *in vitro* model of human vascular endothelial cells (Zeng, 2017). The experiments performed to assess the direct effect of hyperosmolarity on the endothelial cells were selected in order to give a broad range of measures of viability and function. These experiments range from a WST-1 assay to assess viability to the use of a scratch wound healing assay to assess the effect of hyperosmolarity on the ability of the endothelial cells to migrate. A full description of the methodology used for the experiments performed in this chapter can be found in sections 2.2-2.6 of chapter 2.

To investigate the effect of hyperosmolarity on the intensity of Ca^{2+} influx intensity, a live dynamic Ca^{2+} plate reading experiment was performed using the Flexstation3, a microplate reader that can add compounds to wells during reading allowing for a "live" response to be recorded. The measurement of Ca^{2+} influx/efflux was based upon a SOCE calcium imaging experiment performed by Daskouidou et al (2015). Thapsigargin (TG) was used as a Ca^{2+} store depleter, the mechanism of action for this compound is based upon its action as a known SERCA blocker, this leads to an efflux of Ca^{2+} from the endoplasmic reticulum (Sehgal et al, 2017). The influx of Ca^{2+} into the cell is then initiated by the addition of 1.5 mM Ca^{2+} into the bath solution (which is Ca^{2+} free prior to the addition of TG).

Mannitol was used as the additional osmolyte within the experimental hyperosmolar conditions, this is because the sugar is of a similar molecular weight and size to glucose but cannot be metabolised by the cells (Cheng et al., 2013). The experimental hyperosmolar conditions used were 19.5 mM 30 mM 60 mM and 90 mM, the 19.5 mM, these concentrations were selected to ensure that any results generated were comparable to the hyperglycaemic condition used in the Daskidilou et al (2015) paper. This paper used the concentration of 19.5 because it is within the threshold of values that we would expect to initiate ketogenesis and eventually ketoacidosis and it is also not unreasonable for a person with poorly controlled diabetes (type one or two) to reach this level (Kitabchi and Wall, 1995).

It is not easy to model the fluctuations in serum glucose and osmolarity with the methods used in this thesis so in order to understand what effect higher levels of osmolarity would have on the cells and Ca^{2+} influx the concentrations of 30, 60, and 90 mM were used. 30 mM is not an unreasonable level of mannitol to use when trying to replicate the HONK condition observed in poorly controlled type 2 diabetes (REF). The 60 mM condition may be of more limited value when compared to the true clinical condition as such a high serum osmolarity is exceptionally rare, although some patients with HONK may be expected to have glucose concentrations as high as this (Weiss et al, 2010).

The concentrations of 90 mM and 120 mM of mannitol are of limited physiological relevance because such levels are not seen even in the vast majority of extreme hyperglycaemia cases, these concentrations are designed to test the limit of the cellular response as well as what happens in extreme levels of hyperosmolarity (Wolfsdorf et al, 2014). Both sucrose and mannitol were used in the endothelial cell proliferation experiment reported in this chapter mannitol seemed to have a more substantial effect. Also because mannitol is the more commonly used osmolyte within clinical medicine (Wakai et al., 2005) it was decided to use mannitol as the osmotically active sugar throughout.

The negative control groups used in these experiments did not contain any mannitol and would always include the addition of vehicle solvent were appropriate. The negative control group for the Ca^{2+} entry experiments included the addition of DMSO within control wells in order to ensure that any effect observed was not due to the presence of DMSO. Although there are significant limitations in the translation of cell-based assays to the clinical condition these experiments offer preliminary insights as to the cellular effects of the hyperosmolar condition as well as the potential pathway behind these effects.

3.3 Results

3.3.1 Effect of hyperosmolarity on endothelial cell migration

Vascular endothelial cell (EA.hy926) migration was determined by linear wound assay. The cell migration was significantly inhibited by incubating the cells in hyperosmotic media containing either 19.5 mM sucrose or mannitol for 24 hrs at 37°C compared with the control group (Fig 3.1) (mannitol P=<0.001 sucrose P=<0.05). These reductions were 43.4% compared to the negative control in the mannitol group and 37.2% reduction for the sucrose group. However, there was no significant difference between the sucrose group and mannitol group, suggesting that the mobility of endothelial cells is reduced by the increased of osmolarity rather than by any specific effect of the sugar (P= 0.1299 for comparison between sucrose and mannitol groups). Although the difference between the sucrose and mannitol groups is not significant this does not mean that the difference observed is immaterial. As can be clearly seen Fig.3.1 mannitol appears to be more effective in its inhibition of endothelial cell migration. One potential explanation for this could be in the difference in the relative size of the compounds as this has been documented to affect the osmotic effect that they impart (Kawaji, 1979).

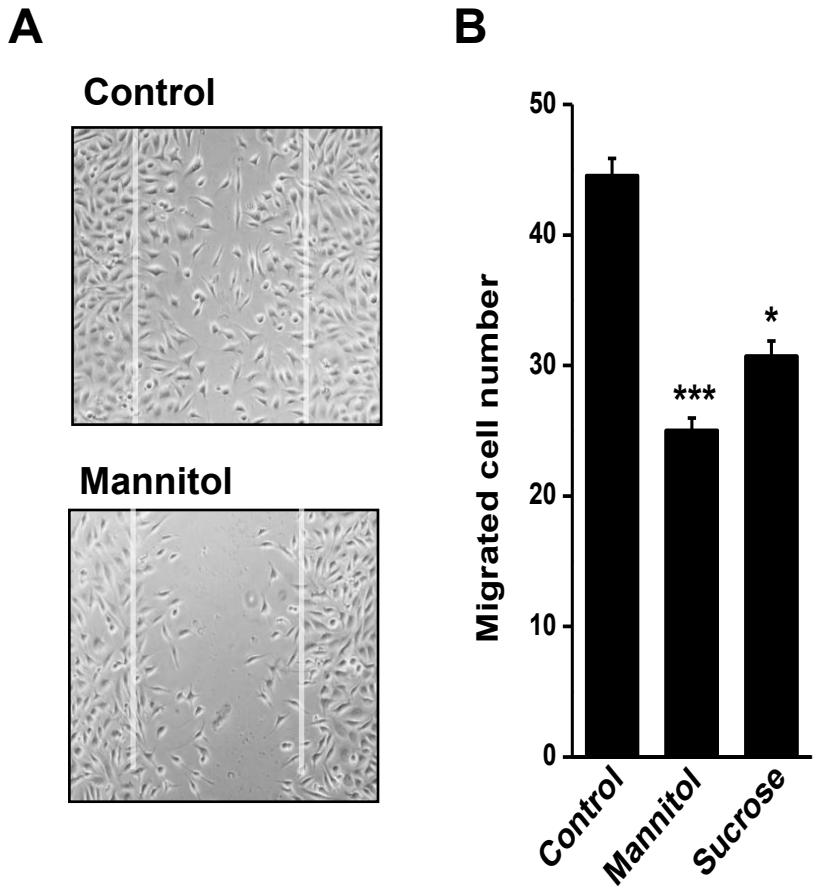

Fig. 3.1 Endothelial cell migration is inhibited by hyperosmolarity. Endothelial cell line (EA.hy926) were incubated with normal DMEM F12 medium (Control) or hyperosmolar culture media (DMEM F12 medium plus 19.5 mM mannitol, or 19.5 mM sucrose) for 24 hr. The migrated cell number across the linear wound scratched area was counted as per microscopic field. (A) Example of migrated cells in the wounded area. (B) Mean ± SEM data. The data was analysed by one way ANOVA (n =12 pictures for each group. * P<0.05, *** P<0.001)(4 pictures taken per experimental group performed in triplicate).

3.3.2 Effect of hyperosmolarity on endothelial cell proliferation

The effect of hyperosmolarity on cell proliferation was assessed using WST-1 assay kit. The hyperosmotic conditions that caused an inhibited migration (Fig 3.1) did not produce any significant change in cell proliferation after incubating the cells for 24 hours (Fig. 3.2). This result was confirmed with a manual cell count method. No significant difference was observed between any groups (control/hyper or hyper/hyper) P=>0.05 for all groups.

The implication of this result is that the effect of inhibited migration under the hyperosmolar condition seen in Fig 3.1 is not due to a reduced proliferative ability of the EA.hy926 cells under the hyperosmolar condition. Fig 3.2 does not only show that there is no significant effect on proliferation in the hyperosmolar conditions but also no effect in the hyperglycaemic conditions. This result is unexpected because hyperglycaemia is a known inhibitor of cellular proliferation (Duraisamy et al, 2003) although contemporary research using the same method only saw significant inhibition of proliferation at higher concentrations of glucose (25 mM and above) (Buranasin et al, 2018). This suggests that the concentration of glucose used in this experiment may not have been enough to cause the anti-proliferative effect noted in other studies. Another observation that can be made from Fig 3.2 is that there was no significant difference between the sucrose and mannitol hyperosmolar groups, further suggesting that mannitol, as a clinically useful osmolar agent, would be the better option for creating the hyperosmolar condition in future experiments.

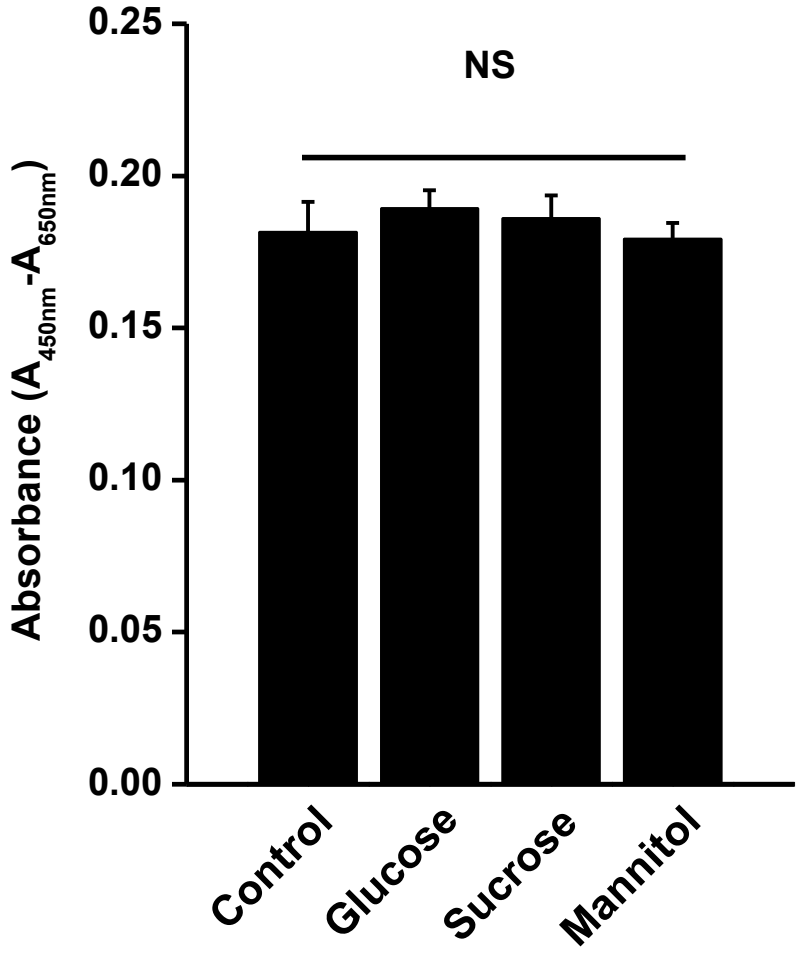

Fig. 3.2 Hyperosmolarity does not affect the proliferation of EA.hy926 cells. EA.hy926 cells were treated with 19.5 mM glucose, 19.5 mM sucrose and 19.5 mM mannitol for 24 hr and the cell proliferation was measured with WST-1 assay. The absorbance was measured at 450 nm with a reference wavelength of 650 nm. No significant difference among the groups (One way ANOVA, n = 8 for each group. NS: non-significant)

3.3.3 Effect of hyperosmolarity on cell death

The effect of hyperosmolarity on cell death was observed using nuclear staining with propidium iodide (Fig. 3.4). There was a significant increase in dead cells per field when treated with either 19.5 mM sucrose (P=0.0006) or 19.5 mM mannitol (P=0.0007) compared with the negative control group. As reported in Figures 3.1 and 3.2 there was no significant difference between the sucrose and mannitol hyperosmolar groups (P=0.768) this is a consistent finding throughout the cell viability assays performed on the EA.hy926 cells. The increase in cell death under the hyperosmolar conditions is similar to that observed in aortic endothelial cells by (Poullis et al, 2008), although interestingly the increase in cell death increased by a similar proportion despite the fact that this experiment used a lower concentration of osmotic sugar. One potential explanation for this could be that there may be a difference in sensitivity between primary aortic endothelial cells (Poullis et al, 2008) and the EA.hy926 cells used in this experiment.

Fig 3.3 also shows that the proportion of dead cells per field increases in the hyperglycaemic condition (19.5 mM mannitol) this result is aligned with evidence showing a similar effect in aortic endothelial cells (Stout, 1982). Interestingly the proportion of dead/dying cells is not significantly different between the hyperosmolar groups and the hyperglycaemic group (P=0.759). One potential reason for this could be that hyperglycaemia has been found to have a greater effect on cell death in the 48-72 hour period, which is not covered in this data (Ido et al., 2002). This may suggest that in the early phase of hyperglycaemia initiated cell death the physical property of hyperosmolarity is one of the more important factors to consider.

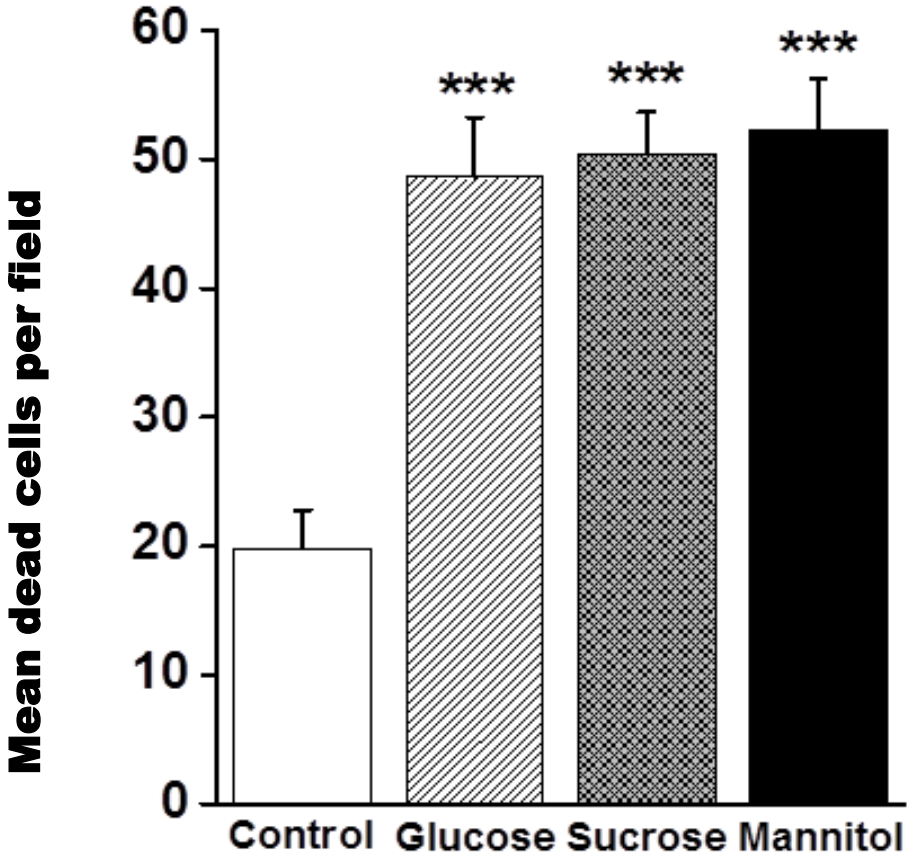

Fig. 3.3 Hyperosmolarity increases endothelial cell death. Nuclear condensation (taken as a marker of cellular death) was measured using propidium iodide nuclear staining method. The densely stained EA.hy926 cells are counted as dead cells by CellC counting software following 24 hrs incubation with either control or experimental group conditions. A one-way ANOVA was used to analyse significance among groups (n =16 fields/pictures for each group) all experiments were performed in triplicate. Data are presented as mean ± SEM. ***P<0.001 all groups were normalised to the total number of cells in the well.

To confirm the dead cell counting result, a fluorescence-based assay was used to determine the total fluorescence intensity of propidium iodide (PI) in a well using a plate reader. This is because, although automated, the cell counting software relies on unbiased image selection and is calibrated against a manual cell count by the observer. Direct measurement of fluorescence within the wells, on the other hand, would not be subject to these potential biases.

Cells were treated with the hyperosmolar condition, mannitol was chosen for this experiment as sucrose has thus far shown no difference as a hyperosmolar condition compared to mannitol. A positive control group, H_2O_2, was also used and all conditions were applied to the EA.hy926 cells for 24 hours prior to plate reading. H_2O_2 was selected as a positive control because it is a well-established initiator of cellular death and has been used in other publications as a means of calibrating the sensitivity of cell death assays (Xiang et al., 2016).

The increased fluorescence intensity of PI was seen in both hyperosmolarity and H_2O_2 groups in a concentration-dependent manner. However, the PI fluorescence dropped to a level similar to the control group at the groups treated with very high concentration (100 mM) of mannitol or H_2O_2 (>500 µM), perhaps because the cells were destroyed due to membrane leak at the extreme conditions (Fig. 3.4A, B). The result from the fluorescence-based assay was similar to the result from the manual dead cell counting (Fig. 3.4 C, D), which further confirms the effect of the hyperosmotic condition can cause cell death. Additional concentrations of mannitol were used in this experiment to assess the effect of more extreme levels of hyperosmolarity on endothelial cell death. The use of the plate reader is a novel technique designed to offer further clarity and assurance of the established cell counting method.

The 90 mM concentration of mannitol leads to the greatest level of cell death (177 AU) which was significantly higher than the level observed in the negative control group (*P*=0.013*)*. The 120 mM concentration of mannitol was chosen as an exceptionally extreme example of hyperosmolarity, this would not be achievable within the clinical situation (Wolfsdorf et al, 2014). This very high concentration of mannitol produced a statistically significant reduction in the number of dead cells compared to the negative control (*P*=0.046).

As discussed previously regarding the high concentration H_2O_2 groups, this reduction in the number of dead cells observed within the 120 mM mannitol group may not be due to a true reduction in dead cell numbers. At such extreme hyperosmolar conditions, even after only 24 hours, a large number of cells would have undergone complete fragmentation and would no longer be visible as cells. This would lead to less densely stained nuclei but this would be due to a reduced number of total cells in the sample so this is likely not a true reduction in the number of dead cells present within the wells measured. Fig 3.4 demonstrates that there is a similar pattern between the increasing concentration of H_2O_2 on the number of dead cells as there is with the increasing hyperosmolarity and the number of dead cells.

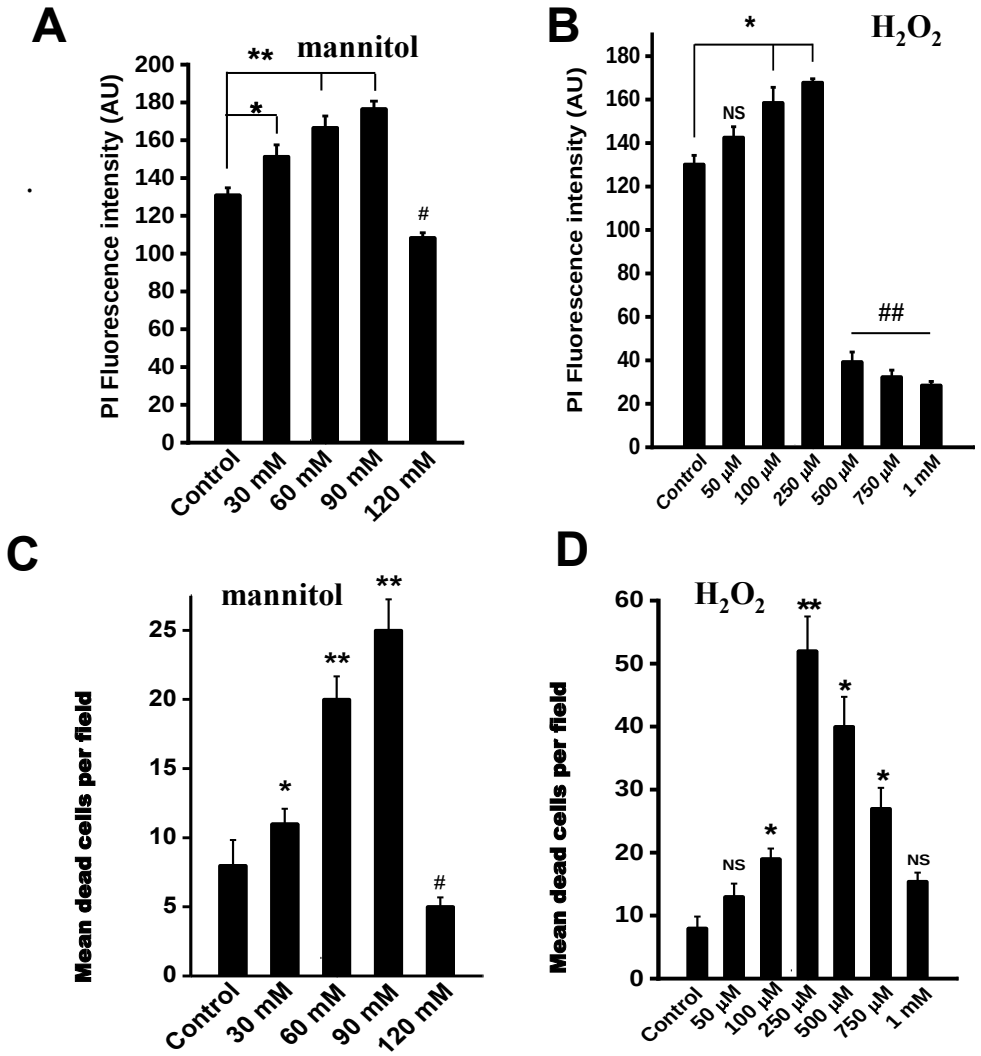

Fig 3.4 Hyperosmolarity increases cell death in EA.hy926 cells. Cells were treated with either the hyperosmotic stimuli or H_2O_2 and compared to a negative control. The cells were incubated for 6 hours prior to propidium iodide (PI) staining. (A) PI fluorescence intensity is increased after exposure to mannitol (30, 60, 90 and 120 mM) detected by plate reader. (B) PI fluorescence intensity is increased after incubation with H_2O_2 (50 µM- 1 mM) detected by plate reader. (C) Hyperosmolarity increased the number of dead cells per field when measured via automated cell counting (CellC). (D) H_2O_2 increases dead/dying cell count when measured via automated cell counting. One way ANOVA was used for each experiment with comparison between the control and test groups (* P<0.05, ** P<0.005, ## P<0.05 n=8 per group)

3.2.4 Cell volume/ surface area reduced by hyperosmolarity

Hyperosmolarity can cause cell shrinkage (Duzgun et al, 1999), therefore it was decided that cell volume should form part of the endothelial cell viability experiments to determine the effect of hyperosmolarity. As can be seen in Fig 3.5 the cell volume reduction was significant after incubation with higher concentrations of mannitol (30 mM, 60 mM and 90 mM) (30 mM-*P*=0.042 60 mM-*P*=0.032 90 mM-*P*=0.019). Due to methodological restrictions in assessing the change in cell size, it was decided to use higher concentrations of mannitol than in previous experiments. It was also no longer necessary to investigate the effect of 120 mM mannitol having seen the ability of this concentration to kill cells in a 24 hour time period and seeing as how this is not a physiologically relevant concentration it was prudent to focus elsewhere. The method used for this experiment controlled for temperature (37°C maintained throughout) as this is another factor that can have contributed to a cell shrinkage response (Kajimura, 1997).

Arguably, the assay used in this experiment could be better described as a cell surface area experiment because it fails to take into account the Z-axis and therefore would not be a true predictor of cell volume. With this being said similar methods have reported the results as volume as the reduction in surface area approximates for the reduction in overall cell volume as water is lost to the extracellular fluid (Kajimura et al, 1999).

The cell shrinkage response occurred quickly and reached a plateau within 10 min (Fig. 3.5), suggesting that the acute cell volume change within minutes would not be able to explain the cell mobility change within 24 hours. Therefore, it may be more likely that alteration of intracellular signalling processes could be the main underlying mechanism for this response.

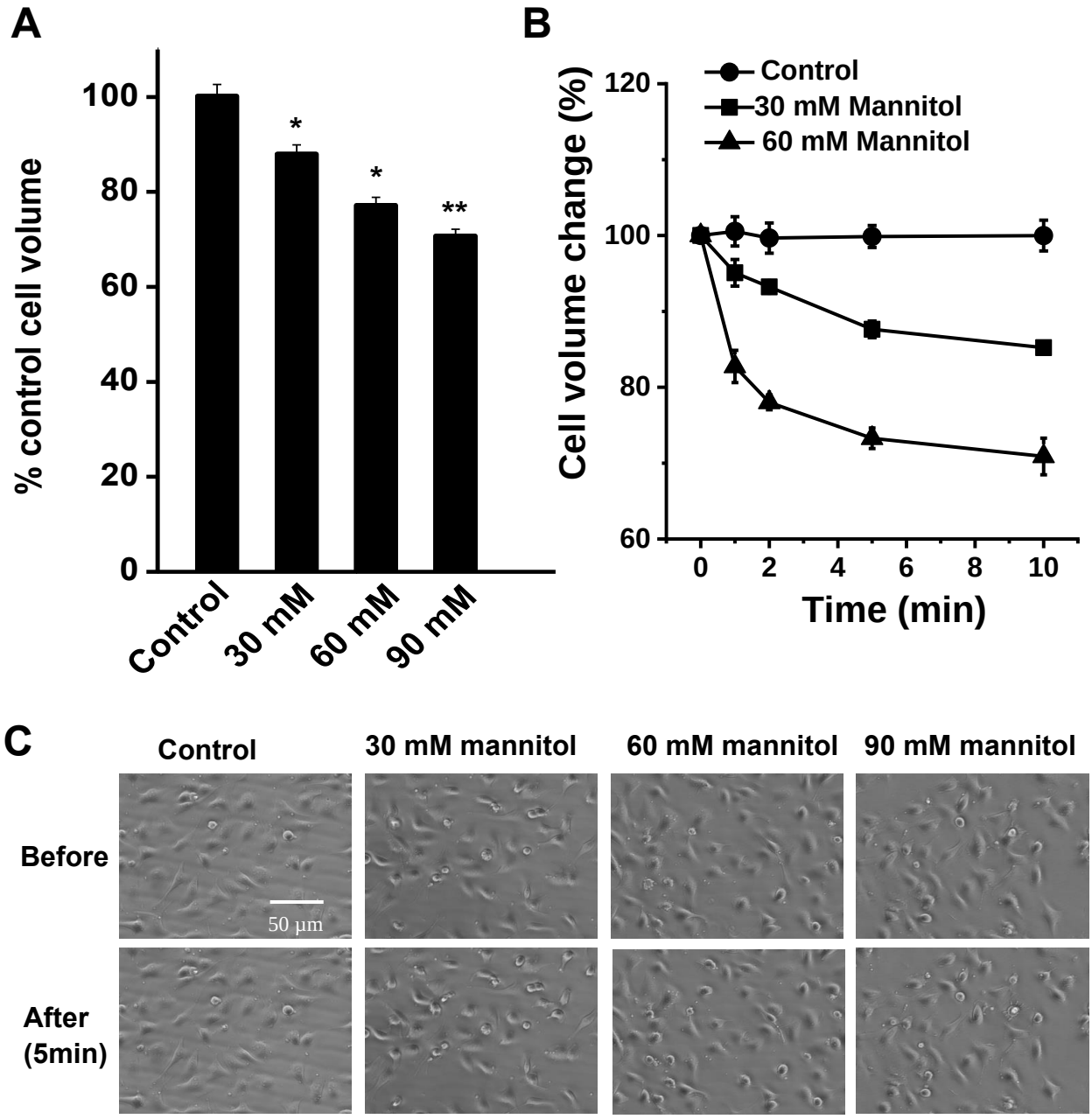

Fig. 3.5 Hyperosmolarity significantly decreases cell volume in EA.hy926 cells. (A) Mannitol at concentrations from 30 mM to 90 mM induced endothelial cell shrinkage. (B) Time course for the cell volume reduction under hyperosmotic conditions. (C) Examples of the cells (EA.hy926) before and after exposure to different concentrations of mannitol for 5 min. One way ANOVA test (* $P < 0.05$, ** $P < 0.01$, $n = 5$ wells for each group)

3.3.5 Ca^{2+} influx is sensitive to hyperosmolarity in endothelial cells

SOCE has been found to be increased in a hyperglycaemic condition (Daskoulidou et al., 2015), so it is important to observe if hyperosmolarity, a concomitant factor to hyperglycaemia, affects SOCE. The intracellular Ca^{2+} was measured by Flexstation 3 using FuraPE3 AM Ca^{2+} dye. The Ca^{2+} stores were depleted using TG (1 μM) followed by the addition of 1.5 mM Ca^{2+} bath solution to initiate SOCE.

Fig 3.6 clearly shows that mannitol is capable of reducing the peak Ca^{2+} fluorescence intensity associated with Ca^{2+} influx into the cell. A concentration of 19.5 mM mannitol was shown to significantly reduce the peak fluorescence intensity from by 35.4 % (P=0.037) and at 30 mM was shown to reduce peak intensity by 39.2% (P=0.026) both of which were compared to the negative control group. The highest concentration of mannitol (60 mM) produced a further reduction in peak fluorescence intensity of 52.3 % compared to the negative control (P=0.015). These concentrations of mannitol were chosen to reflect the breadth of hyperosmolarity that may reasonably be expected from a patient with poorly controlled diabetes as some of the other extreme values (e.g. 90 & 120 mM) would either not exist in the clinical condition or not exist in a reasonable number of patients (Wolfsdorf et al, 2014). The pre-treatment of endothelial cells with the hyperosmolar conditions had no significant effect on the peak intensity of TG mediated Ca^{2+} efflux fluorescence suggesting that it is not initial store depletion after the initial addition of mannitol that leads to diminished Ca^{2+} influx intensity. Although this technique has been adapted from (Zeng et al, 2017) who has attributed the responses to being responses in SOCE. It is important to be clear that what has been measured is Ca^{2+} influx which can be mediated by several channel types, including TRPC4 which is known to play a role in the generation of SOCE like currents (Kim et al, 2012).

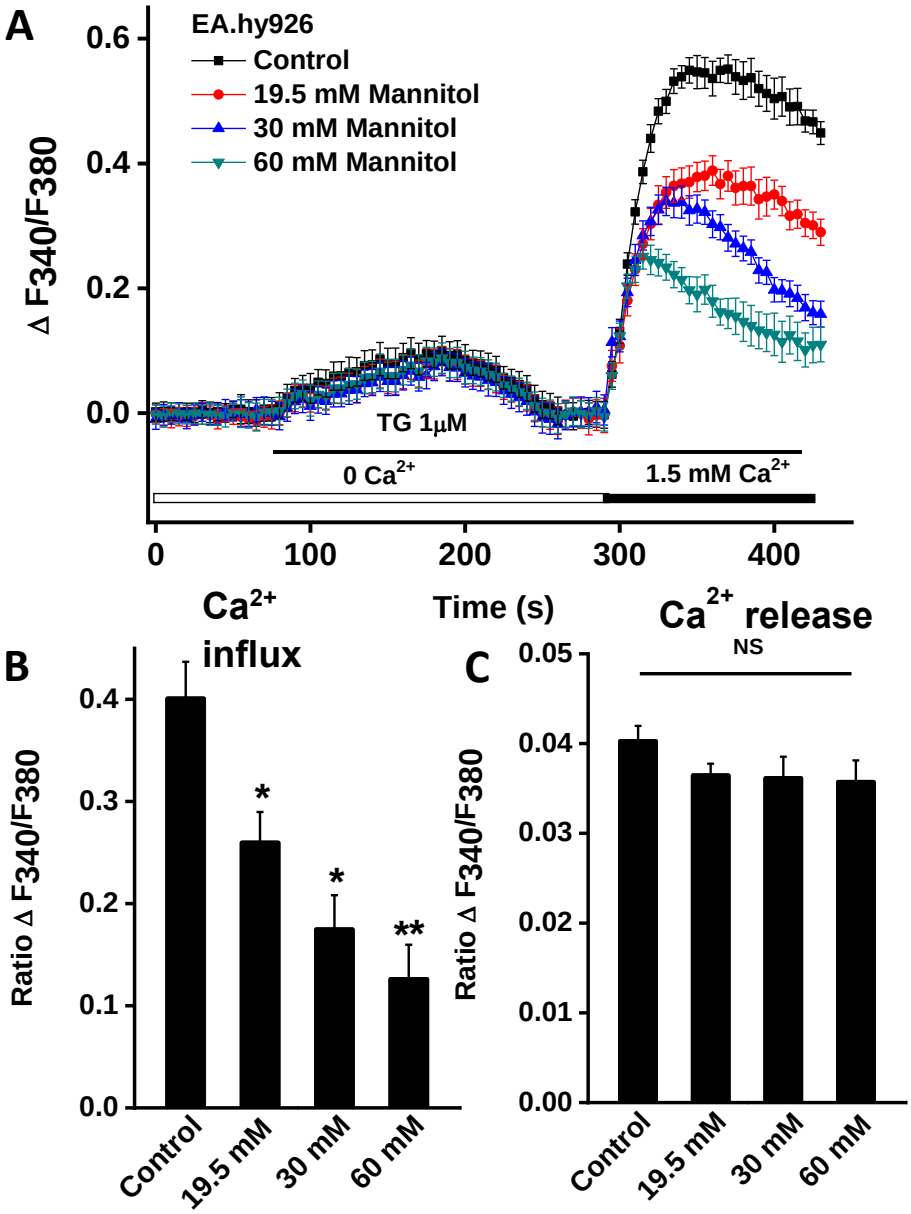

Fig. 3.6 Hyperosmolarity reduces Ca^{2+} influx and has no effect on Ca^{2+} release in EA.hy926 cells. Cells were loaded with FuraPE3-AM Ca^{2+} dye (5 μM) for 1 hr prior to experiment. Cells were treated with hyperosmolar Ca^{2+} free solution or control solution containing no additional osmolytes for 5 min prior to experiment. Intracellular Ca^{2+} stores were depleted using 1 μM TG and 1.5 mM Ca^{2+} to initiate SOCE**.** (A) Traces for Ca^{2+} release induced by TG and SOCE under hyperosmotic conditions. (B) Mean data for peak fluorescence intensity of SOCE under hyperosmolar and control conditions (C) Mean ± SEM data for peak fluorescence intensity of Ca^{2+} release (n=8 per group *P<0.05 ** P<0.01

To understand the effect of hyperosmolarity on endothelial cells in the physiological condition, the same hyperosmolarity protocol was used on primary cultured human aortic endothelial cells (HAEC). These primary cells provide a better *in vitro* model for studying the vascular endothelium because they are known to maintain the natural endothelial morphological and biochemical markers, unlike the immortalised EA.hy926 cells which are known to lack some of the key endothelial biomarkers and receptors.

As with the EA.hy926 cells the HAECs also demonstrated a reduction in the peak fluorescence intensity associated with Ca^{2+}influx, the same as was seen in the endothelial cell line EA.hy926 cells, Ca^{2+} influx was also significantly inhibited by the 5-minute hyperosmolar pre-treatment in the HAEC line (Fig. 3.7). The 19.5 mM mannitol group significantly reduced the intensity of Ca^{2+} influx associated fluorescence by 47.8% as did the 30 mM group by 54.6% compared to the negative control group (19.5 mM-P=0.02 30 mM-P=0.0412). It is interesting to note that for this experiment (as with the EA.hy926) there was no significant difference of the intensity associated Ca^{2+} efflux as triggered by the addition of TG (P=>0.05 for all groups) compared with the control group. 60 mM caused a greater percentage reduction in peak fluorescence intensity than when compared with the lower concentrations of mannitol as well as being a greater reduction than with the EA.hy926 cell experiment at 65.3% compared with the negative control group. These results suggest that the hyperosmolar condition has the ability to reduce the intensity of Ca^{2+} influx but this may not be due to a reduced Ca^{2+} efflux.

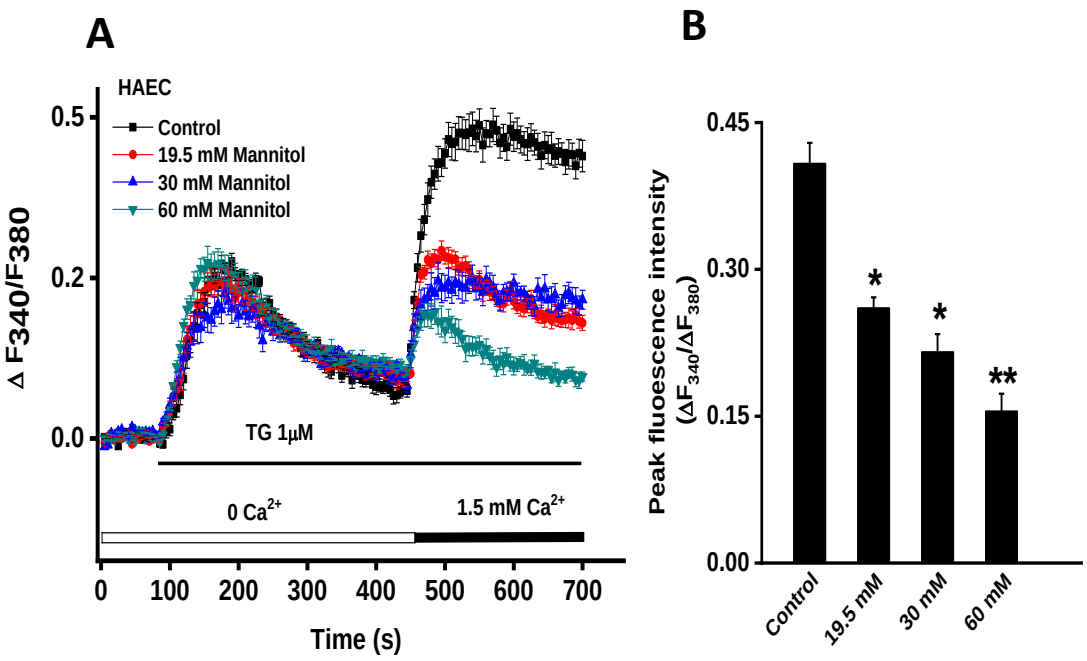

Fig 3.7 Hyperosmolarity reduces store operated Ca^{2+} release in HAEC cells. HAEC cells were loaded with Fura PE3-AM Ca^{2+} dye (5 μM) and then treated with either control or hypertonic Ca^{2+} free solution for 5 min prior to experiment after aspiration of the dye loading solution. Intracellular Ca^{2+} stores were depleted using 1 μM TG and 1.5 mM Ca^{2+} bath solution was added to initiate SOCE**.** (A) Mean florescence intensity in control and hyperosmotic groups following Ca^{2+} store depletion and SOCE. (B) Mean peak fluorescence intensity of SOCE trace in control and hypertonic groups. n=8 per group, one-way ANOVA was used to test significance $P<0.05$ $^{**}P<0.01$.

To further confirm the effect of hyperosmolarity on SOCE rather than simply on Ca^{2+} influx EA.hy926 cells underwent the experiment (exposed to 30 mM mannitol) but with the additional test included to see if TG added prior to Ca^{2+} would affect the result. As can be seen in Fig 3.8, where the cells were not treated with TG there was no significant effect of attributed to the treatment with hyperosmolarity (P=>0.05).

Although the other group that was treated with TG before the addition of Ca^{2+} showed a robust reduction in Ca^{2+} influx by 42.7% (P=0.015). Suggesting that the sensitivity of Ca^{2+} influx intensity to hyperosmolarity is dependent upon the emptying of ER Ca^{2+} stores before the re-introduction of Ca^{2+} into the system, this would be characteristic of the STIM/Orai SOCE apparatus (Feske et al., 2006). Something that is also worth noting within Fig 3.8 is the fact that the 30 mM osmolarity + TG group showed a quicker recovery to baseline than with the negative control group. This could be due to the mannitol hyperosmolar condition causing cytoskeletal or ER changes resulting in a quicker Ca^{2+} efflux signal. Although this is speculative and based only on the importance of cytoskeletal rearrangement for the activation of these channels (Babich and Burkhardt, 2013). There is no significant difference between the peak TG related fluorescence (P=0.124) although this difference in intensity does become significant at 250 seconds (P=0.048).

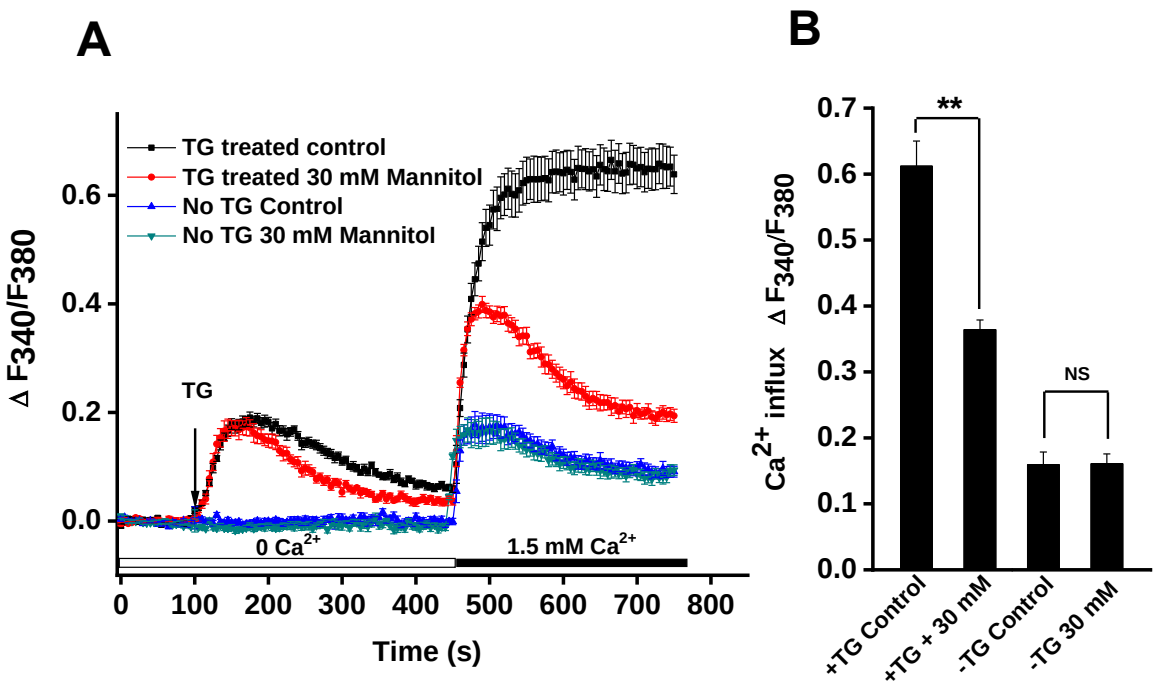

Fig. 3.8 Hyperosmolarity impairs SOCE, but not non-store depleted basal Ca^{2+} entry. TG (1 µM) was added prior to 1.5 mM Ca^{2+} being added in order to deplete ER Ca^{2+} stores in the store depleted groups. (DMSO vehicle control**)** was used in the non-TG treated groups. All cells were loaded with FuraPE3-AM dye for 30 min prior to experiment. (A) FuraPE3-AM dye fluorescence intensity of cells treated with mannitol compared to control both with and without pre-treatment with TG. (B) Control and 30 mM mannitol groups from both the TG-treated groups and the vehicle control (no-TG) groups. One way ANOVA used to determine significance group $^{**}P<0.01$ $n=8$

3.2.6 SOCE in endothelial cells is mediated by Orai channels

Fig 3.9 shows the results of the Orai 1-3 siRNA transfection on the intensity of the Ca^{2+} efflux and influx in EA.hy926 endothelial cells. There was no significant difference in peak TG induced ER Ca^{2+}efflux between any of the Orai siRNA transfected groups (*P*=>0.05 for all groups). Fig 3.9 shows that the Ds-red transfection efficiency tracer did not have a significant effect on the intensity of peak Ca^{2+} intensity, thereby suggesting that the lipofectamine 3000 transfection protocol did not have a significant effect on the Ca^{2+} dynamics of these cells which are in line with other published literature (Li et al., 2019). The Orai-1 siRNA had the greatest effect on the intensity of Ca^{2+} influx, reducing peak intensity by 64.83% compared with the negative control, a result with reached significance (*P*=0.0011).

The Orai 2&3 siRNA transfected cells showed a significant reduction in peak Ca^{2+} influx (21.3% and 29.8% reduction compared to control respectively). Although both Orai 2&3 transfection did not cause as great a reduction as observed in the Orai 1 siRNA transfected cells. As is to be expected, none of the siRNA transfections completely prevented the Ca^{2+} influx response. This is because it is known that no singular Orai subtype will be responsible for the entirety of the SOCE response (Barr et al., 2009), but also these cells are known to express Orai 1-3 proteins (Zeng et al, 2017). As well as other Ca^{2+} channels that are known to contribute to the store-operated influx response such as TRPC channels (Kin et al, 2012)

Orai 1-3 genes are required for the full generation of the classical SOCE response to ER Ca^{2+} store depletion (Bogeski et al., 2010). The strength of influx inhibition associated with the three siRNA's confirms the classical model of Orai subtype expression in human cells is found in these EA.hy926 cells (Mercer *et al.*, 2006). This data shows us that it is likely that Orai 1 is the predominant subtype responsible for the generation of the SOCE current in the EA.hy926 cells. It is also apparent that the Orai 2&3 variants contribute to this SOCE signal to a lesser extent as can be seen by the relatively small reduction of SOCE intensity associated with the Orai 2&3 subtypes in the siRNA transfections reported in Fig. 3.8.

It is apparent that the EA.hy926 cell line expresses Orai 1-3 genes as well as the STIM proteins that would be needed to allow for the SOCE signal (although not directly measured in the previous experiments). EA.hy926 cells are a well-established endothelial cell model although it is recognised that there are limitations in how applicable results generated with these cells are to human cells *in vivo* due to the potential loss of some endothelial markers with prolonged culture time (Bouïs *et al.*, 2001). Endothelial cells are not the only cell type that would be susceptible to fluctuations in plasma osmolarity; several other tissues would be considered as important in the osmotic response in the body such as in the kidney.

For this reason, the same experimental conditions were applied to the human proximal tubular cells (HK2 cells). These HK2 cells are used as a common *in vitro* model for investigations into kidney damage in diabetic nephropathy (Panchapakesan et al, 2004). They were selected to understand whether hyperosmolarity could effect a functionally and morphologically distinct cell type, which still has physiological relevance to clinical hyperosmolarity.

As shown in Fig. 3.10, Orai 1 siRNA transfection significantly reduced the intensity of Ca^{2+} influx by 57.6% (*P*=0.012). Orai 2 & 3 transfection also significantly reduced the intensity of Ca^{2+} influx although to a lesser degree than with Orai 1 (13.6% & 13.7% respectively). Fig 3.10 also shows that there is no significant difference between the groups that were transfected with Orai 1-3 siRNA and the control group in respect to TG induced Ca^{2+} efflux. The second graph in Fig 3.10 shows that the hyperosmolar conditions found to reduce Ca^{2+} influx intensity in EA.hy926 cells also reduced the intensity of Ca^{2+} influx in HK2 cells. Both 19.5 mM and 30 mM mannitol were shown to reduce the peak intensity of Ca^{2+} influx by 23.2% and 24.1% respectively (*P*=<0.05 for both groups compared to negative control).

60 mM mannitol caused the greatest reduction of peak Ca^{2+} influx intensity (67.5% reduction compared to negative control) (*P*=<0.01). One particularly interesting finding from applying the hyperosmolar stimuli to the HK2 cells was that there was also a significant reduction in the peak intensity of TG induced Ca^{2+}efflux) (*P*=<0.01). This is different from the findings described earlier in the Ea.hy926 cells, which showed no such response this is discussed in greater detail within the discussion section of this chapter.

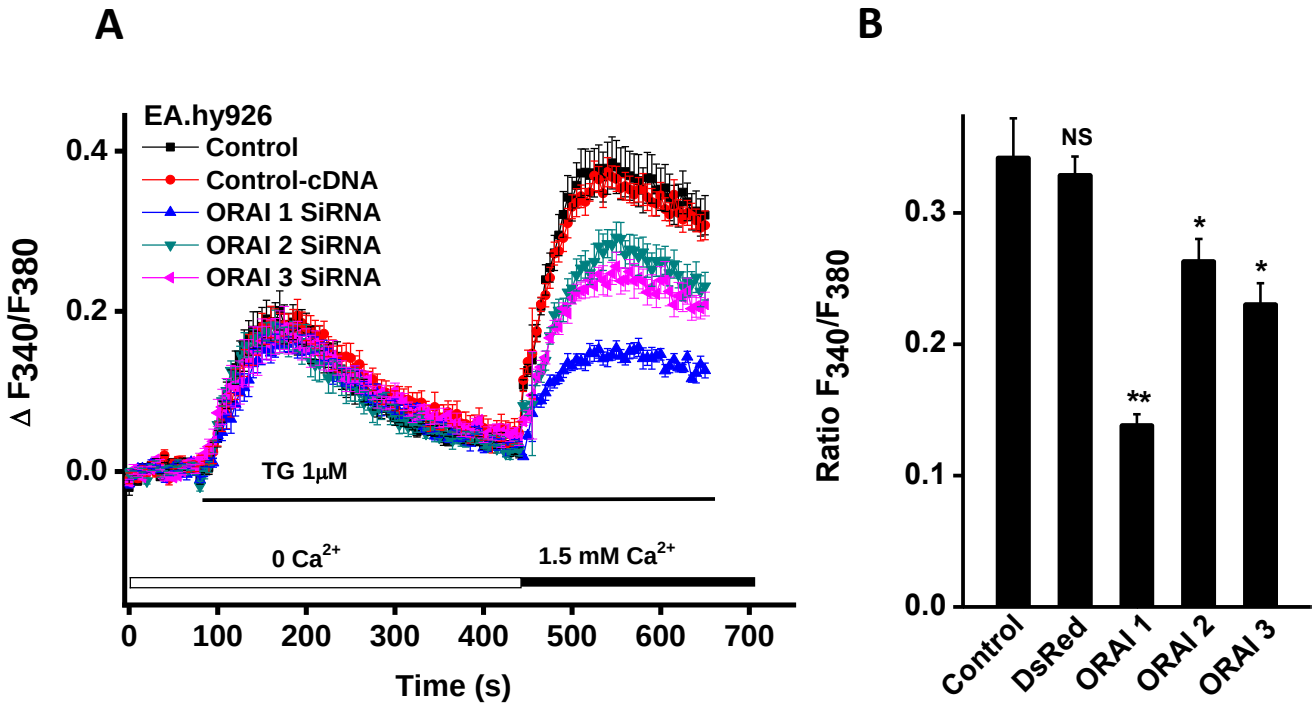

Fig. 3.9 SOCE intensity is reduced in EA.hy926 cells after 48 hr transfection with Orai siRNAs. (A) Mean fluorescence intensity (340/380nm) of FuraPE3-AM intracellular Ca^{2+} dye following Ca^{2+} store depletion and activation of SOCE following transfection with the three Orai subtype targeted siRNAs. (B) Comparison of mean peak intensity of store-operated Ca^{2+} influx between transfected and un-transfected groups. The data were analysed with one-way ANOVA n=8 per group *P<0.05 **P=<0.01

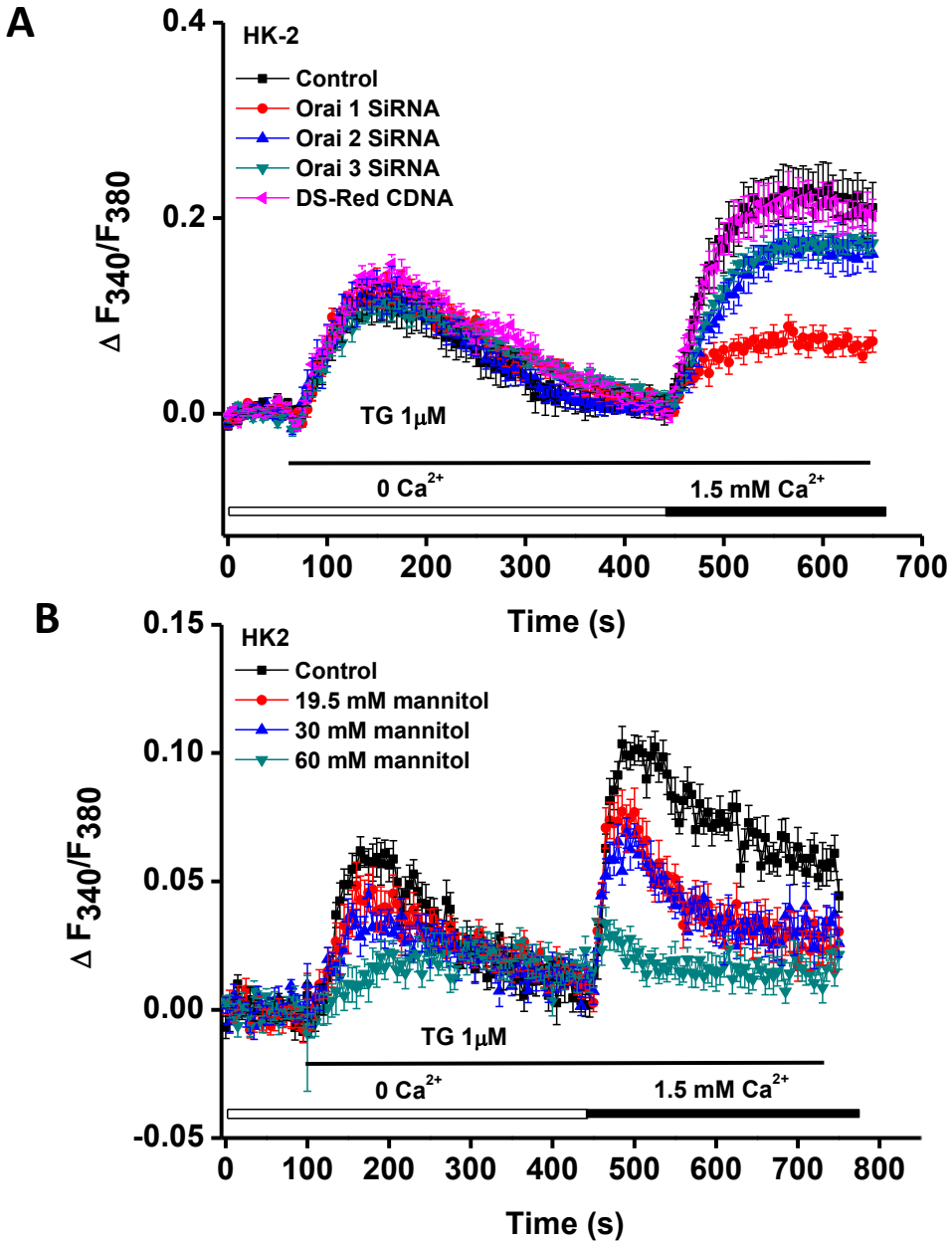

Fig. 3.10 Hyperosmolarity reduces store operated Ca^{2+} entry in HK2 cells. Cells were loaded with FuraPE3-AM dye (5 μM) and were pre-treated with hyperosmotic Ca^{2+} free bath solution for 5 minutes before addition of TG and 1.5 mM Ca^{2+} solution. (A) SOCE in HK2 cells after transfection with siRNAs targeting the Orai-3 genes for 48 hrs. (B) Effect of hyperosmolarity on SOCE in HK2 cells.

3.3 Discussion

Hyperosmolarity, as induced by the addition of mannitol, reduced endothelial cell migration by 43.4% compared to the negative control group (P=<0.01) (Fig 3.1). This same condition was found to be capable of increasing the proportion of dead cells per well as seen in figures 3.2 and 3.3 but it did not affect endothelial cell proliferation as seen in Fig. 3.4. The hyperosmolar condition was also seen to reduce endothelial cell volume/surface area by 22.3% compared to the negative control group (60 mM at 10 minutes), although this reduction in cell surface area reached a plateau following 10 minutes treatment with the hyperosmolar condition. This data indicates that hyperosmolarity, such as that observed in diabetic HHS, has the potential to negatively affect the cells that make up the vascular endothelium and therefore could contribute to the vascular complications of DM. This finding is supported within other published material regarding endothelial cell function (Luh et al, 1996).

The methodology used to assess endothelial cell viability in this chapter paints a broad picture of the effects of hyperosmolarity although it must be stated that these methods may not be as sensitive or as precise as others available. For example, propidium iodide has been challenged as a tool used to detect apoptosis as it has been found stain necrotic cells as well as pre-apoptotic cells (Loo & Rilliema, 1998). Similarly, the scratch wound healing assay has been challenged within publications with regards to its potential for observer bias as well as questions being raised over whether this scratch model is a better model for injury response rather than true “migration” due to the continued presence of extracellular matrix in the “wound” (Hellewel et al, 2017).

The experiments reported in this chapter have attempted to control for observer bias wherever possible and arguably the results of the migration assay are just as significant if they pertain to injury rather than true migration. As this is something that is impacted by hyperglycaemia and the effect of osmolarity would therefore still be a reasonable line of investigation. This is because it is known that diabetic patients have a decreased ability to recover from vascular injury and the results presented in this chapter (Fig 3.1) may suggest that elevated osmolarity could be a contributing factor, although much more in-depth work would need to be performed to make this conclusion fully (Okonkwo and DiPietro, 2017).

The increased cell death seen under the hyperosmolar condition is interesting as it may indicate that cell death can be triggered by prolonged hyperosmolarity, separate from the metabolic changes associated with hyperglycaemia as previously reported in (Meng et al, 2014). The increase in cell death caused by hyperglycaemic conditions seen in this chapter is similar to that found in previous studies investigating ways to prevent this damage (Wu et al., 1999). Prolonged hyperosmolarity is known to be damaging to cells although this evidence helps us to see that hyperglycaemia is capable of having a deleterious physical effect due to its ability to raise osmolarity (Amin et al., 2008).

The major conclusion that can be made from the endothelial cell viability data reported in Figures 3.1-5 is that hyperosmolar condition is capable of significantly altering some of the key cellular processes needed to maintain an optimum physiological environment. This data does add to the published work on the effect of hyperosmolarity on endothelial cell viability, although ideally some additional methods would be employed to better understand and confirm this effect, for example, the use of fluorescence assisted cell sorting in order to determine the effect of hyperosmolarity on apoptosis specifically as opposed to cell death (Fig 3.3,4).

As the cell shrinkage response did not appear to be capable of causing the changes in endothelial cell motility and cell death due to the adaptive response of the cells (Fig 3.5) it was therefore prudent to investigate intracellular processes what may be affected by the hyperosmolar conditions.

Data presented in figures 3.6-7 of this chapter identified that the hyperosmolar condition that caused the alteration in cell viability also reduced the peak intensity of Ca^{2+} influx in EA.hy926 cells (35.4% reduction compared to negative control). This is a novel finding within the field and does offer a potential mechanism by which the hyperosmolarity was altering the function of the endothelial cells as it is known that a reduction in Ca^{2+} signal intensity can lead to cell death and inhibited migration.

The Ca^{2+} influx experiments reported in this chapter utilised a methodology that although published as a SOCE measurement method it may be better termed a store-depletion dependant calcium influx measurement (Zeng et al, 2017). This is because what is being measured is the changes in cytoplasmic Ca^{2+} concentration not the direct activity of the SOCE channels. This is why a siRNA knockdown of the Orai channels was performed (Fig. 3.8) as this confirmed that the intensity of Ca^{2+} influx was reduced when the Orai channels were knocked down. This knockdown showed reductions in intensity that conformed to the known proportion of Orai expression in non-excitable cells (Li et al, 2019), with Orai 1 siRNA producing the greatest reduction in Ca^{2+} influx (>50%) and with Orai 2&3 siRNA's producing a less dramatic reduction in Ca^{2+} influx.

These results increase the confidence that what was observed in earlier experiments in regards to the reduction in Ca^{2+} influx would be due, at least in part, to the alteration of Orai channel activity. Even though other channels are known to contribute to the SOCE process, for example, TRPC (Kim et al, 2012) it is known that the Orai channels are the major contributors as other work has shown that when all three channels are inhibited or silenced the SOCE signal is undetectable (Li et al, 2019). As such further investigation into the effect of hyperosmolarity on Ca^{2+} will focus upon the SOCE apparatus STIM/Orai.

Data shown in this chapter provides evidence that the effect caused by the hyperosmolar condition is dependent upon the depletion of ER Ca^{2+} by TG indicating that alterations in the Store-Operated Ca^{2+} channels have caused the change in Ca^{2+} dynamics (Fig. 3.8). The Ca^{2+} entry observed in the non-store-depleted group is significantly lower in intensity when compared with the store-depleted group (P=0.0256) which suggests that this entry effect would not be capable of confounding the SOCE response. This is an important finding when we consider the number of non-store operated Ca^{2+} channels that are capable of producing a similar signal (Moccia et al., 2015).

HAEC cells were used to confirm the results of the hyperosmolar experiments because these primary cells more closely model the *in vivo* endothelium due to these cells coming directly from human aortic tissue (Sprague et al, 1997). The data presented in this chapter shows that the SOCE reduction effect caused by hyperosmolarity is not unique to EA.hy926 cells but is also seen in the primary HAEC cells. This finding may provide evidence that this effect may not just be experimentally exciting but could be of clinical interest due to seeing this effect in primary human cells that are a very well-established cellular model of the aortic endothelium (Sprague et al., 1997).

One of the impressive results reported in this chapter is the effect that extreme hyperosmolarity (60 mM mannitol) has not just on Ca^{2+} influx but it also appears to reduce the intensity of the store-release signal (initiated by TG) in HK2 cells. This may mean that these cells could be more sensitive to the stimulus, perhaps due to more significant changes in cell volume as these cells are smaller in surface area than EA.hy926 cells. 60 mM mannitol is without a doubt an extreme hyperosmolar condition and such extreme hyperosmolarity would be exceptionally rare within even the poorly controlled diabetes disease state. So, although this result is interesting in comparison to the EA.hy926 cell results it is important to note that this condition may not occur easily within the real body situation.

HK2 cells were also used in these experiments to determine if a cell type that would be key in the regulation of hyperosmolarity is also affected by the hyperosmolar condition (Panchapakesan et al., 2013). The HK2 cells are a cell line derived from the proximal tubule and as such, it is a cell type that would be of interest when assessing the impact of hyperosmolarity on these cells. This is because of the role that the proximal tubule plays in the reabsorption of various substances (and of course pH regulation) but the proximal tubule is of particular interest in the progression of diabetic nephropathy (Vallon, 2011). It was therefore interesting to see in Fig. 3.10 that the intensity of peak Ca^{2+} influx was significantly reduced by pre-treatment with the hyperosmolar condition.

Although the response was less profound in the HK2 cells (reductions of ~20% compared with negative control) there was still a significant reduction in SOCE intensity under the hyperosmolar condition, indicating that the response is not cell-type specific and that this effect could be capable of causing damage to cells of several tissue types and not just the vascular endothelium.

These findings provide evidence that hyperosmolarity is capable of reducing the peak intensity of SOCE; although interestingly the hyperglycaemic conditions reported in (Daskoulidou et al., 2014) increased the intensity of SOCE whereas the hyperosmolar condition used in these experiments decreases the intensity of SOCE.

One potential reason for this difference could be that the Orai channels are osmosensitive but this osmosensitivity is overcome in the hyperglycaemic conditions alterations in cell signalling. Another reason for the difference in response between the hyperglycaemic and hyperosmotic stimuli could be the fact that glucose can enter the cells and change intracellular pathways whereas the mannitol used as the hyperosmolar agent is not able to be taken up by the cells, therefore, producing a greater cell shrinkage response and possibly altering SOCE through an alternative pathway.

To summarise, the major findings presented in this chapter were first that the hyperosmolar stimuli reduces the migration of endothelial cells as well as increasing their rate of cell death compared to the control. Secondly, the hyperosmolar condition reduced the peak intensity of SOCE in endothelial cells and proximal tubule cells. These findings warrant further investigation to ascertain the role of the Orai/STIM apparatus in the generation of this reduced SOCE effect.

Chapter 4

Hyperosmolarity reduces SOCE through modulation of Orai 1-3 channels

4.1 Introduction

In chapter 3, it was found that hyperosmolarity reduces the migration of endothelial cells and increases cell death (Figures 3.1-3.5). Such effects are associated with a significant reduction in peak Ca^{2+} influx intensity (Fig 3.6-9) in the EA.hy926 endothelial cell model. This is a novel finding and warrants a more detailed investigation into the effects that this hyperosmolar condition has on the specific SOCE apparatus-STIM/Orai. As discussed in the previous chapter the experiments performed to determine the effect of hyperosmolarity on TG induced Ca^{2+} efflux and influx could not be considered specific to the activity of the Orai channels because only Ca^{2+} movement and concentration was being measured (Daskoulidou et al, 2015).

In order to understand the effects of hyperosmolarity on individual Orai subtypes, the inducible expression system TREx Orai mCherry GFP STIM will be used in this chapter. The HEK T-REx cells overexpressing Orai1/STIM1, Orai2/STIM1 and Orai3/STIM1 will be tested under the hyperosmolar condition. One aim behind using these transfected cells is to see whether specific subtypes of the Orai channel are more susceptible than others to the hyperosmolar condition, as this would provide a greater understanding as to which subtype may be producing this effect within the endothelial cells (Figures 3.5-9). It is not unreasonable to expect different responses in the subtypes because structural differences between the variants are known to lead to unique pharmacological modulation of these channels (Bogeski et al, 2012). For example, 2-APB is a potent inhibitor of Orai 1&2 but has been found to be a highly selective activator of Orai 3,(Bernhard et al, 2018), we, therefore, may postulate that any sensitivity to osmolarity could likewise be affected by the structural variations present in the Orai subtypes.

An investigation was also performed into whether the Orai/STIM channels are contributing to the surface area reduction response that was observed in the EA.hy926 cells (Fig 3.4). This was done in order to see whether the modulation of SOCE under the hyperosmolar condition is due, in part; to an effort to limit cell volume changes as Ca^{2+} could one of the osmolytes lost by the cell under the hyperosmolar condition.

Other work reported on in this chapter includes the initial investigation into pharmacological agents in order to ascertain any protective effect that they may have on against this reduction of SOCE under hyperosmolar conditions. The two compounds screened were mibefradil and TH1177. These are both T-type voltage-gated Ca^{2+} channel blockers that are known to have off-target effects (Viskoper et al., 1997) for example, mibefradil is known to inhibit the activity of the K^+ channel Kv10.1 (Wang et al., 2017). Another off-target effect of mibefradil and TH1177 which is now used clinically is in the reduction of proliferation (Lijnen et al., 1999). As such this drug is now being explored as an anti-cancer drug (Cove-Smith et al., 2013). Work performed in the lab by other researchers has revealed that mibefradil and TH1177 were capable of reducing the intensity of SOCE (Li et al, 2019). Although what was not known, was the effect of higher concentrations of the compound on SOCE. Because the SOCE proteins are known to respond differently to different concentrations of pharmacological inhibitors/activators (Bogeski et al, 2010) it is postulated that a high dose of these compounds could offer a protective effect against the reduction in SOCE under hyperosmolarity.

1st Hypothesis- Hyperosmolarity will reduce the intensity of SOCE in HEK cells overexpressing Orai-1-3/STIM1

2nd Hypothesis- The overexpression of these channels will increase the intensity of hyperosmolarity related cell shrinkage

3rd Hypothesis- High dose mibefradil/TH1177 will offer a potential protective effect against hyperosmolarity by increasing the intensity of SOCE

4.2 Methods

The HEK-296 cells used in this experiment were transfected using the pcDNA4/TOSPI tetracycline (Tet) regulatory vector system in a process published by (Zeng et al, 2017). The genes transfected were Orai 1-3 (GenBank accession numbers: Orai1, NM_032790; Orai2, NM_032831; Orai3, NM_152288) as well as all transfected cells being transfected with STIM 1 (GenBank accession number: NM_001277961). The Orai genes were tagged with the mcherry fluorescent protein marker and the STIM 1 gene was tagged with green fluorescent protein (GFP), this allowed for visual confirmation of overexpression under fluorescence microscopy prior to experimentation. Native (un-transfected) HEK 293 cells were used as the true "negative control group" in these experiments as well as the un-induced transfected cells. This is because the STIM-1 gene is not induced by the presence of tetracycline, unlike the Orai genes meaning that even though the Orai channels would not be overexpressed in the non-Tet control group there could still be a confounding effect caused by the overexpression of STIM/1. All negative control groups used in this experiment also contained 1 µM tetracycline in order to ensure that this did not have an effect in and of itself on the outcome of the experiments.

The negative control groups also did not contain any additional mannitol. Cell volume experiments were performed according to the protocol described in the Methods section of this thesis. The high concentration of mibefradil and TH1177 (100 µM) used in the compound test experiment was decided upon because the EC_{50} of this compound was found to be 3.6 µM by other researchers (Li et al, 2019). As such, it was decided to use a concentration that greatly exceeded this in order to determine if such high levels could have a stimulatory effect on the activity of SOCE.

4.3 Results

4.3.1 Effect of hyperosmolarity on SOCE in T-REx cells overexpressing Orai 1 channels

Fig. 4.1 shows that the hyperosmolar condition (19.5 mM mannitol) significantly reduced SOCE in HEK 293 T-REx cells overexpressing Orai 1/STIM1 (P=0.042). This represents a relative reduction of 22.2% compared with the negative control group (no mannitol). However, the hyperosmolar condition had no effect on ER Ca^{2+} release, which was induced by TG (P=>0.05). The un-transfected (native) HEK 293 T-REx cells were used as a second negative control group, and the same hyperosmolar condition did not have a significant effect on SOCE and TG induced ER Ca^{2+} release (P=>0.05 for both groups). This data suggests that hyperosmolarity can inhibit SOCE through Orai1 channel. Interestingly when we compare the two control mannitol groups (native HEK cell- no mannitol- transfected cell overexpressing Orai 1- no mannitol) we see that the intensity of peak SOCE (Ca^{2+}influx) is 51.3% lower in the cells not overexpressing the Orai 1 channels (Fig 4.1). This indicates that the native HEK293 cells are capable of generating the SOCE signal, as seen in other published data (Daskoulidou et al 2015) but this is significantly increased in the HEK293 cells that are overexpressing the Orai 1 channel (P=0.0015).

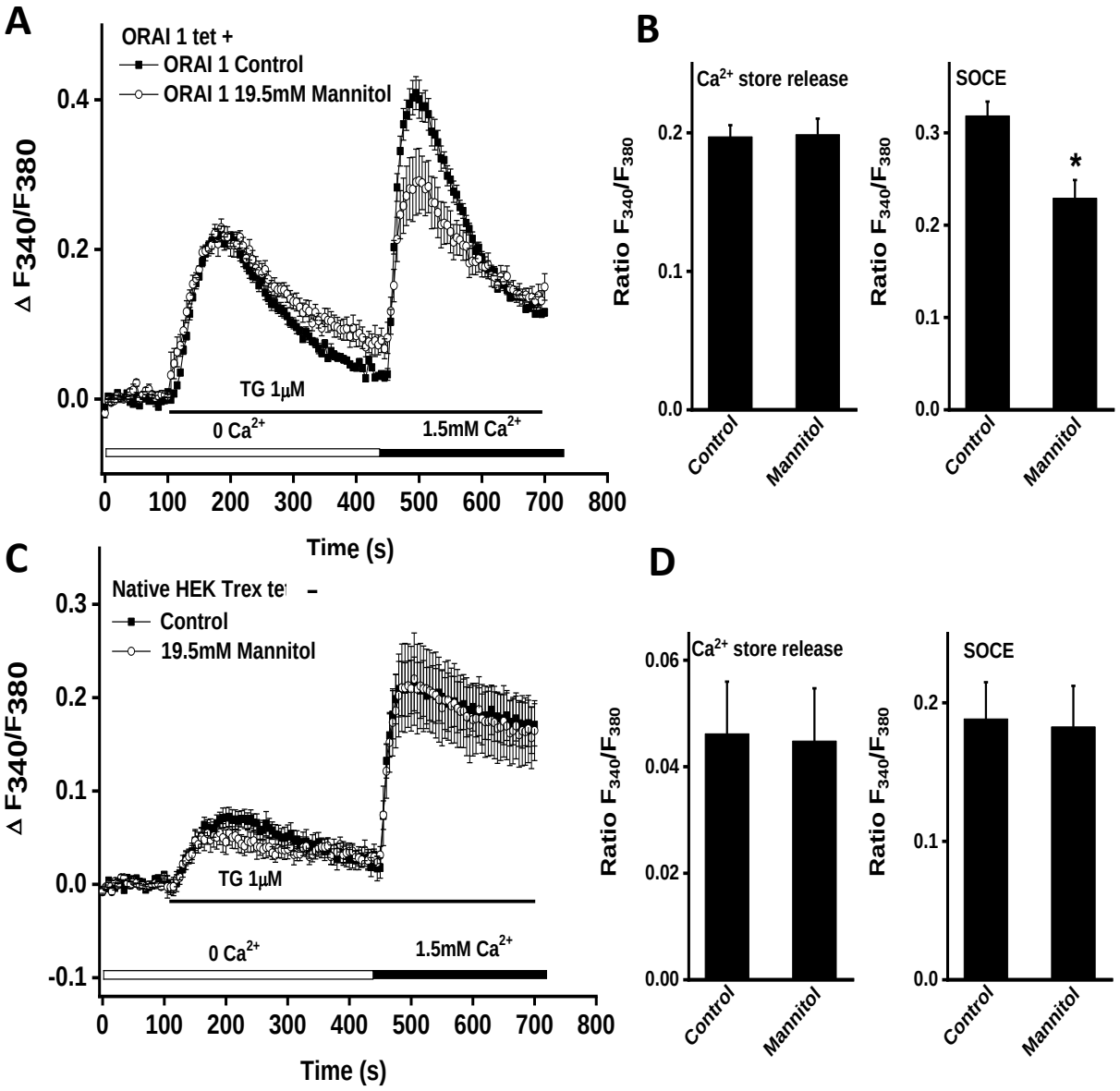

Fig. 4.1 Hyperosmolarity reduces SOCE via Orai1 channels. HEK293 T-REx cells over-expressed STIM1/Orai1, which was induced by 1 μg/ml tetracycline. Two control groups were used, firstly the cells overexpressing Orai 1 are compared to a no mannitol control, secondly non-transfected cells were also treated with the mannitol or no-mannitol condition .Cells were loaded with 5 μM Fur PE3-AM Ca^{2+} dye and detected by Flexstation 3. Both transfected and un-transfected cells were pre-treated with 19.5 mM mannitol or control for 5 min prior to experiment **(**A) Mean fluorescence intensity in hyperosmolar and normal osmolarity control groups in Orai1/STIM1 overexpressing cells. (B) Mean peak fluorescence intensity for both Ca^{2+} store release and SOCE in STIM1/Orai 1 overexpressing cells. (C) Mean florescence intensity in hyperosmolar and control groups in un-transfected cells. (D) Mean peak fluorescence intensity for both Ca^{2+} store release and SOCE in un-transfected cells. *n*=8 wells per group * *P*<0.05

4.3.2 Effect of hyperosmolarity on SOCE in T-REx cells overexpressing Orai2 channels

Fig.4.2 shows that pre-treatment with the hyperosmolar condition (19.5 mM mannitol) lead to a significant reduction of SOCE in HEK 293 T-Rex cells overexpressing Orai 2/ STIM 1 (P=0.041). This represents a relative reduction of 33.4% compared with the co mannitol control group (Fig 4.2). The hyperosmolar condition did not have a significant effect on the TG induced ER Ca^{2+} release (P=>0.05). This indicates that this hyperosmolar effect is not effecting the release of Ca^{2+} from the cells but rather the influx of Ca^{2+}.

The same hyperosmolar condition did not have a significant effect on the peak intensity SOCE in the un-transfected HEK 293 T-REx cells used for the negative control group (P=>0.05). The peak intensity of Ca^{2+} influx within the un-transfected cells was not only not affected by hyperosmolarity but was also significantly lower than the non-hyperosmolar control group of the Orai 2 overexpressing cells (P=0.001). The intensity of Ca^{2+} influx was 44.5% lower in the non-hyperosmolar Orai 2 overexpressing cells than in the non-hyperosmolar native control cells. This not only indicates that the overexpression of Orai 2/STIM 1 is capable of increasing the intensity of Ca^{2+} influx, a well-known concept (Zeng et al, 2017) but it suggests that native HEK cells also express the SOCE proteins.

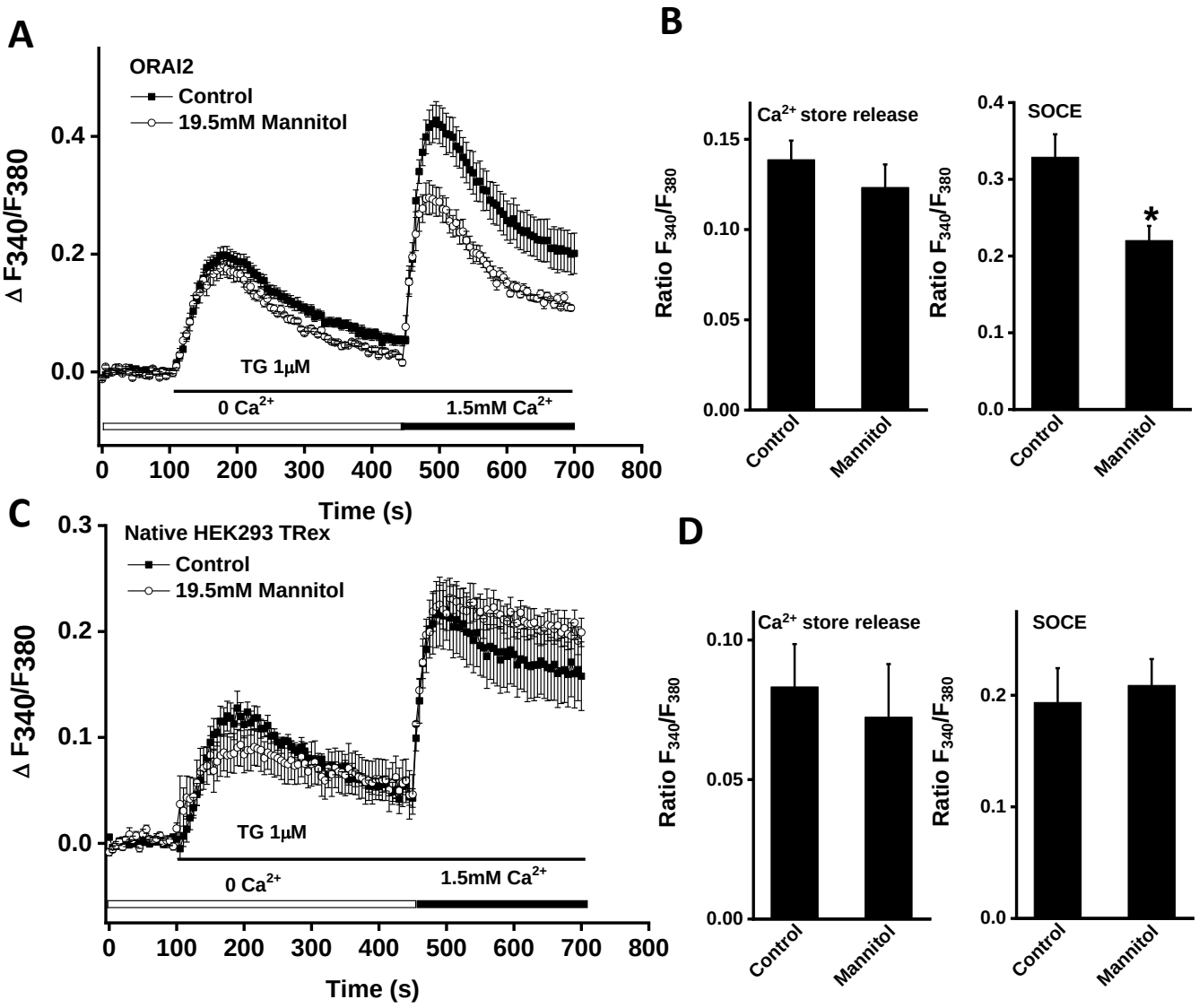

Fig. 4.2 Hyperosmolarity reduces SOCE via Orai2 channels. HEK293 T-REx cells over-expressed STIM1/Orai2, which was induced by 1 µg/ml tetracycline. Two control groups were used, firstly the cells overexpressing Orai 2 are compared to a no mannitol control, secondly non-transfected cells were also treated with the mannitol or no-mannitol condition. Cells were loaded with 5 µM FuraPE3-AM Ca^{2+} dye and detected by Flexstation 3. Both transfected and un-transfected cells were pre-treated with 19.5 mM mannitol or control for 5 min prior to experiment **(**A) Mean fluorescence intensity in hyperosmolar and normal osmolarity control groups in Orai2/STIM1 overexpressing cells. (B) Mean peak fluorescence intensity for both Ca^{2+} store release and SOCE in STIM1/Orai 2 overexpressing cells. (C) Mean florescence intensity in hyperosmolar and control groups in un-transfected cells. (D) Mean peak fluorescence intensity for both Ca^{2+} store release and SOCE in un-transfected cells. *n*=8 wells per group * *P*<0.05

4.3.3 Effect of hyperosmolarity on SOCE in T-Rex cells overexpressing Orai3 channels

Fig.4.3 shows that the hyperosmolar condition (19.5 mM mannitol) leads to a significant reduction of SOCE in HEK 293 T-Rex cells overexpressing Orai 3/ STIM 1 (P=0.032). This represented a reduction in peak Ca^{2+} fluorescence intensity of 32.6% compared to the non-hyperosmolar control group. The same hyperosmolar condition did not have a significant effect on the level of SOCE in the un-transfected HEK 293 T-REx cells used for the negative control group (P=0.980). TG induced Ca^{2+} efflux from the ER was not affected in either experimental or the un-transfected control groups (P=>0.05 for both groups). The peak Ca^{2+} influx fluorescence intensity was far greater in the HEK293 cells overexpressing the Orai 3 channel (non-hyperosmolar control) compared with the non-transfected cells (non-hyperosmolar control), this is a 46% increase in favour of the Orai 3 overexpressing HEK293 TRex cells.

It is also interesting that the peak intensity of Ca^{2+} influx in the HEK293 TRex cells overexpressing the Orai 3 channel is higher than in the other HEK293 TRex cells overexpressing the Orai 1 and Orai 2 channels (Figures 4.1-3). Orai 3 overexpressing cells had a mean peak influx intensity of 4.4 Arbitrary units (AU) whereas Orai 1 had a peak mean influx intensity of 3.1 AU and Orai 2 a mean peak of 3.4. None of these differences reached statistical significance (all groups P=>0.05) although the higher signal intensity associated with Orai 3 has been discovered and published in other work (Daskoulidou et al, 2015).

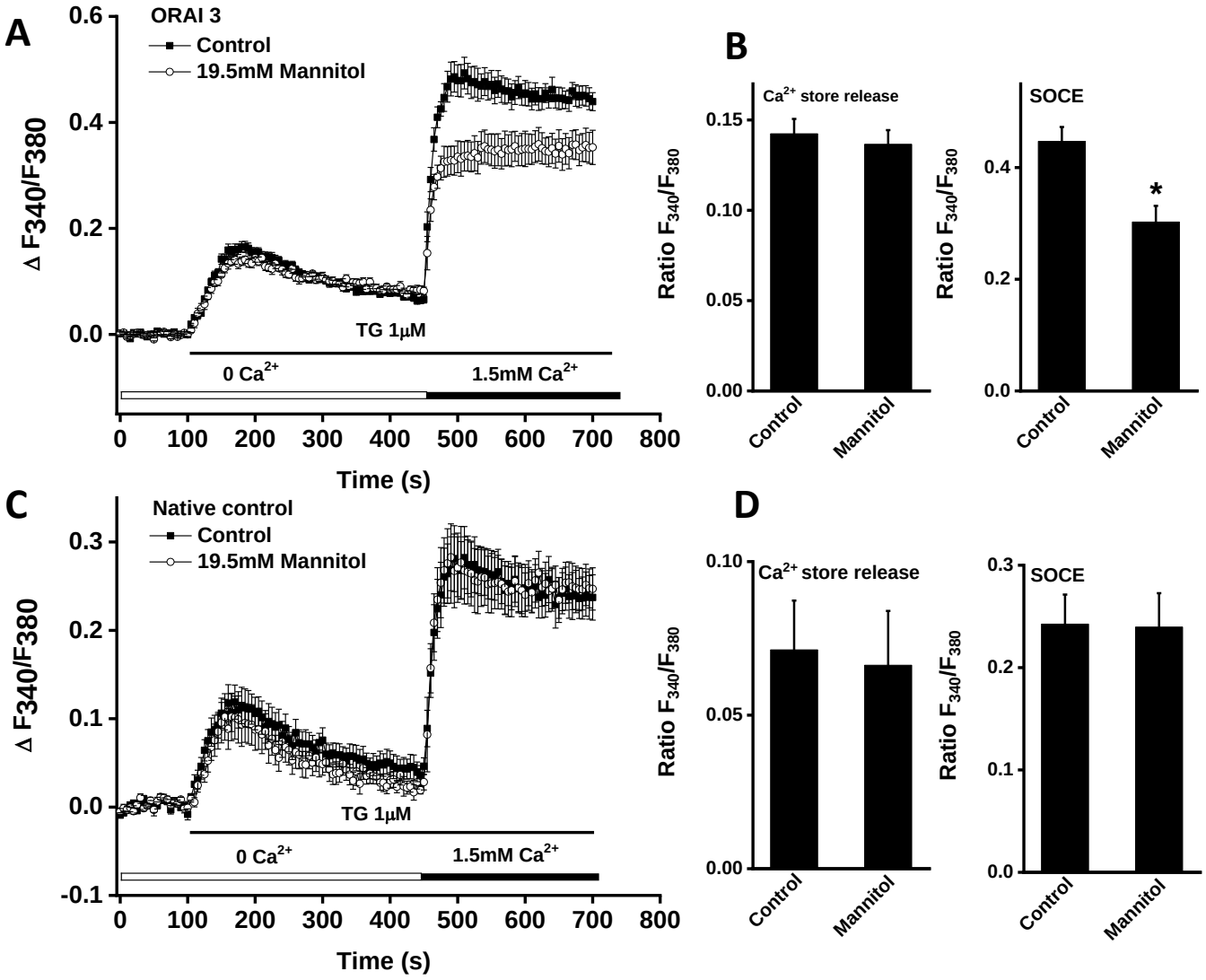

Fig. 4.3 Hyperosmolarity reduces SOCE via Orai3 channels. HEK293 T-REx cells over-expressed STIM1/Orai3, which was induced by 1 μg/ml tetracycline. Two control groups were used, firstly the cells overexpressing Orai 3 are compared to a no mannitol control, secondly non-transfected cells were also treated with the mannitol or no-mannitol condition .Cells were loaded with 5 μM FuraPE3-AM Ca^{2+} dye and detected by Flexstation 3. Both transfected and un-transfected cells were pre-treated with 19.5 mM mannitol or control for 5 min prior to experiment **(**A) Mean fluorescence intensity in hyperosmolar and normal osmolarity control groups in Orai3/STIM1 overexpressing cells. (B) Mean peak fluorescence intensity for both Ca^{2+} store release and SOCE in STIM1/Orai 3 overexpressing cells. (C) Mean florescence intensity in hyperosmolar and control groups in un-transfected cells. (D) Mean peak fluorescence intensity for both Ca^{2+} store release and SOCE in un-transfected cells. *n*=8 wells per group * *P*<0.05

4.3.4 Effect of extreme hyperosmolarity on SOCE in TREx cells overexpressing Orai 1-3 channels

Fig.4.4 shows that extreme hyperosmolarity (30, 60 & 90 mM mannitol) causes a significant reduction of SOCE intensity in HEK 293 T-REx cells overexpressing Orai 1, Orai 2 & Orai 3/ STIM 1 proteins. Within the Orai 1 overexpressing cells the extreme hyperosmolar conditions (30 & 60 mM) reduced the intensity of Ca^{2+} influx by >50% compared to the non-hyperosmolar control group (Fig 4.4 A+B). The 90 mM condition reduced the intensity of Ca^{2+} influx intensity by 91.1%, which nearly prevented the response entirely. Although this level of experimentally induced hyperosmolarity does not easily translate to the clinical condition due to its extremity, it does offer interesting insight into the powerful effect that extreme hyperosmolarity can have on the activity of these channels.

Another finding revealed within this figure is that TG induced Ca^{2+} store-release was significantly inhibited in the extreme hyperosmolar conditions. Both 30 and 60 mM mannitol groups showed a reduction of greater than 50% compared to the non-hyperosmolar control, and the 90 mM mannitol group demonstrated a 73% reduction compared to control compared to the non-hyperosmolar control group (all results significant at the P=<0.001 level). This same significant reduction on Ca^{2+} store release was observed in all of the subtype variant (Orai 1-3) overexpressing HEK293 TRex cells.

Such reductions in TG induced efflux intensity have been described before in experiments in rat liver explants having significant alterations made to their circadian rhythms (Ref Ruiz 2011). In addition to this, work done by Jan *et al* revealed that the antifungal agent econazole is capable of inhibiting this TG induced release of Ca^{2+} from the ER of dog kidney cells (although this was due to econazole depleting the Ca^{2+} stores before the addition of TG) (Jan et al, 1999).

The Orai 3 channel can be activated by 2-APB at a 50 µM dosage (Bogeski et al, 2010). To further confirm the effect of extreme hyperosmolarity on Orai3 channels, 2-APB at 50 µM was used as an activator for Orai3 (Bogeski et al., 2010). Fig 4.5 shows that mannitol at concentrations of 30, 60 & 90 mM all showed a significant reduction in the intensity of Ca^{2+} influx as mediated by Orai 3. 30 mM mannitol yielded a 29.8% reduction in mean peak intensity compared with the no-mannitol control group. Likewise, fig 4.5 shows that 60 & 90 mM mannitol reduced the peak Ca^{2+} influx intensity by 52% & 67% respectively compared to no-mannitol control. All of the reductions from control stated reached statistical significance (P=<0.05). Because this dosage of 2-APB activates Orai 3 specifically this result suggests that the activity of the Orai 3 channel is significantly inhibited under extreme hyperosmolarity.

This adds helpful insight to the body of evidence presented in figures 4.1-5 because although they are overexpressing the Orai 1-3 channels there is still a chance that native channels may be contributing to the Ca^{2+} influx observed, all be it expected to be less than cells not overexpressing the channels. Because the 2-APB is a specific activator of this channel at the concentration used, as the evidence stands thus far, this allows us to observe that it is likely that it is this family of proteins that may be responsible for the reduction in Ca^{2+} influx in response to hyperosmolarity.

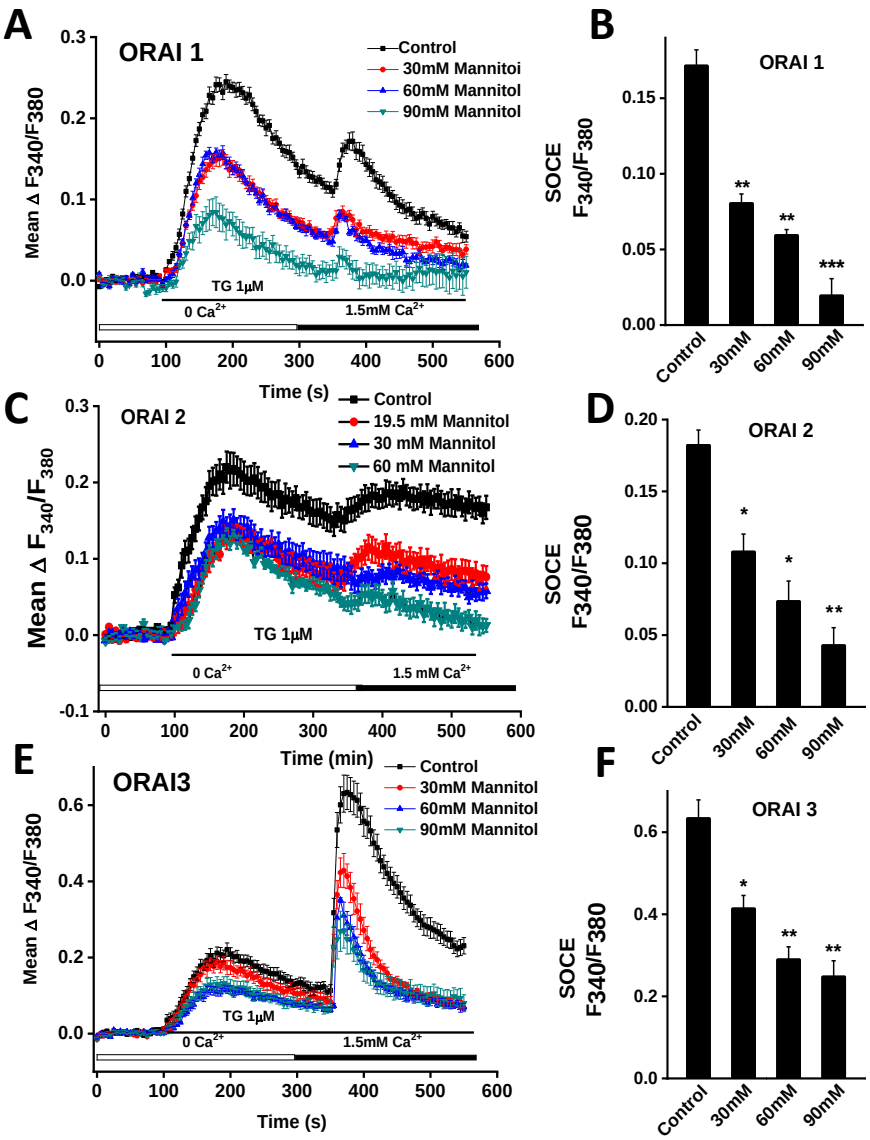

Fig. 4.4 Extreme hyperosmolarity reduces store operated Ca^{2+}entry in HEK293 T-Rex cells over expressing the STIM 1/Orai1-3. All over-expressing cells were activated using 1 µg/ml tetracycline for 24hrs prior to experiment and all cells were loaded with FuraPE3-AM dye (5 µM) for 1 hour prior to experiment. (A), (C) & (E). Charts showing normalised mean florescence intensity in hyperosmolar and control groups in Orai1-3/STIM1 overexpressing cells. (B), (D) & (F). Bar charts showing normalised peak florescence intensity during SOCE in STIM1/Orai1-3 overexpressing cells. Significant difference between groups was determined by one-way ANOVA n=8 wells per group *P<0.05 ** P<0.01 *** P<0.001

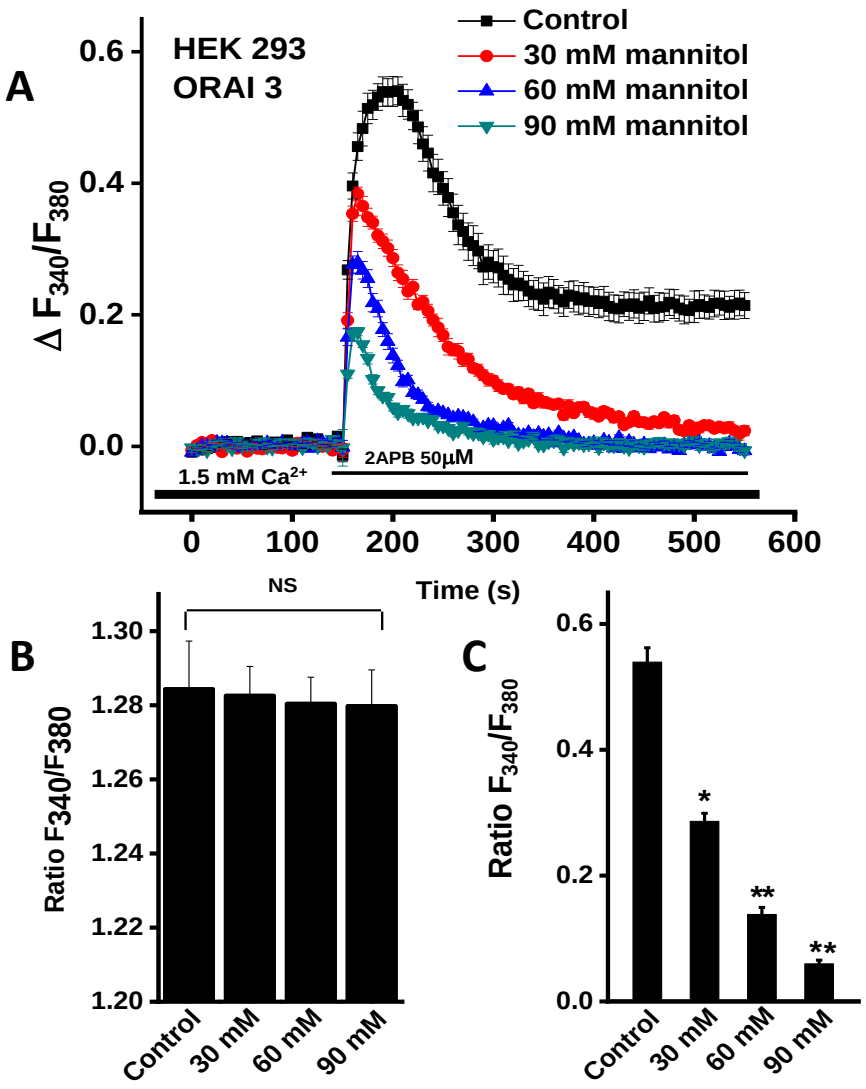

Fig. 4.5 Hyperosmolarity reduces Ca^{2+} influx in STIM1/Orai3 cells using the activator of 2APB. All cells were induced with tetracycline 1 µg/ml 24 hrs prior to experiment and the cells were loaded with 5 µM Fura PE3- AM prior to experiment. (A) Mean normalised fluorescence intensity (Δ340/380) of HEK293 T-Rex cells after the addition 2APB (50 µM). (B) Mean fluorescence intensity of all cell groups at the start of experimentation. (C) Mean peak fluorescence intensity of Ca^{2+} influx induced by 2-APB following treatment with normal or hypertonic solution. Significance was determined using one-way ANOVA (n = 8 wells per group, *P<0.05, **P<0.01).

4.3.6 Hyperosmolarity induced HEK 293 T-REx cell shrinkage is not affected by Orai/STIM overexpression

Having confirmed the effect of hyperosmolarity on the activity of the STIM1/Orai channels, the next logical step of this investigation was to see whether the overexpression of these channels affects the cell volume response, since hyperosmolarity cause cell shrinkage as shown in chapter 3. Therefore, the cell volume response experiments were performed on the HEK293 T-REx cells overexpressing STIM1/Orai. Overexpression of Orai channels did not significantly affect the cell shrinkage response to hyperosmolarity (Fig. 3.6), although the hyperosmolar conditions (30, 60 & 90 mM mannitol) did significantly reduce the surface area/volume of the cells compared with the no-mannitol control groups. For example, after 5 minutes incubation with the 30 mM hyperosmolar condition all groups, whether overexpressing Orai channels or not, demonstrated a significant reduction in surface area/volume (>10% for all groups) compared to the negative (no-mannitol) control groups.

There was also no significant difference in the shrinkage response between cells overexpressing the different Orai subtypes (Orai 1-3) at any of the concentrations of mannitol used. This suggests that there is not one specific subtype that could contribute to the cell shrinkage response more than the others and that the overexpression all subtypes is unrelated to the cell shrinkage response in response to the hyperosmolar stimuli.

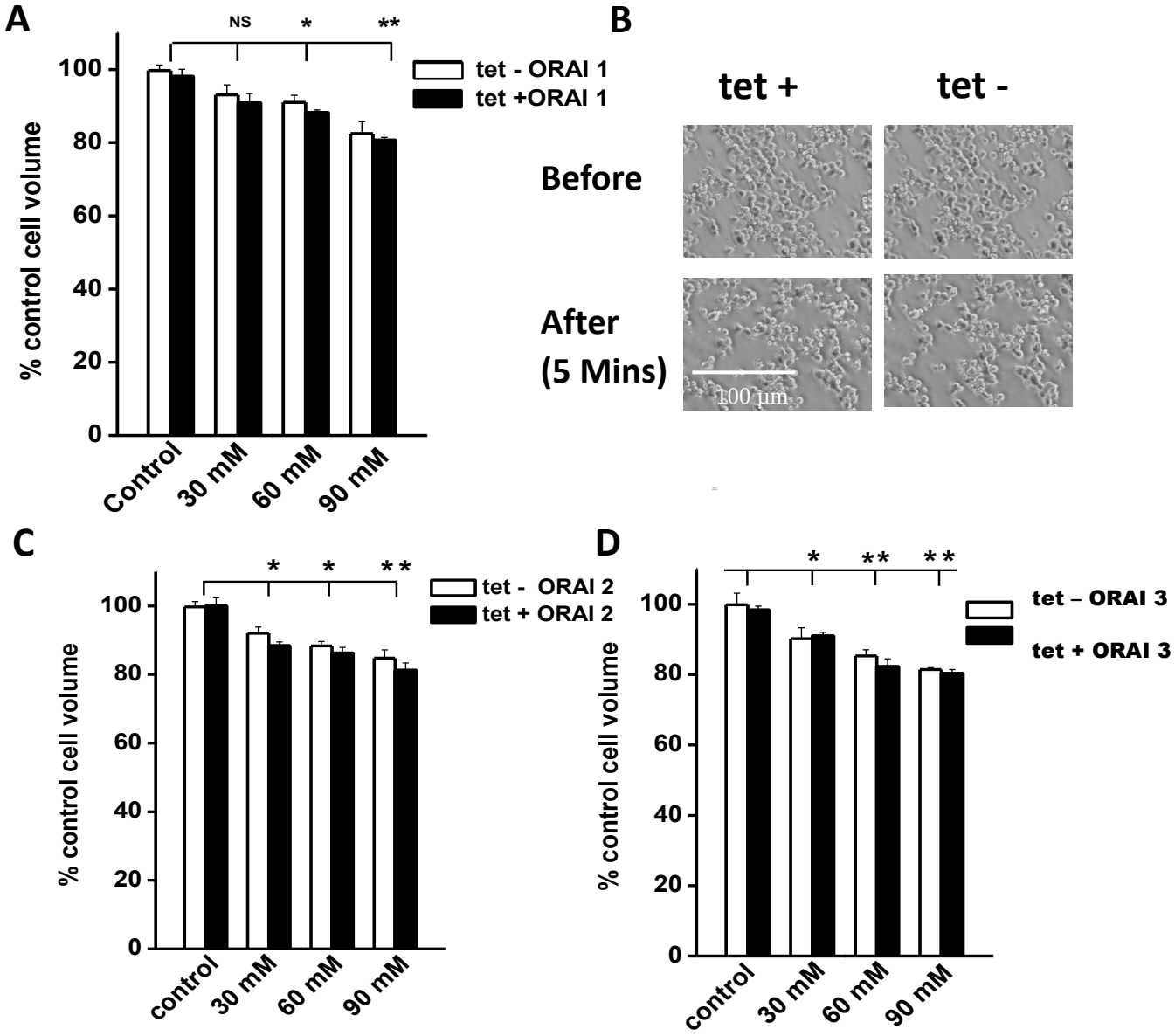

Fig. 4.6 Overexpression of Orai 1-3/STIM 1 in inducible HEK293 TRex cells did not affect the hyperosmotic cell volume response. (A) Cell volume reduction at 30, 60 and 90 mM mannitol, comparing cells over-expressing Orai1/STIM1 and non-induced (Tet-) HEK T-REx cells. (B) Examples for Orai 1 HEK 296 cell volume response to mannitol (30 mM). (C) Cell volume response to mannitol for Orai2/STIM1. (D) Orai3/STIM1 cells. One way ANOVA was used for comparison among the different concentrations of mannitol compared to the control group. T-test was also be used for comparison between tet+ and tet- groups at a same concentration. (n = 6 wells per group (3 photographs per well) * P<0.05 ** P<0.01).

4.3.7 SOCE inhibited by TH1177 and mibefradil in EA.hy926 and HK2 cells

TH1177 and mibefradil are T-type channel blockers, although mibefradil has been shown to inhibit the activity of L type calcium channels as well (Viscoper et al, 1997). It has also been demonstrated that the two compounds significantly inhibited Orai channels with a relatively low EC_{50} of 3.6 µM (Li et al, 2019). As was explained in the introduction of this chapter, because of the unique response that the Orai channels have to some pharmacological compounds we postulated that a higher dose of these compounds might offer a protective effect to the inhibition caused by hyperosmolarity. Therefore, the effect of two compounds on SOCE in the endothelial cell line (EA.hy926) and human proximal tubular cells (HK2 cells) were tested. As shown in Fig. 4.7, TH1177 at 100 µM inhibited TG-induced Ca^{2+} release and completely abolished SOCE in HK-2 cells and EA.hy926 cells. As demonstrated in chapter 3, hyperosmolarity inhibited the SOCE in both cell types. Similar results were observed for mibefradil (Fig. 4.8) whereby SOCE peak intensity was significantly reduced to the point of preventing Ca^{2+} in its entirety (P=0.001). These data suggest TH1177 and mibefradil even at high concentrations, are inhibitors for SOCE therefore not offering any protective effect against the hyperosmolar condition.

Although this outcome was not hypothesised it does not mean that this data is no longer of any value, on the contrary, another major finding reviewed in Fig 4.7 is that the two compounds significantly inhibited the release of Ca^{2+} from the ER as triggered by TG. This is a novel finding and suggests another off-target effect for these compounds, which may not make then effective voltage-gated Ca^{2+} antagonists but this may better help us to understand the anti-proliferative effects of these drugs within cancer treatment.

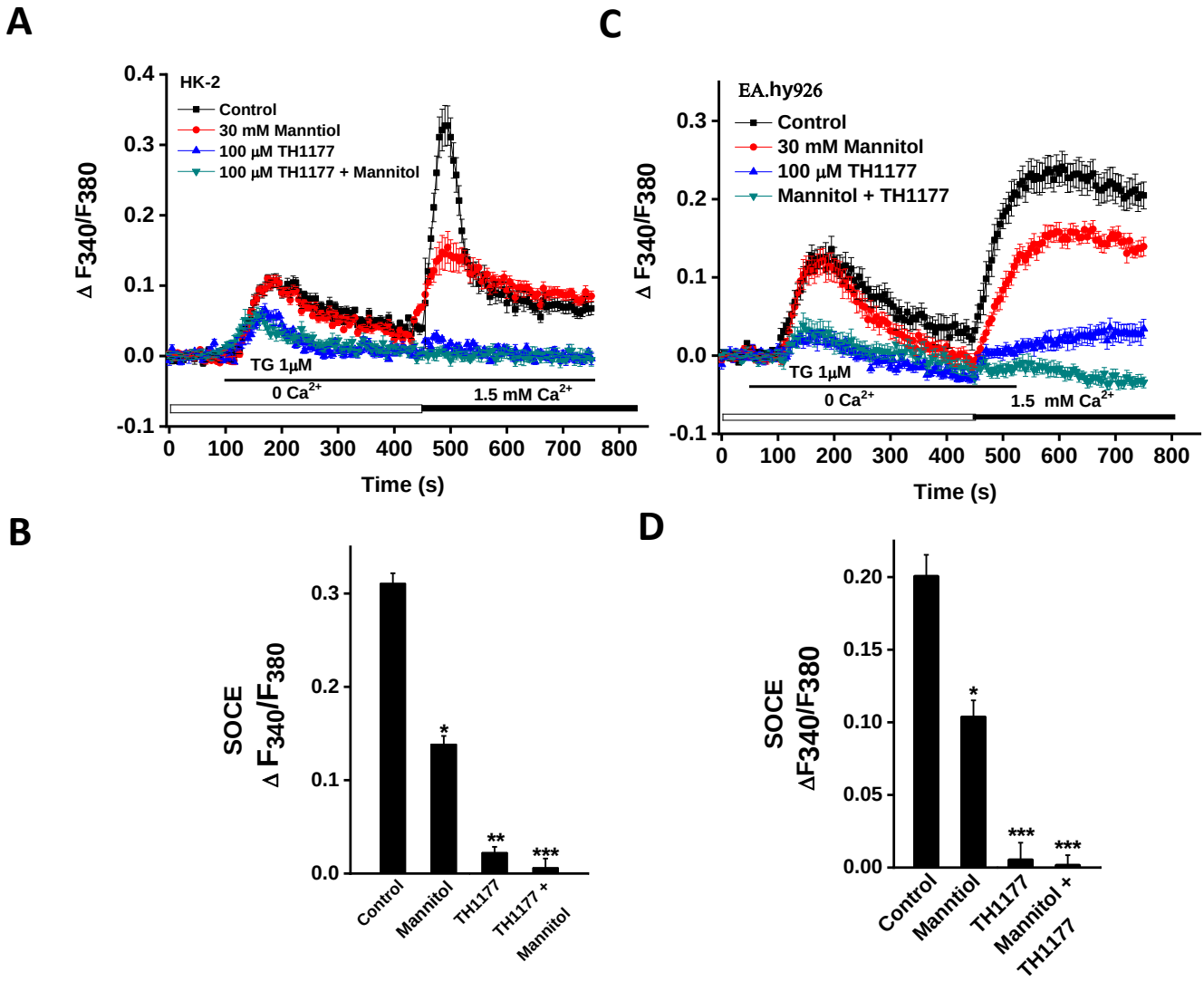

Fig. 4.7 TH1177 reduces SOCE and Ca^{2+} store-release in both HK2 and EA. hy926 cells. Cells were treated with either the mannitol/compound for 5 minutes prior to experimentation. The control condition did not get pre-treated with mannitol or compound. (A) Mean fluorescence intensity in control, mannitol, TH1177, and mannitol + TH1177 groups in HK2 cells. (B) Peak mean fluorescence intensity of SOCE in. (C) Mean florescence intensity in EA.hy926 cells treated with TH1177 and mannitol. (D) Peak mean fluorescence intensity for SOCE . One-way ANOVA was used to test for significance. (n=8 per group * P<0.05 ** P<0.01 *** P<0.001)

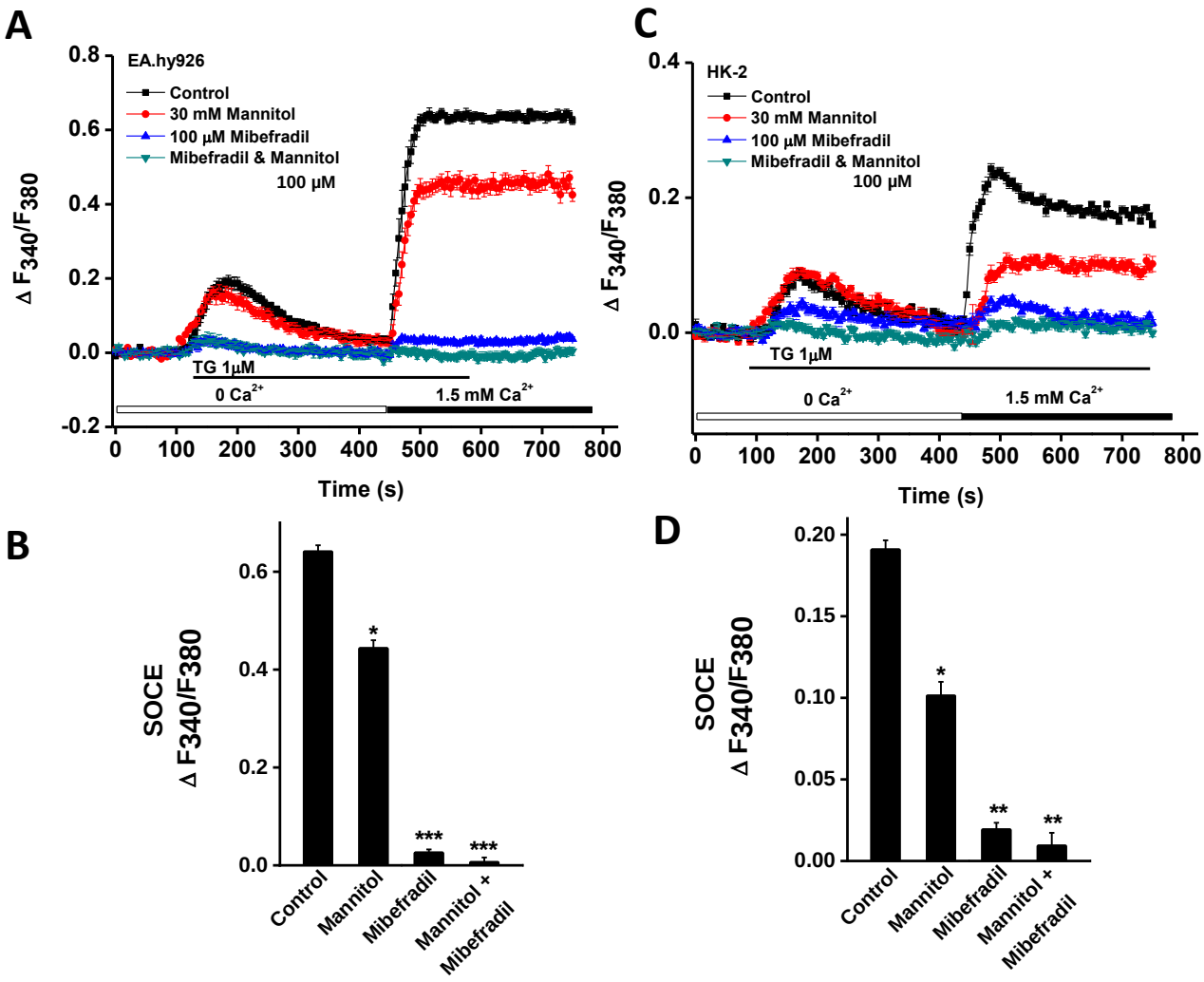

Fig. 4.8 Mibefradil reduces SOCE and Ca^{2+} store-release in both HK2 and EA. hy926 cells. Cells were treated with mibefradil and mannitol 5 minutes prior to experimentation in the test condition and were not subject to this pre-treatment as control. (A) Mean fluorescence change in mannitol, mibefradil and mannitol + mibefradil groups in EA.hy926 cells. (B) Peak mean normalised fluorescence intensity of SOCE in (A). (C) Mean fluorescence intensity in HK2 cells treated with mibefradil and mannitol. (D) Peak mean florescence intensity for SOCE in (C). (n=8 per group * P<0.05 ** P<0.01 *** P<0.001)

4.4 Discussion

All three of the Orai subtypes are sensitive to hyperosmolarity as seen by the reduction of SOCE in HEK293 T-REx cells overexpressing the STIM1/Orai1-3 channels (Fig 4.1-3) all of the subtypes demonstrated a >20% reduction in peak Ca^{2+} intensity compared with the control. The un-transfected HEK293 TREx control cells did not respond to the hyperosmolar stimulus, which allows the conclusion to be drawn that the effect is not being caused by another Ca^{2+} channel that is natively expressed in this cell line. These native cells demonstrated a significantly lower peak Ca^{2+} influx compared to the Orai overexpressing cells this is similar to results published by (Zeng et al, 2007) which also showed that the un-transfected demonstrated a lower intensity than the cells overexpressing the channels.

The data presented in this chapter also revealed an interesting effect caused by more extreme hyperosmolar conditions (30 60 and 90 mM mannitol) this extreme hyperosmolarity was capable of not only reducing the intensity of Ca^{2+} influx but it also significantly reduced the intensity of the TG mediated ER Ca^{2+} efflux (Fig 4.4). This reduction in Ca^{2+} efflux intensity is a novel finding in regards to being caused by hyperosmolarity although other researchers have shown inhibition of this signal in other cell types unrelated to hyperosmolarity (Bissonnotte et al, 2008). As discussed in the previous chapter the extreme hyperosmolarity used is of limited value when trying to compare the *in vitro* results to the clinical condition because only in some of the extreme circumstances would one expect to see plasma glucose levels greater than 30 mM.

The fact that the reduction in SOCE is not seen in the un-transfected HEK293 cells but the same condition significantly reduces SOCE intensity in the EA.hy926 cells is of interest (Figures 4.1-3). One possible explanation for this could be a reduced expression of the Orai proteins in these cells in comparison to other cell types although data to suggest this is absent in the literature. Another possible explanation of the difference in response could be that these cells may be more resistant to the hyperosmolar condition. Because the more extreme hyperosmolar conditions were not applied in the un-transfected HEK293 cell experiments the effect could still be present but was not seen under the 19.5 mM mannitol condition.

Interestingly the results of these investigations show the opposite response to hyperglycaemic stimuli. Hyperglycaemia has been shown to upregulate the activity of Orai 1-3 in endothelial cells (Daskadiliou et al 2015) whereas these data show the opposite effect for hyperosmolarity even though it is a concomitant factor with hyperglycaemia. This need not be thought of contradicting evidence but rather may be explained through an exploration of the previous methods used and the clinical condition being modelled in this body of work.

The methodology described in Daskadiliou *et al* (2015) indicates that what was being modelled was acute hyperglycaemia which was modelling a "typical transient" hyperglycaemic condition and their work may have described a more transient effect on the activity of these channels. Further to this, it is possible that the glucose used in these experiments would have a different effect due to the cells ability to uptake this glucose in the incubation period and therefore produce a different cellular effect to the mannitol used in this work, which would not be able to enter the endothelial cell model.

The methodology used in the experiments described in this chapter describe a less transient cause of hyperosmolarity, this is the condition of the hyperosmolar hyperglycaemic state. The plasma osmolarity in this condition will be elevated for a longer period than in other cases of hyperglycaemia seen in diabetic patients and as such could have a different effect on SOCE activity than the transient hyperglycaemia modelled in Daskadiliou *et al* (2015).

This is a very different condition than what was used in the hyperglycaemia study; it should therefore not be surprising that the response of the channel to this extreme short term condition should be different. What is of significance is that in both of these conditions Ca^{2+} regulation is altered within vascular endothelial cells and both can contribute to major complications. Plasma osmolarity is closely controlled through not just maintenance of water balance but also at the cellular level by sodium/potassium pumps combating to osmolar changes as well as the kidneys actively retaining water during cases of serum hyperosmolarity.

As can be seen in Fig. 4.6 the overexpression of the STIM1/Orai1-3 proteins does not affect the intensity of the cell shrinkage response to the hyperosmolar condition. Therefore, it is not likely a direct effect of hyperosmolarity upon the conformation of the channel that is producing the reduction in SOCE intensity effect, although this cannot be fully proven by such a simple experiment. If these channels were contributing to the overall osmosensitivity and osmoregulation of the cell, similar to other channels that are known to be directly sensitive to changes (Christensen and Corey, 2007). it would have been expected that the overexpression of these channels would alter the cell shrinkage response. This may indicate that although the activity of the channels is altered under increased hyperosmolarity it may not be a true "function" of the channel to help regulate the overall intracellular/extracellular osmotic gradient.

Because the Orai channels do not contribute to the cell shrinkage response, as seen in Fig. 4.6 the reduction in SOCE intensity is likely due to an indirect effect. Because ROS have been shown to modulate the activity of SOCE proteins, albeit in a way that is multifactorial and complex (Bogeski *et al.*, 2010). It is prudent in the next steps in this investigation to understand whether the hyperosmolar condition used in this experiment is capable of significantly increasing intracellular/extracellular ROS. Should this be the case; the role of ROS in the SOCE reduction response to hyperosmolarity can be further investigated and perhaps explored as a means of preventing the effect. Any direct effect that the overexpression of Orai channels could have on the cell shrinkage response could be easily masked by the more intense activity of the Na^+/K^+ exchange pumps which are directly implicated in the regulation of cellular volume in response to osmotic changes (Johnson, Shapiro and Risbud, 2014). This is further supported by foundational data which describes K^+& Na^+ as the primary cellular osmolytes (Sedj et al, 2010) and in the response to hyperosmolarity, it would not be Ca^2 that would be preferentially lost from the cell. This is due, in part, to the key roles that the ion plays in so many cellular mechanisms, as discussed in chapter 1 of this thesis.

The results of the mibefradil compound screening revealed some interesting and novel results, which better helps us to understand this interesting compound. Mibefradil was taken off the market due to potentially deadly drug interactions (Mullins *et al.*, 1998). This drug may have fallen out of favour as an anti-hypertensive compound but its non-specific effects have been predicted to be of benefit in cancer therapy (Keir *et al.*, 2013). TH1177 is a T-type Ca^{2+} channel blocker known for its diverse effect from an anti-proliferative effect known to aid glomerular degeneration (Cove-Smith *et al.*, 2013). As well as effectively blocking the TRPV6 channel as shown in (Landowski *et al.*, 2010).

As yet both of these compounds have not been tested for their effect on SOCE so this data will provide novel insight into these compounds but as well as this a potential for a protective effect against the hyperosmolar condition can be investigated simultaneously. The final finding of this chapter is that both mibefradil and TH1177 do not provide a protective effect against the hyperosmolar response although it is novel to discover that these compounds are capable of producing such a marked reduction in Ca^{2+} release and SOCE currents.

This exacerbates the reduction already caused by the hyperosmolar condition of interest in these experiments. Although this finding is very interesting and novel, further work was needed in order to determine a dosage curve as well as better understand the effect that this effect has on the viability of cells and whether this reduction in SOCE is contributing to the anti-proliferative effect noted in other studies. This work was performed by other researchers within the laboratory and has been published (Li et al, 2019) in-depth work performed using electrophysiology confirmed the dosage response of the Orai channels to these compounds. Interestingly the higher dosage (as used in fig 4.8,9) was found to be capable of inhibiting the proliferation of endothelial cells as well as increasing the proportion of apoptotic cells (as measured by FACS) (Li et al, 2010). The inhibitory effect of higher dose mibefradil on the TG induced Ca^{2+} influx (as shown in figures 4.8-9) may help us to understand the anti-proliferative effect that the compounds have if Ca^{2+} cannot be released from ER stores or replenished through SOCE these cells will have many cellular processes negatively affected, including proliferation.

These compounds can be considered “dirty” in the sense that they are found to have an ever-increasing list of off-target effects, which is added to by the data in this chapter. Although it was in part because of the many off-target effects that these compounds have that they were screened for a potentially protective effect against hyperosmolar SOCE reduction. Initial data suggested their inhibitory effect but there was potential for a dosage response similar to that seen in 2-APB which could have combated the reduction in SOCE intensity caused by hyperosmolarity (Bogeski et al, 2010). The off-target effects do mead that the results described in this chapter would not be considered proof of a direct effect, due to being unable to determine if the drugs reduced the SOCE by having an action on an important messenger or molecule that leads to SOCE downregulation.

Because the compounds tested did not produce a protective effect (i.e. increase SOCE intensity and thereby resisting the hyperosmolarity related inhibition) and because the pharmacological screening of multiple compounds is beyond the scope of this work it is logical to instead perform deeper study into the mechanism by which hyperosmolarity is capable of reducing the intensity of SOCE. The data in this chapter revealed that it is the STIM1/Orai1-3 apparatus that is the major contributor to the effect and as such, it is wise to explore endogenous factors that are known to alter (and indeed reduce) the intensity of SOCE under a stress stimulus such as hyperosmolarity.

Reflecting upon the hypothesis that the experiments were intended to test set out in the introduction of this chapter it is clear that SOCE is reduced under the hyperosmolar condition (Figs 4.1-4) and more extreme hyperosmolarity is capable of reducing Ca^{2+} store-release intensity as well as Ca^{2+} influx (Fig 4.4&5). The overexpression of these channels did not affect the cell shrinkage response, so as such the shrinkage of these cells may not be linked to Orai channel activity reduction under hyperosmolar conditions (Fig 4.6). It was also hypothesised that the compounds mibefradil and TH1177 would offer a protective benefit to this Orai response to hyperosmolarity although the opposite was the case, as treatment with these compounds essentially totally inhibited both SOCE and Ca^{2+} store release from the ER (Figures 4.7 & 4.8).

One factor that may provide an answer to the question of the underlying mechanism may be found in the production (or indeed overproduction of ROS within these cells under the hyperosmolar condition). If the cells used in the experiment do produce a greater amount of ROS then this could be a potential mechanism leading to the reduction in SOCE intensity because an increase in ROS is known to have many effects on the SOCE apparatus, including a reduction in Orai activity (Bogeski et al., 2010).

Chapter 5

Hyperosmolarity increases ROS production potentially contributing to the impairment of SOCE

5.1 Introduction

The effect of ROS on the activity of STIM/Orai is complex, this is partly due to the exact nature of many ROS species and SOCE protein interaction not been clearly elucidated. As well as seemingly contradictory inhibitory and stimulatory effects that have been documented (Bogeski, Kilch and Niemeyer, 2012). The application of exogenous ROS (in the form of H_2O_2 as well as other oxidants) has been shown to reduce the intensity of SOCE (Törnquist *et al.*, 2000). There are sources of ROS that are independent of the mitochondrial electron transport chain, for example via the activity of membrane-bound nicotinamide adenine dinucleotide phosphate (NADPH) Oxidase (Bedard and Krause, 2007) which in phagocytes are capable of producing an oxidative burst to aid lytic activity (Rossi, 1986). Although NADPH is a key energetic molecule in all cell types. Of interest to this body of work is the major role that NADPH oxidase plays in the generation of ROS in vascular endothelial cells and the role that they can play in endothelial dysfunction (Ray et al., 2005).

There are multiple sources of intracellular ROS but one of the more common sources of endogenous ROS is the mitochondrion, via the escape of free electrons from the respiratory electron transport chain (Bedard and Krause, 2007). When the free electrons are transferred to a molecular Oxygen the Superoxide molecule is formed this Superoxide molecule can then go on to combine into Hydrogen Peroxide (H_2O_2) as well as other ROS such as NO and Peroxinitrite (Ray et al, 2005).

The interaction between the STIM/Orai and ROS appears to be mediated via the cysteine residues present within the STIM/Orai proteins and subsequent S-glutathionylation of these residues following exposure with ROS, thereby bringing about post-translational modification of some key sites in the STIM & Orai structures (Bogeski *et al.*, 2010). It is the S-glutathionylation of the SOAR region of STIM 1 by Hydrogen peroxide that has been shown to activate SOCE independent of ER Ca^{2+} store depletion (Grupe *et al.*, 2010). Although inhibition of SOCE is seen when ROS is applied for longer periods of time (10-minute pre-treatment) and this has been linked to the cysteine residues of Orai 1 & 2 found within the transmembrane domain although this same effect was not seen in Orai 3 overexpressing cells (Griesemer *et al.*, 2010).

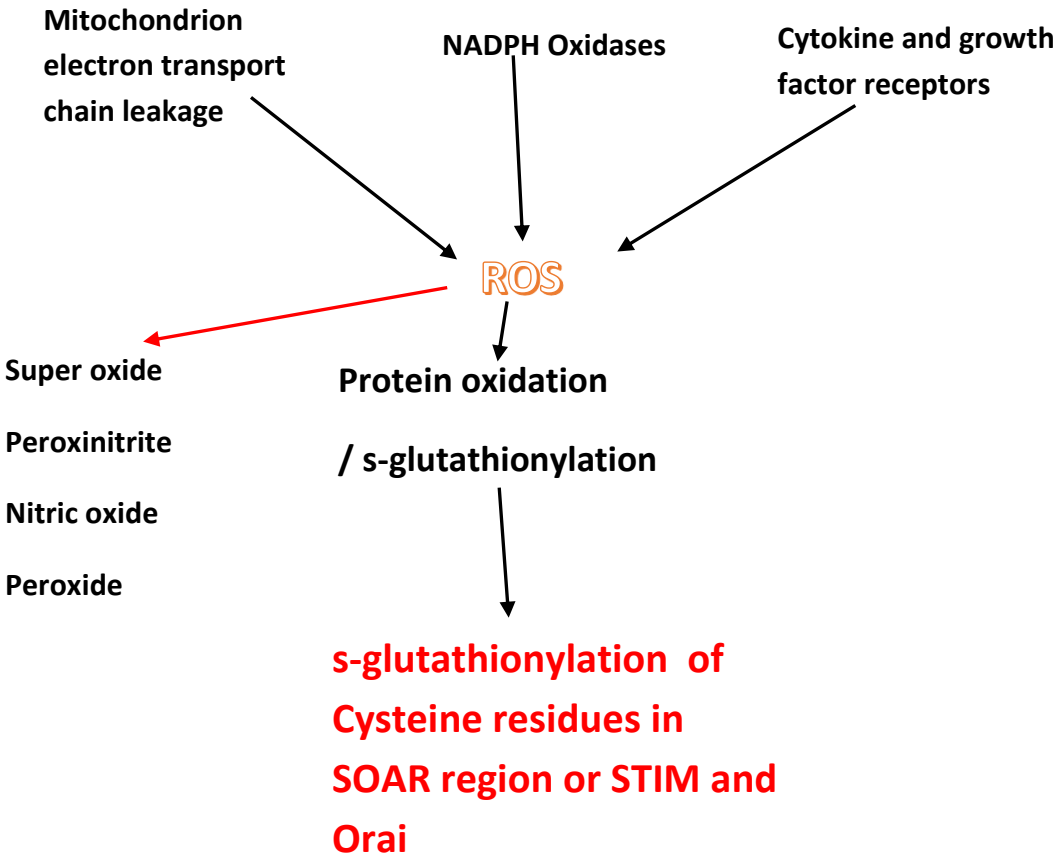

Fig. 5.1.1 Summary of major sources and types of intracellular ROS which lead to the modulation of STIM/Orai activity. Figure is original but with information taken from (Rossi, 1986) & (Bedard and Krause, 2017).

Data presented in the previous chapters have shown that SOCE intensity is inhibited in both endothelial cells and in HEK296 cells overexpressing the STIM & Orai proteins (Figures 3.5&6, 4.1-5). Although this does not appear to be directly mediated by the physical cell shrinkage response as overexpression of the Orai channels did not have any effect on this cell shrinkage (Fig 4.6). Therefore, it was reasonable to assume that this inhibition of SOCE may be caused by intracellular changes modifying the activity of the channels. Because there has been extensive work, showing the modulation of SOCE through reactive oxygen species this was identified as the primary target for the investigation. Further justification for this line of enquiry is found in the data generated by Deng *et al* as this demonstrated that hyperosmolarity greatly increased the concentrations of ROS within an endothelial cell model (Deng et al, 2015). This the same effect is established in the EA.hy926 cells used in the previous experiments then there is the potential to demonstrate a pathway by which hyperosmolarity decreases the intensity of Orai/ STIM mediated SOCE.

The aim of this chapter is to examine whether the hyperosmolar condition can alter the production of intracellular ROS; and. if a causative link can be drawn between the two factors then work will also be performed to combat this inhibitory effect through the use of antioxidants. As well as more in-depth work to investigate the types of ROS being generated in order to better understand their intracellular source.

Hypothesis 1: Hyperosmolarity will increase the intracellular ROS in EA.hy926 cells

Hypothesis 2: ROS will be able to reduce the intensity of SOCE in EA.hy926 as an independent factor to hyperosmolarity

Hypothesis 3: The use of an antioxidant will be able to rescue SOCE under the hyperosmolar condition

5.2 Methods

The determination of which method to use for the detection of intracellular ROS species was a major question that had to be addressed in the development of the methodologies used for generating the data within this chapter. One of the most common ways to measure intracellular ROS is through the use of dies/indicators, other methods exist for example the use gas chromatography and mass spectroscopy to detect specific ROS, although this is a less well-established methodology whit a much higher cost and time investment (Xiao et al, 2016).

2',7'-dichlorodihydrofluorescein diacetate (H_2DCFDA) was selected as a non-specific intracellular ROS indicator, this is essentially a cell-permeable version of fluorescein which has been used in many studies to measure intracellular ROS. H_2DCFDA can very easily be oxidised in air and as such is dissolved in high purity DMSO that is both an effective solvent but helps to prevent oxidation of the dye.

Because the H_2DCFDA was prepared in DMSO all negative control groups contained the equivalent volume of DMSO to ensure that the DMSO was not capable of causing a change in and of itself. H_2DCFDA is also highly susceptible to photobleaching (as is Amplex red, another indicator used in this set of experiments) so to prevent this all experiments were performed in a dark room with special care taken to prevent direct light exposure to the dye solution.

Sodium pyruvate was chosen as a ROS scavenger as it has been found to effectively reduce the levels of intracellular peroxide ROS at a concentration of 10 mM (Giandomenico et al, 1997). Because such a high concentration is needed to achieve this ROS scavenging effect care was taken in solution preparation to ensure that the osmolarity of this final solution was no different due to the addition of sodium pyruvate.

All H_2O_2 used in these experiments was prepared on the day of experimentation from recently purchased and well-sealed concentrated stock solution in order to avoid issues with the decay of the compound, as it can readily degenerate into O_2 & H_2O. For the Mitosox experiments, Sodium azide was used as a "positive-negative" control, this term is used because Mitosox should cause any mitochondria within a living cell to appear red under fluorescence microscopy as the dye is only activated by mitochondrial superoxide. In order to check the specificity of this dye sodium azide can be used to inhibit mitochondrial bioenergetics and as such any cells treated would not display the characteristic Mitosox staining hence the term "positive-negative control".

Carbonyl cyanide-p-trifluoromethoxyphenylhydrazone commonly abbreviated to FFCP is used as a positive control in the Mitosox superoxide detection experiment described in this chapter. This is because FCCP is known to un-couple the mitochondrial electron transport chain leading to an increase in superoxide production (To et al, 2010).

5.3 Results

5.3.1 Detection of cytosolic ROS and the effects of hyperosmolarity

The cell-permeant intracellular ROS indicator H_2DCFDA was used to detect cytosolic ROS production. The fluorescence intensity of H_2DCFDA was significantly increased in the groups pretreated with H_2O_2 and the effect was concentration-dependent (Fig. 5.1A) (*P*=>0.05 in all groups compared with negative control).

This suggests that the cytosolic ROS production is significantly enhanced in EA.hy926 cells under the oxidative stress condition mimicked by the addition of H_2O_2. Then the effect of hyperosmolarity was examined, mannitol at concentrations of 19.5, 30, 60, 90 and 120 mM was applied and the fluorescence intensity of ROS indicator was also significantly increased in all of the groups compared to the negative control (*P*=<0.05 for all groups)(Fig. 5.1B). This result suggests that hyperosmolarity can enhance cytosolic ROS production. 19.5 mM was found to increase the intracellular ROS level by 12.3% compared to the negative control and 30 mM mannitol increased the level of intracellular ROS by 25.7% compared with the negative control. As discussed previously the extreme values of hyperosmolarity created in this experiment (particularly 90 mM and 120 mM) would not be seen within even very poorly controlled diabetic patients, though this data is still interesting as it shows that the EA.hy926 endothelial cells are undergoing a huge amount of metabolic stress in their response to this extreme hyperosmolarity.

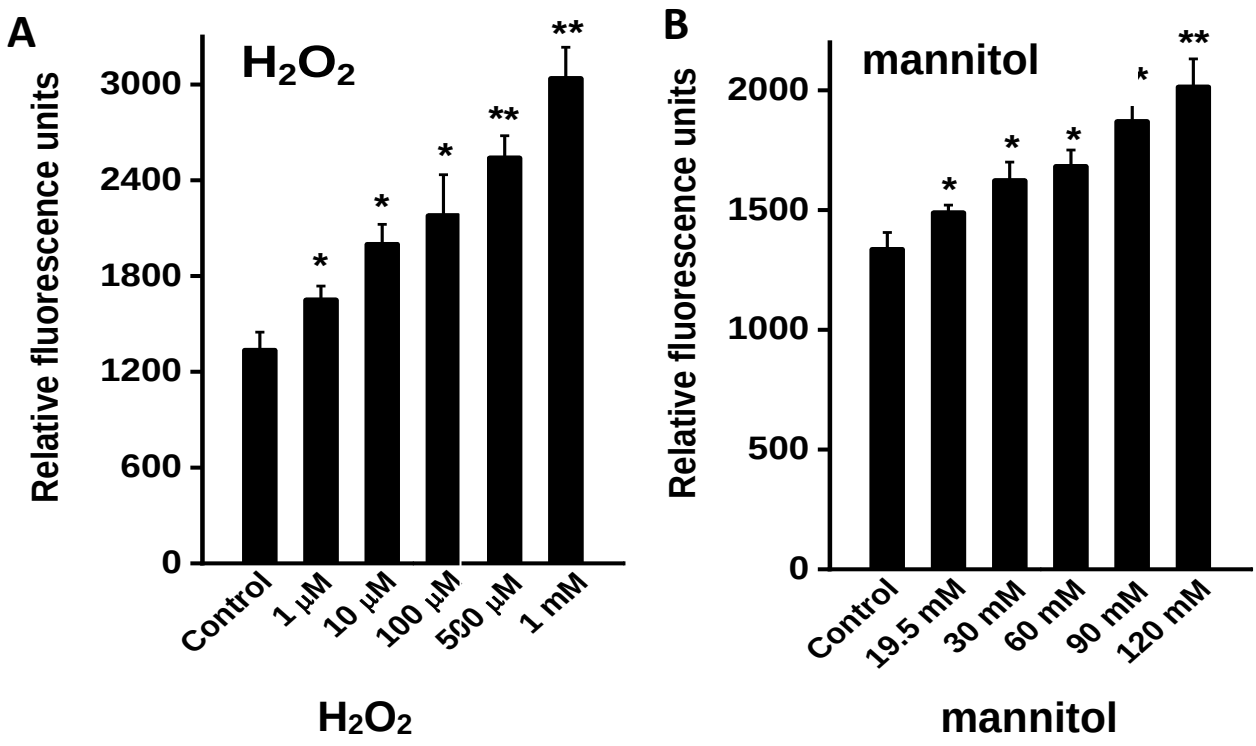

Fig. 5.1 Cytosolic ROS production under hyperosmolarity conditions in EA.hy926 cells. EA.hy926 Cells were treated with either the hyperosmolar condition (mannitol) or the positive control condition (H_2O_2) for 4 hrs prior to loading with intracellular ROS indicator H_2DCFDA (2 μM). After incubation with H_2DCFDA for 30 mins, the florescence was measured at excitation wavelength of 493 nm and emission wavelength of 520 nm. (A) Fluorescence intensity for EA.hy926 cells treated with H_2O_2 (1-1000 μM) for 4 hrs as a positive control experiment. (B) Fluorescence intensity for EA.hy926 cells incubated with hyperosmotic conditions for 4 hrs. Statistical significance was determined using a one-way ANOVA (n=8 wells per group *P<0.05, **P<0.01)

Fig 5.1 shows that the hyperosmolar condition (even at the lower 19.5 mM concentration) is capable of significantly increasing the concentration of intracellular ROS. The next step is to investigate this phenomenon using a time course sample to see if this increase in intracellular ROS is observed at the 5-15 minute time point at which the SOCE experiments were performed. Although the Ca^{2+} assay used a 5-minute pre-treatment for the experimental hyperosmolar condition the reality is that the cells were in the hyperosmolar condition for a further 10 minutes for the length of the assay (SOCE is induced at 10 minutes via the addition of extracellular Ca^{2+}).

5.3.2 Time course of cytosolic ROS measurement under hyperosmolarity condition

The time course of dynamic cytosolic ROS production in EA.hy926 cells was measured using H_2DCFDA dye. Cells pretreated with H_2O_2 at 50 µM or 100 µM gradually increased ROS production, and the slope of the curves was significantly greater than the control group (Fig. 5.2A) (50 µM P=0.042 100 µM P=0.037). Using similar procedures, the dynamic effect of hyperosmolarity on cytosolic ROS production was also monitored. Mannitol significantly increased the ROS fluorescence intensity in a concentration-dependent manner compared with the control group even at the 19.5 mM concentration (P=0.029), further suggesting that the cytosolic ROS is increased under the hyperosmolar condition. The 19.5 mM concentration of mannitol increased the level of intracellular ROS by 41.2% compared with the negative control and the 30 mM group increased the intensity by 63.1% compared with the negative control. Both 50 µM and 100 µM concentrations of H_2O_2 were used in this experiment in order to better compare the levels of intracellular ROS with an extracellular ROS stimulus with greater granularity than a single positive control.

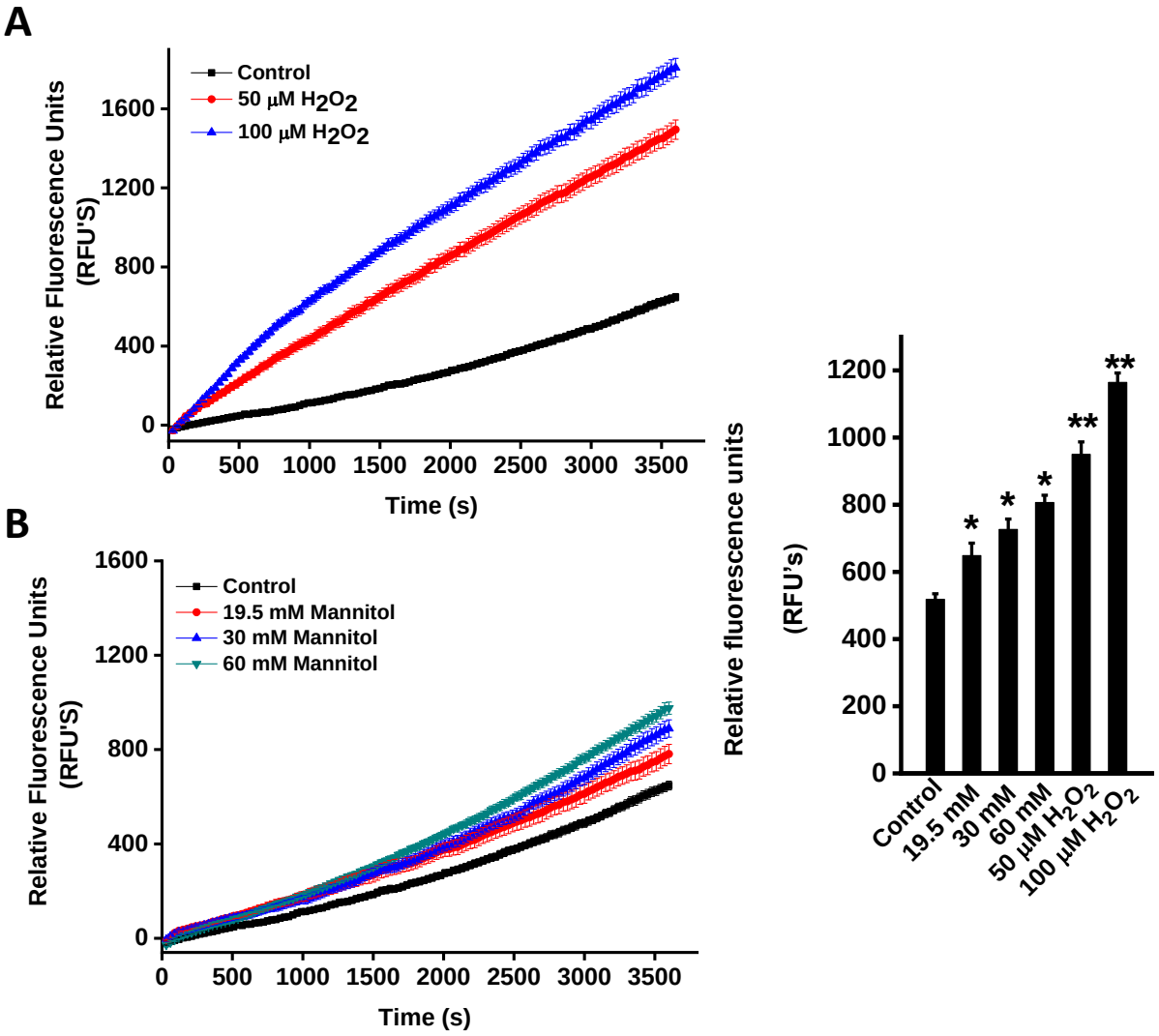

Fig. 5.2 Intracellular ROS production is increased in endothelial cells in hyperosmotic conditions. All cells were loaded with H_2DCFDA (2 µM) intracellular ROS indicator and were incubated for 30 mins prior to experiment, the florescence was measured at 493nm/520nm. Hyperosmotic or positive control condition was applied at time 0 s by live fluidic addition with Flexstation 3. (A) Time course for mean +SEM intracellular ROS dye florescence intensity comparing vehicle control and positive H_2O_2 control groups. (B) Mean change in intracellular ROS indicator florescence under hyperosmolar conditions. (C) Mean ± SEM data for the fluorescence intensity at 3000 s. Significance was tested using one-way ANOVA. *P<0.05 **P<0.01 n = 8 wells per group.

Fig.5.2 shows that the increase in intracellular ROS is still significantly increased within the pre-treatment and experimental time frame used in the SOCE experiments. At t 800s the results of the ANOVA with post hoc Bonferroni revealed that when compared with control all of the hyperosmolar conditions were significantly increased (P<0.05). This difference only increased over time and although the control groups ROS also increased, the difference between the test and control groups had increased steadily until the end of the sampling. This increase in intracellular ROS concentration can be explained by the progressive activation of the dye by normal metabolic by-products rather than being caused by cellular stress (Bogeski et al, 2012).

5.3.3 Ca^{2+} dependence of hyperosmolarity-induced cytosolic ROS production

To investigate whether the presence of extracellular Ca^{2+} may affect the ROS production response to hyperosmolarity, the extracellular Ca^{2+} was omitted/removed using Ca^{2+}-free bath solution. This was achieved using the appropriate concentration of EDTA as well as the omission of CaCl from the formula. The difference in H_2DCFDA fluorescence intensity between 1.5 mM Ca^{2+} and 0 mM Ca^{2+} groups was significant (>50% reduction compared to Ca^{2+} containing solution control P=>0.05 for all groups). This suggests that the cytosolic ROS production was higher in the cells incubated in Ca^{2+} containing solution, implying that Ca^{2+} dynamics may have an important role in this intracellular ROS response to hyperosmolarity. Although this difference for Ca^{2+}-dependent ROS production was seen in the hyperosmolarity condition and the presence of H_2O_2 and the control cells, suggesting more generally that the removal of intracellular Ca^{2+} can impair intracellular ROS production. This result does make sense considering the importance of Ca^{2+} as a messenger of cell stress and death as, if there was less of the messenger the increased ROS in response to stress could be affected (Basset et al, 2006).

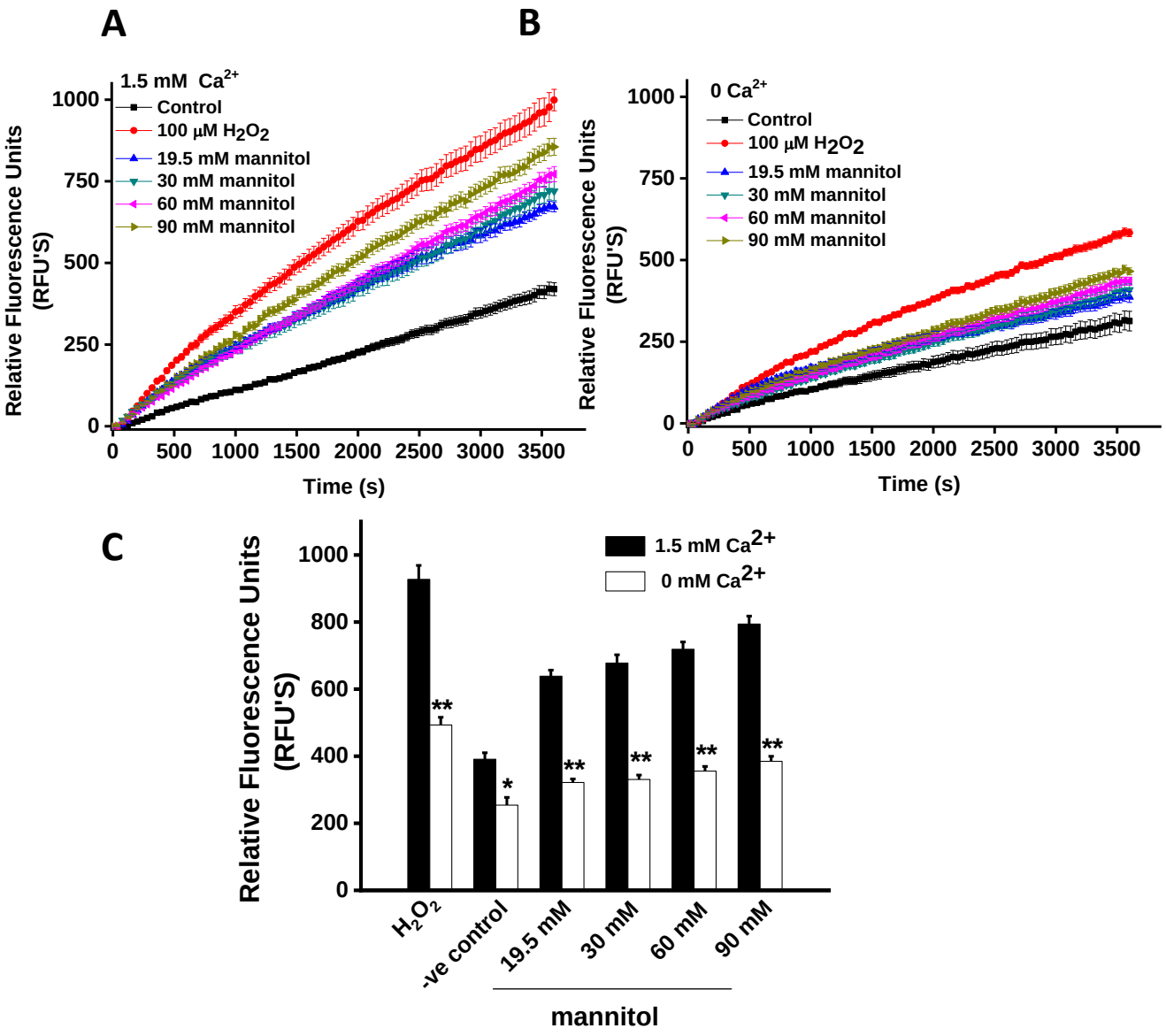

Fig. 5.3 Hyperosmolarity-induced cytosolic ROS production is Ca^{2+}-dependent. EA.hy926 Cells were loaded with intracellular ROS indicator H_2DCFDA (2 µM) for 30 mins prior to experiment, the fluorescence was measured at 493nm/520nm. Hyperosmotic or H_2O_2 were applied at time 0 s. (A) Mean ±SEM fluorescence intensity of H_2DCFDA intracellular ROS indicator over time in 1.5 mM Ca^{2+} bath solution. (B) Mean ±SEM fluorescence intensity of H_2DCFDA in EA.hy926 Cells in Ca^{2+} free bath solution and under the same conditions as in (B). (C) Mean +SEM fluorescence intensity over time in 0 Ca^{2+} bath solution. Statistical significance was determined using one-way ANOVA n=8 wells per group *P<0.05 **P<0.01.

5.3.4 ROS increase effect with hyperosmolarity is dependent upon the presence of cells and not due to dye degradation or artefact

Since the fluorescence of ROS indicator in the control cells was increasing, it is important to test if such increase is due to basal ROS generation in cells under the control condition or the artefact of fluorescent dye bleaching. Therefore, an experiment without cells was set in parallel. As shown in Fig. 5.4, the fluorescence of ROS indicator H_2DCFDA was relatively stable without significant bleaching in the wells without cells. Cells treated with H_2O_2 100 µM significantly increased the intensity of fluorescence, while the fluorescence in the cells without H_2O_2 pre-treatment was also increasing, suggesting that the increase in the control group is due to the basal production of cytosolic ROS. The relatively small increase over time of fluorescence in the group containing only the H_2DCFDA dye and no cells indicates that this dye is specific to intracellular ROS although after significant time elapsed some of the dye began to be activated, this may have been due to oxidation as a result of prolonged exposure to hydrogen peroxide.

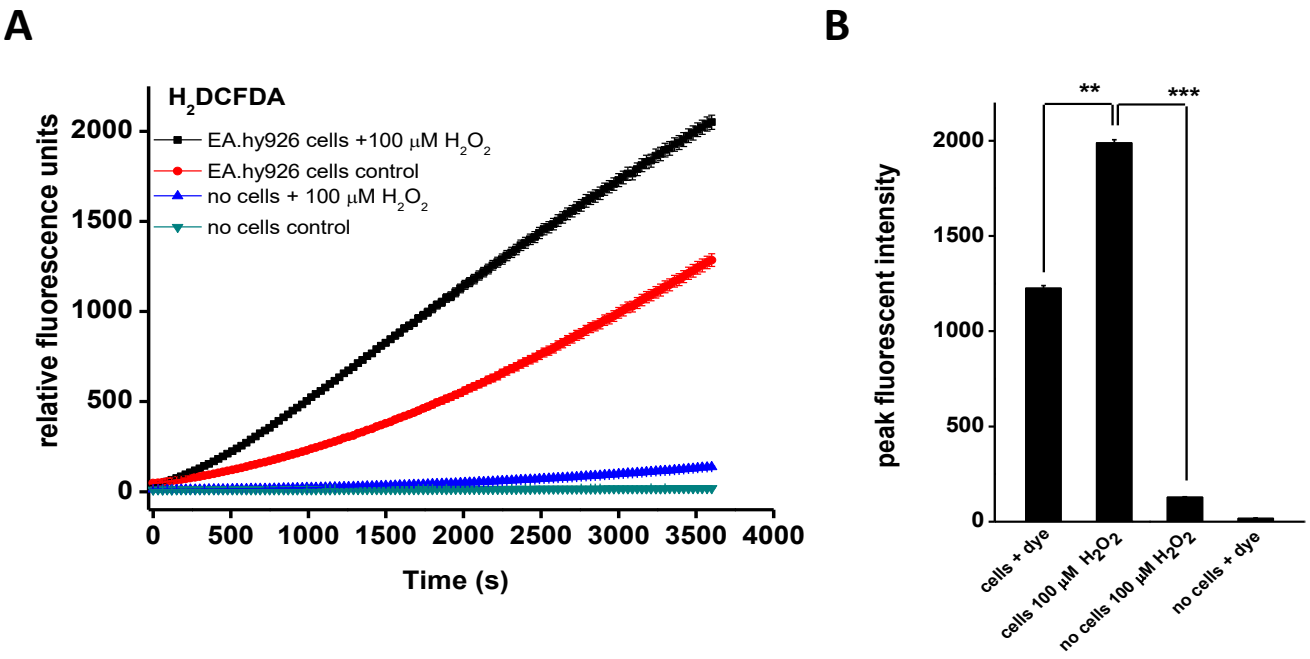

Fig. 5.4 Specificity test of ROS detection using H2DCFDA. All wells were loaded with H_2DCFDA (2 μM) intracellular ROS indicator and were incubated for 30 mins prior to experiment, the florescence was measured at 493nm/520nm. In wells containing no cells, the wells were not washed so as not to completely remove the dye. (A) Mean +SEM fluorescence intensity of H_2DCFDA intracellular ROS indicator comparing the groups containing both cells and dye and wells only containing dye (B) Mean +SEM fluorescence intensity of H_2DCFDA intracellular ROS indicator comparing the positive and negative control groups sampled at 3000 seconds. n=8 wells per group significance tested between Ca^{2+} and 0 Ca^{2+} groups measured using one-way ANOVA **p<0.01 ***p<0.001

5.3.5 Cytosolic ROS is increased by hyperosmolarity in HK2 cells

The Kidney is essential for osmolarity regulation, therefore the effect on ROS production was also examined in the HK2 cells under hyperosmolar conditions. Similar to the response in endothelial cells, (Fig. 5.1&2) hyperosmolarity also significantly increased cytosolic ROS in HK2 cells (P=<0.05 for all hyperosmolar groups compared with negative control) (Fig. 5.5). The results of this experiment suggest that the increase in intracellular ROS in response to hyperosmolarity is not unique to EA.hy926 cells; interestingly it is worth noting that the peak fluorescence intensity (even in the positive control group) was considerably lower in the HK2 cells than in the EA.hy926 cells. 632 RFU's in HK2 compared with 1172 RFUs in EA.hy926 cells (P=<0.01).

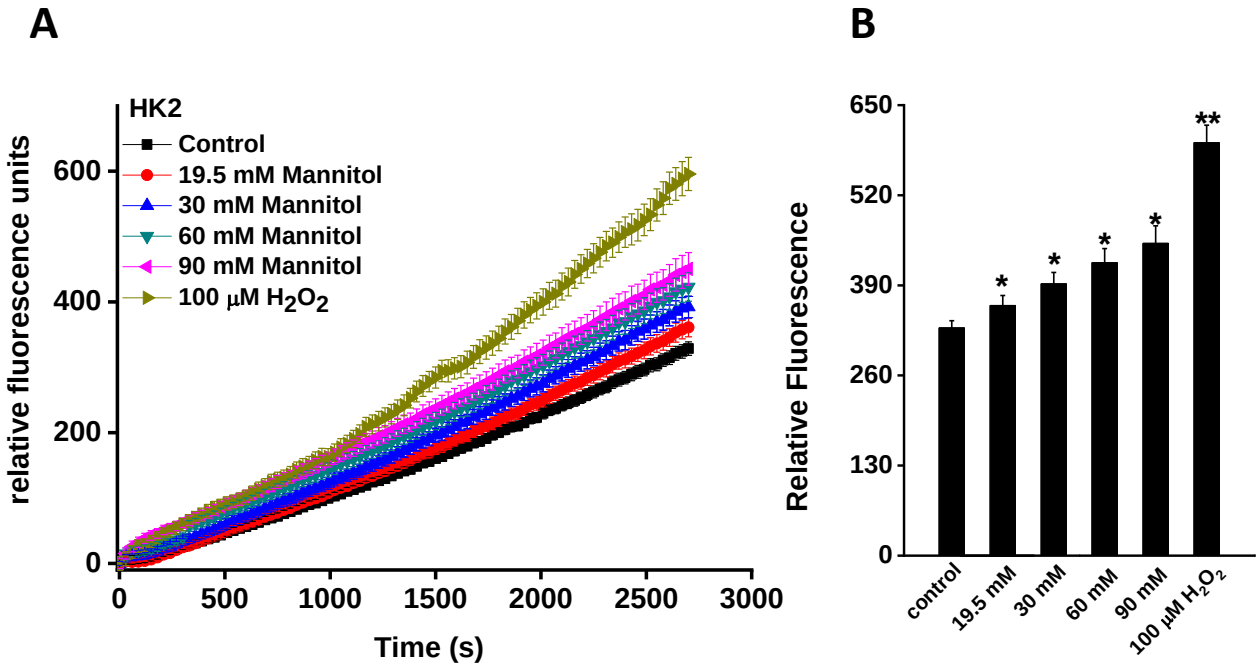

Fig. 5.5 Cytosolic ROS production is increased in HK2 cells under hyperosmotic conditions. All cells were loaded with H_2DCFDA (2 μM) intracellular ROS indicator and were incubated for 30 min prior to experiment, the florescence was measured at 493nm/520nm. Hyperosmotic or H_2O_2 was applied at time 0 s. (A) Time course of mean ± SEM intracellular ROS dye florescence intensity comparing vehicle control condition and positive H_2O_2 control groups. (B) Mean +SEM data measured at 2500s. Significance was tested using one-way ANOVA n=8 per group. * P<0.05 ** P<0.01

5.3.6 Hyperosmolarity increases mitochondrial superoxide

Having established the cytosolic ROS increasing effect by hyperosmolarity, the next step is to investigate which specific reactive oxygen species are propagating such an increase. Superoxide and hydrogen peroxide are often considered as the ROS, which is the most common forms of ROS in a cell (Phaniendra *et al., 2015*). **S**pecific dyes are used in order to ascertain the effect of hyperosmolarity on these specific reactive oxygen species. In Fig. 5.6, the Mitosox dye was used to detect mitochondrial superoxide. The fluorescence intensity of Mitosox was significantly increased over time in EA.hy926 cells compared to the negative control. Hydrogen peroxide was not able to produce a significant increase, indicating that Mitosox is specific for mitochondrial superoxide.

The 19.5 mM mannitol condition did increase by 7.3% compared with the control group but this result was not significant (P=0.062) whereas the 30 mM condition showed an increase in Mitosox fluorescence of 12.4% which was a statistically significant increase (P=0.031). The group containing no-dye sought so show the results obtained were not due to auto-fluorescence. The increase in mitochondrial superoxide concentration under the hyperosmolar condition is an interesting result as this indicates that there could be a metabolic shift that these cells undergo in response to the hyperosmolar condition which in turn leads to greater production of mitochondrial ROS. This is a novel finding and although preliminary in nature this could lead to a greater understanding as to how endothelial cells are responding to hyperosmolar conditions such as hyperglycaemia or hyponatraemia.

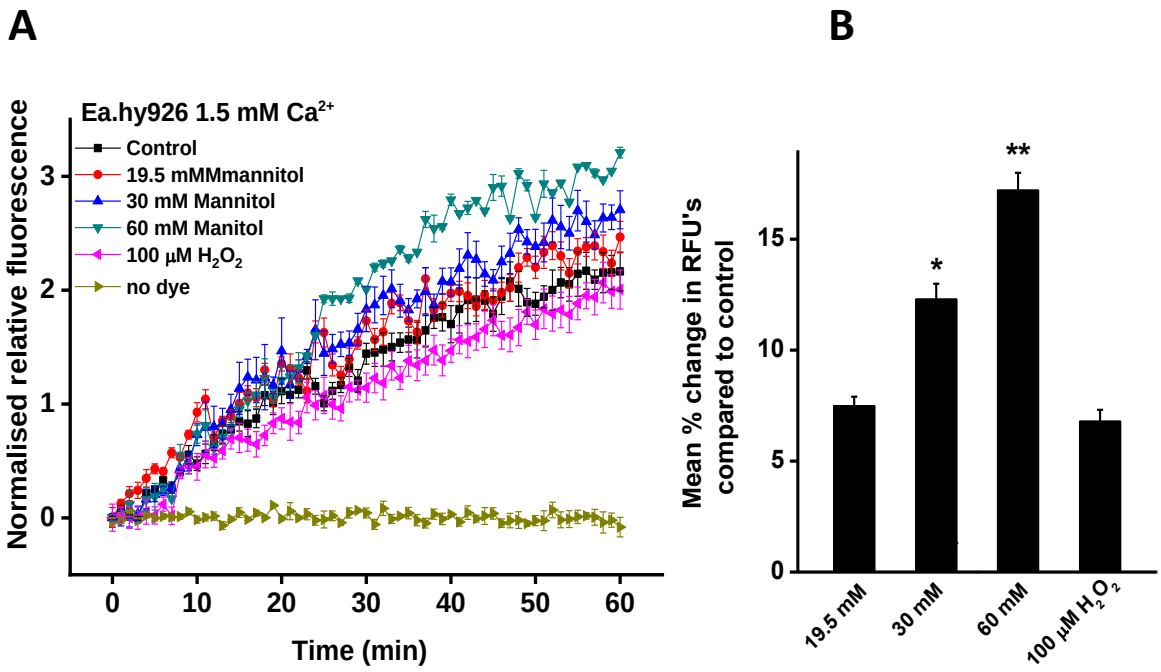

Fig. 5.6 MitoSOX detection of superoxide reveals that hyperosmolarity increases the level of intracellular superoxide. (A). results of the hyperosmolarity experiment in EA.hy926 cells, cells were loaded with MitoSOX (1µg/ml) at the beginning of the experiment (37°C for 30 minutes prior to experiment) and the hyperosmolar condition and H_2O_2 were added at 0 s. (B) Mean data for MitoSOX detection in EA.hy926. Percentage change was shown compared to the no-dye control group. *P<0.05 **P<0.01 n =8 wells per group.

5.3.7 Ca^{2+} independent increase in mitochondrial superoxide

Having identified that hyperosmolarity is capable of increasing the concentration of intracellular superoxide. It is important to establish whether the presence of extracellular Ca^{2+} 1.5 mM can affect the intensity and the pattern of this inhibition. The results of this experiment can be seen in Fig.5.7.

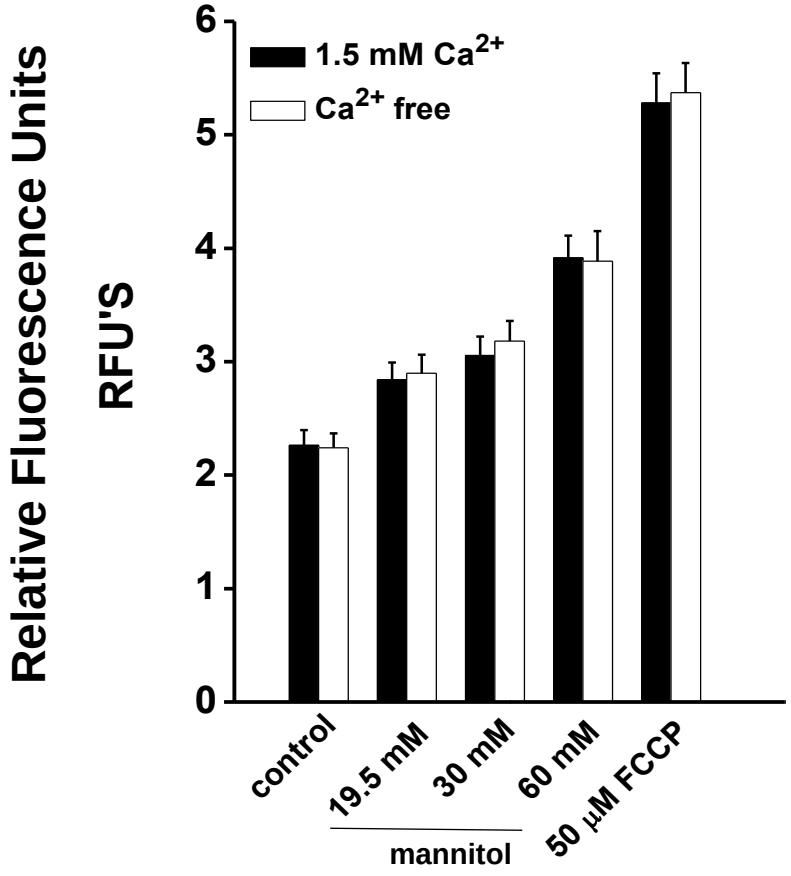

Fig. 5.7 MitoSOX detection of superoxide reveals the increase in superoxide concentration caused by hyperosmolarity is affected by reduced extracellular Ca^{2+}. Mean fluorescence of the MitoSOX dye after 1 hr incubation with either the control or the test condition. The MitoSOX dye was loaded into the cells 20 minutes prior to the experiment in the dark and incubated at 37°C. Statistical comparison (students t test) was performed between the 1.5 mM Ca^{2+} groups and the 0 Ca^{2+} groups, although there was no significant difference that could be attributed to the presence or absence of Ca^{2+}. Although not shown for clarity all of the hyperosmolar groups (and positive control groups) were significantly (one-way ANOVA) increased from the control groups at least at the $p<0.05$ level. $n=8$ wells for each group **=$P<0.01$

As can be seen in Fig 5.7 the production of superoxide in response to hyperosmolarity does not appear to be dependent upon the presence of extracellular Ca^{2+} as there is no significant difference between any of the Ca^{2+} containing and the Ca^{2+} free groups (*P=<0.05* for all groups). Although all groups did have significantly higher levels of mitochondrial superoxide as compared with the control groups, regardless of Ca^{2+} status. The FCCP performed as expected showing very high levels of superoxide production, nearly 3 fold the control group level (*P*=<0.01)

5.3.8 Ca^{2+} dependent peroxide overproduction

In order to measure the effect of hyperosmolarity on the production of peroxide ROS species, an Amplex red dye was used. This dye in combination with hydrogen peroxide in the presence of horseradish peroxidase (HRP) produced a fluorescent by-product proportional to the concentration of peroxide in a sample. EA.hy926 cells in the Ca^{2+} free group exhibited a significantly reduced increase in Amplex Red fluorescence compared with control when treated with the hyperosmolar conditions. This is an interesting finding because Amplex red is a detection kit that is specific to hydrogen peroxide (Voltyakova et al, 2006), and one of the major intracellular sources of superoxide is the NADPH oxidase proteins, although the source of H_2O_2 could also be the mitochondrion as the conjugation of superoxide radicles can form H_2O_2. Although both Endoplasmic reticulum and peroxisomal ROS cannot be discounted as contributing to this effect. All hyperosmolar groups had significantly increased Amplex red fluorescence (peroxide levels) compared to the negative control group (*P*=<0.01 for all 1.5mM Ca^{2+} hyperosmolar groups vs control). Hydrogen peroxide (50 μM) produced nearly double the fluorescence intensity compared to the control group.

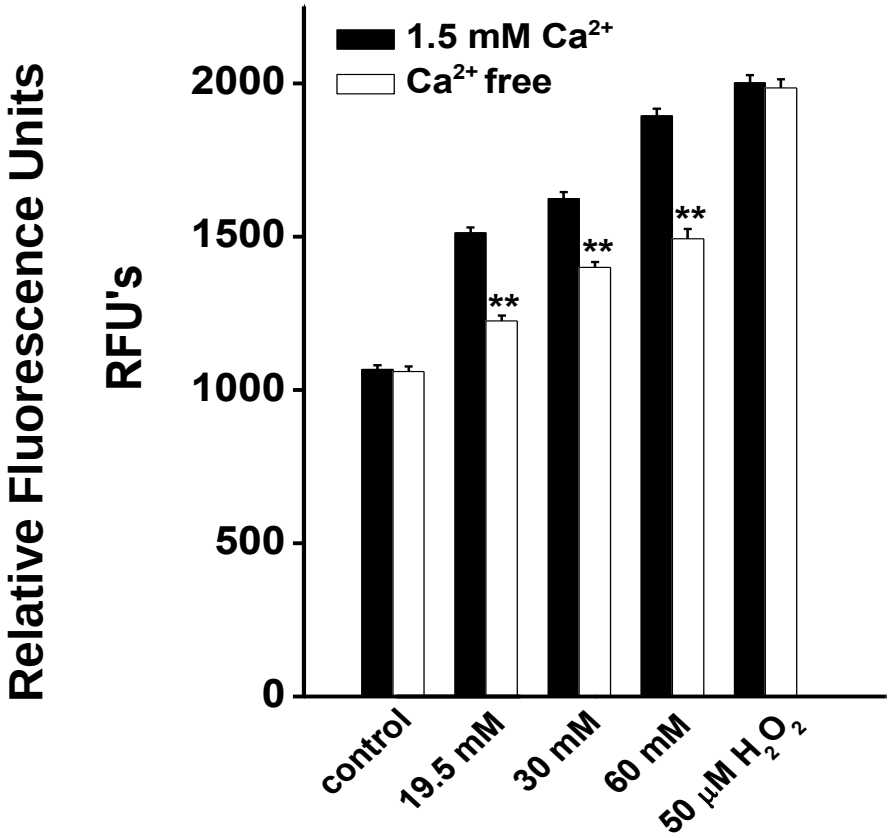

Fig. 5.8 Hydrogen peroxide detected by Amplex Red and the effects of hyperosmolarity and Ca^{2+}. The mean fluorescence of Amplex Red dye after 1 hr incubation with mannitol or H_2O_2 in EA.hy926 cells. Cells were grown to 80% confluence using a 96 well plate. The Amplex Red was added to the solutions (either 1.5 mM Ca^{2+} or Ca^{2+} free) at the 0 second time point. The statistical comparison (one-way ANOVA) was performed between the 1.5 mM Ca^{2+} groups and the 0 Ca^{2+} groups. All of the hyperosmolar groups and positive control groups were significantly increased from

5.3.9 H_2O_2 decreases the intensity of SOCE in EA.hy926 and HK2 cells

One major step remains in the investigation of ROS and SOCE inhibition and that is the need to establish the link between increased ROS and the decreased intensity of SOCE. Fig. 5.9 shows the results of a Ca^{2+} dynamics assay but on this occasion, Hydrogen peroxide is used as the test group instead of hyperosmolarity.

Fig. 5.10 shows the effects that H_2O_2 has on the intensity of SOCE generated within HK2 cells in order to determine the presence of any cell type-specific effect. As can be seen in Figs. 5.10&11 H_2O_2 is capable of significantly reducing the intensity of SOCE in both EA.hy926 cells and HK2 cells following 5 minutes pre-treatment with the ROS stimuli. The HK2 cells were exposed to some very extreme concentrations of H_2O_2 (500 & 1000 µM). These two concentrations caused a very large reduction in both SOCE and Ca^{2+} efflux from the ER (seen by the response to TG) one possible explanation for the reduction in the intensity of both efflux and SOCE could be that the H_2O_2 concentrations used are very likely cytotoxic (even with only a 5-minute pre-treatment). These higher levels of H_2O_2 would likely cause cell lysis and death, similar to what is reported in the cell death experiments in chapter 3 of this thesis.

The lower concentrations of H_2O_2 used with the HK2 cells did not reduce the intensity of fluorescence associated with Ca^{2+} efflux but did significantly reduce the intensity of SOCE. This same effect is true in the EA.hy926 cells and because lower concentrations were used and there was no reduction in Ca^{2+} efflux intensity this implies that it is not an effect that H_2O_2 is bringing about via cell death but instead the increase in intracellular ROS is causing the epigenetic and structural changes to the Orai/STIM proteins.

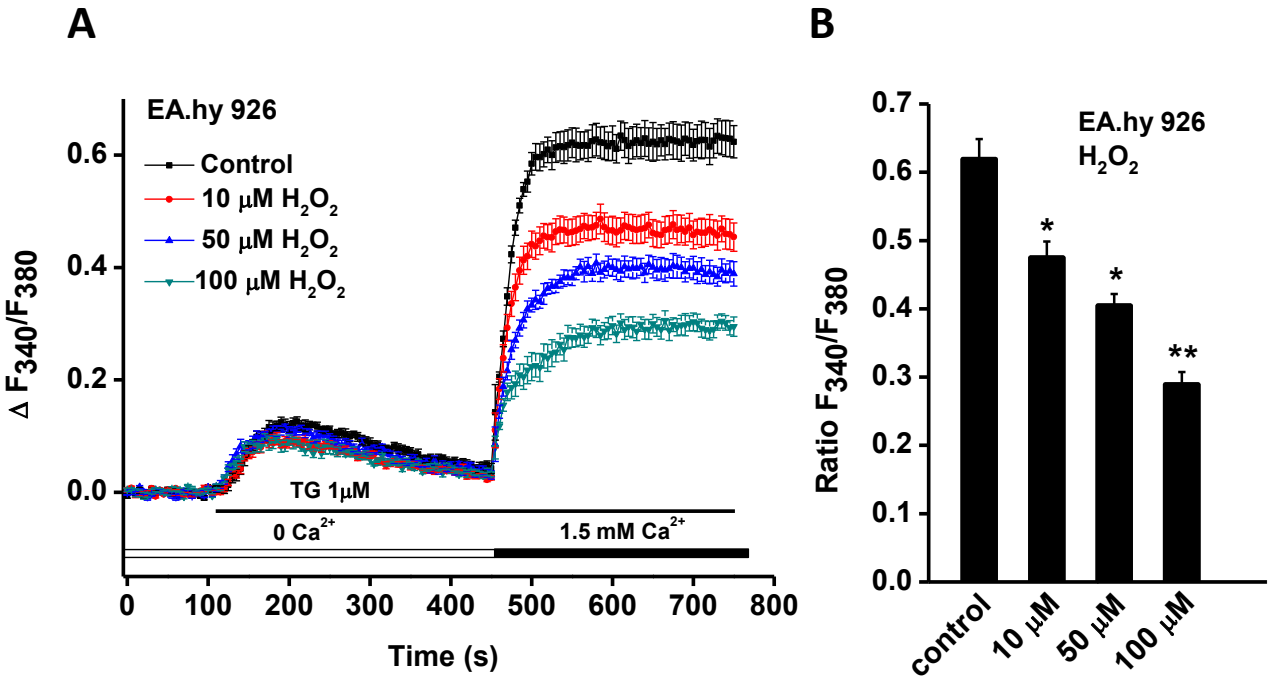

Fig. 5.9 H_2O_2 has an inhibitory effect on SOCE in EA.hy926 cells. Cells were loaded with FuraPE3-AM Ca^{2+} dye (5 μM) for 30 mins prior to experiment and the cells were treated with either control or H_2O_2 containing solution for 5 minutes prior to experimentation (A) Time course fluorescence intensity of EA.hy926 cells under the hydrogen peroxide test conditions. (B) Mean peak fluorescence of the Fura-PE3 AM. One-way ANOVA was used. * P<0.05, ** P<0.01, n = 8 per group.

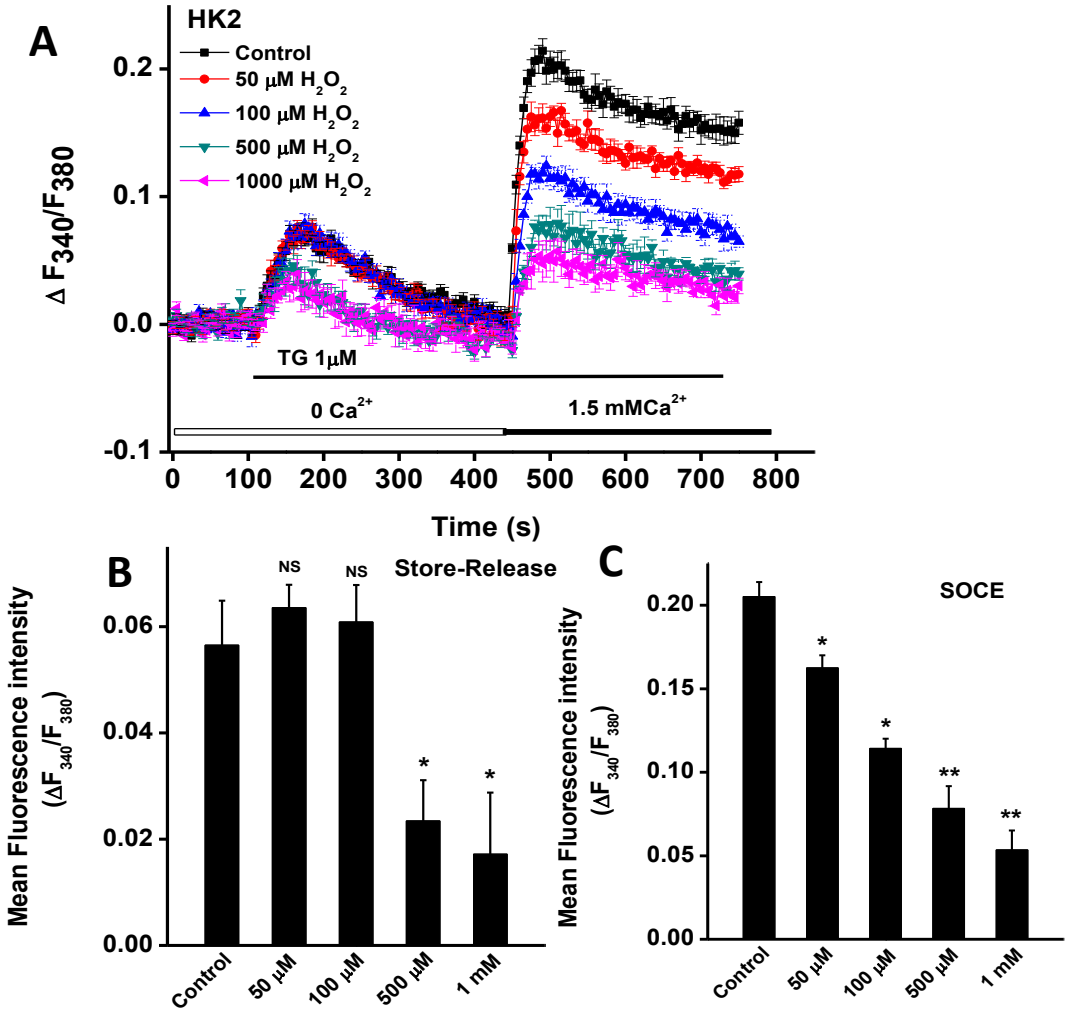

Fig. 5.10 SOCE is inhibited by H_2O_2 in HK2 cells. Cells were loaded with FuraPE3-AM Ca^{2+} dye (5 μM) for 30 mins prior to experiment and the cells were treated with either control or H_2O_2 containing solution for 5 minutes prior to experimentation (A) Time course fluorescence intensity of HK2 cells under the hydrogen peroxide test conditions. (B) Mean peak fluorescence of the FuraPE3AM all peak fluorescence intensities are significantly lower then the Control group that was not treated with the H-$_2O_2$. (10 μM H_2O_2 P=<0.05, μ50 H_2O_2 P=<0.05 , 100 μM H_2O_2 P= <0.01) significance was tested by one-way ANOVA n=8 per group.

5.3.10 Hyperosmolarity induced ROS production is prevented by sodium pyruvate

The final step into this investigation between the SOCE and increased intracellular ROS is to investigate whether an antioxidant is capable of reducing the level of intracellular ROS and in doing so, is it capable of rectifying the reduction of SOCE caused by the ROS? The antioxidant used for this experiment is sodium pyruvate (10 mM) which is a well-known scavenger of H_2O_2 (Giandomenico *et al.*, 1997).

Sodium pyruvate was chosen specifically because of other off-target effects caused by other ROS scavengers that could have interfered with the results of the experiment Fig. 5.11 shows that Sodium Pyruvate reduced the level of intracellular ROS (as measured by H_2DCFDA) in both the hyperosmolar groups and the positive control (Hydrogen peroxide) groups. The antioxidant did not have a significant effect on the 19.5 mM group although for the higher concentrations the sodium pyruvate significantly reduced the level of ROS produced by the cells compared to the groups not treated with the antioxidant. Fig. 5.12 shows that SOCE intensity is restored in EA.hy926 cells that have been co-incubated with both mannitol and sodium pyruvate.

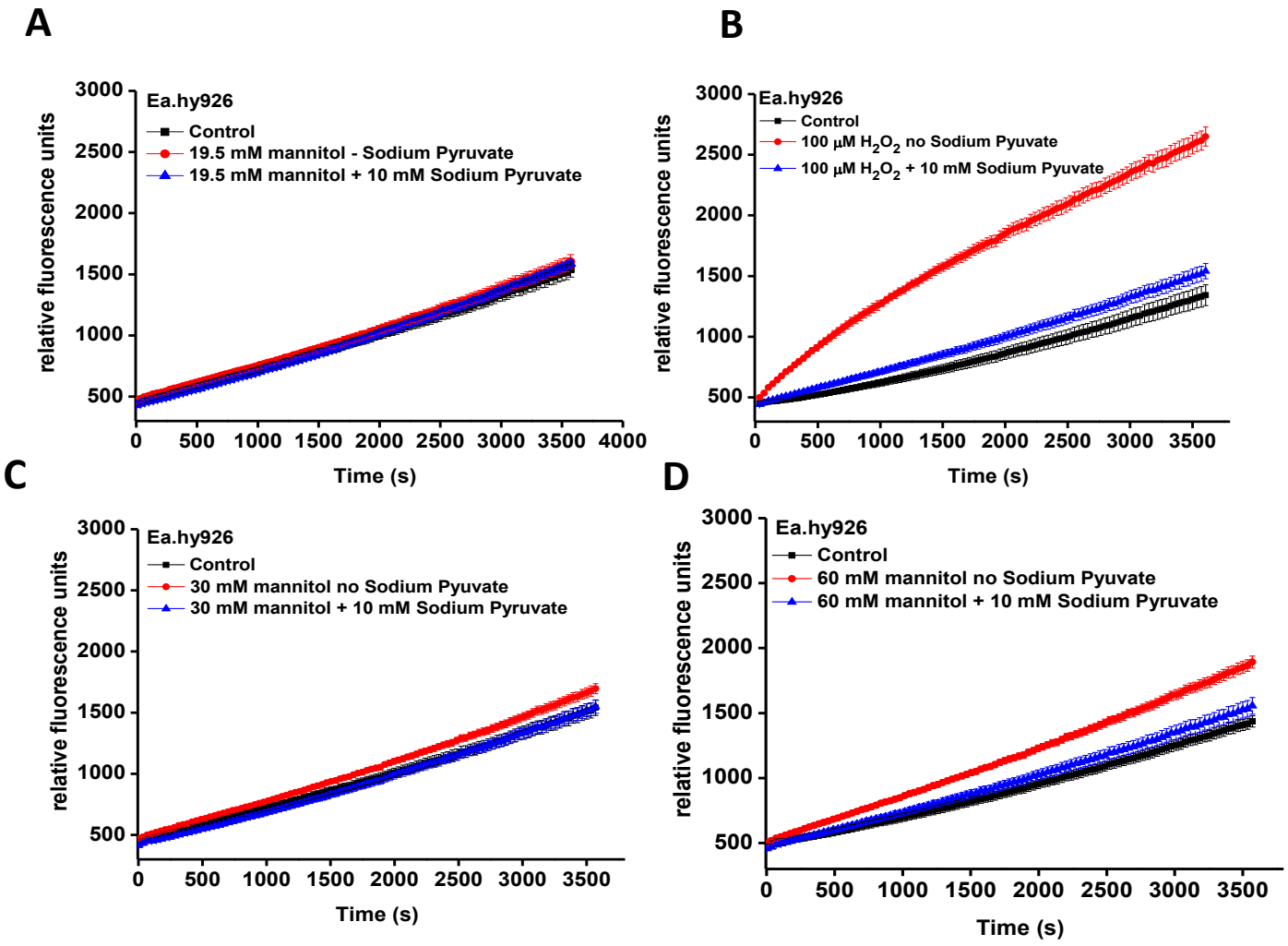

Fig. 5.11 Sodium Pyruvate is capable of reducing the level of intracellular ROS (detected by H2DCFDA) produced by EA.hy926 cells under hyperosmotic conditions. (A) Fluorescence intensity of the control 100 μM H_2O_2 both with and without the 10 mM Sodium pyruvate as well as a negative control (no peroxide and no sodium pyruvate) group for comparison. (B) H_2DCFDA fluorescence intensity of the 19.5 mM Mannitol group. (C) Fluorescence intensity of the 30 mM Mannitol group. (D) Fluorescence intensity of the 60 mM mannitol group. The reduction in the 19.5 mM group was not statistically significant. The reduction in fluorescence intensity in the positive control group was highly significant at the 2000 s time point (P=<0.001). n=8 wells per group, significance was tested using one-way

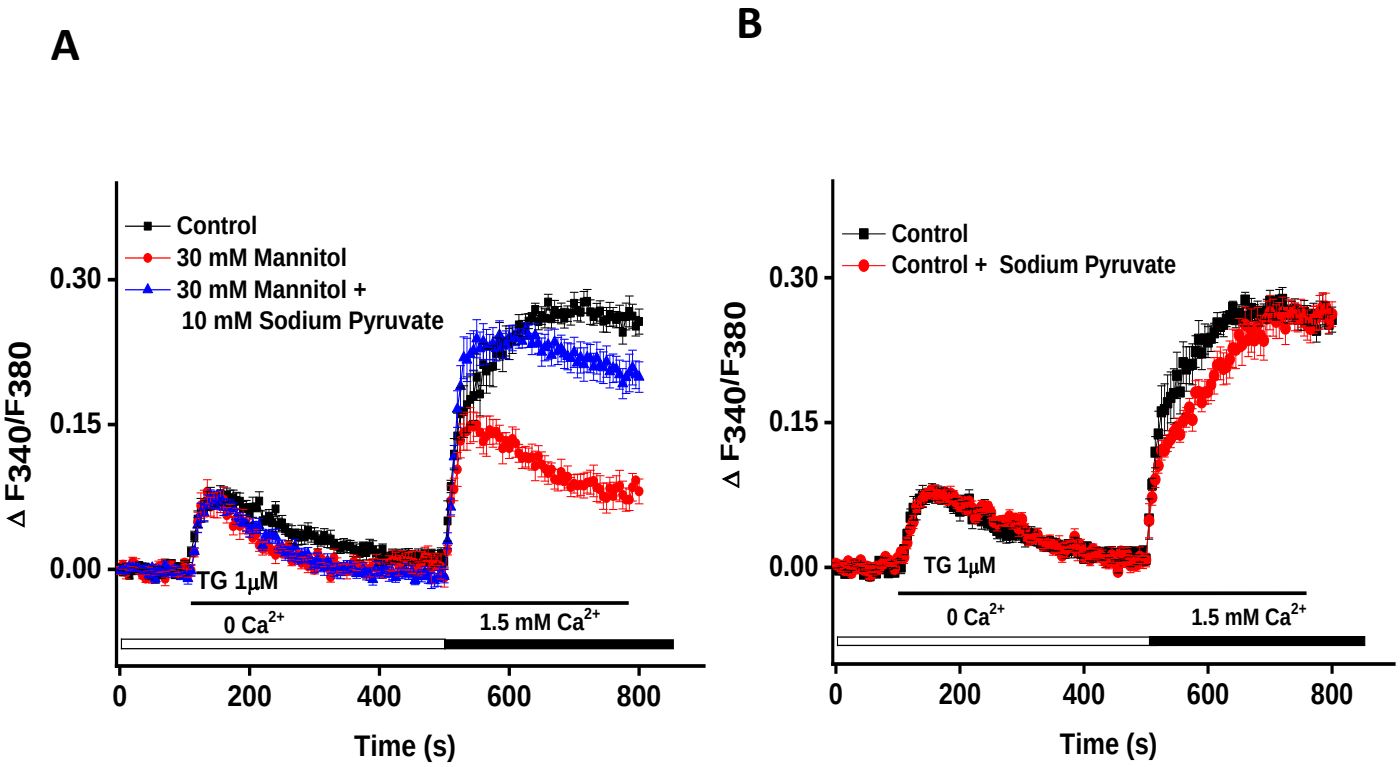

Fig. 5.12 10 mM Sodium Pyruvate is capable of restoring the normal SOCE intensity in EA.hy926 cells treated with 30 mM mannitol for 5 minutes. (A) Mean fluorescence intensity of Ea.hy926 cells that were loaded with 2 μM FuraPE3AM for 30 minutes prior to experiment. (B) Mean fluorescence intensity of the cells in both the negative control group and the 10 mM Sodium Pyruvate alone group. This shows that there is not difference in peak intensity when cells are treated with Sodium Pyruvate and not hyperosmolarity 5 minutes prior to reading the plate. The improvement of the Sodium Pyruvate group is statistically significant (P=<0.05) although there is no significant difference between the Sodium pyruvate group and the negative control group. n= wells8 for each group, significance was tested using one-way ANOVA

5.4 Discussion

The first major finding of this chapter is that the hyperosmolar condition is capable of increasing the intracellular ROS concentration in both endothelial and kidney cells. The second major finding of this chapter is that the increase of intracellular ROS production due to hyperosmolarity is linked to the presence of 1.5 mM extracellular Ca^{2+}. Although it is not only the hyperosmolar groups that showed this dependency upon extracellular Ca^{2+} but also the positive control groups whereby increased ROS was generated by hydrogen peroxide. Although some difference was expected between hyperosmolar groups, in the 1.5 mM Ca^{2+} vs 0 Ca^{2+} groups the presence of such a marked reduction in even the positive control groups lead to questions as to the true mechanism for this reduction. As the removal of Ca^{2+} from the extracellular environment was not predicted to produce such a reduction in the ROS concentration between the positive control groups. Literature has demonstrated that the generation of some NOX variants is Ca^{2+} dependant, such a decrease in global ROS (of which nitric oxide is just one element) was not anticipated (Guzik *et al* 2008).

One possible contributing factor for the reduction of positive control group intracellular ROS intensity is the possibility that the EDTA used in the Ca^{2+} free solution could have been acting as an antioxidant and thereby "mopping up" a proportion of the H_2O_2 used in the positive control group, this antioxidant capability has been documented previously (González-Cuevas *et al.*, 2011).

This does not render the results of this experiment useless though, as EDTA's primary mode of action would have been the chelating of free Ca^{2+}. The fact that an antioxidant compound can reduce the intensity of hyperosmolarity induced increased intracellular ROS confirms that hyperosmolarity is contributing to an increase in ROS and theoretically if intracellular ROS were lowered then it could be expected to reduce the SOCE hyperosmolarity effect.

Following the determination of the importance of Ca^{2+} in the ROS increase related to hyperosmolarity, the decision was made to ensure that the dye was not reduced or inhibited by the additional mannitol or hydrogen peroxide. This was done to ensure that the experimental conditions were not capable of producing a change in fluorescence separate from the cells, as this would render the results of the previous assays useless (Fig. 5.4). This was also an important confirmatory experiment because during the time within the experimental conditions these cells are deprived of all nutrients but glucose and this in itself could lead to oxidative stress (Affonso et al, 2003).

The results shown in Fig. 5.3 and 5.4 show that although these cells may not be in ideal metabolic conditions, the bath solution does not appear to significantly affect the production of ROS within the experimental time frame. It was found that if cells were not present the dye did not emit a significant fluorescent signal, although a small amount of fluorescence was detected in the positive control (hydrogen peroxide) group.

This relatively small increase in fluorescence is probably due to the H_2DCFDA being designed for the detection of intracellular ROS which even in some ROS microdomains found within immune cells would not reach such a high concentration as 100 μM (Rhee *et al.*, 2010). This could have an activating effect on the dye outside of its usual intracellular cleaving effect. Another possible explanation could be the increase in pH (although somewhat buffered by the contents of the bath solution) like this, over time, could have contributed to the H_2DCFDA activation as the dye is known to be sensitive to alterations in extracellular pH (Van Acker *et al*, 2016).

Although the difference in magnitude between the cell containing and the blank (cell-free) hydrogen peroxide-containing groups shows that any extracellular activation of the dye would not significantly change the outcome of the experiment. The intracellular cleavage of this dye produces a much more intense fluorescence, quite possible masking any extracellular fluorescence. The most important finding of the experiment presented in Fig. 5.5 is that the increase in fluoresce intensity seen in the negative control groups over time is dependent upon the presence of cells and not caused by dye degradation or a bleaching effect. A number of factors could cause these cells to produce intracellular ROS, one being the natural production of ROS linked to mitochondrial respiration as well as the fact that these readings are taken at room temperature (perhaps adding to extracellular stress).

Another contributing factor could be a short-term lack of nutrients due to the fact that although intended to mimic normal extracellular fluid there are no amino acids or lipids present within the experimental bath solution and unlike with cell culture media there are fewer buffers in this solution that can resist the production of cellular waste. This could be causing alterations in pH or a reduction in glucose concentration thereby causing an increase intracellular ROS.

The effect of hyperosmolarity on the production of cytosolic ROS was investigated in HK2 cells as well as endothelial cells in order to determine if this same mechanism could be present in a kidney cell line. Cytosolic ROS was still increased by the hyperosmolar condition in HK2 cells although it was to a lesser degree than that observed in the endothelial cell line. One possible reason for the reduced intensity of the fluorescent signal could be due to a decrease in dye loading efficiency. Some kidney cell types, for example, podocytes, are known to actively efflux some dyes and imaging compounds (Zennaro et al, 2013). Despite the reduction in fluorescence intensity, the important finding can still be seen in the increase of intracellular ROS being caused by the hyperosmolar condition. Another possible reason that the HK2 cells may be more resistant to increased ROS due to hyperosmolarity could be that the HK2 cells have a naturally lower volume and as such may have a greater ability to regulate cytosolic water and thereby resist changes to osmolarity to a greater capacity than the endothelial cell line. This is based on the well-established relationship between increasing cellular size and a decreasing inability to buffer large changes in ionic flux due to osmolarity (Bortner and Cidlowski, 2007).

After the work had been done with the general ROS indicator the decision was taken to assess the effect of the hyperosmolarity on both the superoxide and peroxide. This decision was made in order to better ascertain what the source of intracellular ROS is, as superoxide increase would indicate a change in mitochondrial bioenergetics whereas an increase in peroxide could indicate an increase in NADPH oxidase activity (Lee et al, 2003).

This could then be explored in future work as a potential pathway to preventing the ROS increase in response to hyperosmolarity and subsequent SOCE inhibition, The most likely source of this superoxide production is the mitochondrion due to its respiratory chain producing superoxide. Interestingly in this experiment, the positive control (H_2O_2) did not produce the largest increase in fluorescence intensity, this is likely because H_2O_2 is a product of Superoxide formation.

The mitochondrion is an organelle that is known to play a vital role in the regulation of cytosolic Ca^{2+} and in the case of Ca^{2+} overload the mitochondrion is known to enter into a hyper-energetic state (Contreras *et al.*, 2010). This hyper-energetic state would produce more ROS and is detrimental to cellular function. In addition, these experiments suggest a link between the hyperosmolar condition and increasing Peroxide radicles this could be one of the contributing factors to the reduction in SOCE intensity seen in both the endothelial cells and HK2 cells reported earlier in this thesis. The finding that when Ca^{2+} is not present in the extracellular environment the increase in H_2O_2 is diminished suggests that the ROS reaction to hyperosmolarity may be dependent upon a Ca^{2+} signal, with SOCE being the prime candidate in this instance. The hyperosmolar state applied in these experiments could be causing an increase in intracellular ROS because of increased energy demands caused by the active transport of ions across a concentration gradient. Because the ROS produced reduces the intensity of SOCE the potential for the SOCE channels to overload the cell with Ca^{2+} is reduced thereby potentially avoiding cell death and promoting cellular survival. Although data presented in chapter 3 of this thesis does show that there is an increase in endothelial cell death associated with this hyperosmolarity and therefore if the increased ROS is a compensatory mechanism to reduce SOCE intensity it does not seem to be effective.

A third major finding in this chapter was that pre-treatment with H_2O_2 for 5 minutes significantly reduced that SOCE intensity in the EA.hy926 cells and the HK2 cells as well. The very strong increase caused by the H_2O_2 is to be expected due to the concentration of exogenous ROS being many times higher than physiologically acceptable (Huang and Sikes, 2014). Finally, the use of an antioxidant Sodium Pyruvate was capable of reducing the concentration of intracellular ROS and was also shown to have a protective/restorative effect on EA.hy926 treated with the hyperosmolar condition and causing the reduction in SOCE intensity to be revered/prevented.

One of the major conclusions of this chapter is that intracellular ROS are implicated in the altered SOCE response that has been discovered in endothelial and kidney cells treated with hyperosmolar conditions. Although this data may not be directly applicable to a clinical situation as it would not be plausible for patients to be infused with 10 mM Sodium Pyruvate in order to protect endothelial cells during HHS. The reason for only using one concentration of Sodium Pyruvate (10 mM) in these previous two experiments is because work has already performed investigating the antioxidant properties of Sodium pyruvate at this was found to be the optimum concentration for the scavenging of H_2O_2 radicles (Wang *et al.*, 2007).

This experiment provides further evidence that the SOCE reduction response in hyperosmolar conditions could be mediated by an increase in intracellular ROS and that the scavenging of these ROS may be able to combat the decrease in SOCE intensity caused by hyperosmolarity.

This data opens up a new line of enquiry about the general use of known antioxidants in emergency situations such as HHS. If a safe and effective antioxidant was found that could prevent the reduction on SOCE and in turn protect endothelial cells from hyperosmolarity related dysfunction then this could, in theory, deliver clinical benefit.

As the work currently stands the important finding to emphasise is that this data elucidates a potential damage pathway and a new relationship associating hyperosmolarity with the decrease of SOCE via the increase of ROS. It is only by better understanding the mechanisms of damage that new therapeutic interventions can be devised in a targeted manner. This information provides novel information into the effects of hyperosmolarity on the endothelial cell a mechanism that possibly contributes to this effect.

Chapter 6

General discussion

6.1 Main findings

One of the major novel findings presented is that the STIM/Orai SOCE apparatus activity is reduced by hyperosmolarity, as mediated by increased intracellular ROS (Both superoxide and hydrogen peroxide) and it is the reduction in SOCE that may contribute to hyperosmolarity induced endothelial dysfunction. A schematic showing the significant findings of this work can be seen in Fig. 6.1

The reduction of SOCE signal intensity under the hyperosmolar condition is not a phenomenon that has been described before and this discovery contributes to our understanding of clinical hyperosmolarity and its associated injuries. For example in the diabetic vascular complications caused by the extreme hyperosmolarity found in the HHS disease state. As well as contributing to understanding this work, when investigated in greater detail, and expanded could help to inform the clinical management of HHS and other clinical causes of elevated osmolarity.

The findings presented in chapter 5 of this thesis indicate that this decrease in SOCE intensity is not due to a direct effect on the channel apparatus but rather is caused by an increase in intracellular ROS caused by the stressful hyperosmolar condition.

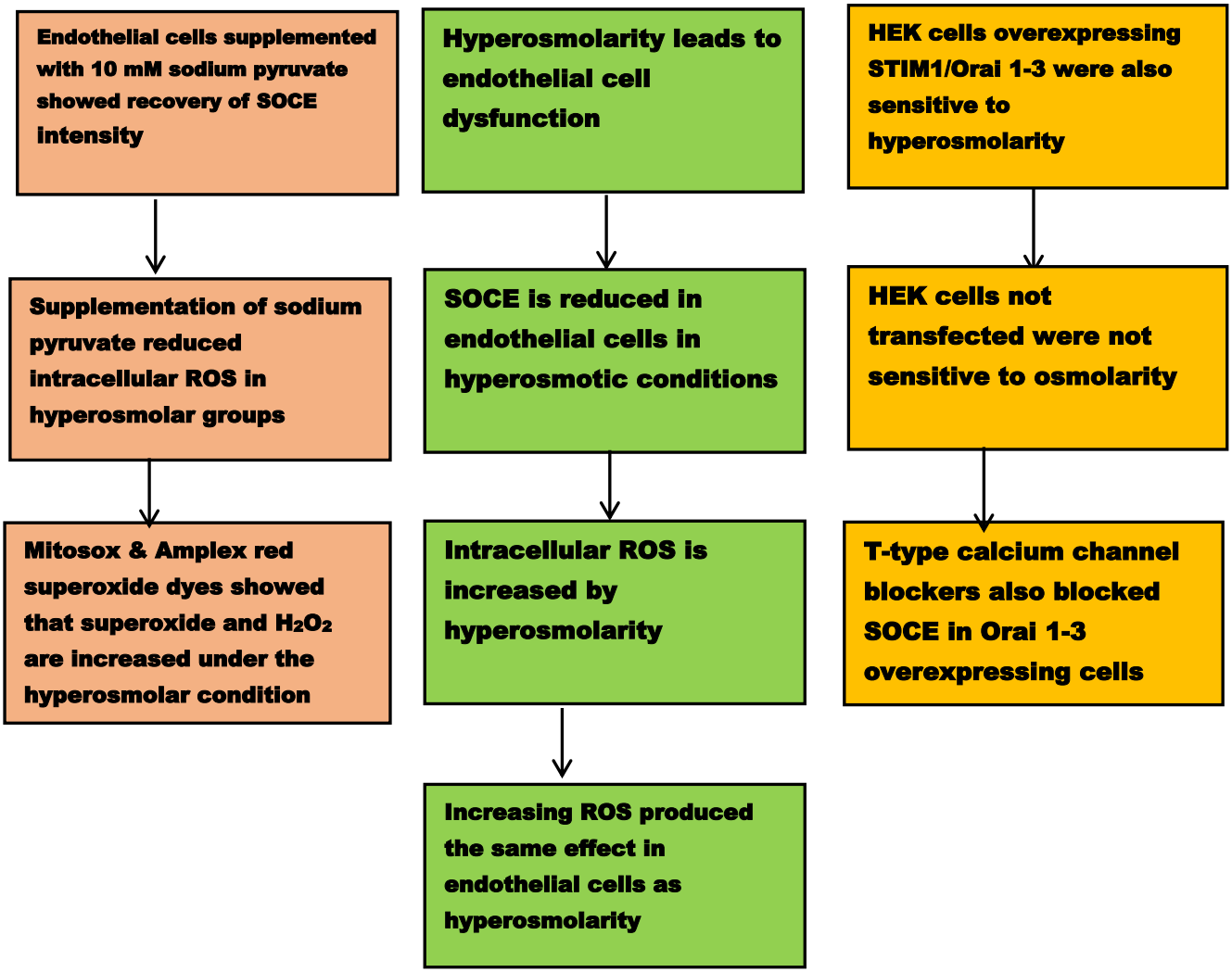

Fig 6.1 Schematic showing the major findings of this thesis. Green boxes denote the central story of SOCE inhibition under hyperosmolarity potentially mediated by increased ROS. Red Boxes denote specific ROS work undertaken. Yellow boxes denote channel specific work and pharmacological investigations into T channel blockers as potential remediative agents.

The restoration of normal serum osmolarity is already a goal of HHS treatment and is often a consequence of treating the hypovolemia associated with the condition (Baldrighi *et al.*, 2018). The body of work presented in this thesis could still help to improve patient outcomes. This is because this work reveals that the reduced SOCE seen in hyperosmolar conditions occurs as an indirect effect produced by elevated intracellular ROS and this effect can be corrected by the use of the antioxidant sodium pyruvate. Although the clinical benefit of antioxidant supplementation as a protective effect against oxidative stress is not well-proven (Rodrigo, Guichard and Charles, 2007). It may be the case that a clinically significant dose of sodium pyruvate or another effective peroxide scavenger could be beneficial in restoring the SOCE response within vascular endothelial cells and thereby reduce the risk of vascular injury caused by this emergency HHS state. Sodium pyruvate has been used to significantly reduce ROS in the clinical setting when delivered at a clinically relevant concentration (Votto *et al.*, 2008).

The discovery of SOCE reduction under the hyperosmotic condition is not only significant to the understanding and treatment of DM but, because serum osmolarity is elevated in a number of conditions, SOCE reduction may be found to be a contributing factor to a number of pathologies. For example, it has been found that elderly stroke sufferers have a higher degree of morbidity and mortality following acute stroke if their serum osmolarity is elevated prior to the acute ischaemic episode (Bhalla *et al.*, 2000). It could be possible that alterations in Ca^{2+} homeostasis, potentially mediated by the reduction in SOCE intensity via increased ROS, could be contributing to the death and dysfunction of neuronal cells.

One of the reasons that hyperosmolarity is a negative predictor of survival within cardiovascular disease and stroke could be the contribution of SOCE reduction within vascular endothelial cells under this hyperosmotic condition leading to endothelial dysfunction (Wang et al., 2014). Although it is worth noting that the hyperosmolar serum alone is not responsible for this poor survivability because haemodilution was found to be ineffective at combating this increased mortality following acute stroke (Chang and Jensen, 2014).

The cell-based models used in this experiment have some limited applicability when it comes to determining the potential impact on diabetic patients. This is because consistently, throughout this thesis there has been a focus on the hyperosmolarity as a solitary factor, whereas in order for patients with diabetes to directly benefit from this work further work would have to be done in linking the hyperglycaemia, and hyperosmolarity. Secondly, there are, of course, significant limitations in seeking to translate cell-based findings to a confirmed mechanism within the human body.

For example, the vascular endothelium is not a tissue that exists in isolation, it has complex interactions with the smooth muscle layer which supports it and these interactions could affect the response of the endothelial cells in the hyperosmotic condition. These are important limitations to consider when planning the next stage of the investigation. Although, the findings within this thesis do offer a basis for a potential cause for hyperosmotic endothelial damage and these results will be able to inform the best way forward.

The data in this thesis may have even wider implications in the understanding of how elevated serum osmolarity is correlated with poor prognosis in critically ill patients as identified in Holtfreter et al., 2006. This is because this work has identified that SOCE is suppressed under hyperosmolar conditions and this leads to endothelial dysfunction, if hyperosmolarity has the same effect *in vivo* then this will be increasing the cardiovascular risk of critically ill patients with hyperosmolarity.

A second major finding of this thesis is that hyperosmolarity produces a significant increase in intracellular ROS (both superoxide and H_2O_2) production. This finding builds upon previously discovered knowledge that cellular stress and hyperglycaemia are capable of increasing ROS (Yao and Brownlee, 2010). Another finding that this data builds upon is the knowledge that ROS are capable of altering the activity of SOCE proteins and reducing the SOCE current at high concentrations (Bogeski et al., 2012). The novel finding that this research adds to this body of knowledge is the effect of hyperosmolarity as a distinct stimulus on the production of ROS and the subsequent effect on the intensity of SOCE, perhaps providing insight as to how hyperosmolarity may be causing cellular damage within the vascular endothelium. It would appear that the results of this thesis support the theory that the major source of this elevated ROS is the mitochondrion, although no in depth work was performed in order to investigate the effect of hyperosmolarity on ER or peroxisomal specific ROS generation.

It is possible that these effects occur through the inhibition of the Orai channels undergoing chemical and conformational change due to the increased presence of intracellular ROS in the hyperosmolar condition. Being able to link the already known relationships between ROS and SOCE to the reduction of SOCE intensity under the hyperosmolar condition allowed for additional research into a potential antioxidant effect of sodium pyruvate and the restoration of SOCE under the hyperosmolar condition when the cells were also treated with this compound.

One of the other significant findings within this body of work is the discovery of a novel inhibitory effect that the T type Ca^{2+} channel blockers, mibefradil & TH1177, have on SOCE in EA.hy926 cells and HK2 cells. This effect has not been described before and is an important insight into potential off-target effects that these drugs may exhibit. Although their inhibitory effect on SOCE is not beneficial, to the hyperosmolar condition being investigated, these drugs are being explored as an anti-proliferative agent and this effect on SOCE needs to be considered in future studies. As described in chapter 4 these drugs are not available for their intended indications because of their ever-increasing list of off-target effects. This data both highlights a potentially serious off-target effect in the reduction of SOCE intensity although this may be a useful finding when investigating the action of these drugs as anti-proliferative agents.

A separate investigation into the exact activity and effect that these compounds have on SOCE, beyond the initial screening done in this work, has been performed and reported on by others members of the laboratory (Li et al 2019). This included ascertaining the EC_{50} of the compounds inhibitory effect as well as any effects that this inhibition of SOCE would have on the viability of endothelial cells.

It is also worth noting that SOCE is very important in multiple immune cell processes and if this inhibitory effect is present in immune cells then this could render these drugs un-usable if they have an immunosuppressant effect (Shaw and Feske, 2012). As with any drug, the benefits must outweigh the risks of use, although the findings of the Li paper do suggest that the inhibitory effects of the compounds can be tissue/cell type-specific depending on the proportion of Orai subtypes expressed by the target cells. This is due to a decreased inhibitory effect of the compounds on Orai 2+ 3 in comparison to Orai1 (Li et al. 2019)

6.2 limitations

One major limitation that is associated with the work presented within this thesis is that all results shown are based on *in vitro* experiments. Even though the cell models used are well established as being experimentally useful and representative of the *in vivo* situation there are still limitations as to the clinical conclusions that can be drawn from these data. One reason the *in vitro* data generated is of limited usefulness is due to the fact that the experiments are tightly controlled with homogenous cellular populations. This is good for the analysis of specific cellular effects but cannot accurately predict the reaction of cells in the physiological situation where they have interactions with a host of cells and cytokines which are not present within the *in vitro* situation. The *in vitro* data presented in this thesis may not be easily translatable to a clinical scenario but it does allow for the description of a novel damage mechanism, which can inform further translational research.

Therefore, a prudent next step within this investigation would be to generate *in vivo* data, this would be technically difficult within a mouse knockout model because any chronic hyperosmolarity induced could lead to either the model drinking and rectifying the condition before measurement can be taken or premature death of the murine model. It may then be better to use tissue samples from patients that have undergone a hyperosmotic episode to determine any effect on the expression of the STIM/Orai proteins in order to show that hyperosmolarity is capable of producing the same effect seen in the previous chapters in a human.

Another methodological limitation is to be found within the cell death assay. The PI dye is a well-established tool for the detection of cell death although it is well established that this method lacks any specificity in the determination of apoptosis (Pollack and Ciancio, 1990). As such, the results presented in this thesis are termed "cell death" because there is no way of confidently predicting which distinct form of cell death is occurring using such a basic method. Therefore, a future direction of investigation would be to determine the effect of hyperosmolarity on the distinct cell death pathways of necrosis and apoptosis.

The second limitation to this PI technique of measuring cell death is the potential for observer bias during manual cell counting. It was this reason that automated cell image processing was used although the gold-standard for analysing the dye uptake and fluorescence in such an assay is fluorescence assisted cell sorting and, where the resources available, this would have been performed in order to further confirm the results of the PI cell death assay. Of course, using FACS to measure the number of dead cells would only be of limited additional value when still using a non-specific dye such as PI.

As such it would be beneficial to explore the use of specific markers of apoptosis and necrosis if a technique such as FACS were to be used. One such specific probe that could be used to confirm these results would be Alexa Fluor 488 annexin V which has shown specificity for apoptotic cells and allowing for the differentiation from necrotic cell death (Stepanek et al., 2011).

Another probe that is specific to FACS apoptosis detection is the Fluorochrome Inhibitor of Caspases (FLICA) probe, which binds to active caspases within the cell and becomes activated. Therefore being specific to apoptosis and allowing for an accurate count of apoptotic cells within the sample (Darzynkiewicz et al., 2011). Should the resource be available; ideally the effect of Hyperosmolarity on the Orai channels would be confirmed using a direct measurement method such as electrophysiology ("Patch-clamp") in order to avoid the confounding Ca^{2+} currents being expressed within the cell models used in this thesis. One major advantage of this technique is the ability to clamp (lock) the membrane potential of the cell and as such measure ionic movement with a high degree of accuracy.

6.2 Future work

One potential future direction that this work could take would be to better develop a model of diabetic hyperosmolarity outside of the HHS emergency condition that this data is based upon. In HHS the plasma osmolarity rises and keeps getting higher until the patient is either treated or they die.

This is not the “normal” outcome for DM patients with poorly controlled blood glucose. It is more likely that the plasma osmolarity would undergo fluctuations from normal to hyperosmotic and back again several times per day. This fluctuation could itself affect endothelial cells in a way that is different from what is reported in previous chapters. It is also within this fluctuating osmolarity condition that the majority of endothelial cell damage is done over the course of the disease and as such would be an important condition to model in order to ascertain any effect on SOCE. This would allow for the findings of this thesis to be translated to a broader hyperglycaemic condition (as found within DM) if a similar damage pathway was identified.

One way to determine whether the described damage pathway suggested in this thesis is present in the clinical situation would be to use human tissue samples from patients that have undergone hyperglycaemic/hyperosmotic shock. An investigation could be performed to ascertain whether the SOCE proteins are expressed in key tissues such as the kidney. It would be possible to measure the activity of the SOCE channels from these samples through the use of Ca^{2+} imaging and electrophysiology. If the same reduction in SOCE intensity is observed this could open up potential research areas into the potential therapeutic effects of antioxidants for patients with highly elevated plasma osmolarity.

Another potential future direction that this research could be taken in would be to assess whether a different source of hyperosmolarity, other than mannitol, is capable of producing the same effect. One such source could be urea, which is a major osmolyte capable of increasing the plasma osmolarity in acute kidney failure (Josa-Laorden *et al.*, 2018). This would not only act as a control for the mannitol induced hyperosmolarity (although this compound is not known to have any effect on cells beyond functioning as an extracellular osmolyte) but this would reveal another clinical condition that can lead to this reduction in SOCE.

Because this work focused in on an underlying mechanism for the SOCE reduction hyperosmolar effect some detail was not covered that could still be of clinical and scientific interest. For example, electrophysiological techniques were not used on these cells and channels which would have shown with near experimental certainty that the effect was mediated by the Orai channels. Also not investigated was the effect that longer-term hyperosmolarity had on the expression of the STIM/Orai genes and proteins which would have revealed how in the longer term, the cells handle this SOCE reduction.

6.3 Conclusion

The data presented is scientifically novel and although of limited clinical importance in and of itself this data can underpin deeper studies into the activity of SOCE proteins and their interaction with hyperosmotic stimuli. The data builds upon known relationships between ROS and SOCE to suggest a novel pathway of endothelial damage as caused by bu hyperosmolarity. The findings presented in this thesis also have the potential, upon further study, to inform the treatment of both the hyperosmolar hyperglycaemic state and other conditions leading to acute and chronic hyperosmolarity.

As is to be expected within any scientific study there is always work to be done but what is important is that even though it was beyond the scope of this experiment it is still imperative to screen compounds that could offer a protective effect against this damage.

The vascular complications of DM remain one of the greatest health threats in the western world due to the high number of DM patients as well as the severity of the disease it is imperative that studies such as this continue to reveal the many ways in which these disease states affect aspects of human physiology. It is only by knowing how DM causes damage that we can learn to prevent it and it would appear from this work that hyperosmolarity is not just a result of hyperglycaemia but is a pathological state in its own right and should be treated as such. For any state capable of altering such an important process as SOCE is worthy of further investigation for its effects could be more numerous and severe than previously imagined.

References

Publications and presentations

Publications

Zeng, B., Chen, G.L., Garcia-Vaz, E., Bhandari, S., Daskoulidou, N., Berglund, L.M., Jiang, H., Hallett, T., Zhou, L.P., Huang, L., Xu, Z.H., Nair, V., Nelson, R.G., Ju, W., Kretzler, M., Atkin, S.L., Gomez, M.F., Xu, S.Z., 2017. ORAI channels are critical for receptor-mediated endocytosis of albumin', *Nature Communications*.8(1), p. 1920.

LI, P., RUBAIY, H. N., CHEN, G. L., HALLETT, T., ZAIBI, N., ZENG, B., SAURABH, R. & Xu, S. Z. 2019. Mibefradil, a T-type Ca(2+) channel blocker also blocks Orai channels by action at the extracellular surface. *Br J Pharmacol,* 176**,** 3845-3856.

Conference presentations

Hallett T.G., Daskoulidou. N., Xu, S., 2016.Involvement of ORAI/STIM store-operated Ca2+ Channels in hyperosmolarity-induced endothelial dysfunction. Proc Physiol Soc 37 PCB19, Dublin. Ireland.

Li P., Hussein N.R., Chen. G., Hallett. T., Xu.S.Z., 2018. T-Type Ca^{2+} blocker mibefradil inhibits ORAI store-operated channels. Europhysiology, London.

References

ADINOLFI, E., CALLEGARI, M. G., FERRARI, D., BOLOGNESI, C., MINELLI, M., WIECKOWSKI, M. R., PINTON, P., RIZZUTO, R. & VIRGILIO, F. D. 2005. Basal Activation of the P2X7 ATP Receptor Elevates Mitochondrial Calcium and Potential, Increases Cellular ATP Levels, and Promotes Serum-independent Growth. *Molecular Biology of the Cell,* 16**,** 3260-3272.

AFFONSO, F., PEIXOTO, S., PINTO, L., GOMES, M. & TIBIRIÇÁ, E. 2003. Effects of high glucose concentrations on the endothelial function of the renal microcirculation of rabbits. *Arquivos brasileiros de cardiologia,* 81**,** 161-5, 156.

AHN, K., PAN, S., BENINGO, K. & HUPE, D. 1995. A permanent human cell line (EA.hy926) preserves the characteristics of endothelin converting enzyme from primary human umbilical vein endothelial cells. *Life Sci,* 56**,** 2331-41.

ÅKERBLOM, H. K., VAARALA, O., HYÖTY, H., ILONEN, J. & KNIP, M. 2002. Environmental factors in the etiology of type 1 diabetes. *American Journal of Medical Genetics,* 115**,** 18-29.

AL-GOBLAN, A. S., AL-ALFI, M. A. & KHAN, M. Z. 2014. Mechanism linking diabetes mellitus and obesity. *Diabetes, metabolic syndrome and obesity : targets and therapy,* 7**,** 587-591.

AL-QABANDI, W., OWAYED, A. F. & DHAUNSI, G. S. 2012. Cellular Oxidative Stress and Peroxisomal Enzyme Activities in Pediatric Liver Transplant Patients. *Medical Principles and Practice,* 21**,** 264-270.

AL-SHAREA, A., LEE, M. K. S., WHILLAS, A., MICHELL, D. L., SHIHATA, W. A., NICHOLLS, A. J., COONEY, O. D., KRAAKMAN, M. J., VEIGA, C. B., JEFFERIS, A.-M., JACKSON, K., NAGAREDDY, P. R., LAMBERT, G.,

WONG, C. H. Y., ANDREWS, K. L., HEAD, G. A., CHIN-DUSTING, J. & MURPHY, A. J. 2019. Chronic sympathetic driven hypertension promotes atherosclerosis by enhancing hematopoiesis. *Haematologica,* 104**,** 456-467.

ALBERTI, K. G. M. M. & ZIMMET, P. Z. 1998. Definition, diagnosis and classification of diabetes mellitus and its complications. Part 1: diagnosis and classification of diabetes mellitus. Provisional report of a WHO Consultation. *Diabetic Medicine,* 15**,** 539-553.

ALESSANDRI-HABER, N., DINA, O. A., YEH, J. J., PARADA, C. A., REICHLING, D. B. & LEVINE, J. D. 2004. Transient receptor potential vanilloid 4 is essential in chemotherapy-induced neuropathic pain in the rat. *J Neurosci,* 24**,** 4444-52.

AMBUDKAR, I. S., DE SOUZA, L. B. & ONG, H. L. 2017. TRPC1, Orai1, and STIM1 in SOCE: Friends in tight spaces. *Cell Calcium,* 63**,** 33-39.

AMIN, A. K., HUNTLEY, J. S., BUSH, P. G., SIMPSON, A. H. R. W. & HALL, A. C. 2008. Osmolarity Influences Chondrocyte Death in Wounded Articular Cartilage. *JBJS,* 90**,** 1531-1542.

AQUILANO, K., FILOMENI, G., RENZO, L. D., VITO, M. D., STEFANO, C. D., SALIMEI, P. S., CIRIOLO, M. R. & MARFÈ, G. 2007. Reactive oxygen and nitrogen species are involved in sorbitol-induced apoptosis of human erithroleukaemia cells K562. *Free Radical Research,* 41**,** 452-460.

ARAKI, N., GREENBERG, J. H., SLADKY, J. T., UEMATSU, D., KARP, A. & REIVICH, M. 1992. The Effect of Hyperglycemia on Intracellular Calcium in Stroke. *Journal of Cerebral Blood Flow & Metabolism,* 12**,** 469-476.

ARBEL-ORNATH, M., HUDRY, E., BOIVIN, J. R., HASHIMOTO, T., TAKEDA, S., KUCHIBHOTLA, K. V., HOU, S., LATTARULO, C. R., BELCHER, A. M., SHAKERDGE, N., TRUJILLO, P. B., MUZIKANSKY, A., BETENSKY, R.

A., HYMAN, B. T. & BACSKAI, B. J. 2017. Soluble oligomeric amyloid-β induces calcium dyshomeostasis that precedes synapse loss in the living mouse brain. *Molecular Neurodegeneration,* 12**,** 27.

ARMSTRONG, C. M. & HILLE, B. 1998. Voltage-Gated Ion Channels and Electrical Excitability. *Neuron,* 20**,** 371-380.

ARTIM-ESEN, B., SMOKTUNOWICZ, N., MCDONNELL, T., RIPOLL, V. M., PERICLEOUS, C., MACKIE, I., ROBINSON, E., ISENBERG, D., RAHMAN, A., IOANNOU, Y., CHAMBERS, R. C. & GILES, I. 2017. Factor Xa Mediates Calcium Flux in Endothelial Cells and is Potentiated by Igg From Patients With Lupus and/or Antiphospholipid Syndrome. *Scientific Reports,* 7**,** 10788.

ARUNDINE, M. & TYMIANSKI, M. 2003. Molecular mechanisms of calcium-dependent neurodegeneration in excitotoxicity. *Cell Calcium,* 34**,** 325-337.

ATKINSON, M. A. & EISENBARTH, G. S. 2001. Type 1 diabetes: new perspectives on disease pathogenesis and treatment. *The Lancet,* 358**,** 221-229.

BABICH, A. & BURKHARDT, J. K. 2013. Coordinate control of cytoskeletal remodeling and calcium mobilization during T-cell activation. *Immunological reviews,* 256**,** 80-94.

BADOU, A., JHA, M., MATZA, D. & FLAVELL, R. 2013. Emerging Roles of L-Type Voltage-Gated and Other Calcium Channels in T Lymphocytes. *Frontiers in Immunology,* 4.

BANSAL, N. 2015. Prediabetes diagnosis and treatment: A review. *World journal of diabetes,* 6**,** 296-303.

BARR, V. A., BERNOT, K. M., SHAFFER, M. H., BURKHARDT, J. K. & SAMELSON, L. E. 2009. Formation of STIM and Orai complexes: puncta and distal caps. *Immunological reviews,* 231**,** 148-159.

BASSET, O., BOITTIN, F.-X., COGNARD, C., CONSTANTIN, B. & RUEGG, U. T. 2006. Bcl-2 overexpression prevents calcium overload and subsequent apoptosis in dystrophic myotubes. *The Biochemical journal,* 395**,** 267-276.

BAUER, J., MARGOLIS, M., SCHREINER, C., EDGELL, C.-J., AZIZKHAN, J., LAZAROWSKI, E. & JULIANO, R. L. 1992. In vitro model of angiogenesis using a human endothelium-derived permanent cell line: Contributions of induced gene expression, G-proteins, and integrins. *Journal of Cellular Physiology,* 153**,** 437-449.

BECKMAN, J. A., CREAGER, M. A. & LIBBY, P. 2002. Diabetes and atherosclerosis: epidemiology, pathophysiology, and management. *JAMA,* 287**,** 2570-81.

BEDARD, K. & KRAUSE, K.-H. 2007. The NOX Family of ROS-Generating NADPH Oxidases: Physiology and Pathophysiology. *Physiological Reviews,* 87**,** 245-313.

BERNHARDT, M. L., STEIN, P., CARVACHO, I., KRAPP, C., ARDESTANI, G., MEHREGAN, A., UMBACH, D. M., BARTOLOMEI, M. S., FISSORE, R. A. & WILLIAMS, C. J. 2018. TRPM7 and Ca_V3.2 channels mediate Ca²⁺ influx required for egg activation at fertilization. *Proceedings of the National Academy of Sciences,* 115**,** E10370-E10378.

BETTER, O. S., RUBINSTEIN, I. & WINAVER, J. 1995. Osmotic Diuretics: Mannitol. *In:* GREGER, R. F., KNAUF, H. & MUTSCHLER, E. (eds.) *Diuretics.* Berlin, Heidelberg: Springer Berlin Heidelberg.

BISSONNETTE, P., LAHJOUJI, K., COADY, M. J. & LAPOINTE, J. Y. 2008. Effects of hyperosmolarity on the Na+ -myo-inositol cotransporter SMIT2 stably transfected in the Madin-Darby canine kidney cell line. *Am J Physiol Cell Physiol,* 295**,** C791-9.

BITTREMIEUX, M. & BULTYNCK, G. 2015. p53 and Ca(2+) signaling from the endoplasmic reticulum: partners in anti-cancer therapies. *Oncoscience,* 2**,** 233-238.

BLOCK, K., GORIN, Y. & ABBOUD, H. E. 2009. Subcellular localization of Nox4 and regulation in diabetes. *Proceedings of the National Academy of Sciences,* 106**,** 14385-14390.

BOCKENHAUER, D. & BICHET, D. G. 2015. Pathophysiology, diagnosis and management of nephrogenic diabetes insipidus. *Nature Reviews Nephrology,* 11**,** 576-588.

BOGESKI, I., AL-ANSARY, D., QU, B., NIEMEYER, B. A., HOTH, M. & PEINELT, C. 2010. Pharmacology of ORAI channels as a tool to understand their physiological functions. *Expert Review of Clinical Pharmacology,* 3**,** 291-303.

BOGESKI, I., KILCH, T. & NIEMEYER, B. A. 2012. ROS and SOCE: recent advances and controversies in the regulation of STIM and Orai. *J Physiol The Journal of Physiology S,* 59017**,** 4193-4200.

BONEKAMP, N. A., VÖLKL, A., FAHIMI, H. D. & SCHRADER, M. 2009. Reactive oxygen species and peroxisomes: Struggling for balance. *BioFactors,* 35**,** 346-355.

BORTNER, C. D. & CIDLOWSKI, J. A. 2007. Cell shrinkage and monovalent cation fluxes: role in apoptosis. *Archives of biochemistry and biophysics,* 462**,** 176-188.

BRANDT, A., KHIMICH, D. & MOSER, T. 2005. Few Ca_V1.3 Channels Regulate the Exocytosis of a Synaptic Vesicle at the Hair Cell Ribbon Synapse. *The Journal of Neuroscience,* 25**,** 11577-11585.

BRAUN, M., RAMRACHEYA, R., BENGTSSON, M., ZHANG, Q., KARANAUSKAITE, J., PARTRIDGE, C., JOHNSON, P. R. & RORSMAN, P.

2008. Voltage-Gated Ion Channels in Human Pancreatic β-Cells: Electrophysiological Characterization and Role in Insulin Secretion. *Diabetes,* 57**,** 1618-1628.

BRERETON, M. F., ROHM, M., SHIMOMURA, K., HOLLAND, C., TORNOVSKY-BABEAY, S., DADON, D., IBERL, M., CHIBALINA, M. V., LEE, S., GLASER, B., DOR, Y., RORSMAN, P., CLARK, A. & ASHCROFT, F. M. 2016. Hyperglycaemia induces metabolic dysfunction and glycogen accumulation in pancreatic β-cells. *Nature Communications,* 7**,** 13496.

BROWNLEE, M. 2005. The pathobiology of diabetic complications: a unifying mechanism. *Diabetes,* 54**,** 1615-25.

BUETLER, T. M., KRAUSKOPF, A. & RUEGG, U. T. 2004. Role of superoxide as a signaling molecule. *News in physiological sciences : an international journal of physiology produced jointly by the International Union of Physiological Sciences and the American Physiological Society,* 19**,** 120-3.

BUOITE STELLA, A., YARDLEY, J., FRANCESCATO, M. P. & MORRISON, S. A. 2018. Fluid Intake Habits in Type 1 Diabetes Individuals during Typical Training Bouts. *Ann Nutr Metab,* 73**,** 10-18.

CABALLERO, A. E. 2003. Endothelial Dysfunction in Obesity and Insulin Resistance: A Road to Diabetes and Heart Disease. *Obesity Research,* 11**,** 1278-1289.

CABALLERO, A. E., ARORA, S., SAOUAF, R., LIM, S. C., SMAKOWSKI, P., PARK, J. Y., KING, G. L., LOGERFO, F. W., HORTON, E. S. & VEVES, A. 1999. Microvascular and macrovascular reactivity is reduced in subjects at risk for type 2 diabetes. *Diabetes,* 48**,** 1856-62.

CAILLARD, O., MORENO, H., SCHWALLER, B., LLANO, I., CELIO, M. R. & MARTY, A. 2000. Role of the calcium-binding protein parvalbumin in short-

term synaptic plasticity. *Proceedings of the National Academy of Sciences,* 97**,** 13372-13377.

CALDERON-RIVERA, A., SANDOVAL, A., GONZALEZ-RAMIREZ, R., GONZALEZ-BILLAULT, C. & FELIX, R. 2015. Regulation of neuronal cav3.1 channels by cyclin-dependent kinase 5 (Cdk5). *PLoS One,* 10**,** e0119134.

CALLAGHAN, M. J., CERADINI, D. J. & GURTNER, G. C. 2005. Hyperglycemia-induced reactive oxygen species and impaired endothelial progenitor cell function. *Antioxid Redox Signal,* 7**,** 1476-82.

CANUGOVI, C., STEVENSON, M. D., VENDROV, A. E., HAYAMI, T., ROBIDOUX, J., XIAO, H., ZHANG, Y.-Y., EITZMAN, D. T., RUNGE, M. S. & MADAMANCHI, N. R. 2019. Increased mitochondrial NADPH oxidase 4 (NOX4) expression in aging is a causative factor in aortic stiffening. *Redox Biology,* 26**,** 101288.

CAO, S. S. & KAUFMAN, R. J. 2014. Endoplasmic reticulum stress and oxidative stress in cell fate decision and human disease. *Antioxidants & redox signaling,* 21**,** 396-413.

CAON, M. 2008. Osmoles, osmolality and osmotic pressure: clarifying the puzzle of solution concentration. *Contemp Nurse,* 29**,** 92-9.

CARDARELLI, F., DIGIACOMO, L., MARCHINI, C., AMICI, A., SALOMONE, F., FIUME, G., ROSSETTA, A., GRATTON, E., POZZI, D. & CARACCIOLO, G. 2016. The intracellular trafficking mechanism of Lipofectamine-based transfection reagents and its implication for gene delivery. *Scientific Reports,* 6**,** 25879.

CARPÉNÉ, C., HASNAOUI, M., BALOGH, B., MATYUS, P., FERNÁNDEZ-QUINTELA, A., RODRÍGUEZ, V., MERCADER, J. & PORTILLO, M. P.

2016. Dietary Phenolic Compounds Interfere with the Fate of Hydrogen Peroxide in Human Adipose Tissue but Do Not Directly Inhibit Primary Amine Oxidase Activity. *Oxidative medicine and cellular longevity,* 2016**,** 2427618-2427618.

CASTELLANI, J. W. & YOUNG, A. J. 2016. Human physiological responses to cold exposure: Acute responses and acclimatization to prolonged exposure. *Auton Neurosci,* 196**,** 63-74.

CAULFIELD, J. P. & FARQUHAR, M. G. 1975. The permeability of glomerular capillaries of aminonuceoside nephrotic rats to graded dextrans. *The Journal of Experimental Medicine,* 142**,** 61-83.

CAVOUNIDIS, A. & MANN, E. H. 2020. SARS-CoV-2 has a sweet tooth. *Nature reviews. Immunology,* 20**,** 460-460.

CHAI, Z., WANG, C., HUANG, R., WANG, Y., ZHANG, X., WU, Q., WANG, Y., WU, X., ZHENG, L., ZHANG, C., GUO, W., XIONG, W., DING, J., ZHU, F. & ZHOU, Z. 2017. CaV2.2 Gates Calcium-Independent but Voltage-Dependent Secretion in Mammalian Sensory Neurons. *Neuron,* 96**,** 1317-1326.e4.

CHANG, T. S. & JENSEN, M. B. 2014. Haemodilution for acute ischaemic stroke. *Cochrane Database of Systematic Reviews*.

CHATTERJEE, J. S. 2006. From compliance to concordance in diabetes. *Journal of medical ethics,* 32**,** 507-510.

CHAU, B. N., CHEN, T.-T., WAN, Y. Y., DEGREGORI, J. & WANG, J. Y. J. 2004. Tumor necrosis factor alpha-induced apoptosis requires p73 and c-ABL activation downstream of RB degradation. *Molecular and cellular biology,* 24**,** 4438-4447.

CHENG, K. T., ONG, H. L., LIU, X. & AMBUDKAR, I. S. 2013. Contribution and regulation of TRPC channels in store-operated Ca2+ entry. *Current topics in membranes,* 71**,** 149-79.

CHIASSON, J.-L., ARIS-JILWAN, N., BÉLANGER, R., BERTRAND, S., BEAUREGARD, H., EKOÉ, J.-M., FOURNIER, H. & HAVRANKOVA, J. 2003. Diagnosis and treatment of diabetic ketoacidosis and the hyperglycemic hyperosmolar state. *CMAJ : Canadian Medical Association journal = journal de l'Association medicale canadienne,* 168**,** 859-866.

CHIDGEY, J., FRASER, P. A. & AARONSON, P. I. 2016. Reactive oxygen species facilitate the EDH response in arterioles by potentiating intracellular endothelial Ca2+ release. *Free Radical Biology and Medicine,* 97**,** 274-284.

CLAPHAM, D. E. 2007. Calcium Signaling. *Cell,* 131**,** 1047-1058.

CLAPHAM, D. E., RUNNELS, L. W. & STRÜBING, C. 2001. The trp ion channel family. *Nature Reviews Neuroscience,* 2**,** 387-396.

CLARK, R. J., MCDONOUGH, P. M., SWANSON, E., TROST, S. U., SUZUKI, M., FUKUDA, M. & DILLMANN, W. H. 2003. Diabetes and the accompanying hyperglycemia impairs cardiomyocyte calcium cycling through increased nuclear O-GlcNAcylation. *The Journal of biological chemistry,* 278**,** 44230-7.

CNOP, M., WELSH, N., JONAS, J.-C., JÖRNS, A., LENZEN, S. & EIZIRIK, D. L. 2005. Mechanisms of pancreatic beta-cell death in type 1 and type 2 diabetes: many differences, few similarities. *Diabetes,* 54 Suppl 2**,** S97-107.

COLLIN, F. 2019. Chemical Basis of Reactive Oxygen Species Reactivity and Involvement in Neurodegenerative Diseases. *International journal of molecular sciences,* 20**,** 2407.

COLLINS, A. R., LYON, C. J., XIA, X., LIU, J. Z., TANGIRALA, R. K., YIN, F., BOYADJIAN, R., BIKINEYEVA, A., PRATICÒ, D., HARRISON, D. G. & HSUEH, W. A. 2009. Age-Accelerated Atherosclerosis Correlates With Failure to Upregulate Antioxidant Genes. *Circulation Research,* 104**,** e42-e54.

CONTE, G., CANTON, A. D., IMPERATORE, P., DE NICOLA, L., GIGLIOTTI, G., PISANTI, N., MEMOLI, B., FUIANO, G., ESPOSITO, C. & ANDREUCCI, V. E. 1990. Acute increase in plasma osmolality as a cause of hyperkalemia in patients with renal failure. *Kidney International,* 38**,** 301-307.

COOPER, M. E., BONNET, F., OLDFIELD, M. & JANDELEIT-DAHM, K. 2001. Mechanisms of diabetic vasculopathy: an overview. *American journal of hypertension,* 14**,** 475-86.

COVE-SMITH, A., MULGREW, C. J., RUDYK, O., DUTT, N., MCLATCHIE, L. M., SHATTOCK, M. J. & HENDRY, B. M. 2013. Anti-Proliferative Actions of T-Type Calcium Channel Inhibition in Thy1 Nephritis. *The American Journal of Pathology,* 183**,** 391-401.

CUMMINGS, B. S. & SCHNELLMANN, R. G. 2004. Measurement of cell death in mammalian cells. *Current protocols in pharmacology,* Chapter 12**,** 10.1002/0471141755.ph1208s25-12.8.

D'APOLITO, M., DU, X., PISANELLI, D., PETTOELLO-MANTOVANI, M., CAMPANOZZI, A., GIACCO, F., MAFFIONE, A. B., COLIA, A. L., BROWNLEE, M. & GIARDINO, I. 2015. Urea-induced ROS cause endothelial dysfunction in chronic renal failure. *Atherosclerosis,* 239**,** 393-400.

DANEMAN, D. 2006. Type 1 diabetes. *The Lancet,* 367**,** 847-858.

DANZIGER, J. & ZEIDEL, M. L. 2015. Osmotic homeostasis. *Clinical journal of the American Society of Nephrology : CJASN,* 10**,** 852-62.

DARDANO, A., PENNO, G., DEL PRATO, S. & MICCOLI, R. 2014. Optimal therapy of type 2 diabetes: a controversial challenge. *Aging,* 6**,** 187-206.

DARZYNKIEWICZ, Z., POZAROWSKI, P., LEE, B. W. & JOHNSON, G. L. 2011. Fluorochrome-labeled inhibitors of caspases: convenient in vitro and in vivo markers of apoptotic cells for cytometric analysis. *Methods in molecular biology (Clifton, N.J.),* 682**,** 103-114.

DASHTI, H. M., MATHEW, T. C., HUSSEIN, T., ASFAR, S. K., BEHBAHANI, A., KHOURSHEED, M. A., AL-SAYER, H. M., BO-ABBAS, Y. Y. & AL-ZAID, N. S. 2004. Long-term effects of a ketogenic diet in obese patients. *Experimental and clinical cardiology,* 9**,** 200-205.

DASKOULIDOU, N., ZENG, B., BERGLUND, L. M., JIANG, H., CHEN, G.-L., KOTOVA, O., BHANDARI, S., AYOOLA, J., GRIFFIN, S., ATKIN, S. L., GOMEZ, M. F. & XU, S.-Z. 2015. High glucose enhances store-operated calcium entry by upregulating ORAI/STIM via calcineurin-NFAT signalling. *Journal of Molecular Medicine,* 93**,** 511-521.

DAVILA, H. M. 1999. Molecular and Functional Diversity of Voltage-Gated Calcium Channels. *Annals of the New York Academy of Sciences,* 868**,** 102-117.

DE VRIES, M. R., NIESSEN, H. W. M., LÖWIK, C. W. G. M., HAMMING, J. F., JUKEMA, J. W. & QUAX, P. H. A. 2012. Plaque Rupture Complications in Murine Atherosclerotic Vein Grafts Can Be Prevented by TIMP-1 Overexpression. *PLOS ONE,* 7**,** e47134.

DEL RÍO, L. A. & LÓPEZ-HUERTAS, E. 2016. ROS Generation in Peroxisomes and its Role in Cell Signaling. *Plant and Cell Physiology,* 57**,** 1364-1376.

DELANEY, M. F., ZISMAN, A. & KETTYLE, W. M. 2000. Diabetic ketoacidosis and hyperglycemic hyperosmolar nonketotic syndrome. *Endocrinology and metabolism clinics of North America,* 29**,** 683-705, V.

DEMURO, A., MINA, E., KAYED, R., MILTON, S. C., PARKER, I. & GLABE, C. G. 2005. Calcium Dysregulation and Membrane Disruption as a Ubiquitous Neurotoxic Mechanism of Soluble Amyloid Oligomers. *Journal of Biological Chemistry,* 280**,** 17294-17300.

DENG, R., HUA, X., LI, J., CHI, W., ZHANG, Z., LU, F., ZHANG, L., PFLUGFELDER, S. C. & LI, D.-Q. 2015. Oxidative Stress Markers Induced by Hyperosmolarity in Primary Human Corneal Epithelial Cells. *PLOS ONE,* 10**,** e0126561-e0126561.

DONNELLY, R., EMSLIE-SMITH, A. M., GARDNER, I. D. & MORRIS, A. D. 2000. ABC of arterial and venous disease: vascular complications of diabetes. *BMJ (Clinical research ed.),* 320**,** 1062-6.

DRUCKER, D. J. 2007. The role of gut hormones in glucose homeostasis. *The Journal of Clinical Investigation,* 117**,** 24-32.

DU, X. L., EDELSTEIN, D., DIMMELER, S., JU, Q., SUI, C. & BROWNLEE, M. 2001. Hyperglycemia inhibits endothelial nitric oxide synthase activity by posttranslational modification at the Akt site. *Journal of Clinical Investigation,* 108**,** 1341-1348.

DUNCAN, B. B., SCHMIDT, M. I., PANKOW, J. S., BALLANTYNE, C. M., COUPER, D., VIGO, A., HOOGEVEEN, R., FOLSOM, A. R. & HEISS, G. 2003. Low-grade systemic inflammation and the development of type 2 diabetes: the atherosclerosis risk in communities study. *Diabetes,* 52**,** 1799-805.

ELLINGER, I. 2016. The Calcium-Sensing Receptor and the Reproductive System. *Frontiers in physiology,* 7**,** 371-371.

ELLIOTT, S. J. & KOLIWAD, S. K. 1995. Oxidant stress and endothelial membrane transport. *Free Radical Biology and Medicine,* 19**,** 649-658.

ENGELMANN, J., VOLK, J., LEYHAUSEN, G. & GEURTSEN, W. 2005. ROS formation and glutathione levels in human oral fibroblasts exposed to TEGDMA and camphorquinone. *Journal of Biomedical Materials Research Part B: Applied Biomaterials,* 75B**,** 272-276.

ENGERMAN, R. L. 1989. Pathogenesis of diabetic retinopathy. *Diabetes,* 38**,** 1203-6.

ENGLAND, K., DRISCOLL, C. O. & COTTER, T. G. 2006. ROS and protein oxidation in early stages of cytotoxic drug induced apoptosis. *Free Radical Research,* 40**,** 1124-1137.

ERTEL, E. A., CAMPBELL, K. P., HARPOLD, M. M., HOFMANN, F., MORI, Y., PEREZ-REYES, E., SCHWARTZ, A., SNUTCH, T. P., TANABE, T., BIRNBAUMER, L., TSIEN, R. W. & CATTERALL, W. A. 2000. Nomenclature of voltage-gated calcium channels. *Neuron,* 25**,** 533-5.

EVANS, J. L., GOLDFINE, I. D., MADDUX, B. A. & GRODSKY, G. M. 2003. Are Oxidative Stress−Activated Signaling Pathways Mediators of Insulin Resistance and β-Cell Dysfunction? *Diabetes,* 52**,** 1-8.

FAIRWEATHER, D. 2015. Sex differences in inflammation during atherosclerosis. *Clinical Medicine Insights. Cardiology,* 8**,** 49-59.

FERENCE, B. A., GINSBERG, H. N., GRAHAM, I., RAY, K. K., PACKARD, C. J., BRUCKERT, E., HEGELE, R. A., KRAUSS, R. M., RAAL, F. J., SCHUNKERT, H., WATTS, G. F., BORÉN, J., FAZIO, S., HORTON, J. D., MASANA, L., NICHOLLS, S. J., NORDESTGAARD, B. G., VAN DE SLUIS,

B., TASKINEN, M.-R., TOKGÖZOĞLU, L., LANDMESSER, U., LAUFS, U., WIKLUND, O., STOCK, J. K., CHAPMAN, M. J. & CATAPANO, A. L. 2017. Low-density lipoproteins cause atherosclerotic cardiovascular disease. 1. Evidence from genetic, epidemiologic, and clinical studies. A consensus statement from the European Atherosclerosis Society Consensus Panel. *European Heart Journal,* 38**,** 2459-2472.

FESKE, S., GWACK, Y., PRAKRIYA, M., SRIKANTH, S., PUPPEL, S.-H., TANASA, B., HOGAN, P. G., LEWIS, R. S., DALY, M. & RAO, A. 2006. A mutation in Orai1 causes immune deficiency by abrogating CRAC channel function. *Nature,* 441**,** 179-185.

FINK, S. L. & COOKSON, B. T. 2005. Apoptosis, pyroptosis, and necrosis: mechanistic description of dead and dying eukaryotic cells. *Infection and immunity,* 73**,** 1907-1916.

FISCHER, K. F., LEES, J. A. & NEWMAN, J. H. 1986. Hypoglycemia in hospitalized patients. Causes and outcomes. *N Engl J Med,* 315**,** 1245-50.

FLOREZ, J. C. 2008. Newly identified loci highlight beta cell dysfunction as a key cause of type 2 diabetes: Where are the insulin resistance genes? *Diabetologia,* 51**,** 1100-1110.

FORTES, Z. B., GARCIA LEME, J. & SCIVOLETTO, R. 1984. Vascular reactivity in diabetes mellitus: possible role of insulin on the endothelial cell. *British journal of pharmacology,* 83**,** 635-43.

FOWLER, M. A., SIDIROPOULOU, K., OZKAN, E. D., PHILLIPS, C. W. & COOPER, D. C. 2007. Corticolimbic expression of TRPC4 and TRPC5 channels in the rodent brain. *PLoS One,* 2**,** e573.

FRANCO, O. H., STEYERBERG, E. W., HU, F. B., MACKENBACH, J. & NUSSELDER, W. 2007. Associations of Diabetes Mellitus With Total Life Expectancy and Life Expectancy With and Without Cardiovascular Disease. *Archives of Internal Medicine,* 167**,** 1145-1145.

FRISCHAUF, I., MUIK, M., DERLER, I., BERGSMANN, J., FAHRNER, M., SCHINDL, R., GROSCHNER, K. & ROMANIN, C. 2009. Molecular determinants of the coupling between STIM1 and Orai channels: differential activation of Orai1-3 channels by a STIM1 coiled-coil mutant. *The Journal of biological chemistry,* 284**,** 21696-706.

FRÖMTER, E., RUMRICH, G. & ULLRICH, K. J. 1973. Phenomenologic description of Na+, Cl− and HCO3−absorption from proximal tubules of the rat kidney. *Pflügers Archiv,* 343**,** 189-220.

GAJEWSKI, E., STECKLER, D. K. & GOLDBERG, R. N. 1986. Thermodynamics of the hydrolysis of adenosine 5'-triphosphate to adenosine 5'-diphosphate. *J Biol Chem,* 261**,** 12733-7.

GARASCHUK, O., MILOS, R.-I., GRIENBERGER, C., MARANDI, N., ADELSBERGER, H. & KONNERTH, A. 2006. Optical monitoring of brain function in vivo: from neurons to networks. *Pflügers Archiv,* 453**,** 385-396.

GARBER, A. J. 1995. Clinical perspectives on type 2 diabetes in North America. *Diabetes/Metabolism Reviews,* 11**,** S81-S86.

GIARDINO, I., EDELSTEIN, D. & BROWNLEE, M. 1994. Nonenzymatic glycosylation in vitro and in bovine endothelial cells alters basic fibroblast growth factor activity. A model for intracellular glycosylation in diabetes. *Journal of Clinical Investigation,* 94**,** 110-117.

GILDEA, J. J., SHAH, I., WEISS, R., CASSCELLS, N. D., MCGRATH, H. E., ZHANG, J., JONES, J. E. & FELDER, R. A. 2010. HK-2 human renal proximal tubule cells as a model for G protein-coupled receptor kinase type 4-mediated dopamine 1 receptor uncoupling. *Hypertension (Dallas, Tex. : 1979),* 56**,** 505-511.

GILMORE, R. M. & STEAD, L. G. 2006. The role of hyperglycemia in acute ischemic stroke. *Neurocritical care,* 5**,** 153-8.

GIORGI, C., BONORA, M. & PINTON, P. 2015. Inside the tumor: p53 modulates calcium homeostasis. *Cell cycle (Georgetown, Tex.),* 14**,** 933-934.

GOMEZ-OSPINA, N., TSURUTA, F., BARRETO-CHANG, O., HU, L. & DOLMETSCH, R. 2006. The C Terminus of the L-Type Voltage-Gated Calcium Channel Ca_V1.2 Encodes a Transcription Factor. *Cell,* 127**,** 591-606.

GOSMANOV, A. R., GOSMANOVA, E. O. & DILLARD-CANNON, E. 2014. Management of adult diabetic ketoacidosis. *Diabetes, metabolic syndrome and obesity : targets and therapy,* 7**,** 255-264.

GOYAL, S. N., REDDY, N. M., PATIL, K. R., NAKHATE, K. T., OJHA, S., PATIL, C. R. & AGRAWAL, Y. O. 2016. Challenges and issues with streptozotocin-induced diabetes - A clinically relevant animal model to understand the diabetes pathogenesis and evaluate therapeutics. *Chem Biol Interact,* 244**,** 49-63.

GRAHAM, K. A., KULAWIEC, M., OWENS, K. M., LI, X., DESOUKI, M. M., CHANDRA, D. & SINGH, K. K. 2010. NADPH oxidase 4 is an oncoprotein localized to mitochondria. *Cancer Biology & Therapy,* 10**,** 223-231.

GROSS, J. L., DE AZEVEDO, M. J., SILVEIRO, S. P., CANANI, L. H., CARAMORI, M. L. & ZELMANOVITZ, T. 2005. Diabetic nephropathy: diagnosis, prevention, and treatment. *Diabetes care,* 28**,** 164-76.

GRUPE, M., MYERS, G., PENNER, R. & FLEIG, A. 2010. Activation of store-operated ICRAC by hydrogen peroxide. *Cell Calcium,* 48**,** 1-9.

GULLANS, S. R. & VERBALIS, J. G. 1993. Control of Brain Volume During Hyperosmolar and Hypoosmolar Conditions. *Annual Review of Medicine,* 44**,** 289-301.

GUNTER, T. E., RESTREPO, D. & GUNTER, K. K. 1988. Conversion of esterified fura-2 and indo-1 to Ca2+-sensitive forms by mitochondria. *American Journal of Physiology-Cell Physiology,* 255**,** C304-C310.

GUTIERREZ, R. C., HUNG, J., ZHANG, Y., KERTESZ, A. C., ESPINA, F. J. & COLICOS, M. A. 2009. Altered synchrony and connectivity in neuronal networks expressing an autism-related mutation of neuroligin 3. *Neuroscience,* 162**,** 208-221.

GUZY, R. D., HOYOS, B., ROBIN, E., CHEN, H., LIU, L., MANSFIELD, K. D., SIMON, M. C., HAMMERLING, U. & SCHUMACKER, P. T. 2005. Mitochondrial complex III is required for hypoxia-induced ROS production and cellular oxygen sensing. *Cell Metabolism,* 1**,** 401-408.

HAN, W., YAN, L. & PANDURANGI, R. 2018. A Priori Activation of Apoptosis Pathways of Tumor (AAAPT) Technology 1: Sensitization of Tumor Cells Using Targeted and Cleavable Apoptosis Initiators in Gastric Cancer. *bioRxiv***,** 492306.

HASHIM, Z. & ZARINA, S. 2012. Osmotic stress induced oxidative damage: Possible mechanism of cataract formation in diabetes. *Journal of Diabetes and its Complications,* 26**,** 275-279.

HASTINGS, A., MCNAMARA, N., ALLAN, J. & MARRIOTT, M. 2016. The importance of social identities in the management of and recovery from 'Diabulimia': A qualitative exploration. *Addictive behaviors reports,* 4**,** 78-86.

HATTING, M., TAVARES, C. D. J., SHARABI, K., RINES, A. K. & PUIGSERVER, P. 2018. Insulin regulation of gluconeogenesis. *Annals of the New York Academy of Sciences,* 1411**,** 21-35.

HAWKINS, B. J., IRRINKI, K. M., MALLILANKARAMAN, K., LIEN, Y.-C., WANG, Y., BHANUMATHY, C. D., SUBBIAH, R., RITCHIE, M. F., SOBOLOFF, J., BABA, Y., KUROSAKI, T., JOSEPH, S. K., GILL, D. L. & MADESH, M. 2010. S-glutathionylation activates STIM1 and alters mitochondrial homeostasis. *The Journal of Cell Biology,* 190**,** 391-405.

HAYASAKA, D., MAEDA, K., ENNIS, F. A. & TERAJIMA, M. 2007. Increased permeability of human endothelial cell line EA.hy926 induced by hantavirus-specific cytotoxic T lymphocytes. *Virus Research,* 123**,** 120-127.

HELLER, S. R., BUSE, J. B., RATNER, R., SEAQUIST, E., BARDTRUM, L., HANSEN, C. T., TUTKUNKARDAS, D. & MOSES, A. C. 2019. Redefining Hypoglycemia in Clinical Trials: Validation of Definitions Recently Adopted by the American Diabetes Association/European Association for the Study of Diabetes. *Diabetes Care*.

HELTON, T. D., XU, W. & LIPSCOMBE, D. 2005. Neuronal L-Type Calcium Channels Open Quickly and Are Inhibited Slowly. *The Journal of Neuroscience,* 25**,** 10247-10251.

HERZOG, K., PRAS-RAVES, M. L., FERDINANDUSSE, S., VERVAART, M. A. T., LUYF, A. C. M., VAN KAMPEN, A. H. C., WANDERS, R. J. A., WATERHAM, H. R. & VAZ, F. M. 2018. Functional characterisation of peroxisomal β-oxidation disorders in fibroblasts using lipidomics. *Journal of inherited metabolic disease,* 41**,** 479-487.

HEWITT, J. A. & PRYDE, J. 1920. The Metabolism of Carbohydrates. Part I: Stereochemical Changes undergone by Equilibrated Solutions of Reducing Sugars in the Alimentary Canal and in the Peritoneal Cavity. *Biochem J,* 14**,** 395-405.

HEX, N., BARTLETT, C., WRIGHT, D., TAYLOR, M. & VARLEY, D. 2012. Estimating the current and future costs of Type 1 and Type 2 diabetes in the UK, including direct health costs and indirect societal and productivity costs. *Diabetic Medicine,* 29**,** 855-862.

HIGGINS, J. P. T., WANG, L., KAMBHAM, N., MONTGOMERY, K., MASON, V., VOGELMANN, S. U., LEMLEY, K. V., BROWN, P. O., BROOKS, J. D. & VAN DE RIJN, M. 2004. Gene expression in the normal adult human kidney assessed by complementary DNA microarray. *Molecular biology of the cell,* 15**,** 649-656.

HILL, N. R., OLIVER, N. S., CHOUDHARY, P., LEVY, J. C., HINDMARSH, P. & MATTHEWS, D. R. 2011. Normal reference range for mean tissue glucose and glycemic variability derived from continuous glucose monitoring for subjects without diabetes in different ethnic groups. *Diabetes Technol Ther,* 13**,** 921-8.

HOENDEROP, J. G., MULLER, D., VAN DER KEMP, A. W., HARTOG, A., SUZUKI, M., ISHIBASHI, K., IMAI, M., SWEEP, F., WILLEMS, P. H., VAN

OS, C. H. & BINDELS, R. J. 2001. Calcitriol controls the epithelial calcium channel in kidney. *J Am Soc Nephrol,* 12**,** 1342-9.

HOLMAN, N., YOUNG, B. & GADSBY, R. 2015. Current prevalence of Type 1 and Type 2 diabetes in adults and children in the UK. *Diabetic Medicine,* 32**,** 1119-1120.

HOOPER, L., ABDELHAMID, A., ALI, A., BUNN, D. K., JENNINGS, A., JOHN, W. G., KERRY, S., LINDNER, G., PFORTMUELLER, C. A., SJÖSTRAND, F., WALSH, N. P., FAIRWEATHER-TAIT, S. J., POTTER, J. F., HUNTER, P. R. & SHEPSTONE, L. 2015. Diagnostic accuracy of calculated serum osmolarity to predict dehydration in older people: adding value to pathology laboratory reports. *BMJ Open,* 5.

HOU, X., PEDI, L., DIVER, M. M. & LONG, S. B. 2012. Crystal Structure of the Calcium Release-Activated Calcium Channel Orai. *Science,* 338**,** 1308-1313.

HOWARTH, F., QURESHI, M. & WHITE, E. 2002. Effects of hyperosmotic shrinking on ventricular myocyte shortening and intracellular Ca2+ in streptozotocin-induced diabetic rats. *Pflügers Archiv,* 444**,** 446-451.

HSUEH, W. A. & ANDERSON, P. W. 1993. Systemic hypertension and the renin-angiotensin system in diabetic vascular complications. *The American Journal of Cardiology,* 72**,** H14-H21.

IDO, Y., CARLING, D. & RUDERMAN, N. 2002. Hyperglycemia-Induced Apoptosis in Human Umbilical Vein Endothelial Cells. *Inhibition by the AMP-Activated Protein Kinase Activation,* 51**,** 159-167.

ISHII, H., KOYA, D. & KING, G. L. 1998. Protein kinase C activation and its role in the development of vascular complications in diabetes mellitus. *Journal of molecular medicine (Berlin, Germany),* 76**,** 21-31.

JACKULIAK, P. & PAYER, J. 2014. Osteoporosis, Fractures, and Diabetes. *International journal of endocrinology,* 2014**,** 820615.

JEFFCOATE, W. J. & HARDING, K. G. 2003. Diabetic foot ulcers. *The Lancet,* 361**,** 1545-1551.

JENKINSON, S. E., CHUNG, G. W., VAN LOON, E., BAKAR, N. S., DALZELL, A. M. & BROWN, C. D. 2012. The limitations of renal epithelial cell line HK-2 as a model of drug transporter expression and function in the proximal tubule. *Pflugers Arch,* 464**,** 601-11.

JIN, Q. & BETHKE, C. M. 2002. Kinetics of Electron Transfer through the Respiratory Chain. *Biophysical Journal,* 83**,** 1797-1808.

JOHNY, J. P., PLANK, M. J. & DAVID, T. 2017. Importance of Altered Levels of SERCA, IP3R, and RyR in Vascular Smooth Muscle Cell. *Biophysical Journal,* 112**,** 265-287.

JOUAVILLE, L. S., PINTON, P., BASTIANUTTO, C., RUTTER, G. A. & RIZZUTO, R. 1999. Regulation of mitochondrial ATP synthesis by calcium: Evidence for a long-term metabolic priming. *Proceedings of the National Academy of Sciences,* 96**,** 13807-13812.

KAHN, B. B. 1998. Type 2 diabetes: when insulin secretion fails to compensate for insulin resistance. *Cell,* 92**,** 593-6.

KAJIMURA, M. & CURRY, F. E. 1999. Endothelial cell shrinkage increases permeability through a Ca2+-dependent pathway in single frog mesenteric microvessels. *The Journal of physiology,* 518**,** 227-38.

KALIMUTHU, S. & SE-KWON, K. 2013. Cell survival and apoptosis signaling as therapeutic target for cancer: marine bioactive compounds. *International journal of molecular sciences,* 14**,** 2334-2354.

KALRA, S., ZARGAR, A. H., JAIN, S. M., SETHI, B., CHOWDHURY, S., SINGH, A. K., THOMAS, N., UNNIKRISHNAN, A. G., THAKKAR, P. B. & MALVE, H. 2016. Diabetes insipidus: The other diabetes. *Indian journal of endocrinology and metabolism,* 20**,** 9-21.

KEFER, J. C., AGARWAL, A. & SABANEGH, E. 2009. Role of antioxidants in the treatment of male infertility. *International Journal of Urology,* 16**,** 449-457.

KIM, J. H., CHOI, E., RHIE, Y. J., LEE, J. H., LEE, K.-H. & NAM, H.-K. 2016. Diabetic Ketoacidosis with Hyperglycemic Hyperosmolar State at the Onset of Type 2 Diabetes Mellitus in an Adolescent Male. *Soonchunhyang Medical Science,* 22**,** 158-162.

KIM, J. J., LEE, S. B., PARK, J. K. & YOO, Y. D. 2010. TNF-alpha-induced ROS production triggering apoptosis is directly linked to Romo1 and Bcl-X(L). *Cell Death Differ,* 17**,** 1420-34.

KIM, M. S., ZENG, W., YUAN, J. P., SHIN, D. M., WORLEY, P. F. & MUALLEM, S. 2009. Native Store-operated Ca2+ Influx Requires the Channel Function of Orai1 and TRPC1. *J Biol Chem,* 284**,** 9733-41.

KING, P., PEACOCK, I. & DONNELLY, R. 1999. The UK prospective diabetes study (UKPDS): clinical and therapeutic implications for type 2 diabetes. *British journal of clinical pharmacology,* 48**,** 643-8.

KITABCHI, A. E. & WALL, B. M. 1995. Diabetic ketoacidosis. *Med Clin North Am,* 79**,** 9-37.

KLARIĆ, M. Š., ŽELJEŽIĆ, D., RUMORA, L., PERAICA, M., PEPELJNJAK, S. & DOMIJAN, A.-M. 2012. A potential role of calcium in apoptosis and aberrant chromatin forms in porcine kidney PK15 cells induced by individual and combined ochratoxin A and citrinin. *Archives of Toxicology,* 86**,** 97-107.

KLEIN, R., KLEIN, B. E., MOSS, S. E., DAVIS, M. D. & DEMETS, D. L. 1984. The Wisconsin epidemiologic study of diabetic retinopathy. IV. Diabetic macular edema. *Ophthalmology,* 91**,** 1464-74.

KLIP, A., RAMLAL, T., BILAN, P. J., CARTEE, G. D., GULVE, E. A. & HOLLOSZY, J. O. 1990. Recruitment of GLUT-4 glucose transporters by insulin in diabetic rat skeletal muscle. *Biochemical and Biophysical Research Communications,* 172**,** 728-736.

KOLM-LITTY, V., SAUER, U., NERLICH, A., LEHMANN, R. & SCHLEICHER, E. D. 1998. High glucose-induced transforming growth factor beta1 production is mediated by the hexosamine pathway in porcine glomerular mesangial cells. *Journal of Clinical Investigation,* 101**,** 160-169.

KONRAD, R. J., DEAN, R. M., YOUNG, R. A., BILLINGS, P. C. & WOLF, B. A. 1996. Glucose-induced Tyrosine Phosphorylation of p125 in Beta Cells and Pancreatic Islets: A NOVEL PROXIMAL SIGNAL IN INSULIN SECRETION. *Journal of Biological Chemistry,* 271**,** 24179-24186.

KOSCHAK, A., REIMER, D., HUBER, I., GRABNER, M., GLOSSMANN, H., ENGEL, J. & STRIESSNIG, J. 2001. alpha 1D (Cav1.3) subunits can form l-type Ca2+ channels activating at negative voltages. *J Biol Chem,* 276**,** 22100-6.

KRAFT, G., COATE, K. C., WINNICK, J. J., DARDEVET, D., DONAHUE, E. P., CHERRINGTON, A. D., WILLIAMS, P. E. & MOORE, M. C. 2017. Glucagon's effect on liver protein metabolism in vivo. *American journal of physiology. Endocrinology and metabolism,* 313**,** E263-E272.

KRASENSKY-WRZACZEK, J. & KANGASJARVI, J. 2018. The role of reactive oxygen species in the integration of temperature and light signals. *J Exp Bot,* 69**,** 3347-3358.

KRAUT, J. A. & KURTZ, I. 2008. Toxic alcohol ingestions: clinical features, diagnosis, and management. *Clinical journal of the American Society of Nephrology : CJASN,* 3**,** 208-25.

KUBOKI, K., JIANG, Z. Y., TAKAHARA, N., HA, S. W., IGARASHI, M., YAMAUCHI, T., FEENER, E. P., HERBERT, T. P., RHODES, C. J. & KING, G. L. 2000. Regulation of endothelial constitutive nitric oxide synthase gene expression in endothelial cells and in vivo : a specific vascular action of insulin. *Circulation,* 101**,** 676-81.

KÜHLBRANDT, W. 2015. Structure and function of mitochondrial membrane protein complexes. *BMC Biology,* 13**,** 89.

KURODA, J., AGO, T., MATSUSHIMA, S., ZHAI, P., SCHNEIDER, M. D. & SADOSHIMA, J. 2010. NADPH oxidase 4 (Nox4) is a major source of oxidative stress in the failing heart. *Proceedings of the National Academy of Sciences,* 107**,** 15565-15570.

KUZNETSOV, A. V., KEHRER, I., KOZLOV, A. V., HALLER, M., REDL, H., HERMANN, M., GRIMM, M. & TROPPMAIR, J. 2011. Mitochondrial ROS production under cellular stress: comparison of different detection methods. *Analytical and Bioanalytical Chemistry,* 400**,** 2383-2390.

KWAN, H.-Y., HUANG, Y. & YAO, X. 2007. TRP channels in endothelial function and dysfunction. *Biochimica et Biophysica Acta (BBA) - Molecular Basis of Disease,* 1772**,** 907-914.

LAMBROS, M. L. & PLAFKER, S. M. Oxidative Stress and the Nrf2 Anti-Oxidant Transcription Factor in Age-Related Macular Degeneration. *In:* BOWES RICKMAN, C., LAVAIL, M. M., ANDERSON, R. E., GRIMM, C.,

HOLLYFIELD, J. & ASH, J., eds. Retinal Degenerative Diseases, 2016// 2016 Cham. Springer International Publishing, 67-72.

LANG, F., BUSCH, G. L., RITTER, M., VOLKEL, H., WALDGGER, S., GULBINS, E. & HAUSSINGER, D. 1998. Functional Significance of Cell Volume Regulatory Mechanisms. *Physiological Reviews,* 78**,** 247-306.

LAPPANO, R. & MAGGIOLINI, M. 2011. G protein-coupled receptors: novel targets for drug discovery in cancer. *Nature Reviews Drug Discovery,* 10**,** 47-60.

LEACH, J. K., VAN TUYLE, G., LIN, P.-S., SCHMIDT-ULLRICH, R. & MIKKELSEN, R. B. 2001. Ionizing Radiation-induced, Mitochondria-dependent Generation of Reactive Oxygen/Nitrogen. *Cancer Research,* 61**,** 3894-3901.

LEIBSON, C. L. & NARAYAN, K. M. V. 2005. Trends in Cardiovascular Complications of Diabetes. *JAMA,* 293**,** 1723-1723.

LI, L., YANG, J., WANG, J. & KOPEČEK, J. 2018. Drug-Free Macromolecular Therapeutics Induce Apoptosis via Calcium Influx and Mitochondrial Signaling Pathway. *Macromolecular Bioscience,* 18**,** 1700196.

LI, P., RUBAIY, H. N., CHEN, G. L., HALLETT, T., ZAIBI, N., ZENG, B., SAURABH, R. & XU, S. Z. 2019. Mibefradil, a T-type Ca(2+) channel blocker also blocks Orai channels by action at the extracellular surface. *Br J Pharmacol,* 176**,** 3845-3856.

LI, Z., WOOLLARD, J. R., WANG, S., KORSMO, M. J., EBRAHIMI, B., GRANDE, J. P., TEXTOR, S. C., LERMAN, A. & LERMAN, L. O. 2011. Increased glomerular filtration rate in early metabolic syndrome is associated with renal adiposity and microvascular proliferation. *American Journal of Physiology-Renal Physiology,* 301**,** F1078-F1087.

LI, Z., XU, J., XU, P., LIU, S. & YANG, Z. 2013. Wnt/β-catenin signalling pathway mediates high glucose induced cell injury through activation of TRPC6 in podocytes. *Cell Proliferation,* 46**,** 76-85.

LIJNEN, P., FAGARD, R. & PETROV, V. 1999. Mibefradil-induced inhibition of proliferation of human peripheral blood mononuclear cells. *J Cardiovasc Pharmacol,* 33**,** 595-604.

LIM, E. L., HOLLINGSWORTH, K. G., ARIBISALA, B. S., CHEN, M. J., MATHERS, J. C. & TAYLOR, R. 2011. Reversal of type 2 diabetes: normalisation of beta cell function in association with decreased pancreas and liver triacylglycerol. *Diabetologia,* 54**,** 2506-2514.

LISMONT, REVENCO, I. & FRANSEN 2019. Peroxisomal Hydrogen Peroxide Metabolism and Signaling in Health and Disease. *International Journal of Molecular Sciences,* 20**,** 3673.

LIU, X., WU, G., YU, Y., CHEN, X., JI, R., LU, J., LI, X., ZHANG, X., YANG, X. & SHEN, Y. 2019. Molecular understanding of calcium permeation through the open Orai channel. *PLoS Biol,* 17**,** e3000096.

LUETHI, N., CIOCCARI, L., CRISMAN, M., BELLOMO, R., EASTWOOD, G. M. & MÅRTENSSON, J. 2016. Prevalence of ketosis, ketonuria, and ketoacidosis during liberal glycemic control in critically ill patients with diabetes: an observational study. *Critical care (London, England),* 20**,** 297-297.

LUH, E. H., SHACKFORD, S. R., SHATOS, M. A. & PIETROPAOLI, J. A. 1996. The effects of hyperosmolarity on the viability and function of endothelial cells. *J Surg Res,* 60**,** 122-8.

LUND, D. D., FARACI, F. M., MILLER, F. J. & HEISTAD, D. D. 2000. Arteries From Diabetic Rabbits Gene Transfer of Endothelial Nitric Oxide Synthase Improves

Relaxation of Carotid Gene Transfer of Endothelial Nitric Oxide Synthase Improves Relaxation of Carotid Arteries From Diabetic Rabbits. *Circulation,* 101**,** 1027-1033.

MA, L., FU, Q., XU, B., ZHOU, H., GAO, J., SHAO, X., XIONG, J., GU, Q., WEN, S., LI, F., SHEN, L., CHEN, G., FANG, H. & LYU, J. 2018. Breast cancer-associated mitochondrial DNA haplogroup promotes neoplastic growth via ROS-mediated AKT activation. *International Journal of Cancer,* 142**,** 1786-1796.

MADONNA, R. & DE CATERINA, R. 2011. Cellular and molecular mechanisms of vascular injury in diabetes — Part I: Pathways of vascular disease in diabetes. *Vascular Pharmacology,* 54**,** 68-74.

MAILE, L. A., CAPPS, B. E., LING, Y., XI, G. & CLEMMONS, D. R. 2007. Hyperglycemia Alters the Responsiveness of Smooth Muscle Cells to Insulin-Like Growth Factor-I. *Endocrinology,* 148**,** 2435-2443.

MAILLOUX, R. J., CRAIG AYRE, D. & CHRISTIAN, S. L. 2016. Induction of mitochondrial reactive oxygen species production by GSH mediated S-glutathionylation of 2-oxoglutarate dehydrogenase. *Redox Biology,* 8**,** 285-297.

MALOUF, R. & BRUST, J. C. 1985. Hypoglycemia: causes, neurological manifestations, and outcome. *Ann Neurol,* 17**,** 421-30.

MAROTO, R., RASO, A., WOOD, T. G., KUROSKY, A., MARTINAC, B. & HAMILL, O. P. 2005. TRPC1 forms the stretch-activated cation channel in vertebrate cells. *Nature Cell Biology,* 7**,** 179-185.

MARUYAMA, I., HASEGAWA, T., YAMAMOTO, T. & MOMOSE, K. 1989. Effects of pluronic F-127 on loading of fura 2/AM into single smooth muscle cells isolated from guinea pig taenia coli. *J Toxicol Sci,* 14**,** 153-63.

MARX, S. O., ONDRIAS, K. & MARKS, A. R. 1998. Coupled Gating Between Individual Skeletal Muscle Ca²⁺ Release Channels (Ryanodine Receptors). *Science,* 281**,** 818-821.

MATTSON, M. P. & CHAN, S. L. 2003. Calcium orchestrates apoptosis. *Nature Cell Biology,* 5**,** 1041-1043.

MENG, X., WANG, X., TIAN, X., YANG, Z., LI, M. & ZHANG, C. 2014. Protection of neurons from high glucose-induced injury by deletion of MAD2B. *Journal of cellular and molecular medicine,* 18**,** 844-851.

MICHIELS, C. 2004. Physiological and pathological responses to hypoxia. *The American journal of pathology,* 164**,** 1875-1882.

MIKAELSSON, M. E. 1991. The Role of Calcium in Coagulation and Anticoagulation. *In:* SIBINGA, C. T. S., DAS, P. C. & MANNUCCI, P. M. (eds.) *Coagulation and Blood Transfusion: Proceedings of the Fifteenth Annual Symposium on Blood Transfusion, Groningen 1990, organized by the Red Cross Blood Bank Groningen-Drenthe.* Boston, MA: Springer US.

MILIONIS, H. J., LIAMIS, G. L. & ELISAF, M. S. 2002. The hyponatremic patient: a systematic approach to laboratory diagnosis. *CMAJ : Canadian Medical Association journal = journal de l'Association medicale canadienne,* 166**,** 1056-62.

MITRAKOU, A., RYAN, C., VENEMAN, T., MOKAN, M., JENSSEN, T., KISS, I., DURRANT, J., CRYER, P. & GERICH, J. 1991. Hierarchy of glycemic thresholds for counterregulatory hormone secretion, symptoms, and cerebral dysfunction. *Am J Physiol,* 260**,** E67-74.

MOCCIA, F., ZUCCOLO, E., SODA, T., TANZI, F., GUERRA, G., MAPELLI, L., LODOLA, F. & D'ANGELO, E. 2015. Stim and Orai proteins in neuronal

Ca(2+) signaling and excitability. *Frontiers in cellular neuroscience,* 9**,** 153-153.

MODIN, A., BJÖRNE, H., HERULF, M., ALVING, K., WEITZBERG, E. & LUNDBERG, J. O. N. 2001. Nitrite-derived nitric oxide: a possible mediator of 'acidic–metabolic' vasodilation. *Acta Physiologica Scandinavica,* 171**,** 9-16.

MP, F., VORHERR, H., CR, K. & TELFER, N. 1971. DIuretic-induced hyponatremia. *Annals of Internal Medicine,* 75**,** 853-863.

NAGASAKA, S., MURAKAMI, T., UCHIKAWA, T., ISHIKAWA, S. E. & SAITO, T. 1995. Effect of glycemic control on calcium and phosphorus handling and parathyroid hormone level in patients with non-insulin-dependent diabetes mellitus. *Endocrine journal,* 42**,** 377-83.

NÄSLUND, U., NG, N., LUNDGREN, A., FHÄRM, E., GRÖNLUND, C., JOHANSSON, H., LINDAHL, B., LINDAHL, B., LINDVALL, K., NILSSON, S. K., NORDIN, M., NORDIN, S., NYMAN, E., ROCKLÖV, J., VANOLI, D., WEINEHALL, L., WENNBERG, P., WESTER, P. & NORBERG, M. 2019. Visualization of asymptomatic atherosclerotic disease for optimum cardiovascular prevention (VIPVIZA): a pragmatic, open-label, randomised controlled trial. *The Lancet,* 393**,** 133-142.

NATARAJAN, R., BAI, W., LANTING, L., GONZALES, N. & NADLER, J. 1997. Effects of high glucose on vascular endothelial growth factor expression in vascular smooth muscle cells. *American Journal of Physiology-Heart and Circulatory Physiology,* 273**,** H2224-H2231.

NAVARRO-GONZÁLEZ, J. F., MORA-FERNÁNDEZ, C., DE FUENTES, M. M. & GARCÍA-PÉREZ, J. 2011. Inflammatory molecules and pathways in the pathogenesis of diabetic nephropathy. *Nature Reviews Nephrology*, 7**,** 327-340.

NGAMWONGSATIT, P., BANADA, P. P., PANBANGRED, W. & BHUNIA, A. K. 2008. WST-1-based cell cytotoxicity assay as a substitute for MTT-based assay for rapid detection of toxigenic Bacillus species using CHO cell line. *Journal of Microbiological Methods,* 73**,** 211-215.

NICHOLS, G. A., HILLIER, T. A. & BROWN, J. B. 2008. Normal fasting plasma glucose and risk of type 2 diabetes diagnosis. *Am J Med,* 121**,** 519-24.

NISHIKAWA, T., EDELSTEIN, D., DU, X. L., YAMAGISHI, S.-I., MATSUMURA, T., KANEDA, Y., YOREK, M. A., BEEBE, D., OATES, P. J., HAMMES, H.-P., GIARDINO, I. & BROWNLEE, M. 2000. Normalizing mitochondrial superoxide production blocks three pathways of hyperglycaemic damage. *Nature,* 404**,** 787-790.

OGRUNC, M., DI MICCO, R., LIONTOS, M., BOMBARDELLI, L., MIONE, M., FUMAGALLI, M., GORGOULIS, V. G. & D'ADDA DI FAGAGNA, F. 2014. Oncogene-induced reactive oxygen species fuel hyperproliferation and DNA damage response activation. *Cell death and differentiation,* 21**,** 998-1012.

OH, M. M., OLIVEIRA, F. A., WATERS, J. & DISTERHOFT, J. F. 2013. Altered Calcium Metabolism in Aging CA1 Hippocampal Pyramidal Neurons. *The Journal of Neuroscience,* 33**,** 7905-7911.

OKONKWO, U. A. & DIPIETRO, L. A. 2017. Diabetes and Wound Angiogenesis. *International journal of molecular sciences,* 18**,** 1419.

OLOKOBA, A. B., OBATERU, O. A. & OLOKOBA, L. B. 2012. Type 2 diabetes mellitus: a review of current trends. *Oman medical journal,* 27**,** 269-273.

PARK, C. Y., SHCHEGLOVITOV, A. & DOLMETSCH, R. 2010. The CRAC Channel Activator STIM1 Binds and Inhibits L-Type Voltage-Gated Calcium Channels. *Science,* 330**,** 101-105.

PASQUEL, F. J. & UMPIERREZ, G. E. 2014. Hyperosmolar hyperglycemic state: a historic review of the clinical presentation, diagnosis, and treatment. *Diabetes care,* 37**,** 3124-31.

PEIRÓ, C., ROMACHO, T., AZCUTIA, V., VILLALOBOS, L., FERNÁNDEZ, E., BOLAÑOS, J. P., MONCADA, S. & SÁNCHEZ-FERRER, C. F. 2016. Inflammation, glucose, and vascular cell damage: the role of the pentose phosphate pathway. *Cardiovascular diabetology,* 15**,** 82-82.

PENG, T.-I. & JOU, M.-J. 2010. Oxidative stress caused by mitochondrial calcium overload. *Annals of the New York Academy of Sciences,* 1201**,** 183-188.

PETERSEN, C. C. H. & BERRIDGE, M. J. 1996. Capacitative calcium entry is colocalised with calcium release in Xenopus oocytes: Evidence against a highly diffusible calcium influx factor. *Pflügers Archiv,* 432**,** 286-292.

PHANIENDRA, A., JESTADI, D. B. & PERIYASAMY, L. 2015. Free radicals: properties, sources, targets, and their implication in various diseases. *Indian journal of clinical biochemistry : IJCB,* 30**,** 11-26.

PINHAS-HAMIEL, O. & ZEITLER, P. 2007. Acute and chronic complications of type 2 diabetes mellitus in children and adolescents. *The Lancet,* 369**,** 1823-1831.

PIZARRO, D., POSADA, G., VILLAVICENCIO, N., MOHS, E. & MM, L. 1983. Oral rehydration in hypernatremic and hyponatremic diarrheal dehydration: Treatment with oral glucose/electrolyte solution. *American Journal of Diseases of Children,* 137**,** 730-734.

PIZZINO, G., IRRERA, N., CUCINOTTA, M., PALLIO, G., MANNINO, F., ARCORACI, V., SQUADRITO, F., ALTAVILLA, D. & BITTO, A. 2017. Oxidative Stress: Harms and Benefits for Human Health. *Oxidative medicine and cellular longevity*, 2017**,** 8416763-8416763.

POLJSAK, B., ŠUPUT, D. & MILISAV, I. 2013. Achieving the Balance between ROS and Antioxidants: When to Use the Synthetic Antioxidants. *Oxidative Medicine and Cellular Longevity,* 2013**,** 956792.

POLLACK, A. & CIANCIO, G. 1990. Chapter 3 Cell Cycle Phase-Specific Analysis of Cell Viability Using Hoechst 33342 and Propidium Iodide after Ethanol Preservation. *In:* DARZYNKIEWICZ, Z. & CRISSMAN, H. A. (eds.) *Methods in Cell Biology.* Academic Press.

POLLACK, M., PHANEUF, S., DIRKS, A. & LEEUWENBURGH, C. 2002. The Role of Apoptosis in the Normal Aging Brain, Skeletal Muscle, and Heart. *Annals of the New York Academy of Sciences,* 959**,** 93-107.

POOLE, C. A., BROOKES, N. H., GILBERT, R. T., BEAUMONT, B. W., CROWTHER, A., SCOTT, L. & MERRILEES, M. J. 1996. Detection of Viable and Non-Viable Cells in Connective Tissue Explants Using the Fixable Fluoroprobes 5-Chloromethylfluorescein Diacetate and Ethidium Homodimer-1. *Connective Tissue Research,* 33**,** 233-241.

PRAKRIYA, M. & LEWIS, R. S. 2003. CRAC channels: activation, permeation, and the search for a molecular identity. *Cell calcium,* 33**,** 311-21.

RAHMAN, M. S., KWON, W.-S. & PANG, M.-G. 2014. Calcium Influx and Male Fertility in the Context of the Sperm Proteome: An Update. *BioMed Research International,* 2014**,** 13.

RAMSEY, I. S., DELLING, M. & CLAPHAM, D. E. 2006. AN INTRODUCTION TO TRP CHANNELS. *Annual Review of Physiology,* 68**,** 619-647.

RASK-MADSEN, C. & KING, G. L. 2013. Vascular complications of diabetes: mechanisms of injury and protective factors. *Cell metabolism,* 17**,** 20-33.

RICCARDI, C. & NICOLETTI, I. 2006. Analysis of apoptosis by propidium iodide staining and flow cytometry. *Nat Protoc,* 1**,** 1458-61.

RINK, T. J. 1990. Receptor-mediated calcium entry. *FEBS Letters,* 268**,** 381-385.

ROBERTS, R. A., JAMES, N. H., WOODYATT, N. J., MACDONALD, N. & TUGWOOD, J. D. 1998. Evidence for the suppression of apoptosis by the peroxisome proliferator activated receptor alpha (PPAR alpha). *Carcinogenesis,* 19**,** 43-48.

ROBISON, P., SUSSAN, T. E., CHEN, H., BISWAL, S., SCHNEIDER, M. F. & HERNÁNDEZ-OCHOA, E. O. 2017. Impaired calcium signaling in muscle fibers from intercostal and foot skeletal muscle in a cigarette smoke-induced mouse model of COPD. *Muscle & Nerve,* 56**,** 282-291.

ROCK, K. L. & KONO, H. 2008. The inflammatory response to cell death. *Annual review of pathology,* 3**,** 99-126.

ROSCOE, J. M., HALPERIN, M. L., ROLLESTON, F. S. & GOLDSTEIN, M. B. 1975. Hyperglycemia-induced hyponatremia: metabolic considerations in calculation of serum sodium depression. *Canadian Medical Association journal,* 112**,** 452-3.

ROSENSTOCK, T. R., CARVALHO, A. C. P., JURKIEWICZ, A., FRUSSA-FILHO, R. & SMAILI, S. S. 2004. Mitochondrial calcium, oxidative stress and apoptosis in a neurodegenerative disease model induced by 3-nitropropionic acid. *Journal of Neurochemistry,* 88**,** 1220-1228.

RYBKA, J. & MISTRÍK, J. 2015. [Hyperosmolar hyperglycemic state]. *Vnitrni lekarstvi,* 61**,** 451-457.

SCHENK, B. & FULDA, S. 2015. Reactive oxygen species regulate Smac mimetic/TNFα-induced necroptotic signaling and cell death. *Oncogene,* 34**,** 5796-5806.

SCHNEDL, W. J., FERBER, S., JOHNSON, J. H. & NEWGARD, C. B. 1994. STZ Transport and Cytotoxicity: Specific Enhancement in GLUT2-Expressing Cells. *Diabetes,* 43**,** 1326-1333.

SCHRAMM, J. C., DINH, T. & VEVES, A. 2006. Microvascular Changes in the Diabetic Foot. *The International Journal of Lower Extremity Wounds,* 5**,** 149-159.

SCHULLA, V., RENSTRÖM, E., FEIL, R., FEIL, S., FRANKLIN, I., GJINOVCI, A., JING, X.-J., LAUX, D., LUNDQUIST, I., MAGNUSON, M. A., OBERMÜLLER, S., OLOFSSON, C. S., SALEHI, A., WENDT, A., KLUGBAUER, N., WOLLHEIM, C. B., RORSMAN, P. & HOFMANN, F. 2003. Impaired insulin secretion and glucose tolerance in beta cell-selective Ca(v)1.2 Ca2+ channel null mice. *The EMBO journal,* 22**,** 3844-54.

SCIALÒ, F., FERNÁNDEZ-AYALA, D. J. & SANZ, A. 2017. Role of Mitochondrial Reverse Electron Transport in ROS Signaling: Potential Roles in Health and Disease. *Frontiers in Physiology,* 8.

SEDEJ, S., HEINZEL, F. R., WALTHER, S., DYBKOVA, N., WAKULA, P., GROBORZ, J., GRONAU, P., MAIER, L. S., VOS, M. A., LAI, F. A., NAPOLITANO, C., PRIORI, S. G., KOCKSKAMPER, J. & PIESKE, B. 2010. Na+-dependent SR Ca2+ overload induces arrhythmogenic events in mouse cardiomyocytes with a human CPVT mutation. *Cardiovasc Res,* 87**,** 50-9.

SELVARAJ, S., SUN, Y., SUKUMARAN, P. & SINGH, B. B. 2016. Resveratrol activates autophagic cell death in prostate cancer cells via downregulation of STIM1 and the mTOR pathway. *Molecular Carcinogenesis,* 55**,** 818-831.

SELVIN, E., WATTANAKIT, K., STEFFES, M. W., CORESH, J. & SHARRETT, A. R. 2006. HbA1c and peripheral arterial disease in diabetes: the Atherosclerosis Risk in Communities study. *Diabetes care,* 29**,** 877-82.

SHANMUGASUNDARAM, K., NAYAK, B. K., FRIEDRICHS, W. E., KAUSHIK, D., RODRIGUEZ, R. & BLOCK, K. 2017. NOX4 functions as a mitochondrial energetic sensor coupling cancer metabolic reprogramming to drug resistance. *Nature Communications,* 8**,** 997.

SHAW, A., DOHERTY, M. K., MUTCH, N. J., MACRURY, S. M. & MEGSON, I. L. 2014. Endothelial cell oxidative stress in diabetes: a key driver of cardiovascular complications? *Biochem Soc Trans,* 42**,** 928-33.

SHEETZ, M. J. & KING, G. L. 2002. Molecular understanding of hyperglycemia's adverse effects for diabetic complications. *JAMA,* 288**,** 2579-88.

SIVAKUMAR, R., RAVINDRAN, G., MUTHAYYA, M., LAKSHMINARAYANAN, S. & VELMURUGHENDRAN, C. U. 2005. Diabetic Retinopathy Analysis. *Journal of biomedicine & biotechnology,* 2005**,** 20-27.

SOERGEL, K. H., WHALEN, G. E. & HARRIS, J. A. 1968. Passive movement of water and sodium across the human small intestinal mucosa. *Journal of Applied Physiology,* 24**,** 40-48.

SPANAKIS, E. K. & GOLDEN, S. H. 2013. Race/ethnic difference in diabetes and diabetic complications. *Current diabetes reports,* 13**,** 814-823.

SPIRA, A., GOWRISHANKAR, M. & HALPERIN, M. L. 1997. Factors contributing to the degree of polyuria in a patient with poorly controlled diabetes mellitus. *Am J Kidney Dis,* 30**,** 829-35.

SPRAGUE, E. A., LUO, J. & PALMAZ, J. C. 1997. Human Aortic Endothelial Cell Migration onto Stent Surfaces under Static and Flow Conditions. *Journal of Vascular and Interventional Radiology,* 8**,** 83-92.

STADIE, W. C. 1958. Ketogenesis. *Diabetes,* 7**,** 173-180.

STANDL, E., KHUNTI, K., HANSEN, T. B. & SCHNELL, O. 2019. The global epidemics of diabetes in the 21st century: Current situation and perspectives. *Eur J Prev Cardiol,* 26**,** 7-14.

STEPANEK, O., BRDICKA, T., ANGELISOVA, P., HORVATH, O., SPICKA, J., STOCKBAUER, P., MAN, P. & HOREJSI, V. 2011. Interaction of Late Apoptotic and Necrotic Cells with Vitronectin. *PLOS ONE,* 6**,** e19243.

STERNS, R. H., SILVER, S. M. & HIX, J. K. 2013. Treatment of Hyponatremia. New York, NY: Springer New York.

STOJANOVIC, M., GERMAIN, M., NGUYEN, M. & SHORE, G. C. 2005. BAP31 and its caspase cleavage product regulate cell surface expression of tetraspanins and integrin-mediated cell survival. *The Journal of biological chemistry,* 280**,** 30018-24.

STROTMANN, R., HARTENECK, C., NUNNENMACHER, K., SCHULTZ, G. & PLANT, T. D. 2000. OTRPC4, a nonselective cation channel that confers sensitivity to extracellular osmolarity. *Nature Cell Biology,* 2**,** 695-702.

SUNDARARAGHAVAN, V., MAZUR, M. M., EVANS, B., LIU, J. & EBRAHEIM, N. A. 2017. Diabetes and bone health: latest evidence and clinical implications. *Therapeutic advances in musculoskeletal disease,* 9**,** 67-74.

SUTHAMMARAK, W., SOMERLOT, B. H., OPHEIM, E., SEDENSKY, M. & MORGAN, P. G. 2013. Novel interactions between mitochondrial superoxide dismutases and the electron transport chain. *Aging cell,* 12**,** 1132-1140.

TAKAMURA, T., MISU, H., MATSUZAWA-NAGATA, N., SAKURAI, M., OTA, T., SHIMIZU, A., KURITA, S., TAKESHITA, Y., ANDO, H., HONDA, M. & KANEKO, S. 2008. Obesity Upregulates Genes Involved in Oxidative Phosphorylation in Livers of Diabetic Patients. *Obesity,* 16**,** 2601-2609.

TANG, W. H., MARTIN, K. A. & HWA, J. 2012. Aldose reductase, oxidative stress, and diabetic mellitus. *Frontiers in pharmacology,* 3**,** 87-87.

TERLECKY, S. R., KOEPKE, J. I. & WALTON, P. A. 2006. Peroxisomes and aging. *Biochimica et biophysica acta,* 1763**,** 1749-1754.

THOMAS, M. C., BROWNLEE, M., SUSZTAK, K., SHARMA, K., JANDELEIT-DAHM, K. A. M., ZOUNGAS, S., ROSSING, P., GROOP, P.-H. & COOPER, M. E. 2015. Diabetic kidney disease. *Nature Reviews Disease Primers,* 1**,** 15018-15018.

TOJO, A., ONOZATO, M. L., KITIYAKARA, C., KINUGASA, S., FUKUDA, S., SAKAI, T. & FUJITA, T. 2008. Glomerular albumin filtration through podocyte cell body in puromycin aminonucleoside nephrotic rat. *Medical Molecular Morphology,* 41**,** 92-98.

TONG, L., CHUANG, C.-C., WU, S. & ZUO, L. 2015. Reactive oxygen species in redox cancer therapy. *Cancer Letters,* 367**,** 18-25.

TORNQUIST, K., VAINIO, P., TITIEVSKY, A., DUGUE, B. & TUOMINEN, R. 1999. Redox modulation of intracellular free calcium concentration in thyroid FRTL-5 cells: evidence for an enhanced extrusion of calcium. *Biochem J,* 339 (Pt 3)**,** 621-8.

TRIFUNOVIC, A., HANSSON, A., WREDENBERG, A., ROVIO, A. T., DUFOUR, E., KHVOROSTOV, I., SPELBRINK, J. N., WIBOM, R., JACOBS, H. T. & LARSSON, N.-G. 2005. Somatic mtDNA mutations cause aging phenotypes without affecting reactive oxygen species production. *Proceedings of the National Academy of Sciences of the United States of America,* 102**,** 17993-17998.

UEHARA, A., YASUKOCHI, M., IMANAGA, I., NISHI, M. & TAKESHIMA, H. 2002. Store-operated Ca2+ entry uncoupled with ryanodine receptor and junctional membrane complex in heart muscle cells. *Cell Calcium,* 31**,** 89-96.

UMPIERREZ, G. E., KHAJAVI, M. & KITABCHI, A. E. 1996. Review: diabetic ketoacidosis and hyperglycemic hyperosmolar nonketotic syndrome. *The American journal of the medical sciences,* 311**,** 225-33.

VAN CRUCHTEN, S. & VAN DEN BROECK, W. 2002. Morphological and Biochemical Aspects of Apoptosis, Oncosis and Necrosis. *Anatomia, Histologia, Embryologia,* 31**,** 214-223.

VAN DER KLOOT, W. 1978. Calcium and Neuromuscular Transmission. *In:* WEISS, G. B. (ed.) *Calcium in Drug Action.* Boston, MA: Springer US.

VELHO, A. M. & VELHO, R. M. 2013. Anatomy and physiology series: infrastructure of the kidney. *Journal of Renal Nursing,* 5**,** 228-231.

VENDROV, A. E., VENDROV, K. C., SMITH, A., YUAN, J., SUMIDA, A., ROBIDOUX, J., RUNGE, M. S. & MADAMANCHI, N. R. 2015. NOX4 NADPH Oxidase-Dependent Mitochondrial Oxidative Stress in Aging-Associated Cardiovascular Disease. *Antioxidants & redox signaling,* 23**,** 1389-1409.

VENKATACHALAM, K., VAN ROSSUM, D. B., PATTERSON, R. L., MA, H.-T. & GILL, D. L. 2002. The cellular and molecular basis of store-operated calcium entry. *Nature Cell Biology,* 4**,** E263-E272.

VENKATACHALAM, K., ZHENG, F. & GILL, D. L. 2003. Regulation of canonical transient receptor potential (TRPC) channel function by diacylglycerol and protein kinase C. *J Biol Chem,* 278**,** 29031-40.

VERKMAN, A. S., VAN HOEK, A. N., MA, T., FRIGERI, A., SKACH, W. R., MITRA, A., TAMARAPPOO, B. K. & FARINAS, J. 1996. Water transport across mammalian cell membranes. *American Journal of Physiology-Cell Physiology,* 270**,** C12-C30.

VINIK, A. I., ERBAS, T., PARK, T. S., STANSBERRY, K. B., SCANELLI, J. A. & PITTENGER, G. L. 2001. Dermal Neurovascular Dysfunction in Type 2 Diabetes. *Diabetes Care,* 24**,** 1468-1475.

VISKOPER, R. J., BERNINK, P., SCHELLING, A., RIBEIRO, A. B., KANTOLA, I. M., WILKINS, M. R. & KOBRIN, I. 1997. A randomised, double-blind trial comparing mibefradil and amlodipine: two long-acting calcium antagonists with similar efficacy but different tolerability profiles. *Journal of Human Hypertension,* 11**,** 387-393.

VOTYAKOVA, T. V. & REYNOLDS, I. J. 2004. Detection of hydrogen peroxide with Amplex Red: interference by NADH and reduced glutathione auto-oxidation. *Archives of Biochemistry and Biophysics,* 431**,** 138-144.

VUJOVIC, P., CHIRILLO, M. & SILVERTHORN, D. U. 2018. Learning (by) osmosis: an approach to teaching osmolarity and tonicity. *Advances in Physiology Education,* 42**,** 626-635.

WACHTEL, T. J., TETU-MOURADJIAN, L. M., GOLDMAN, D. L., ELLIS, S. E. & O'SULLIVAN, P. S. 1991. Hyperosmolarity and acidosis in diabetes mellitus: a three-year experience in Rhode Island. *Journal of general internal medicine,* 6**,** 495-502.

WAGNER, S., RUFF, H. M., WEBER, S. L., BELLMANN, S., SOWA, T., SCHULTE, T., ANDERSON, M. E., GRANDI, E., BERS, D. M., BACKS, J., BELARDINELLI, L. & MAIER, L. S. 2011. Reactive Oxygen Species–Activated Ca/Calmodulin Kinase IIδ Is Required for Late I_{Na} Augmentation Leading to Cellular Na and Ca Overload. *Circulation Research,* 108**,** 555-565.

WAKAI, A., ROBERTS, I. G., SCHIERHOUT, G. & WAKAI, A. 2005. Mannitol for acute traumatic brain injury. *Cochrane Database of Systematic Reviews*.

WALTON, P. A. & PIZZITELLI, M. 2012. Effects of peroxisomal catalase inhibition on mitochondrial function. *Frontiers in physiology,* 3**,** 108-108.

WANDERS, R. J. A., WATERHAM, H. R. & FERDINANDUSSE, S. 2016. Metabolic Interplay between Peroxisomes and Other Subcellular Organelles Including Mitochondria and the Endoplasmic Reticulum. *Frontiers in Cell and Developmental Biology,* 3.

WANG, B., GONG, Y., YING, B. & CHENG, B. 2018. Association of Initial Serum Total Calcium Concentration with Mortality in Critical Illness. *BioMed Research International,* 2018**,** 8.

WANG, J.-Y., WANG, C.-Y., HUANG, Y.-S., CHEN, P.-F., HUANG, K.-Y., CHOU, P., LIAN, W.-C. & LEE, C.-C. 2014. Increased Risk of Ischemic Stroke after Hyperosmolar Hyperglycemic State: A Population-Based Follow-Up Study. *PLOS ONE,* 9**,** e94155.

WANG, W., ZHANG, X., GAO, Q., LAWAS, M., YU, L., CHENG, X., GU, M., SAHOO, N., LI, X., LI, P., IRELAND, S., MEREDITH, A. & XU, H. 2017. A voltage-dependent K(+) channel in the lysosome is required for refilling lysosomal Ca(2+) stores. *J Cell Biol,* 216**,** 1715-1730.

WANG, Y., FANG, J., LEONARD, S. S. & KRISHNA RAO, K. M. 2004. Cadmium inhibits the electron transfer chain and induces Reactive Oxygen Species. *Free Radical Biology and Medicine,* 36**,** 1434-1443.

WEBER, L. V., AL-REFAE, K., WÖLK, G., BONATZ, G., ALTMÜLLER, J., BECKER, C., GISSELMANN, G. & HATT, H. 2016. Expression and functionality of TRPV1 in breast cancer cells. *Breast cancer (Dove Medical Press),* 8**,** 243-252.

WELCH, B. J. & ZIB, I. 2004. Case Study: Diabetic Ketoacidosis in Type 2 Diabetes: "Look Under the Sheets". *Clinical Diabetes,* 22**,** 198-200.

WELLS-KNECHT, K. J., ZYZAK, D. V., LITCHFIELD, J. E., THORPE, S. R. & BAYNES, J. W. 1995. Mechanism of autoxidative glycosylation: identification of glyoxal and arabinose as intermediates in the autoxidative modification of proteins by glucose. *Biochemistry,* 34**,** 3702-9.

WEWER ALBRECHTSEN, N. J., KUHRE, R. E., HORNBURG, D., JENSEN, C. Z., HORNUM, M., DIRKSEN, C., SVANE, M., GASBJERG, L. S., JØRGENSEN, N. B., GABE, M. N., BALK-MØLLER, E., ALBRECHTSEN, R., WINTHER-SØRENSEN, M., GALSGAARD, K. D., MEISSNER, F., JORSAL, T., LUND, A., VILSBØLL, T., ELIASEN, R., BOJSEN-MØLLER, K. N., IDORN, T., DEACON, C. F., KNOP, F. K., ROSENKILDE, M. M., HARTMANN, B., FELDT-RASMUSSEN, B., MANN, M., MADSBAD, S. & HOLST, J. J. 2017.

Circulating Glucagon 1-61 Regulates Blood Glucose by Increasing Insulin Secretion and Hepatic Glucose Production. *Cell reports,* 21**,** 1452-1460.

WHITING, D. R., GUARIGUATA, L., WEIL, C. & SHAW, J. 2011. IDF Diabetes Atlas: Global estimates of the prevalence of diabetes for 2011 and 2030. *Diabetes Research and Clinical Practice,* 94**,** 311-321.

WILLIX, C., GRIFFITHS, E. & SINGLETON, S. 2019. Hyperglycaemic presentations in type 2 diabetes. *Australian Journal for General Practitioners,* 48**,** 163-167.

WILSON, D. K., BOHREN, K. M., GABBAY, K. H. & QUIOCHO, F. A. 1992. An unlikely sugar substrate site in the 1.65 A structure of the human aldose reductase holoenzyme implicated in diabetic complications. *Science (New York, N.Y.),* 257**,** 81-4.

WOLFSDORF, J. I., ALLGROVE, J., CRAIG, M. E., EDGE, J., GLASER, N., JAIN, V., LEE, W. W. R., MUNGAI, L. N. W., ROSENBLOOM, A. L., SPERLING, M. A. & HANAS, R. 2014. Diabetic ketoacidosis and hyperglycemic hyperosmolar state. *Pediatric Diabetes,* 15**,** 154-179.

WU, D. & YOTNDA, P. 2011. Production and detection of reactive oxygen species (ROS) in cancers. *Journal of visualized experiments : JoVE***,** 3357.

WU, L. & JUURLINK, B. H. J. 2002. Increased Methylglyoxal and Oxidative Stress in Hypertensive Rat Vascular Smooth Muscle Cells. *Hypertension,* 39**,** 809-814.

WU, M.-L., TSAI, K.-L., WANG, S.-M., WU, J.-C., WANG, B.-S. & LEE, Y.-T. 1996. Mechanism of Hydrogen Peroxide and Hydroxyl Free Radical–Induced Intracellular Acidification in Cultured Rat Cardiac Myoblasts. *Circulation Research,* 78**,** 564-572.

WUERTZ, K., URBAN, J. P. G., KLASEN, J., IGNATIUS, A., WILKE, H. J., CLAES, L. & NEIDLINGER-WILKE, C. 2007. Influence of extracellular osmolarity and

mechanical stimulation on gene expression of intervertebral disc cells. *Journal of Orthopaedic Research,* 25**,** 1513-1522.

XIA, Z. & STORM, D. R. 2005. The role of calmodulin as a signal integrator for synaptic plasticity. *Nat Rev Neurosci,* 6**,** 267-76.

XIANG, J., WAN, C., GUO, R. & GUO, D. 2016. Is Hydrogen Peroxide a Suitable Apoptosis Inducer for All Cell Types? *BioMed research international,* 2016**,** 7343965-7343965.

XU, S. Z., SUKUMAR, P., ZENG, F., LI, J., JAIRAMAN, A., ENGLISH, A., NAYLOR, J., CIURTIN, C., MAJEED, Y., MILLIGAN, C. J., BAHNASI, Y. M., AL-SHAWAF, E., PORTER, K. E., JIANG, L. H., EMERY, P., SIVAPRASADARAO, A. & BEECH, D. J. 2008. TRPC channel activation by extracellular thioredoxin. *Nature,* 451**,** 69-72.

YAN, L.-J. 2018. Redox imbalance stress in diabetes mellitus: Role of the polyol pathway. *Animal models and experimental medicine,* 1**,** 7-13.

YANNOUTSOS, A., LEVY, B. I., SAFAR, M. E., SLAMA, G. & BLACHER, J. 2014. Pathophysiology of hypertension: interactions between macro and microvascular alterations through endothelial dysfunction. *Journal of Hypertension,* 32**,** 216-224.

YAO, D. & BROWNLEE, M. 2010. Hyperglycemia-Induced Reactive Oxygen Species Increase Expression of the Receptor for Advanced Glycation End Products (RAGE) and RAGE Ligands. *Diabetes,* 59**,** 249-255.

YAU, S.-Y., LEE, T. H.-Y., LI, A., XU, A. & SO, K.-F. 2018. Adiponectin Mediates Running-Restored Hippocampal Neurogenesis in Streptozotocin-Induced Type 1 Diabetes in Mice. *Frontiers in neuroscience,* 12**,** 679-679.

YEROMIN, A. V., ZHANG, S. L., JIANG, W., YU, Y., SAFRINA, O. & CAHALAN, M. D. 2006. Molecular identification of the CRAC channel by altered ion selectivity in a mutant of Orai. *Nature,* 443**,** 226-229.

YIN, L.-M., WEI, Y., WANG, Y., XU, Y.-D. & YANG, Y.-Q. 2013. Long term and standard incubations of WST-1 reagent reflect the same inhibitory trend of cell viability in rat airway smooth muscle cells. *International journal of medical sciences,* 10**,** 68-72.

YOUNG, B. A., MAYNARD, C. & BOYKO, E. J. 2003. Racial differences in diabetic nephropathy, cardiovascular disease, and mortality in a national population of veterans. *Diabetes care,* 26**,** 2392-9.

ZEESHAN, H. M. A., LEE, G. H., KIM, H.-R. & CHAE, H.-J. 2016. Endoplasmic Reticulum Stress and Associated ROS. *International Journal of Molecular Sciences,* 17.

ZENG, B., CHEN, G.-L., GARCIA-VAZ, E., BHANDARI, S., DASKOULIDOU, N., BERGLUND, L. M., JIANG, H., HALLETT, T., ZHOU, L.-P., HUANG, L., XU, Z.-H., NAIR, V., NELSON, R. G., JU, W., KRETZLER, M., ATKIN, S. L., GOMEZ, M. F. & XU, S.-Z. 2017. ORAI channels are critical for receptor-mediated endocytosis of albumin. *Nature Communications,* 8**,** 1920-1920.

ZHANG, Y., TING, R. Z., YANG, W., JIA, W., LI, W., JI, L., GUO, X., KONG, A. P., WING, Y. K., LUK, A. O., SARTORIUS, N., MORISKY, D. E., OLDENBURG, B., WENG, J. & CHAN, J. C. 2015. Depression in Chinese patients with type 2 diabetes: associations with hyperglycemia, hypoglycemia, and poor treatment adherence. *J Diabetes,* 7**,** 800-8.

ZHAO, R.-Z., JIANG, S., ZHANG, L. & YU, Z.-B. 2019. Mitochondrial electron transport chain, ROS generation and uncoupling (Review). *International journal of molecular medicine,* 44**,** 3-15.

ZHAO, Z. 2019. Iron and oxidizing species in oxidative stress and Alzheimer's disease. *Aging medicine (Milton (N.S.W)),* 2**,** 82-87.

ZHENG, L., STATHOPULOS, P. B., SCHINDL, R., LI, G.-Y., ROMANIN, C. & IKURA, M. 2011. Auto-inhibitory role of the EF-SAM domain of STIM proteins in store-operated calcium entry. *Proceedings of the National Academy of Sciences,* 108**,** 1337-1342.

ZIELONKA, J., CHENG, G., ZIELONKA, M., GANESH, T., SUN, A., JOSEPH, J., MICHALSKI, R., O'BRIEN, W. J., LAMBETH, J. D. & KALYANARAMAN, B. 2014. High-throughput assays for superoxide and hydrogen peroxide: design of a screening workflow to identify inhibitors of NADPH oxidases. *The Journal of biological chemistry,* 289**,** 16176-16189.